CRANFIELD UNIVERSITY

Maurizio Collu

Dynamics of Marine Vehicles with Aerodynamic Surfaces

School of Engineering

Offshore Engineering and Naval Architecture Group

PhD Thesis

CRANFIELD UNIVERSITY
School of Engineering, Department of Structures, Impact & Machine Dynamics
Offshore Engineering and Naval Architecture Group
PhD Thesis
Academic Year 2007-2008

Maurizio Collu

Dynamics of Marine Vehicles with Aerodynamic Surfaces

Supervisor
Prof. M. H. Patel
Co-Supervisor
Dr. F. Trarieux

November 2008

This thesis is submitted in partial fulfilment
of the requirements for the degree
of Doctor of Philosophy

Audentes Fortuna Iuvat
(Fortune favors the bold)
Virgil, Aeneid, book X, line 284

A Chiara,
non solo la donna piu' bella
che abbia mai incontrato,
ma anche la piu' comprensiva.

Abstract

An assessment of the relative speeds and payload capacities of airborne and waterborne vehicles highlights a gap which can be usefully filled by a new vehicle concept, utilizing both hydrodynamic and aerodynamic forces. A high speed marine vehicle equipped with aerodynamic surfaces (called an AAMV, 'Aerodynamically Alleviated Marine Vehicle') is one such concept. The development of this type of vehicle requires a mathematical framework to characterize its dynamics taking account of both aerodynamic and hydrodynamic forces. This thesis presents the development of unified and consistent equations of equilibrium and equations of motion to predict the dynamic performance of such AAMV configurations.

An overview of the models of dynamics developed for Wing In Ground effect 'WIGe' vehicles and high speed marine vehicles (planing craft) is given first. Starting from these models, a generic AAMV configuration is proposed and a kinematics framework is developed. Then, taking into account the aerodynamic, hydrostatic and hydrodynamic forces acting on the AAMV, equations of equilibrium are derived and solved. This is followed by deriving and solving the full equations of motion, using a small perturbation assumption. A static stability criterion, specific for the AAMV configuration, has been developed. This mathematical framework and its results are implemented in MATLAB and validated against theoretical and experimental data. The resultant capability for analysing novel AAMV configurations is presented through two parametric analysis. The analysis demonstrate that these models offer a powerful AAMV design tool.

Acknowledgements

My sincere thanks go to my supervisor, Professor Minoo H Patel and my co-supervisor, Florent Trarieux for their guidance throughout this work. They offered me the chance to do what I love to do; research, and taught me how to do it. I would also especially like to thank Aaron J. Latty and Adair Williams who were a source of help and support both in and out the university: you truly are two of the kindest people I have ever met.

Vorrei esprimere tutta la mia gratitudine a mia moglie Chiara per il suo insostituibile supporto: spero di meritarla, dal momento che pur di lasciarmi coltivare i miei sogni ha accettato di sopportare i sacrifici che derivano dal vivere a distanza. Un grosso grazie va anche alla mia famiglia, inesauribile fonte di affetto e sostegno: papa' Saturnino, mamma Maria, mia sorella Daniela e mio fratello Claudio, i miei 'secondi' papa' e mamma Mauro e Daniela e secondo fratello Cristiano. Ringrazio molto anche tutti i miei amici, primi fra tutti Luca Mauri, Chiara e Gianluca. Tutti loro meritano una parte del mio PhD!

Contents

List of Figures

List of Tables

Notation

a	pitch moment arm of D_F
a_{ah}	pitch moment arm of D_{ah}
a_{ws}	pitch moment arm of D_{ws}
A	characteristic polynomial coefficient
A_{ij}	∂F_i / $\partial \ddot{\eta}_j$
$[A]$	aerodynamic and/or hydrodynamic added mass matrix
$[A_{SS}]$	left state space matrix
AAMV	Aerodynamically Alleviated Marine Vehicle (1.1.1)
AAZ	Aerodynamic Alleviation Zone (1.1.1)
AC_i	Aerodynamic Center, i-th aerodynamic surface
ACV	Air Cushion Vehicle
a.k.a.	also known as
AoA	Angle of Attack
B	characteristic polynomial coefficient
$[B]$	aerodynamic and/or hydrodynamic damping matrix
B_{ij}	∂F_i / $\partial \dot{\eta}_j$
$[B_{SS}]$	right state space matrix
c	pitch moment arm of N
$c_{L,i}$	lift coefficient, i-th aerodynamic surface
$c_{D,i}$	drag coefficient, i-th aerodynamic surface
$c_{m,i}$	pitch moment coefficient, i-th aerodynamic surface
C	characteristic polynomial coefficient
$[C]$	hydrostatic restoring stability derivatives matrix

C_{ij}	∂F_i / $\partial \eta_j$
CG	Center of Gravity
D	characteristic polynomial coefficient
$[D]$	aerodynamic WIGe matrix
D_{ah}	dry hull aerodynamic drag
D_{ai}	aerodynamic drag, i-th aerodynamic surface
D_F	Hydrodynamic frictional drag
D_{ws}	Hydrodynamic whisker spray drag
DHMTU	Department of Hydro-mechanic, Marine Technical University
E	characteristic polynomial coefficient
F	characteristic polynomial coefficient
F_i	surge (i=1), heave (i=3) force or pitch (i=5) moment
Fn	Froude number, beam based $Fn = V/\sqrt{g\,B}$
g	gravitational constant acceleration
h	height above the surface, positive upward, small disturbances variable
$[H]$	state space matrix
HSMV	High Speed Marine Vehicle
HYSUCAT	Hydrofoil Supported Catamaran
I_{55}	pitch moment of inertia
IGE	In Ground Effect
L_{ai}	aerodynamic lift, i-th aerodynamic surface
lcg	longitudinal position of CG, measured from the transom
m	vehicle mass at equilibrium
M_{ai}	aerodynamic moment, i-th aerodynamic surface
mac_i	mean aerodynamic chord, i-th aerodynamic surface
N	hydrodynamic potential force

PC	planing craft
RULM	Rectilinear Uniform Level Motion
S_{ai}	reference surface area of the i-th aerodynamic surface
SES	Surface Effect Vehicle
SPPO	Small Period Pitching Oscillation
T	thrust force
TP	thrust force point of action
V_0	velocity at equilibrium
vcg	vertical position of CG, measured from the keel
W	weight of the vehicle
WIGe	Wing In Ground effect
wrt	with respect to
X	surge force, positive forward
Z	heave force, positive downward
β	deadrise angle
ϵ	angle between the direction of T and the keel
η	angle between the wing mac and the keel
$\underline{\eta}$	small disturbances vector, $[\eta_1\ \eta_3\ \eta_3\ \eta_3\ ]^T$
η_0	height above the surface, positive upward, small disturbances variable
η_1	surge displacement, positive forward, small disturbances variable
η_3	heave displacement, positive downward, small disturbances variable
η_5	pitch rotation, positive bow-up, small disturbances variable
$\dot{\eta}_i$	$\partial\eta_i \quad \partial t$
$\ddot{\eta}_i$	$\partial^2\eta_i \quad (\partial t)^2$

$\underline{\nu}$	state space vector
ρ^i	density, ρ^a air, ρ^w seawater
τ	trim angle, angle between the keel of the planing hull and the waterline
ξ_i	coordinate of the i-th point in the body-fixed axes system, x axis
ζ_i	coordinate of the i-th point in the body-fixed axes system, z axis
$[0]_{i,j}$	zeros matrix, i row times j columns

Chapter 1

Introduction

1.1 Context

During the last five decades, interest in High Speed Marine Vehicles (HSMV) has been increasing for both commercial and military use, leading to new configurations and further development of already existing configurations [30]. To create vehicles that are capable of carrying more payload both farther and faster, many vehicle concepts have been proposed, and these can be classified using the 'Lift or Sustention Triangle' concept (fig. 1.1).

Basically, to sustain the weight of a HSMV, three are the forces that can be used:

- hydrostatic lift (buoyancy),
- powered aerostatic lift,
- hydrodynamic lift.

Buoyancy is the lift force most commonly used by ships, and historically is the oldest. Marine vehicles that exploit only buoyancy to sustain their weight are usually called displacement ships. For high speed marine vehicles it is not feasible

to use only buoyancy, due to the fact that the buoyancy force is proportional to the displaced water volume, and at high speed it is better to minimize this parameter, since as more vehicle volume is immersed in the water the higher the hydrodynamic drag will be.

The Air Cushion Vehicles (ACV) class, such as the Hovercraft, use a cushion of air at a pressure higher than atmospheric to minimize contact with the water, thus minimizing hydrodynamic drag. The air cushion is not closed, and an air flux keeps the pressure in the cushion high. This system is called 'powered aerostatic lift'.

At high speeds a marine vehicle experiences 'hydrodynamic lift', due to the fact that the vehicle is planing over the water surface. This hydrodynamic lift supports the weight otherwise sustained by buoyancy or, through increasing the speed, can also replace the buoyancy force. Planing craft, high speed catamarans (trimarans, quadrimarans) and other similar configurations use this principle to attain high speeds.

If, instead of a simple planing hull, a surface similar to an aerofoil is used underwater, a hydrofoil is obtained. Basically, while in planing mode the hydrodynamic lift is generated by only one surface, the wetted surface of the hull, hydrofoils experience an effect similar to aerofoil, since the hydrodynamic lift is the difference between the pressure acting on the lower surface and the pressure on the upper surface.

As illustrated in fig. 1.1, a high speed marine vehicle can use two or all these three kind of forces to sustain its weight. For example, a SES (Surface Effect Ship) consists of a catamaran hull configuration plus a powered air cushion with a front and a rear skirt in the space between the hulls. Therefore it experiences both hydrostatic and powered aerostatic lift. Other vehicles exploiting more than one

way to sustain their vehicles are Hydrofoil-Supported Catamarans (HYSUCAT).

As presented in the literature review chapter, in section 2.4, there is another lift force that can be exploited to 'alleviate' the weight of the vehicle, leading to a reduced buoyancy and therefore to a decreased hydrodynamic drag: this is aerodynamic lift. The use of one or more aerodynamic surfaces to alleviate the weight of the vehicle requires a modification of the 'Sustention Triangle', leading to the 'Lift Pyramid', illustrated in fig. 1.2. While the 'Sustention Triangle' has three corners defining primary means - buoyant lift, dynamic lift and powered lift - by which lift is generated, the lift pyramid has a fourth corner, representing the aerodynamic lift. As can be seen, there is an extreme case where the aerodynamic forces are sustaining 100% of the weight of the vehicle: WIGe (Wing In Ground effect) vehicles. These vehicles are presented in section 2.2.

1.1.1 Definition of 'Aerodynamic Alleviation Zone' and 'Aerodynamically Alleviated Marine Vehicle (AAMV)'

Two new terms have been introduced by the author to better define a new configuration class and the zone of the 'Lift Pyramid' in which these vehicles operate.

The **Aerodynamic Alleviation Zone (AAZ)**, illustrated in fig. 1.3, can be defined as the area representing the points where a combination of buoyancy, hydrodynamic lift and aerodynamic lift is used to sustain the weight of the vehicle. As the speed increases, hydrostatic force becomes lower, therefore a high speed marine vehicle, equipped with aerodynamic surfaces, operates at cruise speed in a sub-zone called 'AAZ Cruise speed', illustrated in fig. 1.3.

An **Aerodynamically Alleviated Marine Vehicle (AAMV)** is a high speed marine vehicle designed to exploit, in its cruise phase, the aerodynamic lift force,

using one or more aerodynamic surfaces. The AAMV operate in the just defined AAZ.

1.2 Problem Statement

This work is concerned with the development of a method to study the dynamics of an AAMV, a vehicle designed to exploit hydrodynamic and aerodynamic forces that are of the same order of magnitude to sustain its weight. Methodologies for aircraft and marine craft exist and are well documented, but air and marine vehicles have always been investigated with a rather different approach. Marine vehicles have been studied analyzing very accurately hydrostatic and hydrodynamic forces, approximating very roughly the aerodynamic forces acting on the vehicle. On the contrary, the dynamics of Wing In Ground effect (WIGe) vehicles has been modeled focusing mainly on aerodynamic forces, paying much less attention to hydrostatic and hydrodynamic forces.

An AAMV experiences aerodynamic and hydrodynamic forces of the same order of magnitude, therefore neither the high speed marine vehicles nor the airborne vehicles models of dynamics can be adopted. The main objective of this work is to bridge this gap by developing a new model of dynamics, that takes into account the equal importance of aerodynamic and hydrodynamic forces. In particular two mathematical models have been developed:

- a system of equations of equilibrium, to estimate the equilibrium attitude of an AAMV (chapter 6),
- a system of equations of motion, to estimate the static and dynamic stability of an AAMV (chapter 7).

1.3 Methodology

It is true that available models of dynamics cannot take into account both aerodynamic and hydrodynamic forces at the same time with equal accuracy. Nonetheless, to develop a new model of dynamics for an AAMV, it is suitable to start analyzing the models of dynamics used for airborne and waterborne vehicles. As it is illustrated in section 5.3, the chosen AAMV configuration consists of a high speed prismatic planing hull plus one or more aerodynamic surfaces. These aerodynamic surfaces are always operating at very low altitude above the surface, and for this reason they operates 'In Ground Effect (IGE)'. Therefore the models of dynamics of planing craft and of WIGe vehicles are adopted as the starting point, to develop the AAMV model of dynamics.

1.3.1 Literature review

A thorough literature review on both planing craft (section 2.3) and WIGe vehicles (section 2.2) models of dynamics has been conducted. Furthermore, the author has also conducted a literature review on available vehicles that can be classified as 'Aerodynamically Alleviated Marine Vehicles (AAMV)' (section 2.4), for a dual purpose: to analyze the state of the art of the models of dynamics developed for AAMV, and to collect some experimental data on AAMV; this being useful to check the validity of the models developed in this work.

Unfortunately no experimental data on vehicles classifiable as AAMV are available in the public domain, therefore it has not been possible to directly check the developed AAMV model of dynamics against experimental data. For this reason the AAMV mathematical model has been obtained by unifying two sub-models, one developed for planing craft and checked against planing craft experimental

data, and one developed for WIGe vehicles, checked against experimental data obtained for these vehicles. With this approach, the mathematical model of dynamics developed for AAMV is also able to analyze planing craft and WIGe configurations, therefore its numerical results can be validated against available experimental data.

The work has been divided in two parts:

- part I: analysis and implementation in MATLAB of separate dynamics models for a planing craft and a WIGe vehicle, fully validated against experimental data,

- part II: coupling of these two models to develop a system of equations of equilibrium and a system of equations of motion for the AAMV configuration.

1.3.2 Part I: analysis of planing craft and WIGe vehicles models of dynamics

Part I is presented in chapters 3 and 4. In chapter 3 a mathematical model of the dynamics of WIGe vehicles is presented, and its numerical implementation in MATLAB is illustrated. To check the validity of the program some comparisons between numerical results and experimental data are presented. The same approach has been adopted to develop the planing craft MATLAB model of dynamics, presented in chapter 4.

1.3.3 Part II: development of a model of dynamics for Aerodynamically Alleviated Marine Vehicles

1.3.3.1 Configuration and kinematics

In order to develop a mathematical model of the AAMV dynamics, a kinematics framework has been developed to describe the motion of a AAMV and the forces acting on it (section 5.2). Once a reference framework has been established, it is necessary to narrow down the possible configurations of a AAMV, since the qualitative and quantitative nature of the forces and moments acting on a AAMV depends on the elements that compose its configuration (section 5.3).

1.3.3.2 Development of the system of equations of equilibrium

Once a kinematics framework and a configuration has been established, it is possible to derive a system of equations of equilibrium in the longitudinal plane (chapter 6). This system take into account hydrostatic, hydrodynamic, and aerodynamic forces and moments acting on an AAMV. An iterative method to solve this system is proposed, and its solution gives an estimation of the equilibrium attitude of the AAMV, starting from the geometric, inertial, aerodynamic and hydrodynamic characteristics of the vehicle.

1.3.3.3 Development of the system of equations of motions

To analyze how the AAMV, at a given equilibrium state, reacts to external disturbances, it is necessary to develop a system of equations of motion (chapter 7). A set of ordinary differential equations of motion are derived using small-disturbance stability theory, leading to the Cauchy standard form. Analyzing the properties

of this system it is shown that the dynamics of an AAMV configuration is not simply the sum of the planing craft and WIGe vehicles dynamics, but it presents some new characteristics.

1.3.3.4 AAMV stability analysis

The AAMV is characterized by new features in the dynamics, therefore the methods to assess the static and dynamic stability of planing craft and WIGe vehicles cannot be adopted. Starting from the AAMV system of equations of motion developed, a mathematical method to estimate the static stability of a vehicle experiencing both hydrodynamic and aerodynamic forces has been developed (section 8.2). Furthermore, using the approaches used for planing craft and WIGe vehicles, it is also possible to calculate the dynamic stability of the AAMV (section 8.3).

1.3.3.5 Parametric analysis of a AAMV configuration

With the AAMV system of equations of equilibrium developed it is possible to estimate, given the AAMV configuration characteristics, the equilibrium attitude characteristics in a given speed range (chapter 6). With the AAMV system of equations of motion developed (chapter 7), and in particular with the AAMV static and dynamic stability methods developed (chapter 8), it is possible to determine the degree of static and dynamic stability of the AAMV in a given equilibrium state.

Both the AAMV performances and its static and dynamic stability degree depend on several configuration characteristics: mass, pitch moment of inertia, hull length, hull width, aerodynamic surface lengths, aerodynamic and hydrodynamic coefficients, and so on. Using the mathematical methods developed and their

numerical implementation in MATLAB, parametric analysis on the influence of some key parameters of the configuration on the AAMV performances and on the AAMV static and dynamic stability have been conducted (chapter 9).

Through these analysis it is shown how the two mathematical models developed can be used as AAMV design tools.

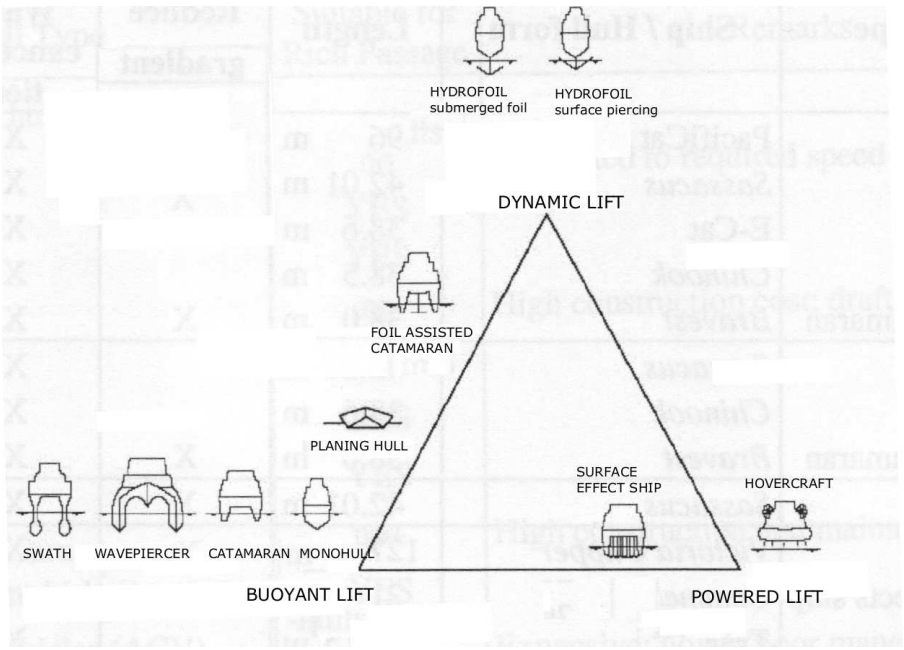

Figure 1.1: Lift or Sustention Triangle [1]

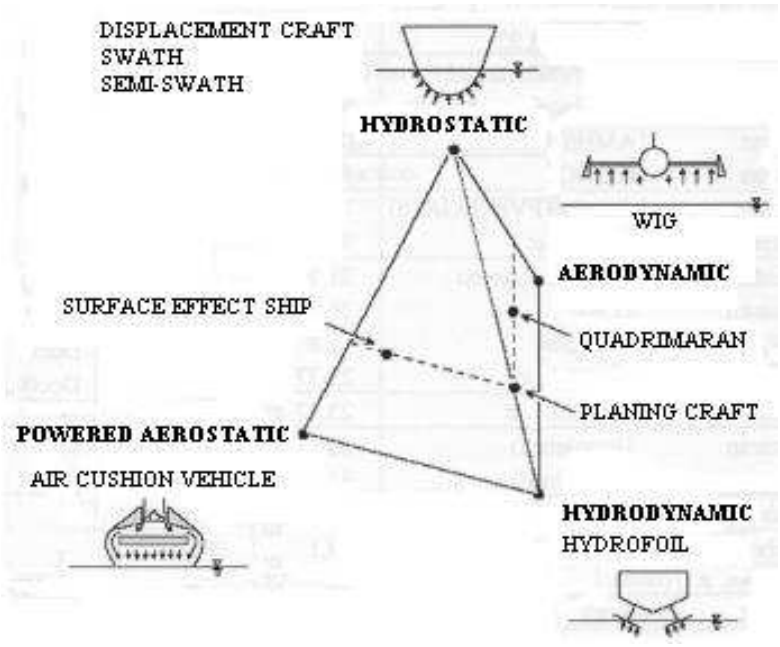

Figure 1.2: Lift Pyramid [1]

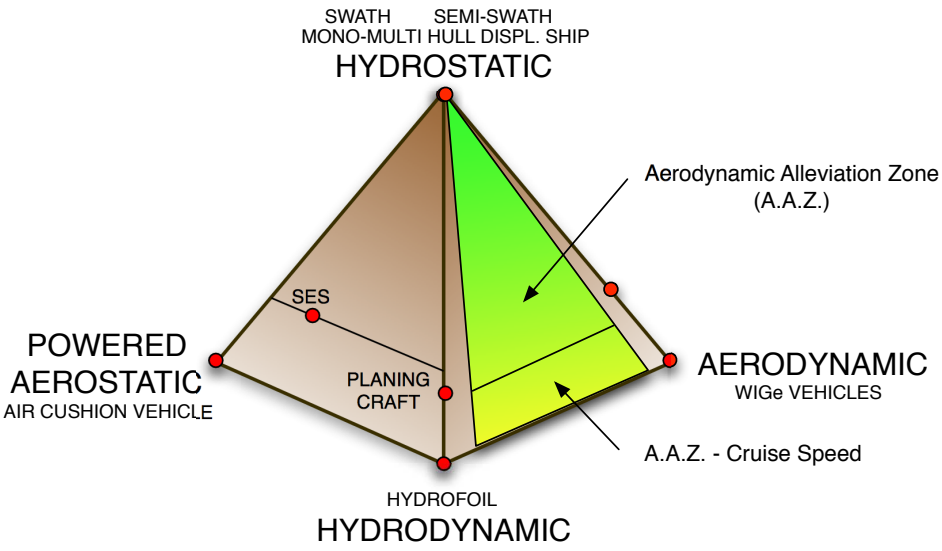

Figure 1.3: Lift Pyramid - Aerodynamic Alleviation Zone

Chapter 2

Literature Review

2.1 Introduction

In order to develop a model to study the dynamics of an 'Aerodynamically Alleviated Marine Vehicle (AAMV)', a literature search on dynamics models for airborne and waterborne vehicles has been carried out. In particular, the static and dynamic stability models of Wing in Ground effect (WIGe) vehicles and planing craft have been used as a starting point in the search.

2.2 Wing in Ground effect vehicles

2.2.1 Short history

As defined by Rozhdestvensky [41], the WIGe is:

> "...an increase of the lift-to-drag ratio of a lifting system at small relative distances from an underlying surface."

Also Rozhdestvensky says that a WIGe vehicle:

> "...can be defined as a heavier than air vehicle with an engine, which is designed to operate in proximity to an underlying surface for efficient utilization of the ground effect."

The enhancement of the lift to drag ratio is due to two main effects: the lift augmentation and the induced drag decreasing as the vehicle approaches the ground. Very simply, the lift enhancement is due to an increment of the pressure experienced by the lower surface of the aerodynamic surface, while the lower induced drag is due to the fact that the induced lift vortices are restrained by the presence of the solid surfaces close by. It should be noticed that some authors, like Moore [32], state that the increase of the lift to drag ratio is due only to the increase of the lift, because the drag actually increases as the profile approaches the ground.

In 1930-31, the Dornier DO-X seaplane exploited ground effect to increase its performances during transatlantic flights, highlighting a new phenomena occurring when a wing is flying at very low altitude above the surface.

In 1935 T. Kaario in Finland built a WIGe vehicle: it was capable of transporting a man over the snow at speeds of up to 12 knots. He obtained the first patent for this kind of vehicle. Later in 1962, Kaario build the Aerosani No.8. This vehicle was essentially a WIGe sled, capable of transporting two men up to speeds of 43 knots.

In 1958, in Russia, R. Y. Alexeyev (a.k.a. R. E. Alekseev) (fig. 2.1) began a project for the Russian Navy: it is the start of the 'Ekranoplan' project. An Ekranoplan, briefly, is an airplane designed to fly at a height above the surface equals to a fraction of the chord of the wing, typically a height of ≤ 0.5 chord, to exploit the 'wing in ground' effect (WIGe). The first series, called SM, were built

and tested in the early to mid 1960's, leading to the 'Project KM', known in the West as the Caspian Sea Monster. It was the first vehicle to demonstrate that a pitch stability solution can be attained using a tail surface operating out of ground effect and out of the effect of the main wing. The test demonstrated that the KM was able to fly in ground effect at 500 km/h (about 310 mph). In 1972 the SM-6 was designed. It is the prototype of the Orlyonok ekranoplan, shown in fig. 2.2. Respectively in 1980's and 1990's the Lun ekranoplan and Spasatel ekranoplan followed (fig. 2.3, 2.4), demonstrating the technology and experimental leadership of the Russian Navy in this field.

In 1963, Dr. W. R. Bertelson of Illinois, USA, developed the GEM-3. This vehicle consisted of a four-seats ram-wing able to operate at speeds of 95 knots over water and snow. In the same year, in Iowa, A. Lippisch of West Germany developed an experimental WIGe vehicle, the X-112 (fig. 2.5). The interesting characteristic of the X-112 configuration was its stability in both free flight and ground effect. In 1970 Lippisch returned to Germany and developed, under a joint program of Rhein-Fleuzeugbau and West German government, the X-113 and X-114 (fig. 2.6, 2.7). During 1971-1972 the vehicle was thoroughly tested to collect data.

In 1972, the HFL-Seaglide Ltd., in England, developed a three-seat aerodynamic ram-wing vehicle called Seabee, under the direction of Ronald Bourn. It was tested only in ground effect.

A more extensive historical review of WIGe vehicles can be found in [34] and [42].

2.2.2 Model of dynamics

As previously stated, research on WIGe vehicles has mainly been carried out in the former Soviet Union, where they were known as 'Ekranoplans'. The Central

Hydrofoil Design Bureau, under the guidance of R. E. Alekseev, developed several test craft and the first production line for ekranoplans: Orlyonok and Lun types [60]. Unfortunately, little has been published in the open domain. In the meantime, several research programs were undertaken in the west to better understand the peculiar dynamics of vehicles flying in ground effect (IGE).

In the 1960's and the 1970's Kumar [24],[25] started research in this area at Cranfield University (College of Aeronautics). He carried out several experiments with a small test craft and provided the equations of motion, the dimensionless stability derivatives and studied the stability issues of a vehicle flying IGE.

In 1970's Irodov [20] presented a simplified analysis for the longitudinal static stability of WIGe vehicles. He linearized the equations of motion about a trimmed, straight and level flight path, deriving a simplified static stability criterion for this configuration. The approach, independently developed, is similar to the Staufenbiel approach to the study of WIGe vehicles dynamics.

Staufenbiel [52] in the 1980s carried out an extensive work on the influence of the aerodynamic surface characteristics on the longitudinal stability in wing in ground effect. Several considerations about the aerofoil shape, the wing planform and other aerodynamic elements were presented, in comparison with experimental data obtained from the experimental WIG vehicle X-114. The equations of motion for a vehicle flying IGE were defined, including non linear effects.

In USA, Gera [16] used Staufenbiel's work to investigate the stability of a Russian ekranoplan, using available data for the F-104 aircraft, a vehicle with an aerodynamic layout similar to the Russian vehicle. The approach is similar to that used for a conventional airplane, although the model is not so accurate, changes of stability derivatives with height are not taken into account.

Hall [17], in 1994, extended the work of Kumar, modifying the equations of motion

of the vehicle flying IGE, taking into account the influence of perturbations in pitch on the height above the surface. Unlike Gera [16], Hall took into account also the variation of the derivatives of lift coefficient (C_L) and drag coefficient (C_D) with respect to the height above the surface.

More recently, Chun and Chang [4] evaluated the stability derivatives for a 20 passenger WIG vehicle, based on wind tunnel results together with a vortex lattice method code. Using the work of Kumar and Staufenbiel, the static and dynamic stability characteristics have been investigated, demonstrating the validity of the approach developed so far in the West.

2.3 Planing craft

Research on high speed planing started in the early twentieth century in order to design seaplanes. Later, this research focused on applications to design planing boats and hydrofoil craft. Between 1960's and 1990's, many experiments have been carried out and new theoretical formulations proposed.

Savitsky [43] carried out an extensive experimental program on prismatic planing hulls and obtained some empirical equations to calculate forces and moments acting on planing vessels. He also provided simple computational procedures to calculate the running attitude of the planing craft (trim angle, draft), power requirements and also the stability characteristics of the vehicle.

Martin [28] derived a set of equations of motion for the surge, pitch and heave degrees of freedom and demonstrated that surge can be decoupled from heave and pitch motion. Using the coefficients of Martin, Zarnick [59] defined a set of highly nonlinear integro-differential equations of motion, with coefficients determined by

a combination of theoretical and experimental results. Since this method obscured some of the physics, Zarnick built a nonlinear numerical simulator.

Troesch and Falzarano [53],[54] studied the nonlinear integro-differential equations of motion and carried out several experiments to develop a set of coupled ordinary differential equations with constant coefficients, suitable for modern methods of dynamic systems analysis. Troesch [19] later extended his previous work and expanded the nonlinear hydrodynamic force equations of Zarnick using Taylor series up to the third order, obtaining a form of equation of motion suitable for path following or continuation methods (e.g. [48]).

The model of Savitsky [43] has been further developed until recently [46], and it is still one of the reference methods used for the preliminary design of planing craft.

Modern motion simulation and control-oriented mathematical models start from these works to define the coordinate systems, the equations of motion and to calculate the hydrodynamic forces (see, for example [57],[58]).

2.4 'Aerodynamically Alleviated Marine Vehicles'

In 1976, Shipps [49], among other air-supported waterborne vehicle (like the SES, Surface Effect Vehicle, fig. 2.10), analyzed a new kind of race boat, known as the "tunnel hull" race boat: the two planing sponsons of the catamaran configuration act as aerodynamic end plates of the central "channel flow" or ram wing.

These race boats immediately demonstrated better performance with respect to conventional monohull race boats and a new race boat class was created. The advantages of this new configuration come from the aerodynamic lift that it generates. The additional lift from aerodynamic forces can be equal to 30-80 % of

the total weight. This means that lower hydrodynamic lift is needed, therefore a lower chine and keel wetted length and a decreased hydrodynamic drag are possible. Furthermore, the flow in the tunnel hull act as an air cushion, dampening heave and pitch oscillations. On the other hand, this aerodynamic lift can create safety and stability problem. Sometimes the craft, for example after a wave, can lose contact with the water. Generally the aerodynamic center is located upward with respect to the CG, therefore when the vehicle jumps off the water the pitch moment is unbalanced and the vehicle performs a pitch-over. More generally, Shipps believed in the possible development of air-supported waterborne vehicle, capable of better performance, and suitable for littoral warfare and other offshore scenarios.

In 1978, Ward et al. [55] published an article on the design and performance of a ram wing planing craft: the KUDU II (KUDU I was mentioned in Shipps' article). This vehicle, represented in fig. 2.8 and 2.9, can be considered an 'Aerodynamically Alleviated Marine Vehicle', since it has two planing sponsons separated by a wing section. Therefore it is a vehicle with aerodynamic and hydrodynamic surfaces, designed to obtain aerodynamic and hydrodynamic lift. In his article Ward presented the results of some trials: the KUDU II was able to run at 78 kts (about 145 km/h, 90 mph).

In 1978, Kallio [21], of the David W. Taylor Naval Ship Research and Development Center (USA), performed comparative tests between the KUDU II and the KAAMA. The KAAMA is a conventional mono hull planing craft. The data obtained during comparative trials show that the KUDU II pitch motion, in sea state 2, at about 40 to 60 knots, is about 30% to 60% lower than the conventional planing hull KAAMA pitch motion. Unfortunately the KUDU II sustained severe damages during the trials, thereafter there is little data available for comparison.

In 1996, Privalov and Kirillovikh [37] presented a design vehicle called TAP, Transport Amphibious Platform. It can be considered an hybrid vehicle. The TAP consists of two hulls, like a catamaran, and a fuselage, a wing and an aerodynamic tail in between the hulls. It moves always in contact with the water and uses an aerodynamic cushion effect, obtained by forcing the powerplant gas jets beneath the platform between the hulls. The authors assess that the advantages of the TAP are:

- high speed, compared to air cushion vehicles and ships (around 250 km/h),
- amphibious capability,
- high cargo-carrying capacity, also due to its higher weight efficiency, obtained by a more simplified structural scheme as compared to hovercraft and WIGe vehicles.

This vehicle seems to be very promising, but the authors presented only performance estimation of the TAP, without disclosing any detail on the dynamics model adopted.

In 1997, Doctors [14] proposed a new configuration called 'Ekranocat' for which he mentioned the 'aerodynamic alleviation concept'. The weight of the catamaran is alleviated by aerodynamic lift, thanks to a more streamlined superstructure than in traditional catamarans. The theoretical analysis and computed results show that reductions in total drag around 50 % can be obtained at very high speed.

In these references are presented some experimental data and theoretical and computed results on vehicles which can be classified as 'AAMV', but none of them presents a mathematical model to estimate the equilibrium attitude of the vehicle, neither a mathematical model of the system of equations of motion. The objective of this thesis is to develop such models.

Figure 2.1: Rostislav Evgenievich Alekseev, father of ekranoplans

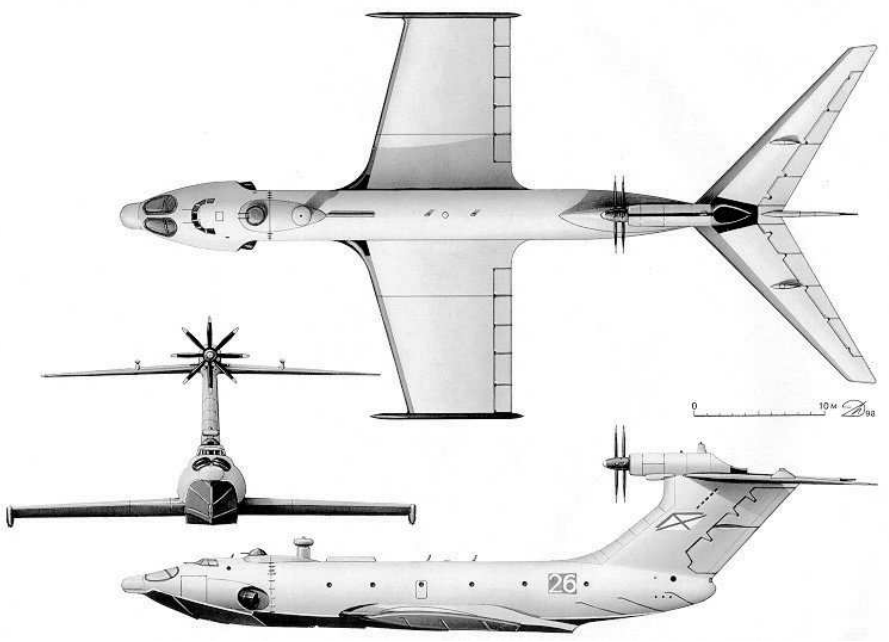

Figure 2.2: 'Orlyonok' ekranoplan, 1972

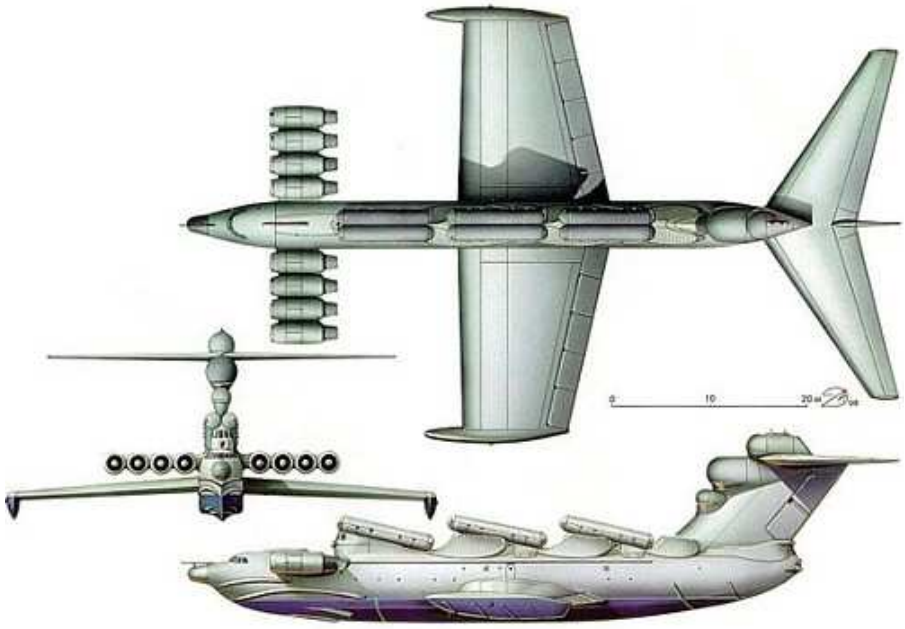

Figure 2.3: 'Lun' ekranoplan, 1980's

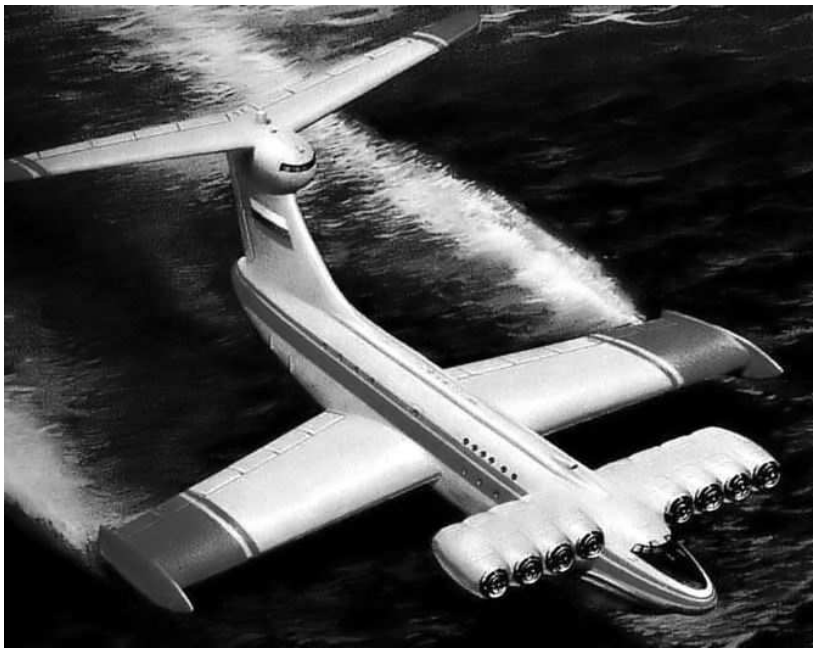

Figure 2.4: 'Spasatel' ekranoplan, 1990's

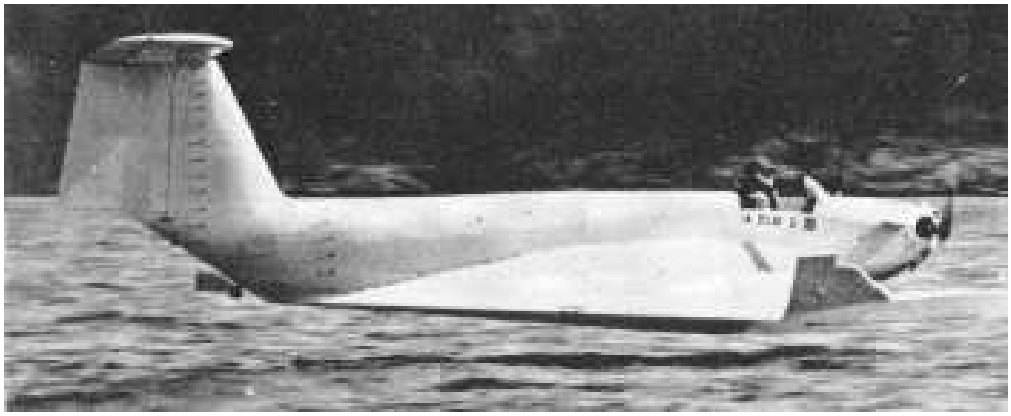

Figure 2.5: Lippisch's experimental WIGe vehicle, X-112

Figure 2.6: Lippisch's experimental WIGe vehicle, X-113

Figure 2.7: Lippisch's experimental WIGe vehicle, X-114

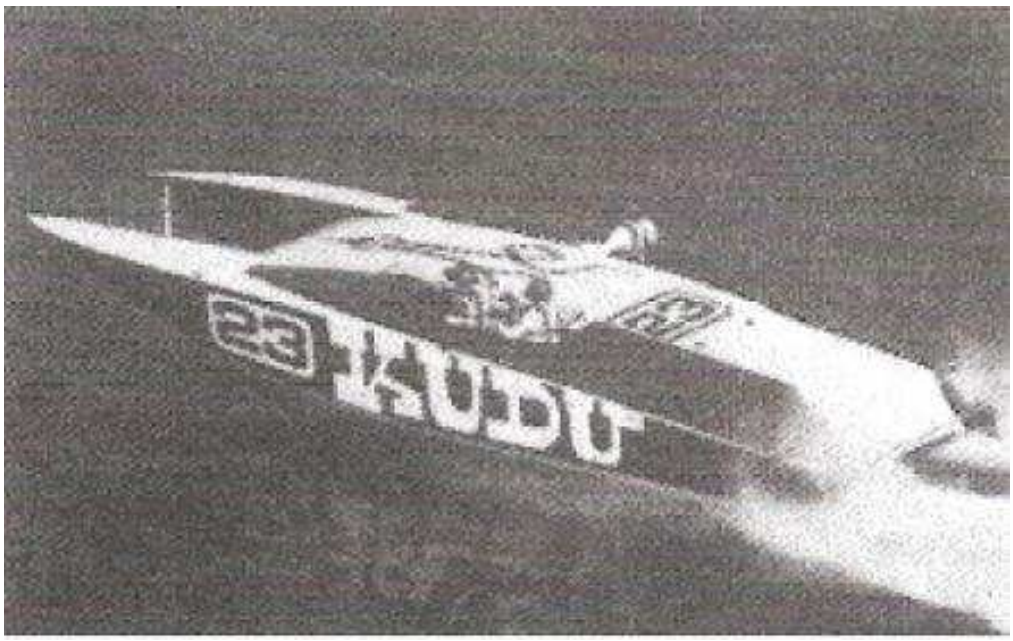

Figure 2.8: Ram wing planing craft KUDU II [55]

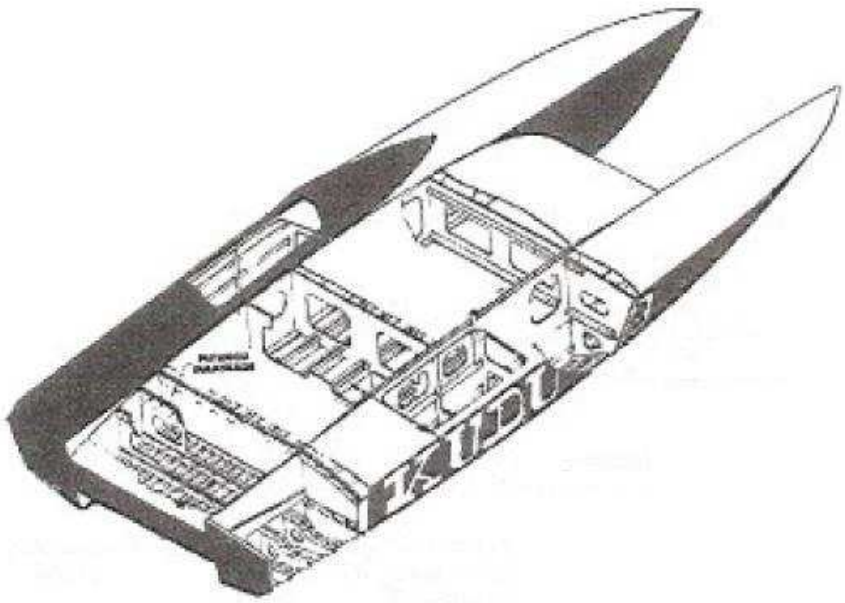

Figure 2.9: Structure of the KUDU II [55]

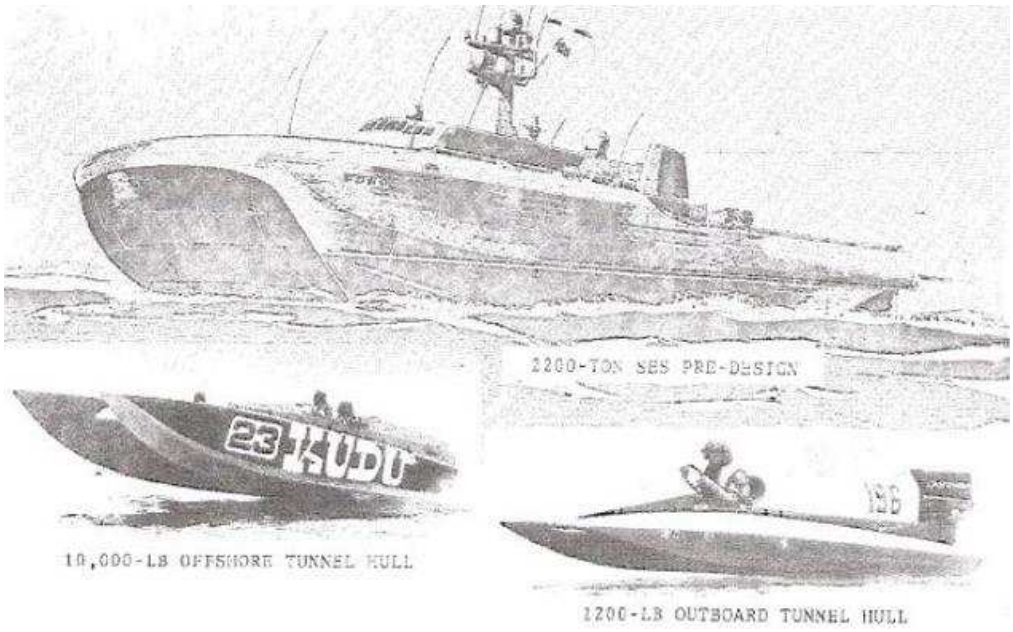

Figure 2.10: Vehicles cited in [49]

Part I

Wing In Ground Effect Vehicles and Planing Craft: Dynamics Models Numerical Implementation

Chapter 3

Wing in Ground Effect Vehicles

3.1 Introduction

The configuration of an 'Aerodynamically Alleviated Marine Vehicle (AAMV)' is still a matter of study. A possible configuration is proposed in section 5.3, and among other elements one or more aerodynamic surfaces are present. If the AAMV speed range analysed starts from zero to the maximum speed, at low speed the hydrodynamic and aerodynamic forces can be considered negligible with respect to the hydrostatic (buoyancy) force. Conversely in the present work only the speed range at which the aerodynamic and hydrodynamic forces are of the same order or of a higher order of magnitude with respect to buoyancy is analysed. Another limitation is that the AAMV is always in contact with the water, therefore the aerodynamic surfaces operate very near the water surface. Therefore it can be assumed that they are in 'wing in ground effect' (see section 2.2).

3.1.1 Methodology

In order to develop a mathematical model for the AAMV dynamics, a WIGe vehicles dynamics mathematical model is analysed and presented in this chapter,

while in chapter 4 a model of the dynamics of planing craft is discussed. In these chapters the following steps are followed:

1. review of the kinematics (geometrical aspects of motion: reference frames, variables, transformations) and the kinetics (effects of forces on the motion: rigid-body dynamics, forces and moments) used in the literature,

2. investigation of the approaches developed to define a control-oriented mathematical model,

3. development of a wing-in-ground effect (WIGe) vehicle (and planing craft) computer based simulation.

The validity of simulations has been checked against data presented in the literature.

3.2 WIGe vehicle model of dynamics

3.2.1 References

Starting from [24], [25], [52], [17], [4] and [12] a linear mathematical model of the longitudinal plane dynamics of a wing in ground effect vehicle is adopted, in the frame of the small disturbances approach. The model is implemented in MATLAB.

3.2.2 Mathematical model

The mathematical model adopted is the system of equations of motion, for the longitudinal plane, developed in the small disturbance framework, for a WIGe vehicle. It differs from the longitudinal system of equations of motion for conventional airplanes, since it takes into account also the influence of the height above the surface on aerodynamic forces.

The small disturbances framework analysis starts from an equilibrium state: this equilibrium state is a 'Rectilinear Uniform Level Motion (RULM)'. This means that the equilibrium state is characterized by a rectilinear trajectory, without any acceleration, and at constant height above the surface.

3.2.2.1 Axis system

To describe the motion of a WIGe vehicle and the forces acting on it, a number of different axis systems are used. Starting from the axis systems used by, for example, Chun and Chang [4], an earth-axis system and two body-axis system are presented below. They are all right-handed and orthogonal as represented in fig. 3.1.

Body-axis systems

The origin O is the center of gravity (CG) position of the WIGe vehicle in equilibrium state. The x and z axis lay in the longitudinal plane of symmetry, x positive forward and z positive downward. The direction of the x-axis depends on the body-axis system. Two are considered:

- **Aerodynamic axes ($\eta_1 \mathbf{O} \eta_3$)**, the direction of the x-axis η_1 being parallel to the steady forward velocity V_0,

- **Geometric axes** ($\xi O\varsigma$), the direction of the x-axis ξ being parallel to a convenient geometric longitudinal datum.

Aerodynamic axes are called wind or wind-body axes in UK and stability axes in USA. Usually the stability derivatives are calculated in this axis system.

Earth-axis systems (xOz)

The direction of the axes are fixed in space. The z-axis is directed vertically downward, the x-axis is directed forwards and parallel to the undisturbed waterline and the origin at the undisturbed waterline level.

3.2.2.2 Longitudinal linearized equations of motion

$$[A]\,\underline{\ddot{\eta}} + [B]\,\underline{\dot{\eta}} + [C]\,\underline{\eta} + [D]h = \mathbf{0} \tag{3.1}$$

where

$$\underline{\eta} \;=\; \begin{bmatrix} \eta_1 \\ \eta_3 \\ \eta_5 \end{bmatrix}$$

and h is the (perturbated) height above the waterline.

The matrix [A] is the sum of the mass matrix and the aerodynamic "added mass" terms (usually in aerodynamics they are not called added mass terms, but simply "acceleration derivatives").

$$[A] = \begin{bmatrix} m & -X^a_{\ddot{\eta}_3} & 0 \\ 0 & m - Z^a_{\ddot{\eta}_3} & 0 \\ 0 & -M^a_{\ddot{\eta}_3} & I_{55} \end{bmatrix} = \begin{bmatrix} m & A_{13} & 0 \\ 0 & m + A_{33} & 0 \\ 0 & A_{53} & I_{55} \end{bmatrix} \tag{3.2}$$

[B] is the damping matrix and is defined as:

$$[B] = \begin{bmatrix} -X^a_{\dot{\eta}_1} & -X^a_{\dot{\eta}_3} & -X^a_{\dot{\eta}_5} \\ -Z^a_{\dot{\eta}_1} & -Z^a_{\dot{\eta}_3} & -Z^a_{\dot{\eta}_5} - mV_0 \\ -M^a_{\dot{\eta}_1} & -M^a_{\dot{\eta}_3} & -M^a_{\dot{\eta}_5} \end{bmatrix} = \begin{bmatrix} B_{11} & B_{13} & B_{15} \\ B_{31} & B_{33} & B_{35} - mV_0 \\ B_{51} & B_{53} & B_{55} \end{bmatrix} \tag{3.3}$$

[C] is the restoring matrix and is defined as:

$$[C] = \begin{bmatrix} 0 & 0 & -mg \\ 0 & 0 & 0 \\ 0 & 0 & 0 \end{bmatrix} \tag{3.4}$$

The matrix [D] represents the wing in ground effect, to take into account the influence of the height above the surface on the aerodynamic forces.

$$[D] = \begin{bmatrix} -X_h^a \\ -Z_h^a \\ -M_h^a \end{bmatrix} = \begin{bmatrix} D_{10} \\ D_{30} \\ D_{50} \end{bmatrix} \tag{3.5}$$

3.2.2.3 Cauchy or state space form

By defining a state space vector $\underline{\nu}$ as

$$\underline{\nu} = \begin{bmatrix} \dot{\eta}_1 & \dot{\eta}_3 & \dot{\eta}_5 & \eta_5 & \eta_0 \end{bmatrix}^T \tag{3.6}$$

the system of equations (3.1) can be transformed in the Cauchy standard form (or state-space form). The state space vector has five variables while the system of equations (3.1) has only 3 equations. The remaining 2 equations are:

$$\begin{cases} \frac{\partial(\eta_5)}{\partial\, t} = \dot{\eta}_5 \\ \\ \frac{\partial(h)}{\partial t} = -\dot{\eta}_3 + V_0\, \eta_5 \end{cases} \tag{3.7}$$

Therefore the system is:

$$[A_{SS}]\dot{\underline{\nu}} = [B_{SS}]\, \underline{\nu} \tag{3.8}$$

where

$$[A_{SS}] = \begin{bmatrix} [A] & [0]_{3x2} \\ [0]_{2x3} & \begin{matrix} 1 & 0 \\ 0 & 1 \end{matrix} \end{bmatrix} \tag{3.9}$$

and

$$[B_{SS}] = \begin{bmatrix} & & -mg & \\ -[B] & & 0 & -[D] \\ & & 0 & \\ 0 & 0 \quad 1 & 0 & 0 \\ 0 & -1 \quad 0 & V_0 & 0 \end{bmatrix} \tag{3.10}$$

The system of equations of motion in state-space form is:

$$\underline{\dot{\nu}} = [H]\,\underline{\nu} \tag{3.11}$$

where

$$[H] = [A_{SS}]^{-1} \quad [B_{SS}] \tag{3.12}$$

3.2.2.4 Modes of oscillation

Once obtained the state space matrix $[H]$, it is possible to solve eq. 3.11 with a Fourier transformation:

$$\begin{aligned} \underline{\dot{\nu}} &= [H]\,\underline{\nu} \\ s \cdot \underline{\nu} &= [H]\,\underline{\nu} \\ (s \cdot [I]_{5*5} - [H])\ \underline{\nu} &= [0]_{5*1} \end{aligned} \tag{3.13}$$

that is, excluding the trivial solution $\underline{\nu} = [0]_{5*1}$:

$$\mathbf{det}\ (s \cdot [I]_{5*5} - [H]) \ = \ 0 \tag{3.14}$$

It gives the polynomial characteristic of the form:

$$A * s^5 + B * s^4 + C * s^3 + D * s^2 + E * s + F = 0 \tag{3.15}$$

The polynomial characteristic coefficients A, B, C, D, E, F are illustrated in Delhaye [12]. The roots of the modes of oscillation of the WIGe vehicle can be obtained solving the characteristic polynomial.

$$\begin{cases} s_{1,2} &= a_1 \pm i \cdot b_1 \\ s_{3,4} &= a_2 \pm i \cdot b_2 \\ s_5 &= a_3 \end{cases} \tag{3.16}$$

For a conventional airplane, the analysis of the longitudinal plane dynamics leads to a characteristic polynomial of the 4th degree, and the solution consists only in the two pair of complex roots. These two roots corresponds to the well known:

- phugoid motion, a low frequency long period oscillation mode, with an oscillation of forward speed, pitch angle and heave position,
- small period pitching oscillation (SPPO), a high frequency small period oscillation mode in pitch.

Since the WIGe vehicle dynamics is characterized by a fifth degree characteristic polynomial, the solution comprehends an additional root, with only the real part (imaginary part is equal to zero). This root represents the influence of the wing in ground phenomenon on both phugoid and SPPO oscillation modes, also if the

effect on the phugoid motion is more pronounced than the effect on the SPPO. This effect is due to the air cushion created between the ground and the wing flying in ground effect, since it acts like a pneumatic dampener.

3.3 Numerical implementation

The program starts from an extended markup language file (xml) as input file: this format has been chose due to its simplicity and adaptability. It contains all the information about the characteristics of the air, the motion, and the geometrical, inertial and dynamical characteristics of the vehicle. Its structure is illustrated in fig. 3.2, and all the elements are illustrated in tab. 3.1 and tab. 3.2.

A MATLAB program uses the xml input data file to calculate the state space matrix $[H]$ of eq. 3.12. The mathematical method to estimate the matrix $[H]$ for WIGe vehicles is available in the literature (for example [12] [4]), and the equations to derive the aerodynamic stability derivatives, starting from the aerodynamic coefficients, is illustrated in appendix A.

Once obtained the state space matrix $[H]$ it is possible to calculate the roots of the modes of oscillation (eq. 3.16) as previously illustrated.

Using the MATLAB algorithm 'ode45' to solve ordinary differential equations of motion, the program can also estimate the WIGe vehicle time response to an external disturbance.

Table 3.1: Input data of the WIGe vehicles: xml file structure (1)

Branch of the tree	Name	Description
medium	g_e $[m\,s^{-2}]$	gravitational constant
”	rho $[kg\,m^{-3}]$	air density
motion	V_e $[m\,s^{-1}]$	steady forward velocity
”	heights $[m]$	height(s) above the surface
”	alpha_e $[deg]$	angle of attack at equilibrium
vehicle		
geometry	mac $[m]$	mean aerodynamic chord
”	S $[m^2]$	wing planform area
”	l_T $[m]$	longitudinal tail arm
”	S_T $[m^2]$	tail planform area
inertial	m_e $[kg]$	mass at equilibrium
”	I_y $[kg\,m^2]$	pitch moment of inertia
dynamics		
stabDer	type	dimensional, aeronormalized, dynanormalized, calculated
”	axes	body axes, wind-stability axes
”	X_h	X force der. wrt height
”	X_u,w,q	X der. wrt surge, heave, pitch velocity
”	X_dw	X der. wrt heave acceleration
”	Z_h	Z force der. wrt height
”	Z_u,w,q	Z der. wrt surge, heave, pitch velocity
”	Z_dw	Z der. wrt heave acceleration
”	M_h	M moment der. wrt height
”	M_u,w,q	M der. wrt surge, heave, pitch velocity
”	M_dw	M der. wrt heave acceleration

Table 3.2: Input data of the WIGe vehicles: xml file structure (2)

Branch of the tree	Name	Description
vehicle		
dynamics		
coefficients		
aerodynamic	C_L	lift coefficient
”	C_LV	lift coeff. der. wrt velocity
”	C_Lalpha	lift coeff. der. wrt AoA
”	C_Lhc	lift coeff. der. wrt height/chord
”	C_D	drag coefficient
”	C_DV	drag coeff. der. wrt velocity
”	C_Dalpha	drag coeff. der. wrt AoA
”	C_Dhc	drag coeff. der. wrt height/chord
”	C_mV	moment coeff. der. wrt velocity
”	C_malpha	mom. coeff. der. wrt AoA
”	C_mhc	mom. coeff. der. wrt height/chord
”	C_LTalpha	tail lift coeff. der. wrt AoA
”	eps_alpha	downwash derivative at tailplane
wing-bodyContr	Z_qWB	body contribution to Z_q
”	M_qWB	body contribution to M_q
”	M_dwWB	body contribution to M_dw
thrust	T_V	thrust force derivative wrt velocity

3.4 Validation

The WIGe dynamics mathematical program has been validated against experimental and numerical data available in literature.

In 1997 Delhaye [12] developed a numerical model to simulate the dynamics of the 'Orlyonok A-90' ekranoplan. With this model the numerical values of the roots in eq. 3.16 have been estimated. It is shown as a new mode appears, the so called 'subsidence mode', and as the phugoid motion is altered by the wing in ground effect. In fig. 3.3 the roots of the A-90 calculated by the author and by Delhaye are compared. Agreement between the two numerical results are good, although there are small discrepancies for the SPPO roots, in particular for the imaginary part of the root (the values of b in eq. 3.16).

In 2002 Chun and Chang [4] investigated the static and dynamic stability of a 20 passenger WIGe vehicle. They conducted wind tunnel tests to estimate the aerodynamic coefficients to calculate the stability derivatives of the WIGe vehicle. With these data the characteristic roots for two heights above the surface have been calculated. As it can be seen in fig. 3.4, the accord between the present work and the roots estimated by Chun and Chang is good for both heights above the surface. It can be observed how, approaching the ground (h/c is the height above the surface divided by the aerodynamic chord of the wing), the influence of the wing in ground effect is similar to the Orlyonok A-90; that is

- the small period pitching oscillation frequency increases,
- the phugoid frequency increases.

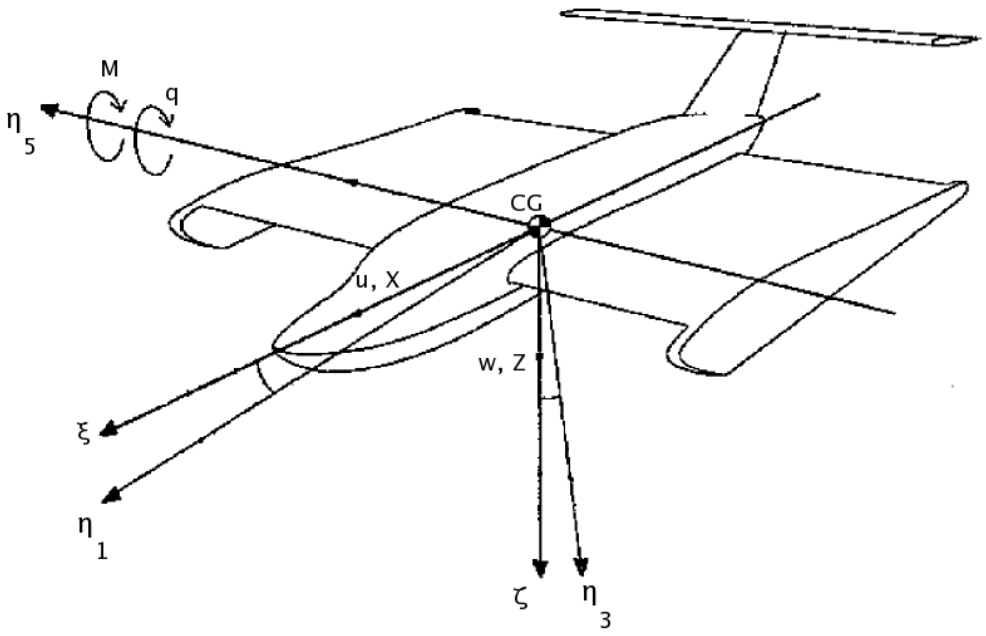

Figure 3.1: Axis systems used in the WIGe vehicle mathematical model

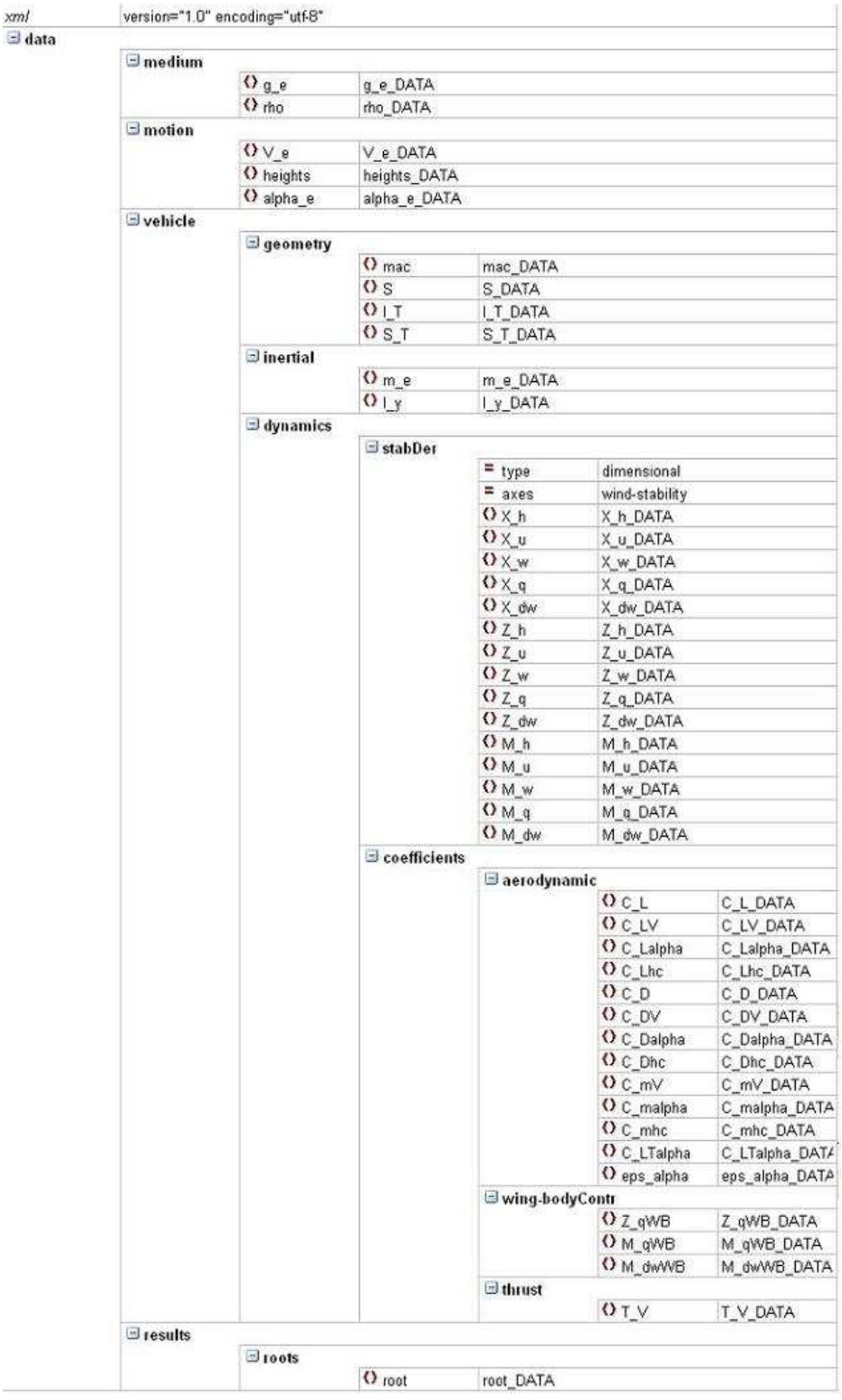

Figure 3.2: Xml input data structure of the WIGe vehicles simulation program

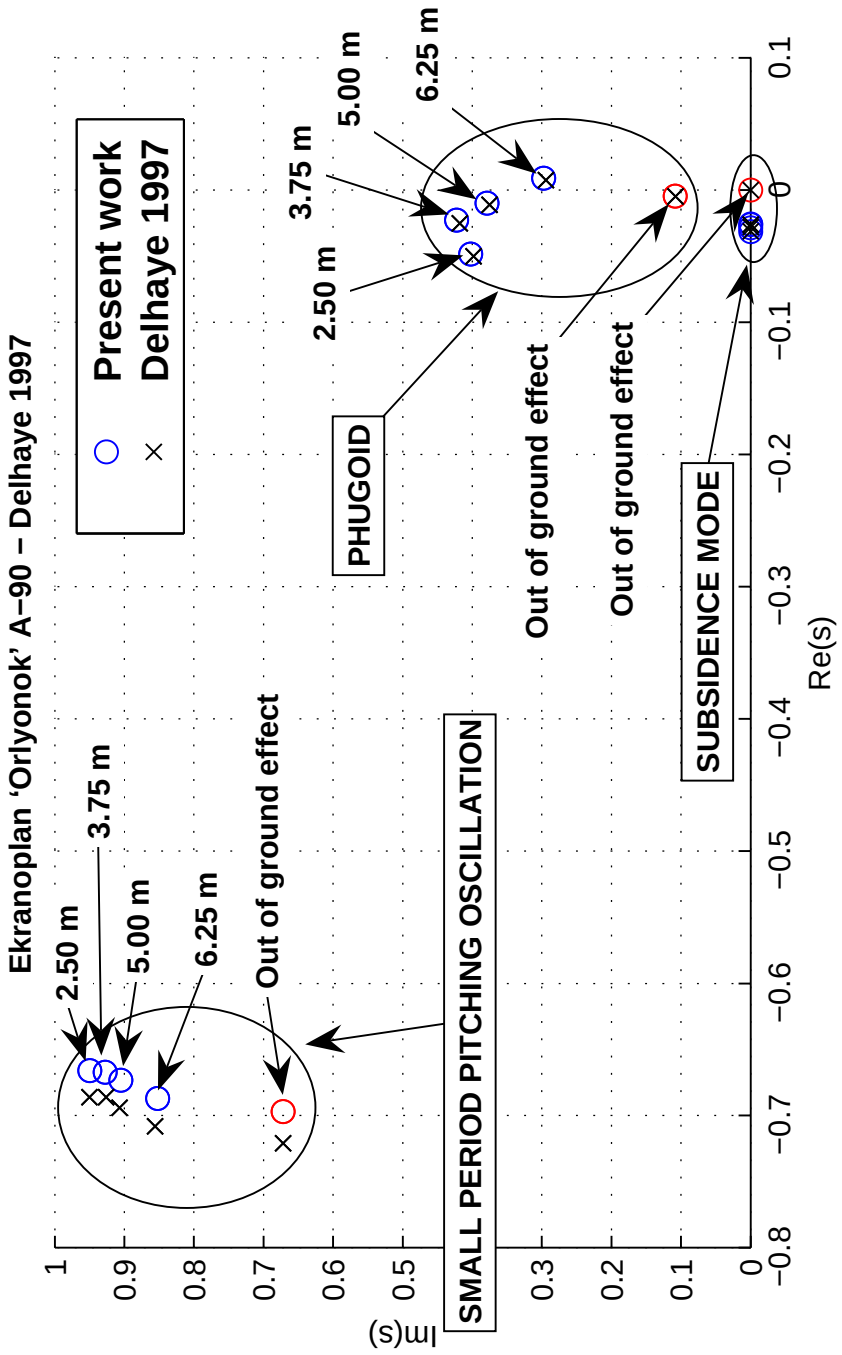

Figure 3.3: WIGe vehicle Orlyonok A-90 roots: Delhaye [12] vs Collu

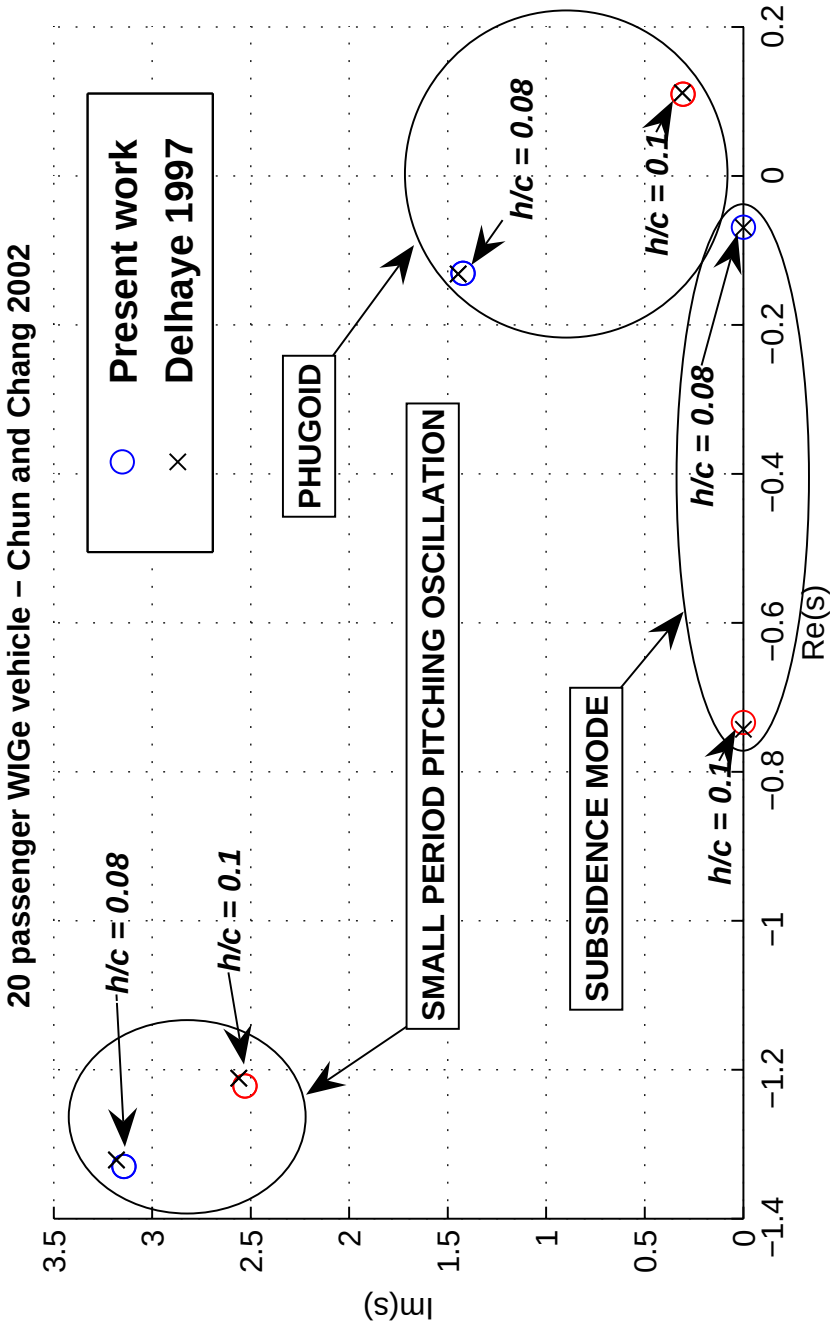

Figure 3.4: WIGe 20 passenger vehicle roots: Chun & Chang [4] vs Collu

Chapter 4

Planing Craft

4.1 Introduction

As previously mentioned in chapter 3, the AAMV configuration has not been fixed. The author proposes a possible configuration in section 5.3. The hydrodynamic surface of this AAMV configuration consists of a rigid, high speed, prismatic planing hull.

4.1.1 Prismatic planing hull

A prismatic planing hull is shown in fig. 4.1. It is characterized, geometrically, by only two parameters:

- B, the width of the planing hull,
- β, the deadrise angle.

Modern planing craft do not use this simple geometry. Variable deadrise angles, round bilges, two or three chines, spray rails, stepped hulls and others solutions are

used to enhance the performance of the high speed marine vehicle. Nonetheless the simple geometry illustrated in fig. 4.1 is the reference model used by the Savitsky method [43](see section 2.3), and this method is still widely used to estimate the performance of modern planing craft, in the preliminary design phase. For this reason the author used the constant deadrise, v-shaped, one chine simple geometry adopted in this model.

4.1.2 Methodology

In order to implement a numerical method to analyse the dynamics of a planing craft, the same approach presented for WIGe is adopted, and it consists of the following steps:

1. review of the kinematics (geometrical aspects of motion: reference frames, variables, transformations) and the kinetics (effects of forces on the motion: rigid-body dynamics, forces and moments) used in the literature,

2. investigation of the approaches already developed to derive a control-oriented mathematical model,

3. development of a planing craft (PC) computer based simulation.

There is a difference between the approach used in the previous chapter to analyze WIGe vehicles and the approach presented here. For WIGe vehicles, a model to estimate the modes of oscillation characteristics of this vehicle are illustrated. That analysis starts from a given equilibrium state, which is specified in the xml input file. This is due to the fact that the equilibrium state attitude, for an airplane as well as for a WIGe vehicle, can be set by designers in the design phase. For example, the angle of attack at a given speed can be chosen by setting

the position of the tail horizontal surfaces (elevators). Conversely, planing craft do not have a control device similar to the tail horizontal surface of airplanes and WIGe vehicles. Therefore the equilibrium attitude of the PC has to be calculated. For these reason the implemented PC model of dynamics consists of two programs:

- the first program estimates the equilibrium state attitude,
- the second program, starting from the calculated equilibrium state characteristics, derives the roots of the characteristic polynomial.

The validity of these programs is checked against data presented in the literature.

4.2 Planing craft models of dynamics

4.2.1 References

The equilibrium attitude estimation model adopted in this work is based on the Savitsky method for prismatic planing hull [43] [46]. It is a semi-empirical mathematical model, which starts from the geometrical and inertial characteristics of the planing craft at a certain speed, and it estimates the equilibrium attitude. A thorough mathematical analysis of the Savitsky method can be found in Doctors [13].

Once the equilibrium attitude of a given PC configuration at a certain speed is estimated, it is possible to analyse the PC stability in the small disturbances framework. The PC system of equations of motion has been investigated by many authors, and in this work the mathematical methods of Martin [28], Troesch and Falzarano [53] [54], and Faltinsen [15] have been adopted.

4.2.2 Equations of equilibrium model

4.2.2.1 Hypotheses

As for the WIGe vehicle model, the present model concentrates on the analysis of an equilibrium state characterized by a rectilinear trajectory and a constant speed. The vehicle is supposed to be always in contact with the water, and in a calm water situation. Waves are not taken into account.

4.2.2.2 Forces and moments analysis

The forces and moments acting on the vehicle are illustrated in fig. 4.2. They can be divided into four groups:

- gravitational force (weight, W),
- thrust force (propulsion force, T),
- aerodynamic force(aerodynamic drag of the section of the hull above the surface, D_{ah}),
- hydrodynamic forces (potential force, N, frictional force, D_F, whisker spray drag, D_{ws}).

The weight (W) acts at the center of gravity (CG), which is also the origin of the body-fixed axis system (CG coordinates are (0,0)). Thrust acts at the thrust point (TP), in a direction determined by the angle ϵ, the angle between the direction of the thrust and the keel, positive for an anticlockwise movement (view from the starboard side of the vehicle). The dry section of the hull experiences an

aerodynamic drag force (D_{ah}). To evaluate its contribution, Savitsky [46] proposes the expression:

$$D_{ah} = \frac{1}{2}\rho_h V_0^2 A_h c_{D,ah} \tag{4.1}$$

where A_h is the frontal area of the planing hull, and $c_{D,ah}$ is the aerodynamic drag coefficient of the hull (approximated as 0.70). Since it is not known where the hull aerodynamic drag acts, D_{ah} is supposed to be acting on the CG. Therefore no moment is generated by this force. Hydrodynamic forces are the potential force N, the friction force D_F, and the whisker spray drag D_{ws}. The potential force direction is supposed to be normal to the keel and acting at the hydrodynamic center HC. The friction force acts parallel to the keel line, half height between the keel and the chine line. The whisker spray drag is assumed to act through the CG of the HV.

All the expressions to evaluate these forces are presented by Doctors in [13].

4.2.2.3 System of equations of equilibrium

Once all the forces and moments are known, a system of equations of equilibrium can be developed. The vehicle, in the longitudinal plane, has three degrees of freedom, and a system of three equations of equilibrium is needed. The system is:

- surge equation: sum of the horizontal forces equals 0,

$$-D_{ah} - N\,sin(\tau) - D_F\,cos(\tau) - D_{ws} + T\,cos(\tau + \epsilon) = 0 \tag{4.2}$$

- heave equation: sum of vertical forces equals 0,

$$N\,cos(\tau) - D_F\,sin(\tau) - W + T\,sin(\tau + \epsilon) = 0 \tag{4.3}$$

- pitch equation: sum of pitch moments equals 0.

$$D_{ah}\,a_{ah} + D_{ws}\,a_{ws} - N\,c - D_F\,a + T\,[\xi_{TP}\,sin(\epsilon) + \zeta_{TP}\,cos(\epsilon)] = 0 \tag{4.4}$$

The CG of the PC is chosen as point of reference for pitch moments.

The surge equation 4.2 states that the sum of the aerodynamic drag, the component of potential and friction hydrodynamic forces parallel to the velocity, and the whisker spray drag has to be equal to the component of the thrust parallel to the velocity.

The heave equation 4.3 states that the sum of the vertical components of the potential and friction hydrodynamic force and the vertical component of the thrust has to be equal to the weight of the PC.

The pitch moment equation 4.4 states that the sum of the aerodynamic moments, hydrodynamic moments and the moment generated by the thrust force has to be equal to zero.

Savitsky proposes an iterative cycle to solve this system of equations of motion, since there are n+1 variables with n equations. The cycle starts guessing a trim angle, then eq. 4.2, eq. 4.3 and eq. 4.4 are evaluated. If all the three balances are fulfilled, the guessed trim angle will be the equilibrium trim angle. If not, another cycle will be required, changing the value ot the guessed trim angle.

4.2.3 Equations of motion model

The mathematical model adopted is the system of equations of motion, for the longitudinal plane, developed in the small disturbance framework, presented by Martin [28].

4.2.3.1 Axis system

To describe the motion of a PC configuration, the same system used for WIGe vehicles is adopted. The reason is that the equations of motion models for WIGe and PC vehicles are analyzed as a basis of the AAMV equations of motion. Therefore it is appropriate to use a common mathematical framework.

Body-axis systems The origin O is taken to be coincident with the center of gravity (CG) position of the PC in equilibrium state. The x and z axis lay in the longitudinal plane of symmetry, x positive forward and z positive downward. The direction of the x-axis depends on the body-axis system. Two are considered:

- **Hydrodynamic axes ($\eta_1 \mathbf{O} \eta_3$)**, the direction of the x-axis η_1 being parallel to the steady forward velocity V_0,
- **Geometric axes** ($\xi \mathrm{O} \varsigma$), the direction of the x-axis ξ being parallel to a convenient geometric longitudinal datum, in our case the keel.

Earth-axis systems (xOz)

The direction of the axes are fixed in space. The z-axis is directed vertically downward, the x-axis is directed forwards and parallel to the undisturbed waterline and the origin at the undisturbed waterline level.

4.2.3.2 Longitudinal linearized equations of motion

$$[A]\,\underline{\ddot{\eta}} + [B]\,\underline{\dot{\eta}} + [C]\,\underline{\eta} = \mathbf{0} \tag{4.5}$$

where

$$\underline{\eta} = \begin{bmatrix} \eta_1 \\ \eta_3 \\ \eta_5 \end{bmatrix}$$

The matrix [A] is the sum of the mass matrix and the hydrodynamic added mass derivatives.

$$\begin{aligned} [A] &= \begin{bmatrix} m - X^h_{\ddot{\eta}_1} & -X^h_{\ddot{\eta}_3} & -X^h_{\ddot{\eta}_5} \\ -Z^h_{\ddot{\eta}_1} & m - Z^h_{\ddot{\eta}_3} & -Z^h_{\ddot{\eta}_5} \\ -M^h_{\ddot{\eta}_1} & -M^h_{\ddot{\eta}_3} & I_{55} - M^h_{\ddot{\eta}_5} \end{bmatrix} = \\ &= \begin{bmatrix} m + A_{11} & A_{13} & A_{15} \\ A_{31} & m + A_{33} & A_{35} \\ A_{51} & A_{53} & I_{55} + A_{55} \end{bmatrix} \end{aligned} \tag{4.6}$$

[B] is the damping matrix and is defined as:

$$
\begin{aligned}
[B] &= \begin{bmatrix} -X^h_{\dot{\eta}_1} & -X^h_{\dot{\eta}_3} & -X^h_{\dot{\eta}_5} \\ -Z^h_{\dot{\eta}_1} & -Z^h_{\dot{\eta}_3} & -Z^h_{\dot{\eta}_5} \\ -M^h_{\dot{\eta}_1} & -M^h_{\dot{\eta}_3} & -M^h_{\dot{\eta}_5} \end{bmatrix} = \\
&= \begin{bmatrix} B_{11} & B_{13} & B_{15} \\ B_{31} & B_{33} & B_{35} \\ B_{51} & B_{53} & B_{55} \end{bmatrix}
\end{aligned} \tag{4.7}
$$

[C] is the restoring matrix and is defined as:

$$
\begin{aligned}
[C] &= \begin{bmatrix} 0 & -X^h_{\eta_3} & -mg - X^h_{\eta_5} \\ 0 & -Z^h_{\eta_3} & -Z^h_{\eta_5} \\ 0 & -M^h_{\eta_3} & -M^h_{\eta_5} \end{bmatrix} = \\
&= \begin{bmatrix} 0 & C_{13} & -mg + C_{15} \\ 0 & C_{33} & C_{35} \\ 0 & C_{53} & C_{55} \end{bmatrix}
\end{aligned} \tag{4.8}
$$

4.2.3.3 Cauchy or state space form

By defining a state space vector $\underline{\nu}$ as

$$\underline{\nu} = \left[\begin{array}{ccccc} \dot{\eta_1} & \dot{\eta_3} & \dot{\eta_5} & \eta_3 & \eta_5 \end{array} \right]^T \tag{4.9}$$

the system of equations (4.5) can be transformed in the Cauchy standard form (or state-space form). The state space vector has five variables while the system of equations (4.5) has only 3 equations. The remaining 2 equations are:

$$\left\{ \begin{array}{rcl} \frac{\partial(\eta_3)}{\partial\, t} & = & \dot{\eta_3} \\ \\ \frac{\partial(\eta_5)}{\partial\, t} & = & \dot{\eta_5} \\ \\ \end{array} \right. \tag{4.10}$$

Therefore the system is:

$$[A_{SS}]\dot{\underline{\nu}} = [B_{SS}]\,\underline{\nu} \tag{4.11}$$

where

$$[A_{SS}] = \left[\begin{array}{ccc} [A] & [0]_{3x2} \\ \\ [0]_{2x3} & \begin{array}{cc} 1 & 0 \\ 0 & 1 \end{array} \end{array} \right] \tag{4.12}$$

and

$$[B_{SS}] = \begin{bmatrix} & & & -C_{13} & mg - C_{15} \\ & -[B] & & -C_{33} & -C_{35} \\ & & & -C_{53} & -C_{55} \\ 0 & 1 & 0 & 0 & 0 \\ 0 & 0 & 1 & 0 & 0 \end{bmatrix} \tag{4.13}$$

The system of equations of motion in state-space form is:

$$\dot{\underline{\nu}} = [H]\,\underline{\nu} \tag{4.14}$$

where

$$[H] = [A_{SS}]^{-1} \quad [B_{SS}] \tag{4.15}$$

4.2.3.4 Reduced order system - equations of motion

As demonstrated by Martin [28], the longitudinal system of equations of motion can be decoupled in two separated systems of equations : first the surge motion, second the heave and pitch motions. This is due to the fact that the stability derivatives in the surge equation are considerably smaller than the stability derivatives in the pitch and heave equation. This hypothesis has been adopted by Troesch and Falzarano [53] [54], and Faltinsen [15].

Adopting this hypothesis, the reduced order longitudinal system of equations of motion is as follow.

$$[A]\,\ddot{\underline{\eta}} + [B]\,\dot{\underline{\eta}} + [C]\,\underline{\eta} = \mathbf{0} \tag{4.16}$$

where

$$\underline{\eta} = \begin{bmatrix} \eta_3 \\ \eta_5 \end{bmatrix}$$

The matrix [A] is the sum of the mass matrix and the hydrodynamic added mass derivatives.

$$\begin{aligned} [A] &= \begin{bmatrix} m - Z^h_{\ddot{\eta}_3} & -Z^h_{\ddot{\eta}_5} \\ -M^h_{\ddot{\eta}_3} & I_{55} - M^h_{\ddot{\eta}_5} \end{bmatrix} = \\ &= \begin{bmatrix} m + A_{33} & A_{35} \\ A_{53} & I_{55} + A_{55} \end{bmatrix} \end{aligned} \tag{4.17}$$

[B] is the damping matrix and is defined as:

$$\begin{aligned} [B] &= \begin{bmatrix} -Z^h_{\dot{\eta}_3} & -Z^h_{\dot{\eta}_5} \\ -M^h_{\dot{\eta}_3} & -M^h_{\dot{\eta}_5} \end{bmatrix} = \\ &= \begin{bmatrix} B_{33} & B_{35} \\ B_{53} & B_{55} \end{bmatrix} \end{aligned} \tag{4.18}$$

[C] is the restoring matrix and is defined as:

$$
\begin{aligned}
[C] &= \begin{bmatrix} -Z^h_{\eta_3} & -Z^h_{\eta_5} \\ \\ -M^h_{\eta_3} & -M^h_{\eta_5} \end{bmatrix} = \\
&= \begin{bmatrix} C_{33} & C_{35} \\ \\ C_{53} & C_{55} \end{bmatrix}
\end{aligned}
\tag{4.19}
$$

4.2.3.5 Reduced order system - state space form

By defining a state space vector $\underline{\nu}$ as

$$
\underline{\nu} = \begin{bmatrix} \dot{\eta_3} & \dot{\eta_5} & \eta_3 & \eta_5 \end{bmatrix}^T \tag{4.20}
$$

the system of equations (4.16) can be transformed in the Cauchy standard form (or state-space form). The state space vector has four variables while the system of equations (4.16) has only 2 equations. The remaining 2 equations are:

$$
\begin{cases} \frac{\partial(\eta_3)}{\partial\, t} = \dot{\eta_3} \\ \\ \frac{\partial(\eta_5)}{\partial\, t} = \dot{\eta_5} \\ \\ \end{cases}
\tag{4.21}
$$

Therefore the system is:

$$
[A_{SS}]\dot{\underline{\nu}} = [B_{SS}]\,\underline{\nu} \tag{4.22}
$$

where

$$[A_{SS}] = \begin{bmatrix} [A] & [0]_{2x2} \\ [0]_{2x2} & \begin{matrix} 1 & 0 \\ 0 & 1 \end{matrix} \end{bmatrix} \tag{4.23}$$

and

$$[B_{SS}] = \begin{bmatrix} -[B] & -[C] \\ \begin{matrix} 1 & 0 \\ 0 & 1 \end{matrix} & \begin{matrix} 0 & 0 \\ 0 & 0 \end{matrix} \end{bmatrix} \tag{4.24}$$

The system of equations of motion in state-space form is:

$$\dot{\underline{\nu}} = [H]\,\underline{\nu} \tag{4.25}$$

where

$$[H] = [A_{SS}]^{-1}\ [B_{SS}] \tag{4.26}$$

4.2.3.6 Reduced order system - modes of oscillation

Once obtained the state space matrix $[H]$ in eq. 4.26, it is possible to solve eq. 4.25 with a Fourier transformation:

$$\begin{aligned} \dot{\underline{\nu}} &= [H]\,\underline{\nu} \\ s \cdot \underline{\nu} &= [H]\,\underline{\nu} \\ (s \cdot [I]_{4*4} - [H])\ \underline{\nu} &= [0]_{4*1} \end{aligned} \tag{4.27}$$

that is, excluding the trivial solution $\underline{\nu} = [0]_{4*1}$:

$$\mathbf{det}\ (s \cdot [I]_{4*4} - [H]) \ = \ 0 \tag{4.28}$$

It gives the polynomial characteristic of the form:

$$A * s^4 + B * s^3 + C * s^2 + D * s + E = 0 \tag{4.29}$$

The polynomial characteristic coefficients A, B, C, D, E can be evaluated using the expressions derived by Faltinsen in [15]. Solving the reduced order characteristic polynomial, the roots of the modes of oscillation of the PC vehicle are obtained.

$$\begin{cases} s_{1,2} \ = \ a_1 \pm i \cdot b_1 \\ s_{3,4} \ = \ a_2 \pm i \cdot b_2 \end{cases} \tag{4.30}$$

These solutions correspond to two oscillatory modes. Usually, for a conventional planing hull configuration in the planing regime, one of the solutions is much less stable than the other, if not unstable ($s_{1,2} = a_1 \pm i \cdot b_1$, with $a_1 > 0$), and characterized by a higher frequency (shorter period). These two aspects makes the second mode of oscillation, characterized by a lower frequency and a higher damping factor, almost negligible with respect to the first one. In fact, usually both in the open sea and in the towing tank test experiment, the least stable mode of oscillation occurs and is predominant with respect to the second one, to the extent that only the first one is measured, and it is called 'porpoising'.

4.3 Numerical implementation

As for the WIGe vehicles program, both the equilibrium attitude estimation program and the equations of motion program start from an extended markup language file (xml) as input data file. It contains all the informations about the characteristics of the air, the water, the speed range analyzed, and the geometrical and inertial characteristics of the planing craft configuration. Its structure is illustrated in fig. 4.3, and all the elements are illustrated in tab. 4.1.

As it can be seen, four parameters called 'computational parameters' are shown in the xml input file. To solve the system of equations of equilibrium (eq. 4.2, 4.3, 4.4), the Savitsky long-form method illustrated by Doctors in [13] has been adopted. It is an iterative method, since it is not a closed system of equations: a trim angle τ has to be guessed, then eq. 4.2, 4.3, 4.4 are checked. If they are equal to zero, the trim angle will be the equilibrium angle, if not a new trim angle will be guessed. The MATLAB program developed starts the τ cycle with $\tau =$ tau_deg_start, then τ is incremented of tau_deg_step at each step, until it reaches the value $\tau =$ tau_deg_stop. At this point the pitch moment versus τ curve is analyzed, and the equilibrium trim angle (which corresponds a moment equal to zero) is estimated with an interpolation method.

The fourth parameter, called the 'derivativesMethod', is related to the mathematical model used to estimate the stability derivatives. In literature two stability derivatives estimation methods have been found, derived by Faltinsen [15] and by Martin [28], and the parameter called 'derivativesMethod' is to choose the preferred method. As for the WIGe vehicles program, once obtained the state space matrix $[H]$ it is possible to calculate the roots of the modes of oscillation as previously illustrated, and the roots illustrated in eq. 4.30 can be obtained. Also here, using the MATLAB algorithm to solve ordinary differential equations

Table 4.1: Input data of the PC MATLAB programs: xml file structure

Branch of the tree	Name	Description
medium	g_e $[m\ s^{-2}]$	gravitational constant
”	rho_a $[kg\ m^{-3}]$	air density
”	rho_h $[kg\ m^{-3}]$	water density
”	nu_h $[m^2\ s]$	water cinematic viscosity
motion	Fn_min [ ]	Minimum Froude number
”	Fn_max [ ]	Max Froude number
”	Fn_delta [ ]	Froude number increment
vehicle		
geometry		
prop	xi_tp $[m]$	thrust point longitudinal position
”	zeta_tp $[m]$	thrust point vertical position
”	eps_deg $[deg]$	angle between keel and thrust direction
hydro	beam $[m]$	planing hull width
”	beta $[deg]$	planing hull deadrise angle
”	A_h $[m^2]$	planing hull frontal area
inertial	lcg $[m]$	CG longitudinal position (from transom)
”	vcg $[m]$	CG vertical position (from keel)
”	m $[kg]$	PC total mass
”	I_55 $[kg\ m^2]$	pitch moment of inertia
computational_parameters		
tau_deg_start $[deg]$	tau cycle - first value	
tau_deg_stop $[deg]$	tau cycle - last value	
tau_deg_step $[deg]$	tau cycle - increment	
derivativesMethod	method to estimate hydrodynamic derivatives	

of motion 'ode45', the program can also estimate the PC vehicle time response to an external disturbance.

4.4 Validation

In 2007 Savitsky, DeLorme and Datla [46] proposed a further development of the Savitsky method to estimate the equilibrium attitude of a PC. The analytical results of this method have been compared against experimental data obtained in three separate towing tank facilities. The method shows good agreement with experimental data. The analytical results obtained with the PC equilibrium attitude program here implemented have been compared against data in Savitsky, as shown in fig. 4.4, fig. 4.5, fig. 4.6, and fig. 4.7. In particular, in Savitsky four planing hull configurations have been analyzed, called here 'Savitsky PC of Tab 3, Tab 4, Tab 5, Tab 6'. These configurations are not proper prismatic planing hulls, since the deadrise angle β is not constant, and in some cases they possess more than one chine. Nonetheless the results are in good agreement through all the speed range investigated.

Only in one case, shown in fig. 4.6, the comparison between the present work and the Savitsky's method highlight a difference of about 10%. Since for the other comparisons the error is very low (fig. 4.4, 4.5, 4.7), it is possible that, in this case, Savitsky used a sligthly different tuning of some coefficients of its model. In fact, this is the only planing craft configuration where the resistance is overestimated by the Savistky method (see the resistance vs velocity graph in table 5 of [46]), and this is the only case where the roughness allowance is set at 0 rather than 0.0004, to counteract this wrong estimate.

The previous comparisons validate the equilibrium attitude program. Unfortunately, as regard the second program, the system of equations of motion program, no experimental data have been found in literature. Briefly the problem is that there are some experimental data but, being obtained in towing tank facilities and not in open sea, they have been calculated imposing a certain equilibrium attitude. On the contrary, the equations of motion program developed by the author starts from the equilibrium attitude estimated by the equilibrium attitude program here developed. Since the porpoising characteristics are strongly dependent on the initial equilibrium state, a comparison is not possible.

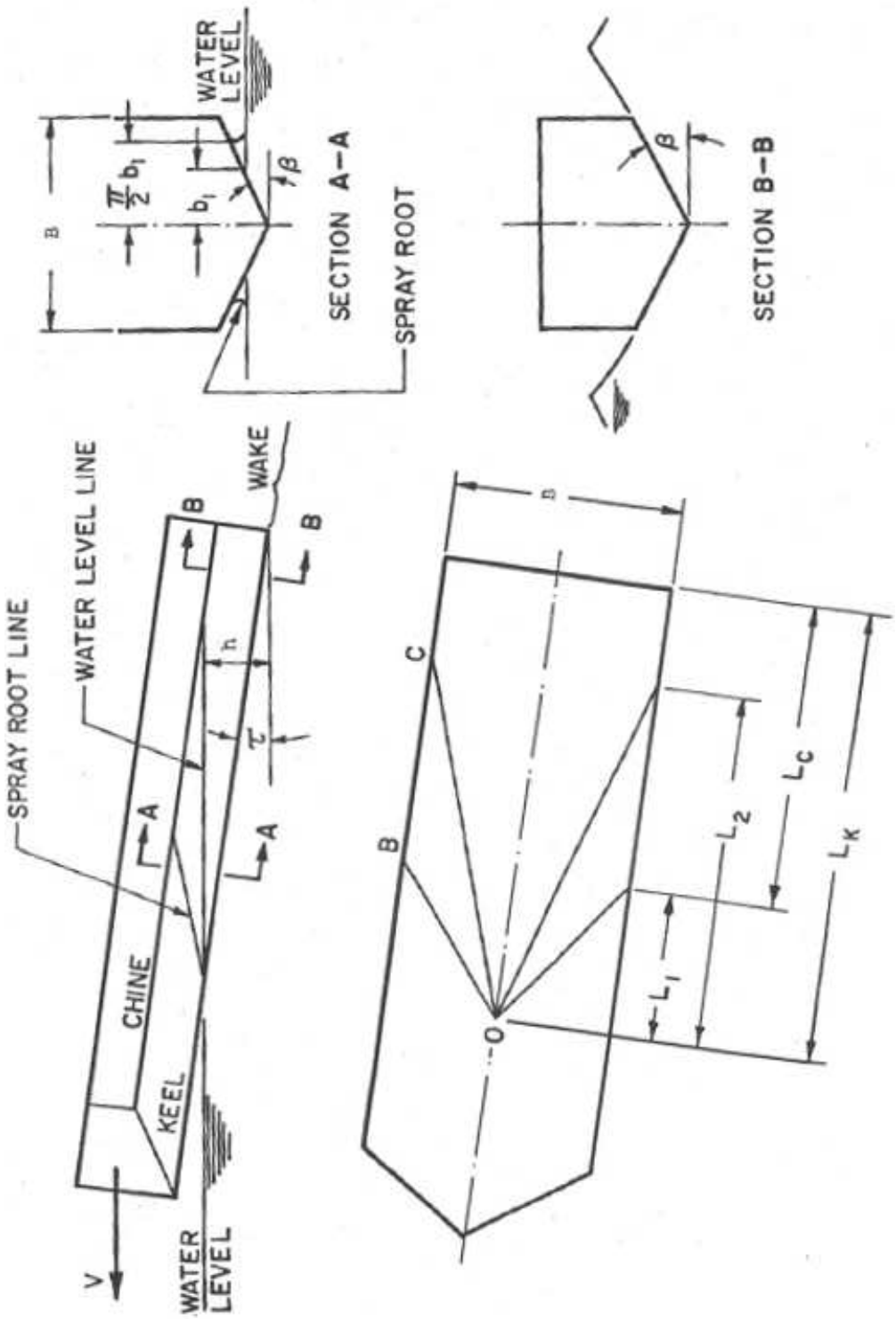

Figure 4.1: Prismatic planing hull: geometrical characteristics and Savitsky model variables [43]

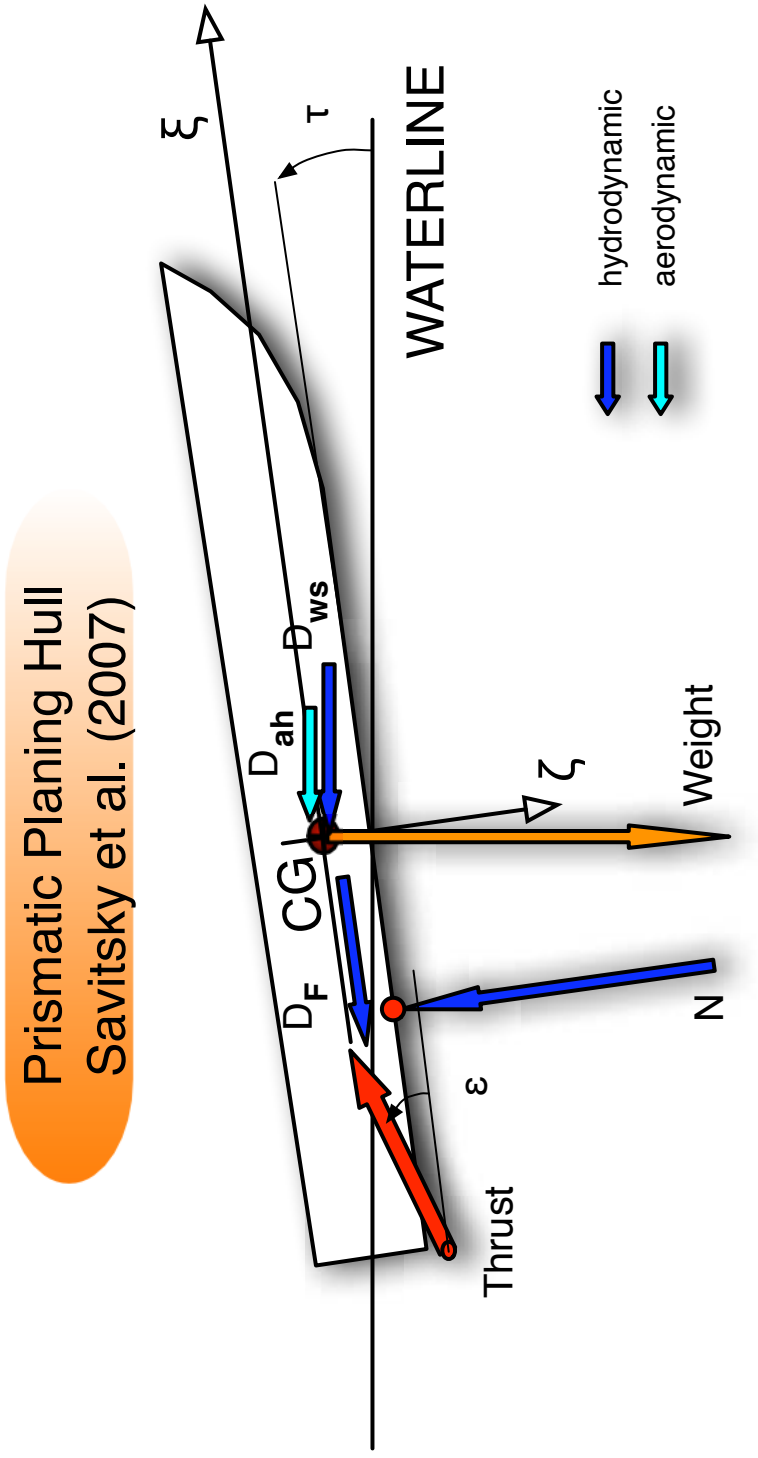

Figure 4.2: Forces and moments acting on planing craft at equilibrium, Savitsky model [46]

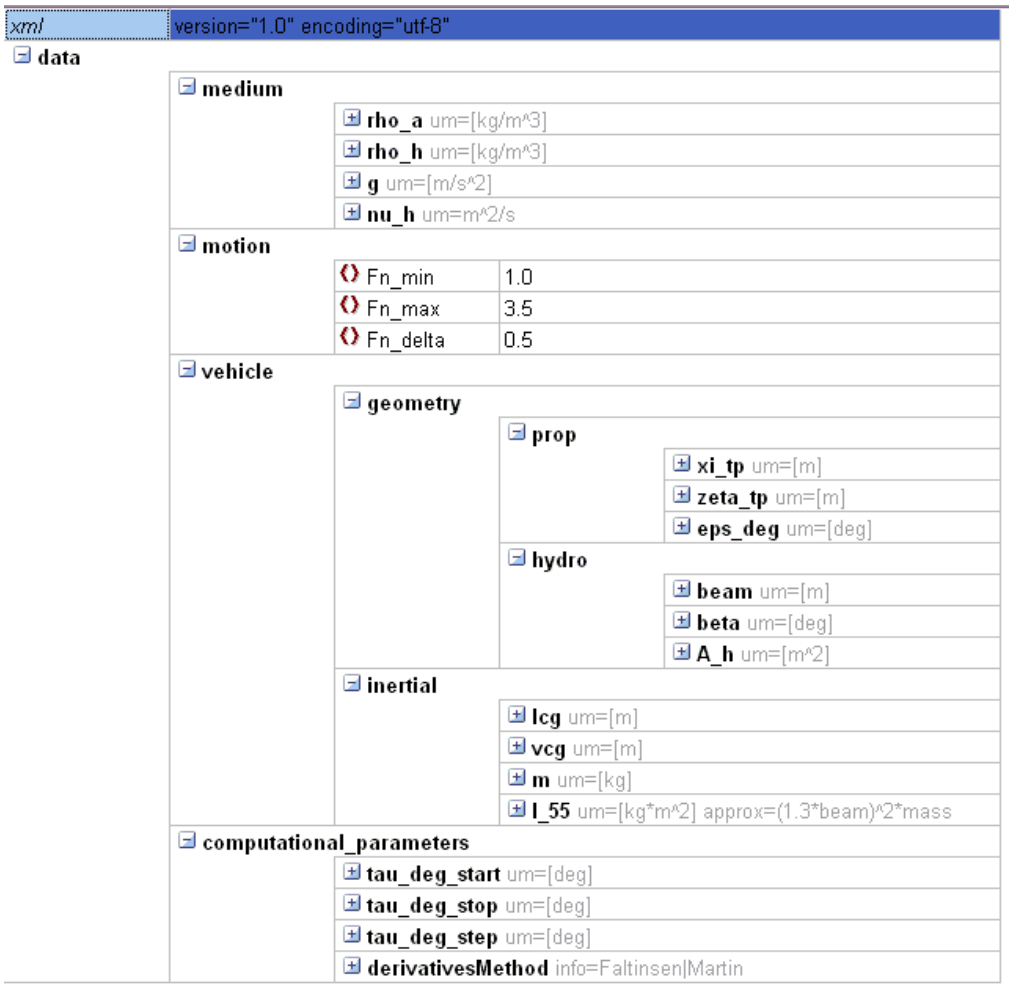

Figure 4.3: Xml input data structure of PC vehicle simulation program

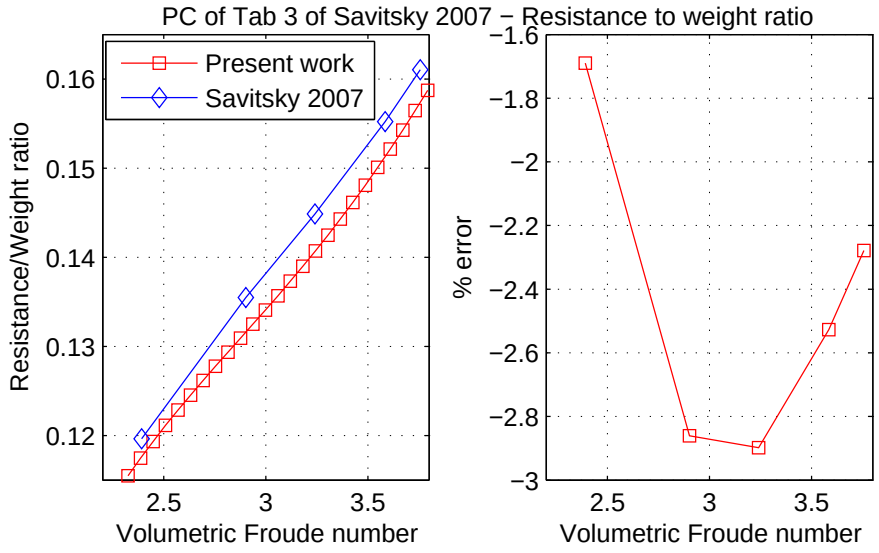

Figure 4.4: Planing craft of tab. 3 of [46]: Savitsky vs Collu

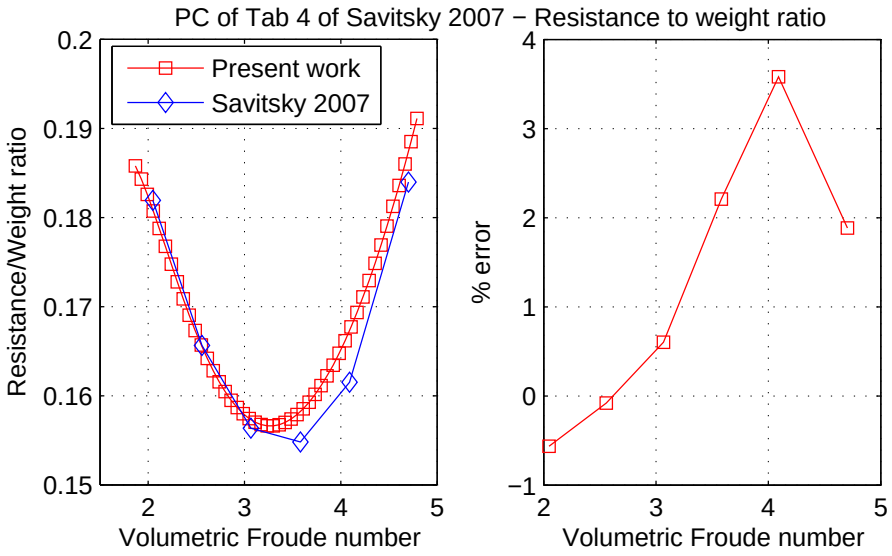

Figure 4.5: Planing craft of tab. 4 of [46]: Savitsky vs Collu

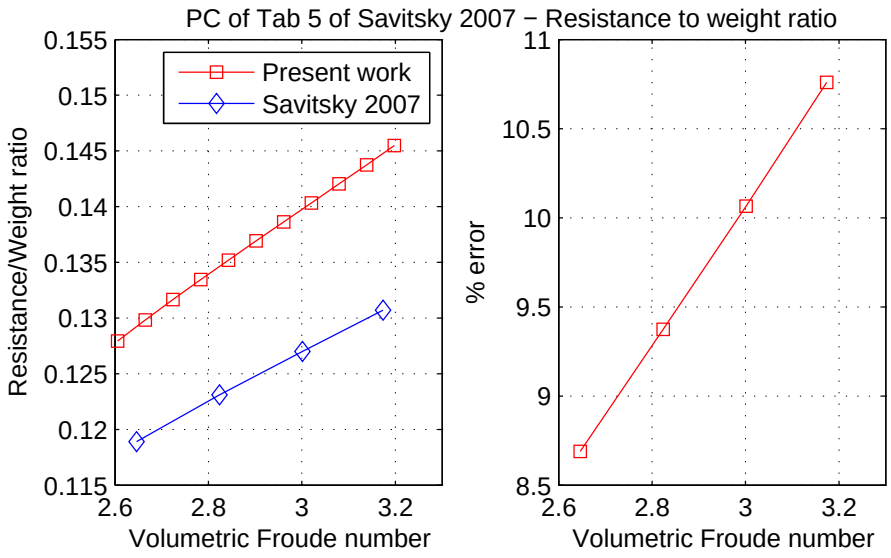

Figure 4.6: Planing craft of tab. 5 of [46]: Savitsky vs Collu

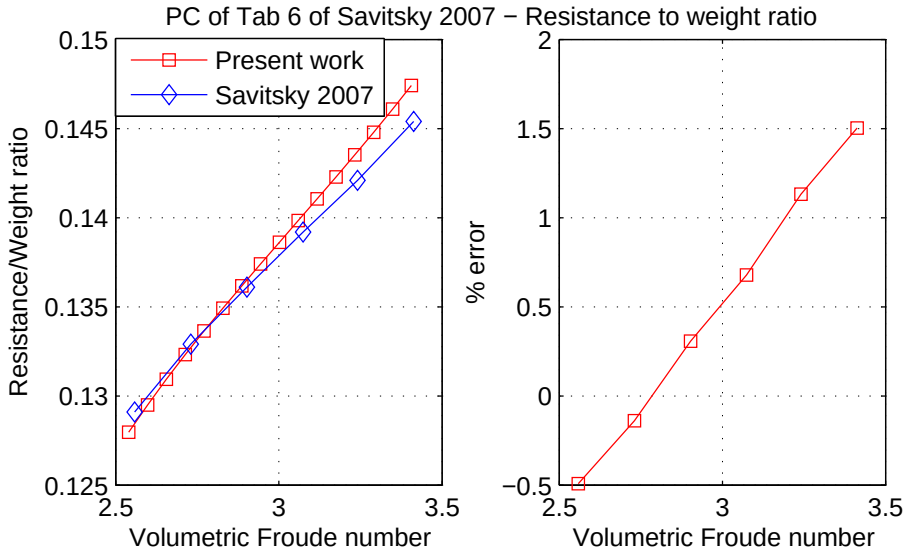

Figure 4.7: Planing craft of tab. 6 of [46]: Savitsky vs Collu

Part II

Aerodynamic Alleviated Marine Vehicles: Development of a New Model of Dynamics

Chapter 5

Configuration and Kinematics

5.1 Introduction

In order to develop a mathematical model for the dynamics of an 'Aerodynamically Alleviated Marine Vehicle (AAMV)', a kinematics framework is proposed to describe the motion of the AAMV and the forces acting on it. Once a reference framework is established, it is necessary to narrow down possible configurations of the AAMV, since the qualitative and quantitative nature of the forces and moments acting on the AAMV depend on the elements that comprise its configuration.

5.2 Kinematics

The study of kinematics requires definition of coordinate frames, of a notation to represent vehicle motion and a technique for a transformation between fixed and moving frames.

To describe the motion of an AAMV and the forces acting on it, a number of

different axis systems are used. Starting from the axis systems used for planing craft [43] [28] and for WIGe vehicles [51] [20], an earth-axis system and two body-axis system are presented below. They are all right-handed and orthogonal, as represented in fig. 5.1. Dashed lines represent the vehicle in a disturbed state (rotation and displacements have been emphasized for clarity).

For body-axis systems, the origin O is taken to be coincident with the center of gravity (CG) position of the AAMV in equilibrium state. The x and z axis lie in the longitudinal plane of symmetry, x positive forward and z positive downward. The direction of the x-axis depends on the body-axis system. Two are considered:

- **Aero-hydrodynamic axes ($\eta_1 \mathbf{O} \eta_3$)**, the direction of the x-axis η_1 being parallel to the steady forward velocity V_0,
- **Geometric axes** ($\xi O \varsigma$), the direction of the x-axis ξ being parallel to a convenient geometric longitudinal datum (as the keel of the hull).

Aero-hydrodynamic axes are used here as the counterpart of aerodynamic axes (called wind or wind-body axes in UK and stability axes in USA) used for airplanes. Usually the stability derivatives are calculated in this axis system.

The direction of the earth-axis systems (xOz) are fixed in space. The z-axis is directed vertically downward, the x-axis is directed forwards and parallel to the undisturbed waterline and the origin at the undisturbed waterline level.

5.3 Configuration

The general approach of this thesis is to start from studies on WIGe vehicles and high speed marine vehicles to derive integrated equations for an AAMV.

This approach can be applied also to the choice of the AAMV configuration. A WIGe vehicle's fundamental elements are the aerodynamic surfaces and the aero-propulsion system, while on a high speed marine vehicle the elements would be hydrostatic surfaces, hydrodynamic surfaces and a hydro-propulsion system. The combination of all these elements can be represented as in fig. 5.2, and it consists in:

- 2 aerodynamic surfaces, one front and one rear surface: both can have control surfaces,
- 2 hydrodynamic surfaces, one front and one rear surface: both can have control surfaces,
- 1 hydrostatic surface (hull),
- 1 aero-propulsion system,
- 1 hydro-propulsion system.

During course of the work [7], it was decided to limit the type of hydro-surfaces to only a prismatic planing hull (fig. 5.3). Therefore the possible configurations was narrowed down to the following:

- 2 aerodynamic surfaces, one front and one rear surface: both can have control surfaces,
- 1 (or more, in the multihull case) hydrostatic and hydrodynamic surface (prismatic planing hull),
- 1 or more hydrodynamic control systems,
- 1 aero-propulsion system,

- 1 hydro-propulsion system.

The main difference is that with the first class of configurations the hydrofoils could be represented. With the latter, only planing surfaces can be taken into account. The author considered that the AAMV should also have the capability of free flight (or wing in ground flight), therefore the configuration with hydrofoils as hydrodynamic surfaces was not considered suitable.

Among all the other possible hydrostatic/hydrodynamic surfaces, a prismatic planing hull has been chosen, and the Savitsky planing hull model is used for this configuration [43]. The available literature on planing craft dynamics is extensive and the approaches used are somewhat similar to the approach used for WIGe vehicles: this aspect makes the coupling of the airborne and waterborne dynamics simpler. Also if the majority of planing hulls used are non-prismatic, it has been demonstrated that the Savitsky approach is suitable also for non-prismatic hulls [46].

A better choice to couple the aerodynamic surface with the hydrodynamic surface would have been the multi-hull planing configuration, such as the catamaran configuration, but eventually a single planing hull model has been chosen. First of all, the planing models used for catamarans start from the Savitsky method and, through the estimation of a factor called 'interference factor' of one hull on the other, estimate the catamaran attitude as the Savitsky method estimates the prismatic planing hull attitude [47] [27] [26]. Secondly, as stated by Pensa [36], the models used to estimate these interference factors depend on a great numbers of parameters and involve quite complicated relations. Therefore it is not possible to generalize the methods neither to extrapolate data. For all these reasons, in the present work the Savitsky method is chosen, and along with it the prismatic planing monohull as the hydrostatic/hydrodynamic surface of the AAMV.

This kinematics approach has been presented by the author at the *2nd International Conference on Marine Research and Transportation, 2007* [8].

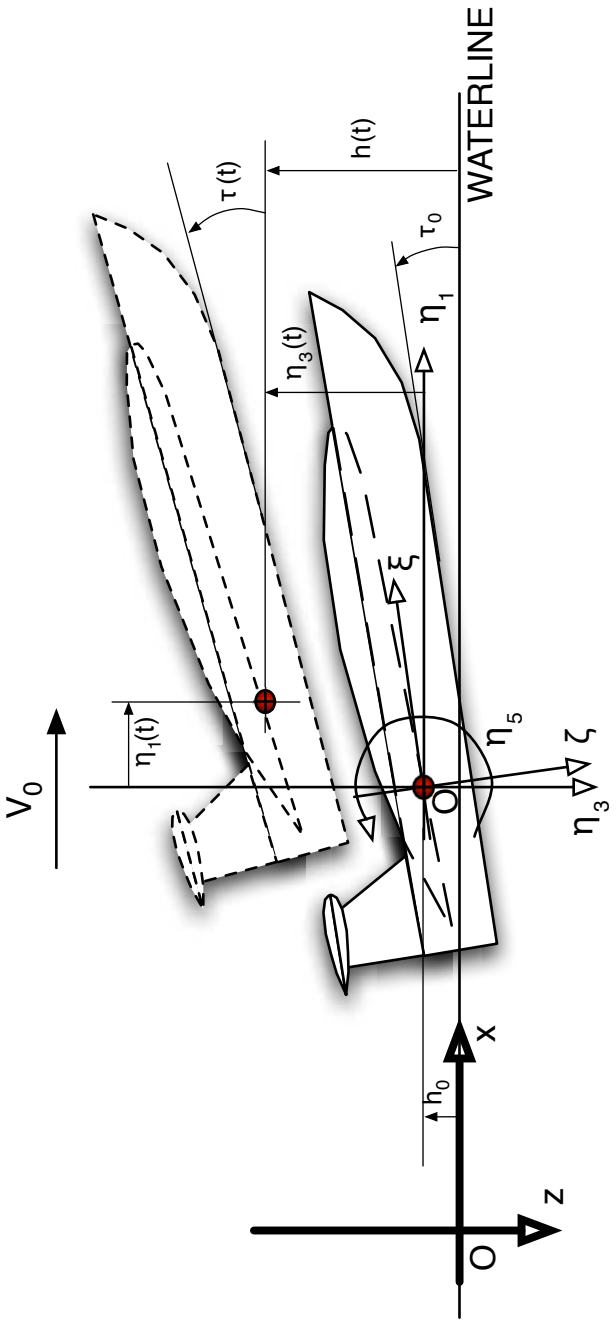

Figure 5.1: AAMV axis system

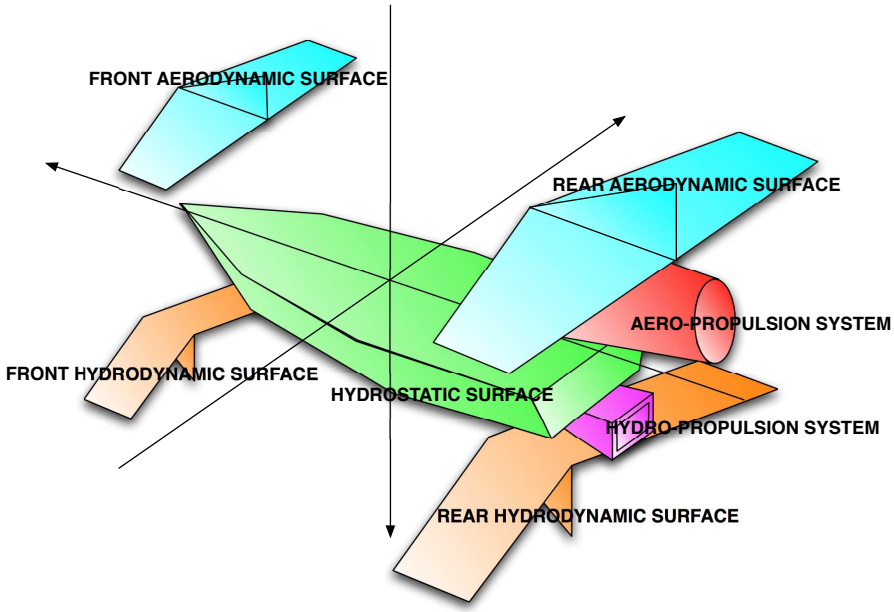

Figure 5.2: Class of configurations for the AAMV - 1st choice

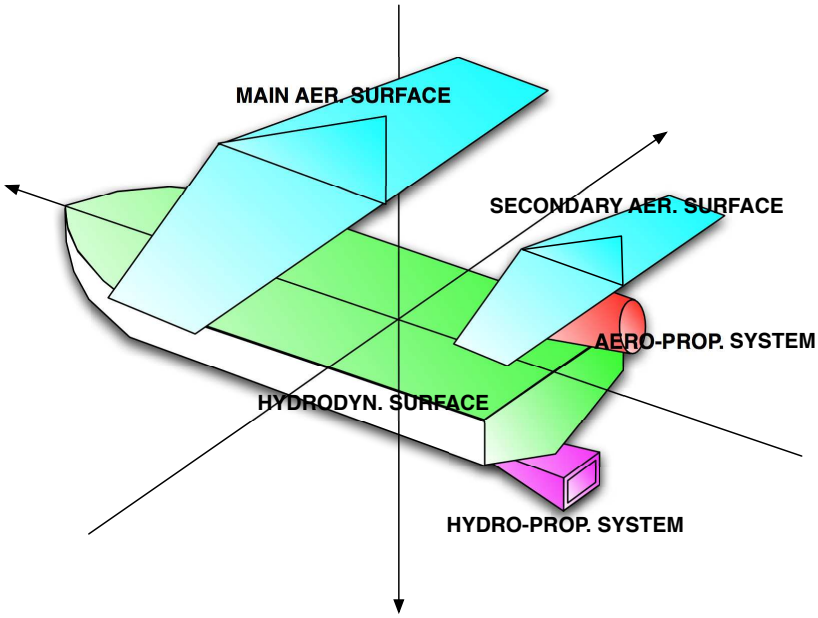

Figure 5.3: Class of configurations for the AAMV - Final choice

Chapter 6

Equations of Equilibrium

6.1 Introduction

In chapter 8 the static and dynamic stability of a AAMV configuration are analyzed. These analyses start from an equilibrium state and studies how the vehicle reacts to a disturbance. In this chapter the author proposes a mathematical method to estimate the equilibrium attitude of an AAMV, starting from the geometric, inertial, aerodynamic and hydrodynamic characteristics of the vehicle.

The approach adopted starts from available mathematical models for WIGe vehicles and PC configurations to develop a mathematical model for the AAMV. This approach is adopted also to develop the mathematical model presented in this chapter. In chapters 3 and 4 are analyzed, respectively, the mathematical models used for WIGe vehicles and a planing craft. Starting from these models:

- an analysis of the forces and moments acting on a AAMV configuration at equilibrium is conducted,
- a system of equations of equilibrium specifically developed for the AAMV configuration is obtained,

- a method to solve the AAMV system of equations of equilibrium is proposed,
- a numerical implementation of the previous method is shown.

6.2 Hypotheses

The present work concentrates on the analysis of an equilibrium state characterized by a rectilinear trajectory, a constant speed and a constant altitude above the surface, which will be referred as 'Rectilinear Uniform Level Motion' (RULM). The vehicle is always in contact with the water, and in a calm water situation. Waves are not taken into account.

6.3 Forces and moments: equilibrium state analysis

The forces and moments acting on a AAMV depend on the configuration chosen. The AAMV configuration proposed is presented in fig. 5.3. Once defined the configuration and the nature of the motion (RULM), it is possible to analyse the forces and moments acting on the vehicle, illustrated in fig. 6.1.

They can be divided in four groups:

- gravitational (weight, W),
- thrust (propulsion force, T),
- aerodynamic (lift, drag and moment from the 1st and 2nd aerodynamic surface, aerodynamic drag of the hull above the surface, D_{ah}),

- hydrodynamic (potential force, N, frictional force, D_F, whisker spray drag, D_{ws}).

6.3.1 Gravitational force

Since the equilibrium state analyzed is a level motion, the height above the surface is constant; therefore the direction of the velocity at equilibrium is normal to the weight direction. The weight (W) acts at the center of gravity (CG), which is also the origin of the body-fixed axis system (CG coordinates are (0,0)).

6.3.2 Power force

As previously mentioned, the thrust can be provided by an aero-propulsion system or a hydro-propulsion system. The thrust acts at the thrust point (TP), in a direction determined by the angle ϵ, the angle between the direction of the thrust and the keel, positive for an anticlockwise movement (view from the starboard side of the vehicle).

6.3.3 Aerodynamic forces

The AAMV can have one or two aerodynamic surfaces. The aerodynamic force acting on a aerodynamic surface is usually represented by two forces plus a moment: lift, defined as perpendicular to the velocity, drag, defined as parallel to the velocity, and pitch moment, positive for a bow up movement. These forces act on the aerodynamic center (AC).

To evaluate their values, the classical approach developed for airplanes has been adopted, used also for WIGe vehicles. Therefore, once known the coefficient of lift, of drag and of moment:

$$\begin{aligned} L_i &= \tfrac{1}{2}\,\rho_a\,V_0^2\,S_i\,c_{L,i} \\ D_i &= \tfrac{1}{2}\,\rho_a\,V_0^2\,S_i\,c_{D,i} \\ M_i &= \tfrac{1}{2}\,\rho_a\,V_0^2\,S_i\,c_{m,i}\,mac_i \end{aligned} \tag{6.1}$$

where

- "i" can be a1 for the first surface and a2 for the second surface,
- ρ_a is the density of the air,
- V_0 is the steady forward velocity,
- S_i is the reference aerodynamic area,
- mac_i is the mean aerodynamic chord and
- $c_{L,i}$, $c_{D,i}$ and $c_{m,i}$ are, respectively, the lift, drag and moment coefficients.

Once chosen the profile, the aerodynamic coefficients $c_{L,i}$, $c_{D,i}$ and $c_{m,i}$ depend both on angle of attack and on height above the surface, since the aerodynamic surfaces are operating in ground effect. The angle of attack depends on how the profile has been set on the keel. Once the trim angle is known, that is the angle between the keel and the surface, the angle of attack can be calculated. The angle of attack is the sum of the trim angle τ and η_{ai}, which is the angle between the mean aerodynamic chord of the wing and the keel of the hull. The aerodynamic center height above the surface is taken as reference height to evaluate the aerodynamic coefficients.

The dry section of the hull experiences an aerodynamic drag force (D_{ah}). In [46] this is estimated with the equation 6.2:

$$D_{ah} = \frac{1}{2}\,\rho_a\,V_0^2\,A_h\,c_{D,ah} \tag{6.2}$$

where

- A_h is the frontal area of the hull,
- $c_{D,ah}$ is the aerodynamic drag coefficient of the hull (approximated as 0.70)

Since it is not known where the hull aerodynamic drag acts, D_{ah} is supposed acting on the CG. Therefore no moment is generated by this force.

6.3.4 Hydrodynamic forces

Referring to the work developed by Savitsky et al. [43], [46], hydrodynamic forces are:

- potential force N,
- frictional force D_F,
- whisker spray drag D_{ws}.

The potential force direction is supposed to be normal to the keel and acting on the hydrodynamic center (HC). The frictional force acts parallel to the keel line, half-height between the keel and the chine. The whisker spray drag D_{ws} has been analyzed in particular in [46]. Like the aerodynamic drag of the hull (D_{ah}), also D_{ws} is assumed to act through the CG. To estimate their values the formulas used in [46] have been used.

6.4 System of equations of equilibrium

A brief summary of all forces and moments acting on a AAMV configuration is presented in tab. 6.1, and the system of equations of equilibrium can be developed. The vehicle, in the longitudinal plane, has three degrees of freedom, and a system of three equations of equilibrium is needed.

- surge equation: sum of the vertical forces = 0,
- heave equation: sum of horizontal forces = 0,
- pitch equation: sum of pitch moments = 0.

The CG of the AAMV is the point of reference for pitch moments.

6.4.1 Surge equation

It states that the sum of aerodynamic drags, of the component of potential and friction hydrodynamic forces parallel to the velocity, and of the whisker spray drag has to be equal to the component of the thrust parallel to the velocity.

$$-D_{a1} - D_{a2} - D_{ah} - N\ sin(\tau) - D_F \cos(\tau) - D_{ws} + T\ \cos(\tau + \epsilon) \quad = \quad 0 \tag{6.3}$$

6.4.2 Heave equation

The sum of aerodynamic lifts, of the vertical components of the potential and friction hydrodynamic forces and the vertical component of the thrust has to be

Table 6.1: Forces and moments acting on AAMV at equilibrium

Name	Description	Point of action (Body-axis system)	
		ξ	ζ
Gravitational			
W	Weight	0	0
Propulsion			
T	Thrust	ξ_{TP}	ζ_{TP}
Aerodynamic			
L_{ai}	Lift of the i-th aer. surf.	ξ_{ai}	ζ_{ai}
D_{ai}	Drag of the i-th aer. surf.	ξ_{ai}	ζ_{ai}
M_{ai}	Moment of the i-th aer. surf.	/	/
D_{ah}	Drag due to the hull	0	0
Hydrodynamic			
N	Potential force	ξ_{hc}	ζ_{hc}
D_F	Frictional drag	/	half-height betw. keel and chine
D_{ws}	Whisker spray drag	0	0

equal to the weight of the AAMV.

$$L_{a1} + L_{a2} + N\ \cos(\tau) - D_F \sin(\tau) - W + T\ \sin(\tau + \epsilon) \ = \ 0 \tag{6.4}$$

6.4.3 Pitch Moment Equation

The sum of aerodynamic moments, of hydrodynamic moments and of the moment generated by the thrust force has to be equal to zero.

$$L_{a1}\ [\xi_{ac1}\ \cos(\tau) + \zeta_a c1\ \sin(\tau)] + D_{a1} * [\xi_{ac1}\ \sin(\tau) - \zeta_{ac1}\ \cos(\tau)] + M_{a1} +$$

$$+ L_{a2}\ [\xi_{ac2}\ \cos(\tau) + \zeta_{ac2}\ \sin(\tau)] + D_{a2}\ [\xi_{ac2}\ \sin(\tau) - \zeta_{ac2}\ \cos(\tau)] + M_{a2} +$$

$$+ D_{ah}\ a_{ah} + D_{ws}\ a_{ws} - N * c - D_F * a +$$

$$+ T\ [\xi_{TP}\ \sin(\epsilon) + \zeta_{TP}\ \cos(\epsilon)] \ = \ 0 \tag{6.5}$$

In particular, since the aerodynamic drag of the hull and the whisker spray are supposed to act through the CG,

$$a_{ah} = a_{ws} = 0$$

6.5 Solution of the system of equations of equilibrium

The method to solve the system of the three equations of equilibrium is a enhancement of the 'Savitsky long-form method' illustrated in [13]. For a conventional planing craft, the weight is sustained by hydrostatic and hydrodynamic forces,

while for a AAMV configuration the weight is sustained by a combination of aerodynamic, hydrostatic, and hydrodynamic forces. Obviously, as it can be seen in eq. 6.3 and in eq. 6.5, also aerodynamic drag and moments are taken into account. As shown in chapter 4, in the original Savitsky method, the trim angle is not known at the start, therefore an initial trim angle is assumed and, through a cycle, the right trim angle that fulfill equations 4.2, 4.3 and 4.4 is eventually found. In this work an additional assumption is needed, since aerodynamic forces depend on both:

- the trim angle (τ), since the angle of attack is the sum of the trim angle and the angle between the mac and the keel ϵ,

- the height above the surface of the aerodynamic center of the wing.

As illustrated in fig. 6.2, this leads to a trim angle (τ) cycle (in red) nested into the height above the surface (h) cycle (in blue). Assuming a value for the height above the surface of the CG h_i and a trim angle τ_i, the aerodynamic forces can be calculated. Then the weight sustained by hydrostatic and hydrodynamic forces is equal to the difference between the total weight and the sum of aerodynamic lifts. At this point the 'long-form method' of Savitsky can be followed, taking into account also aerodynamic drags and moments: the equilibrium trim angle can be derived. The height above the surface of the vehicle h_{i+1} can then be calculated. If h_{i+1} is equal to the h_i assumed, then the equilibrium attitude of the vehicle has been found. If not, a new h cycle is performed.

6.6 Numerical implementation

The WIGe and the PC model programs illustrated respectively in sections 3.3 and 4.3 are developed following a common framework:

1. xml input data file,
2. first MATLAB program to evaluate the equilibrium attitude (equations of equilibrium),
3. second MATLAB program to evaluate the small perturbations motion (equations of motion).

The WIGe model does not have the first MATLAB program, since the equilibrium state characteristics are given in the input xml file.

The AAMV model program is developed following the same structure, and in this section the xml input data file as well as the first MATLAB program to estimate the AAMV equilibrium attitude is illustrated.

6.6.1 AAMV xml input data file

The structure of the AAMV xml input file is illustrated in fig. 6.3 and all the elements are illustrated in tab. 6.2 and tab. 6.3.

As it can be seen, in the AAMV xml data input file both the aerodynamic and hydrodynamic characteristics of the vehicle can be found, along with its inertial characteristics. It can be viewed as the sum of the WIGe vehicle and the PC xml input data files.

Table 6.2: Xml input data structure of the AAMV MATLAB program (1)

Branch of the tree	Name	Description
medium	rho_a $[kg\,m^{-3}]$	air density
”	rho_h $[kg\,m^{-3}]$	water density
”	g $[m\,s^{-2}]$	gravitational constant
”	nu_h $[m^2\,s]$	water cinematic viscosity
motion	Fn_min [ ]	Minimum Froude number
”	Fn_max [ ]	Max Froude number
”	Fn_delta [ ]	Froude number increment
vehicle		
geometry		
prop	xi_tp $[m]$	thrust point longitudinal position
”	zeta_tp $[m]$	thrust point vertical position
”	eps_deg $[deg]$	angle between keel and thrust direction
aero		
first surface	mac_a1 $[m]$	mean aerodynamic chord length
”	S_a1 $[m^2]$	surface area
”	eta_a1 $[deg]$	angle between the mac and keel line
”	xi_ac1 $[m]$	aerodynamic center longitudinal position
”	zeta_a1 $[m]$	aerodynamic center vertical position
”	profile	aerodynamic coefficients excel file name
hydro	beam $[m]$	planing hull width
”	beta $[deg]$	planing hull deadrise angle
”	A_h $[m^2]$	planing hull frontal area
dynamics		
prop	T_V $[N\,m^{-1}\,s]$	thrust derivative wrt speed

Table 6.3: Xml input data structure of the AAMV MATLAB program (2)

vehicle		
dynamics		
aero		
stabDer	type	dimensional, aeronormalized, dynanormalized, calculated
”	axes	body axes, wind-stability axes
”	Z_qWB	wing-body interaction Zq derivative
”	M_qWB	wing-body interaction Mq derivative
”	M_dwWB	wing-body interaction Mdw derivative
”	eps_alpha	downwash angle derivative wrt alpha
”	c_LTalpha	tail lift coeff. derivative wrt alpha
inertial	lcg $[m]$	CG longitudinal position (from transom)
”	vcg $[m]$	CG vertical position (from keel)
”	m $[kg]$	PC total mass
”	I_55 $[kg\,m^2]$	pitch moment of inertia

computational_parameters	
tau_deg_start $[deg]$	tau cycle - first value
tau_deg_stop $[deg]$	tau cycle - last value
tau_deg_step $[deg]$	tau cycle - increment
h_CG_0 $[m]$	h cycle - first value
h_CGEps $[m]$	h cycle - accuracy
derivativesMethod	method to estimate hydrodynamic derivatives

The vehicle → geometry → aero → first → profile value indicates the name of the excel file where are contained the aerodynamic lift, drag and moment coefficients, function of the angle of attack and of the height above the surface, illustrated in fig. 6.5. In the worksheet the lift, drag and moment coefficients function of the angle of attack are presented. As previously said, these coefficients depend also from the height above the surface, and this is indicated in the name of the worksheet (0.5), correspondent to the height-to-mac ratio. The AAMV MATLAB program acquire these data and, with a 2-dimensional interpolation, can evaluate the three aerodynamic coefficients at given height above the surface and at a given angle of attack. In the first worksheet of the excel file there is a summary of the characteristics under which the coefficients have been obtained, as illustrated in fig. 6.4.

With respect to the planing craft xml input file, the AAMV input file has two more parameters in the 'computational_parameters' branch: h_CG_0 and h_CGEps. As said in section 6.5, to solve the system of equations of motion a height above the surface cycle is needed. The cycle starts from the condition:

$$h_0 = h\_CG\_0$$

and then, once h_{i+1} is obtained at the end of the height cycle, there is a 'if' control: if the value $h_{i+1} - h_i \leq h\_CGEps$, then the equilibrium height above the surface has been found, if not a new height above the surface cycle is needed. Therefore the value h_CGEps represents the accuracy of the calculated equilibrium height above the surface. The other 'computational_parameters' values have been already illustrated in section 4.3.

In order to:

- better explain how the program works,

- how the program can be used in MATLAB,
- show the numerical and graphical outputs of the program,

in appendix B a complete example of an AAMV configuration analysis is given.

This approach has been presented by the author at the *8th Symposium on High Speed Marine Vehicles, 2008* [9].

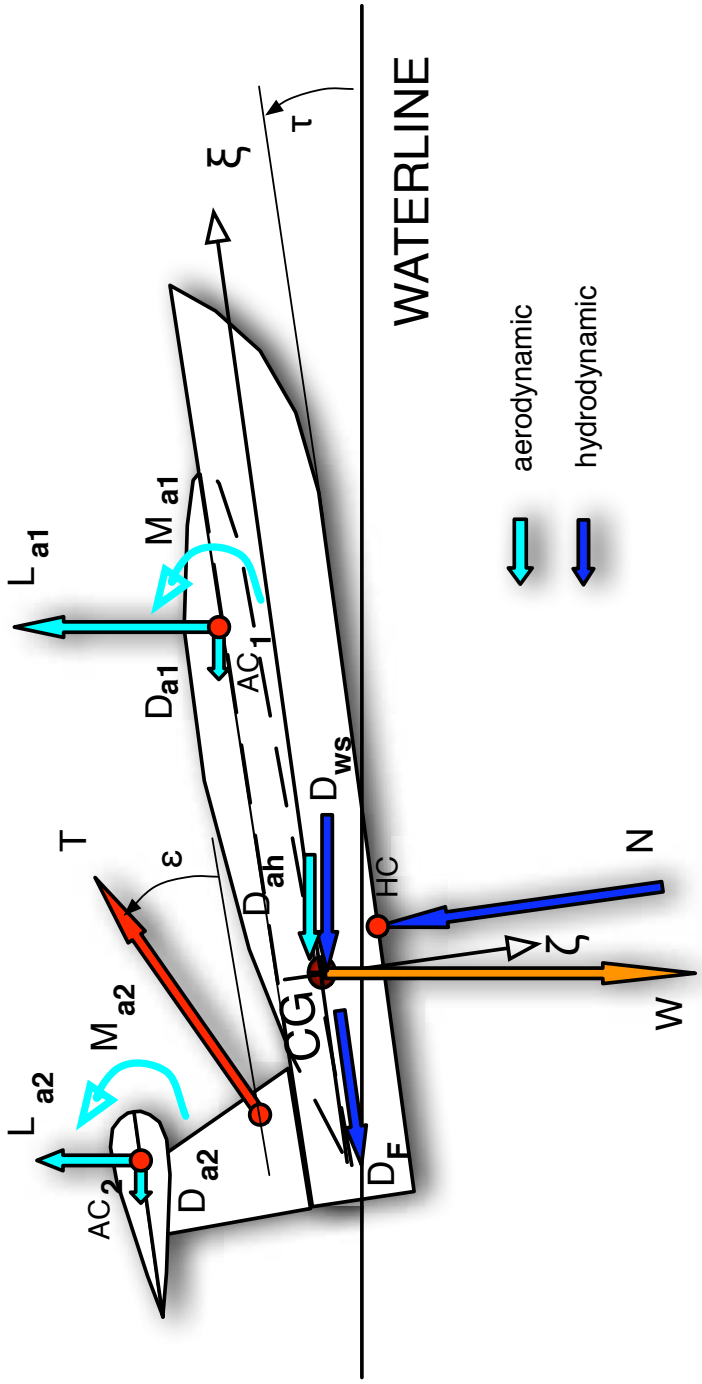

Figure 6.1: Forces and moments acting on a AAMV at equilibrium

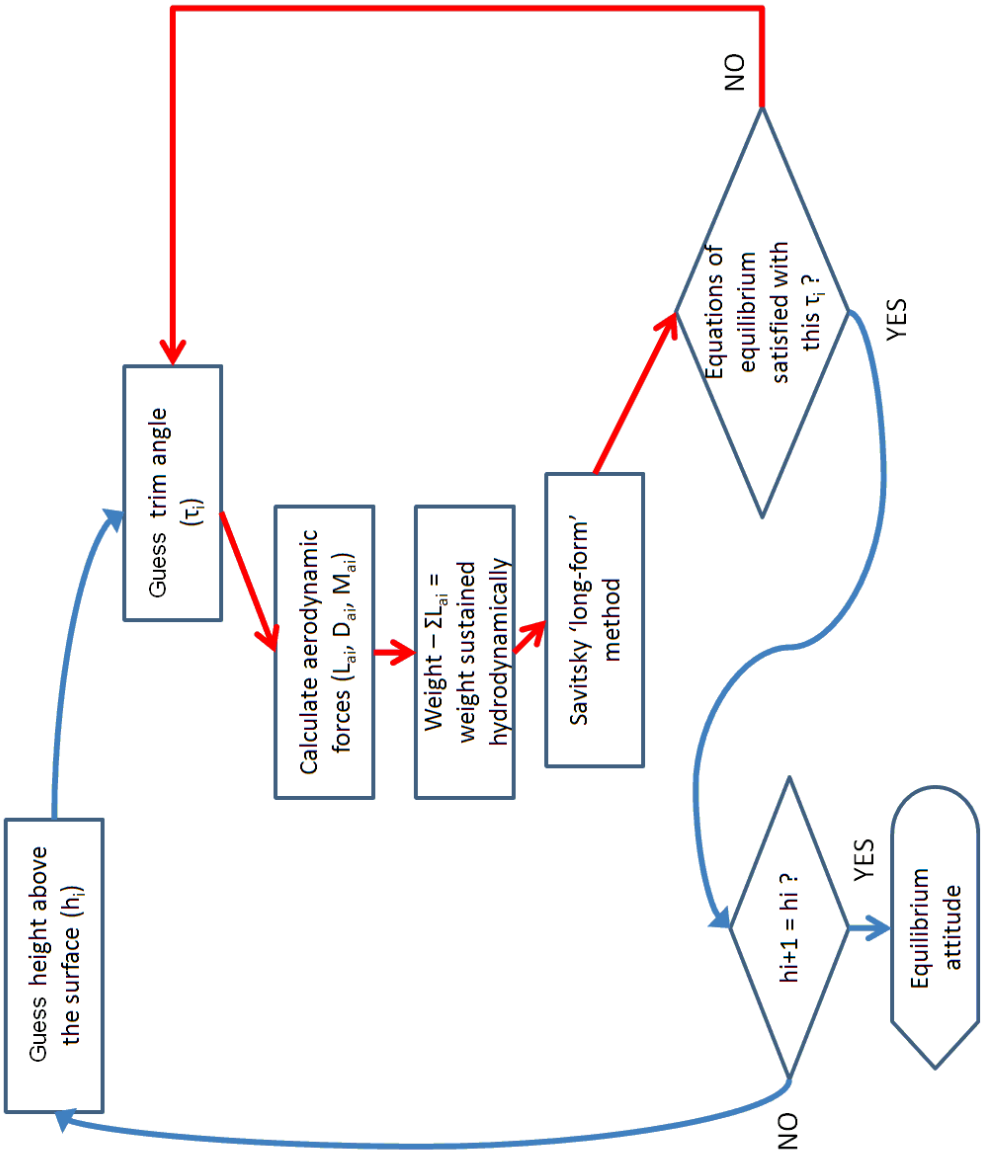

Figure 6.2: Method to solve the AAMV system of equations of equilibrium: flow chart

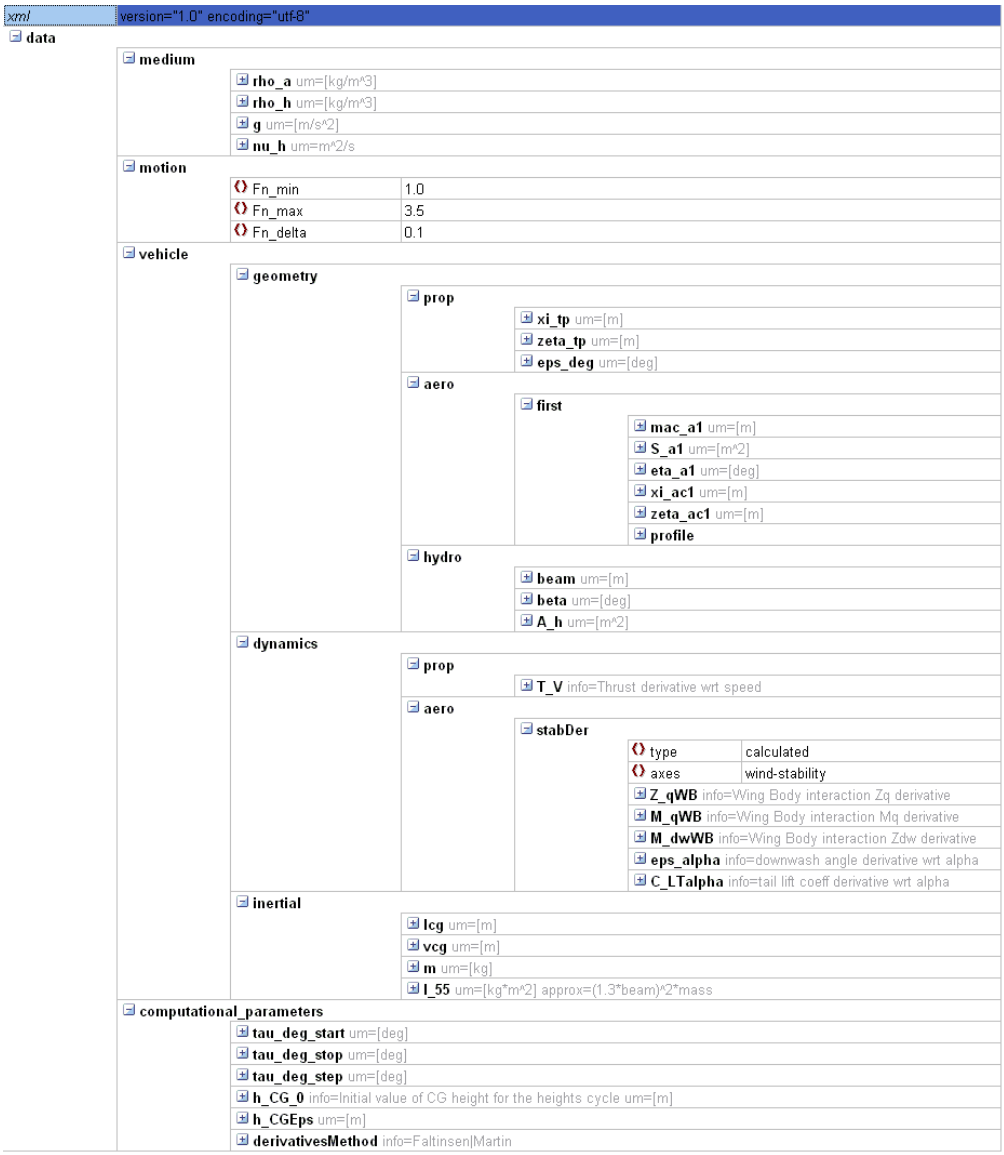

Figure 6.3: Xml input data structure of the AAMV MATLAB program

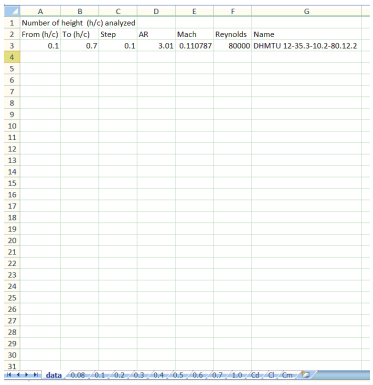

Figure 6.4: Aerodynamic coefficients excel input file: input data characteristics worksheet

	A	B	C	D	E
1	α	Cl	Cd	Cm 0.25	
2	[°]	[-]	[-]	[-]	
3	-5.0	-0.2372	0.0398	0.0546	
4	-4.0	-0.1779	0.0212	0.0477	
5	-3.0	-0.0988	0.0199	0.0392	
6	-2.0	-0.0277	0.0182	0.0315	
7	-1.0	0.0375	0.0179	0.0231	
8	0.0	0.0988	0.0193	0.0154	
9	1.0	0.1581	0.0212	0.0077	
10	2.0	0.2470	0.0226	0.0000	
11	3.0	0.3261	0.0279	-0.0069	
12	4.0	0.4051	0.0385	-0.0138	
13	5.0	0.5336	0.0412	-0.0077	
14	6.0	0.6324	0.0505	-0.0085	
15	7.0	0.7115	0.0571	-0.0123	
16	8.0	0.7905	0.0664	-0.0169	
17	9.0	0.8498	0.0770	-0.0215	
18	10.0	0.9289	0.0863	-0.0262	
19	11.0	0.9783	0.0956	-0.0308	
20	12.0	1.0079	0.1042	-0.0369	
21	13.0	1.0178	0.1142	-0.0377	
22					
23					
24					

0.1 0.2 0.3 0.4 0.5 0.6 0.7 1.0 Cd Cl Cm

Figure 6.5: Aerodynamic coefficients excel input file: n-th height above the surface worksheet

Chapter 7

Equations of Motion

7.1 Introduction

In chapter 6 a mathematical model of the system of equations of equilibrium is developed. It is able to estimate the AAMV equilibrium attitude, given the configuration and the speed. To investigate how the vehicle, in the given equilibrium state, reacts to external disturbances, the static and dynamic stability need to be analyzed. To do so, a system of equations of motion is needed.

In this chapter a mathematical model of the system of equations of motion, in the longitudinal plane, in the small disturbances framework, for an AAMV configuration is developed. This model is based on the systems of equations of motion for WIGe vehicles and planing craft, analyzed respectively in sections 3.2 and 4.2.3.

7.2 Forces and Moments: small disturbance analysis

The forces and moments acting on the vehicle, after an external disturbance, are:

- gravitational force (weight),
- hydrostatic forces, acting on the hull,
- hydrodynamic forces, acting on hydrodynamic high-speed planing hulls,
- aerodynamic forces, acting on aerodynamic surfaces,
- aerodynamic and hydrodynamic control systems' forces (supposed constants, control fixed analysis),
- aero- or hydro-propulsion forces (constant, sufficient to maintain a given steady forward speed).

7.2.1 Decoupling of Equations of Motion

The AAMV, represented as a rigid body in space, has 6 degrees of freedom. To describe its motion a set of six simultaneous differential equations of motion is needed. However, a decoupled system of equations of motion can be derived. For airplanes, in the frame of small perturbations approach, the lateral-longitudinal coupling is usually negligible. This is still valid for WIGe vehicle [4]. For planing craft, as demonstrated in [28], not only the lateral-longitudinal coupling is usually negligible, but also the surge motion can be decoupled from the heave and pitch motion. Therefore it is assumed that the AAMV has a negligible longitudinal-lateral coupling. In this work, the longitudinal motion of the AAMV is analyzed,

then only the forces and moments acting on the longitudinal plane are taken into account: surge, heave forces and pitch moments. Following the nomenclature used for ships and airplanes, the force in x direction is X, in z direction is Z and the moment about the y axis is M.

7.2.2 Forces and moments expressions

The total force acting on the AAMV can be expressed as:

$$\mathbf{F} = \mathbf{F}^g + \mathbf{F}^a + \mathbf{F}^h + \mathbf{F}^c + \mathbf{F}^p + \mathbf{F}^d \tag{7.1}$$

where the components of each force are

$$\mathbf{F}^i \;=\; [\, X^i \quad Z^i \quad M^i \,]^T$$

The total force is the sum of gravitational force, aerodynamic and hydrodynamic forces, control systems forces, propulsion force and environment disturbances forces.

When considering the motion of an airplane or a marine vehicle, after a small perturbation from a datum motion condition, it is usual to express aerodynamic and hydrodynamic forces and moments in Taylor expansions about their values at the datum motion state. The expansion can be nonlinear and expanded up to the n-th order, but in this work a linear expansion will be used. As for airplanes and planing craft, forces and moments are assumed to depend on the values of the state variables and their derivatives with respect to time. Then, each force and moment is the sum of its value during the equilibrium state plus its expansion to take into account the variation after the small disturbance, which is:

$$\mathbf{F} \;=\; \mathbf{F}_0 \;+\; \mathbf{F'} \tag{7.2}$$

$$\mathbf{F}_0 = [\, X_0 \quad Z_0 \quad M_0 \,]^T$$

$$\mathbf{F'} = [\, X' \quad Z' \quad M' \,]^T$$

where the subscript $(_0)$ denotes starting equilibrium state and superscript $(')$ denotes perturbation from the datum. Initially, the AAMV is assumed to maintain a RULM with zero roll, pitch and yaw angle. In this particular motion, the steady forward velocity of the AAMV is V_0 and its component in the aero-hydrodynamic axis system are $[\dot{\eta}_{1,0},\, \dot{\eta}_{3,0}]$, with $\dot{\eta}_{1,0} = V_0$ and $\dot{\eta}_{3,0} = 0$, since this is a level motion (constant height above the surface).

7.2.3 Control, power and disturbances forces

In this analysis, it is assumed that the controls are fixed (similar to the "fixed stick analysis" for airplanes). Then controls' forces and moments variations are equal to zero. The thrust is assumed not to vary during the small perturbation motion and it is equal to the total drag of the vehicle. The effects of environmental disturbances, like waves, are beyond the scope of this work, then a stable undisturbed environment is assumed.

$$\begin{cases} \mathbf{F}^c = \mathbf{F}_0^c \\ \mathbf{F}^p = \mathbf{F}_0^p \\ \mathbf{F}^d = \mathbf{0} \end{cases} \tag{7.3}$$

7.2.4 Gravitational force

The gravitational contribution to the total force can be obtained resolving the AAMV weight into the axis system. Since the origin of the axis system is co-

incident with the CG of the AAMV, there is no weight moment about the y axis. Remembering that the equilibrium state pitch angle is equal to zero and the angular perturbation θ' is small, the gravitational contribution is

$$\mathbf{F}^g = \mathbf{F}_0^g + \mathbf{F}^{g'} \tag{7.4}$$

$$\begin{aligned} \mathbf{F}_0^g &= [\, 0 \quad mg \quad 0 \,]^T \\ \mathbf{F}^{g'} &= [\, -mg\theta' \quad 0 \quad 0 \,]^T \end{aligned} \tag{7.5}$$

7.2.5 Aerodynamic forces

Usually, to evaluate aerodynamic forces and moments, the state variables taken into account in their Taylor linear expansion are the velocity along the x and z axes ($\dot{\eta}_1$ and $\dot{\eta}_3$) and the angular velocity about the y axis ($\dot{\eta}_5$). Among the accelerations, only the vertical acceleration ($\ddot{\eta}_3$) is taken into account in the linear expansion. Since the dynamics of a vehicle flying IGE depends also on the height above the surface, Kumar, Irodov and Staufenbiel introduced for WIGe vehicles the derivatives with respect to height (h).

These derivatives can be evaluated knowing the geometrical and aerodynamics characteristics of the aerodynamic surfaces of the AAMV ([17], [12]), as illustrated in appendix A. As shown by Chun and Chang [4], the Taylor expansion stopped at the 1st order (linear model) is a good approach to have a first evaluation of the static and dynamic stability characteristics of the WIGe vehicle.

The expansion of the generic aerodynamic force (moment) in the aero-hydrodynamic axis system ($\eta_1 O \eta_3$) for a AAMV with a longitudinal plane of symmetry is

$$\mathbf{F}^a = \mathbf{F}_0^a + \mathbf{F}^{a'} \tag{7.6}$$

$$\mathbf{F}_0^a = [\, X_0^a \quad Z_0^a \quad M_0^a \,]^T$$

$$\mathbf{F}^{a'} = \begin{bmatrix} X_h^a \\ Z_h^a \\ M_h^a \end{bmatrix} h' + \begin{bmatrix} X_{\dot\eta_1}^a & X_{\dot\eta_3}^a & X_{\dot\eta_5}^a \\ Z_{\dot\eta_1}^a & Z_{\dot\eta_3}^a & Z_{\dot\eta_5}^a \\ M_{\dot\eta_1}^a & M_{\dot\eta_3}^a & M_{\dot\eta_5}^a \end{bmatrix} \begin{bmatrix} \dot\eta_1 \\ \dot\eta_3 \\ \dot\eta_5 \end{bmatrix}' + \begin{bmatrix} 0 & X_{\ddot\eta_3}^a & 0 \\ 0 & Z_{\ddot\eta_3}^a & 0 \\ 0 & M_{\ddot\eta_3}^a & 0 \end{bmatrix} \begin{bmatrix} \ddot\eta_1 \\ \ddot\eta_3 \\ \ddot\eta_5 \end{bmatrix}'$$

The superscript ^{a} denotes "aerodynamic forces". F_j denotes the derivative of the force (or moment) F with respect to the state variable j, it corresponds to the partial differential $\partial F/\partial j$.

7.2.6 Hydrodynamic forces

In Hicks et al. [19], the nonlinear integro-differential expressions to calculate hydrodynamic forces and moments are expanded in a Taylor series, through the third order. Therefore, equations of motion can be written as a set of ordinary differential equations with constant coefficients. Analytic expressions are available for these coefficients in the work of Hicks [18]. The planing craft dynamics is highly non-linear, but the first step is to linearize the non-linear system of equations of motion and to calculate eigenvalues and eigenvectors, which variations are moni-

tored with quasi-static changes of physical parameters, such as the position of the CG. This approach seems reasonable as a first step for the analysis of the AAMV dynamics too, for which a linear system of equations is developed.

The derivatives are usually divided into restoring coefficients (derivatives with respect to heave displacement and pitch rotation), damping coefficients (derivatives with respect to linear and angular velocities) and added mass coefficients (derivatives with respect to linear and angular accelerations). Martin [28] and Troesch [54] showed that the added mass and damping coefficients are nonlinear functions of the motion but also that their nonlinearities are small compared to the restoring forces nonlinearities : therefore added mass and damping coefficients are assumed to be constant at a given equilibrium motion. Their value can be extrapolated from experimental results obtained by Troesch [53]. For the restoring coefficients, the linear approximation presented in Troesch and Falzarano [54] will be followed:

$$\mathbf{F}^{h,\,restoring} - \mathbf{F}_0^{h,\,restoring} \cong -[C]\,\underline{\eta} \tag{7.7}$$

The coefficients of [C] can be determined using Savitsky's method for prismatic planing hull [43] or the approach presented by Faltinsen [15].

An approach to estimate added mass, damping and restoring coefficients is presented by Martin [28]. Furthermore, an alternative approach is to compute the added mass and damping coefficients as presented in Faltinsen [15].

Then the expansion of the generic hydrodynamic force (moment) with respect to the aero-hydrodynamic axis system $\eta_1 \mathrm{O} \eta_3$ is:

$$\mathbf{F}^h \;=\; \mathbf{F}_0^h \;+\; \mathbf{F}^{h'} \tag{7.8}$$

$$\mathbf{F}_0^h \;=\; [\; X_0^h \quad Z_0^h \quad M_0^h \;]^T$$

$$
\begin{aligned}
\mathbf{F}^{h'} &= \begin{bmatrix} 0 & X^h_{\eta_3} & X^h_{\eta_5} \\ 0 & Z^h_{\eta_3} & Z^h_{\eta_5} \\ 0 & M^h_{\eta_3} & M^h_{\eta_5} \end{bmatrix} \quad \begin{bmatrix} \eta_1 \\ \eta_3 \\ \eta_5 \end{bmatrix}' + \\
&+ \begin{bmatrix} X^h_{\dot{\eta}_1} & X^h_{\dot{\eta}_3} & X^h_{\dot{\eta}_5} \\ Z^h_{\dot{\eta}_1} & Z^h_{\dot{\eta}_3} & Z^h_{\dot{\eta}_5} \\ M^h_{\dot{\eta}_1} & M^h_{\dot{\eta}_3} & M^h_{\dot{\eta}_5} \end{bmatrix} \quad \begin{bmatrix} \dot{\eta}_1 \\ \dot{\eta}_3 \\ \dot{\eta}_5 \end{bmatrix}' + \\
&+ \begin{bmatrix} X^h_{\ddot{\eta}_1} & X^h_{\ddot{\eta}_3} & X^h_{\ddot{\eta}_5} \\ Z^h_{\ddot{\eta}_1} & Z^h_{\ddot{\eta}_3} & Z^h_{\ddot{\eta}_5} \\ M^h_{\ddot{\eta}_1} & M^h_{\ddot{\eta}_3} & M^h_{\ddot{\eta}_5} \end{bmatrix} \quad \begin{bmatrix} \ddot{\eta}_1 \\ \ddot{\eta}_3 \\ \ddot{\eta}_5 \end{bmatrix}'
\end{aligned}
$$

The superscript ^{h} denotes "hydrodynamic forces". X_{η_1}, Z_{η_1} and M_{η_1} are equal to zero since surge, heave and pitch moment are not dependent on the surge position of the AAMV.

7.3 System of Equations of Motion

The generalized system of equations of motion (in 6 degrees of freedom) of a rigid body with a left/right (port/starboard) symmetry is linearized in the frame of small-disturbance stability theory. The starting equilibrium state is a RULM (Rectilinear Uniform Level Motion), with a steady forward velocity equal to V_0. The total velocity components of the AAMV in the disturbed motion are (evalu-

ated in the Earth-axis system):

$$\begin{bmatrix} \dot{\eta}_1 \\ \dot{\eta}_2 \\ \dot{\eta}_3 \\ \dot{\eta}_4 \\ \dot{\eta}_5 \\ \dot{\eta}_6 \end{bmatrix} = \begin{bmatrix} V_0 + \dot{\eta}'_1 \\ \dot{\eta}'_2 \\ \dot{\eta}'_3 \\ \dot{\eta}'_4 \\ \dot{\eta}'_5 \\ \dot{\eta}'_6 \end{bmatrix} \tag{7.9}$$

By definition of small disturbances, all the linear and the angular disturbance velocities (denoted with $'$) are small quantities: therefore, substituting eq. 7.9 in the generalized 6 degrees of freedom equations of motion, and eliminating the negligible terms, the linearized equations of motion can be expressed as

$$\begin{cases} m\ddot{\eta}'_1 &= X \\ m(\ddot{\eta}'_2 + \dot{\eta}'_6 V_0) &= Y \\ m(\ddot{\eta}'_3 - \dot{\eta}'_5 V_0) &= Z \\ I_{44}\ddot{\eta}'_4 - I_{46}\ddot{\eta}'_6 &= L \\ I_{55}\ddot{\eta}'_5 &= M \\ I_{66}\ddot{\eta}'_6 - I_{64}\ddot{\eta}'_4 &= N \end{cases} \tag{7.10}$$

If the system of equations is decoupled, the longitudinal linearized equations of motion are

$$\begin{cases} m\ddot{\eta}_1' &= X \\ m(\ddot{\eta}_3' - \dot{\eta}_5' V_0) &= Z \\ I_{55}\ddot{\eta}_5' &= M \end{cases} \tag{7.11}$$

N.B. From now on the superscript $'$ representing the perturbated state will be omitted.

7.3.1 Equilibrium state

The equilibrium state has been already analyzed in chapter 6: here it is only briefly presented to make the necessary simplifications.

When an equilibrium state has reached, by definition, all the accelerations are zero as well as all the perturbations velocities and the perturbation forces and moments. Then, using eq.s 7.3, 7.4, 7.6 and 7.8 in eq. 7.11:

$$\begin{cases} 0 &= X_0^g + X_0^a + X_0^h + X_0^c + X_0^p + X_0^d \\ 0 &= Z_0^g + Z_0^a + Z_0^h + Z_0^c + Z_0^p + Z_0^d \\ 0 &= M_0^g + M_0^a + M_0^h + M_0^c + M_0^p + M_0^d \end{cases} \tag{7.12}$$

or

$$\begin{cases} 0 &= X_0^a + X_0^h + X_0^c + X_0^p \\ 0 &= mg + Z_0^a + Z_0^h + Z_0^c + Z_0^p \\ 0 &= M_0^a + M_0^h + M_0^c + M_0^p \end{cases} \tag{7.13}$$

For the dynamic stability analysis, a given equilibrium state is assumed. The equilibrium state condition could be calculated using the approach presented in chapter 6.

7.3.2 Longitudinal linearized equations of motion

Taking into account eq. 7.13, the longitudinal linearized equations of motion (eq. 7.11) written in the aero-hydrodynamic axis system can be rearranged as:

$$[A]\,\underline{\ddot{\eta}} + [B]\,\underline{\dot{\eta}} + [C]\,\underline{\eta} + [D]h = \mathbf{0} \tag{7.14}$$

where

$$\underline{\eta} = \begin{bmatrix} \eta_1 \\ \eta_3 \\ \eta_5 \end{bmatrix}$$

and h is the (perturbated) height above the waterline.

The matrix [A] is the sum of the mass matrix, the hydrodynamic added mass derivatives and the aerodynamic "added mass" terms (usually in aerodynamics they are not called added mass terms, but simply "acceleration derivatives").

$$[A] = \begin{bmatrix} m - X^h_{\ddot{\eta}_1} & -X^a_{\ddot{\eta}_3} - X^h_{\ddot{\eta}_3} & -X^h_{\ddot{\eta}_5} \\ -Z^h_{\ddot{\eta}_1} & m - Z^a_{\ddot{\eta}_3} - Z^h_{\ddot{\eta}_3} & -Z^h_{\ddot{\eta}_5} \\ -M^h_{\ddot{\eta}_1} & -M^a_{\ddot{\eta}_3} - M^h_{\ddot{\eta}_3} & I_{55} - M^h_{\ddot{\eta}_5} \end{bmatrix} \tag{7.15}$$

[B] is the damping matrix and is defined as:

$$[B] = \begin{bmatrix} -X^a_{\dot{\eta}_1} - X^h_{\dot{\eta}_1} & -X^a_{\dot{\eta}_3} - X^h_{\dot{\eta}_3} & -X^a_{\dot{\eta}_5} - X^h_{\dot{\eta}_5} \\ -Z^a_{\dot{\eta}_1} - Z^h_{\dot{\eta}_1} & -Z^a_{\dot{\eta}_3} - Z^h_{\dot{\eta}_3} & -Z^a_{\dot{\eta}_5} - Z^h_{\dot{\eta}_5} \\ -M^a_{\dot{\eta}_1} - M^h_{\dot{\eta}_1} & -M^a_{\dot{\eta}_3} - M^h_{\dot{\eta}_3} & -M^a_{\dot{\eta}_5} - M^h_{\dot{\eta}_5} \end{bmatrix} \tag{7.16}$$

[C] is the restoring matrix and is defined as:

$$[C] = \begin{bmatrix} 0 & -X^h_{\eta_3} & -mg - X^h_{\eta_5} \\ 0 & -Z^h_{\eta_3} & -Z^h_{\eta_5} \\ 0 & -M^h_{\eta_3} & -M^h_{\eta_5} \end{bmatrix} \tag{7.17}$$

The matrix [D] represents the wing in ground effect, to take into account the influence of the height above the surface on the aerodynamic forces.

$$[D] = \begin{bmatrix} -X_h^a \\ \\ -Z_h^a \\ \\ -M_h^a \\ \\ \end{bmatrix} \tag{7.18}$$

7.4 Cauchy Standard Form of the Equations of Motion

By defining a state space vector $\underline{\nu}$ as

$$\underline{\nu} = \begin{bmatrix} \dot{\eta_1} & \dot{\eta_3} & \dot{\eta_5} & \eta_3 & \eta_5 & \eta_0 \end{bmatrix}^T \tag{7.19}$$

the system of equations eq. 7.14 can be transformed in the Cauchy standard form (or state-space form). The state space vector has six variables while the system of equations eq. 7.14 has only 3 equations. The remaining 4 equations are:

$$\begin{cases} \frac{\partial(\eta_3)}{\partial\, t} = \dot{\eta_3} \\ \\ \frac{\partial(\eta_5)}{\partial\, t} = \dot{\eta_5} \\ \\ \frac{\partial(h)}{\partial t} = \frac{\partial(\eta_0)}{\partial\, t} = -\dot{\eta_3} + V_0\, \eta_5 \\ \\ \end{cases} \tag{7.20}$$

Therefore the system is:

$$[A_{SS}]\dot{\underline{\nu}} = [B_{SS}]\, \underline{\nu} \tag{7.21}$$

where

$$[A_{SS}] = \begin{bmatrix} [A] & [0]_{3x3} \\ [0]_{3x3} & \begin{matrix} 1 & 0 & 0 \\ 0 & 1 & 0 \\ 0 & 0 & 1 \end{matrix} \end{bmatrix} \tag{7.22}$$

and

$$[B_{SS}] = \begin{bmatrix} & & & & 0 & -mg & \\ & -[B] & & & -C_{33} & -C_{35} & -[D] \\ & & & & -C_{53} & -C_{55} & \\ 0 & 1 & 0 & 0 & 0 & & 0 \\ 0 & 0 & 1 & 0 & 0 & & 0 \\ 0 & -1 & 0 & 0 & V_0 & & 0 \end{bmatrix} \tag{7.23}$$

The system of equations of motion in state-space form is:

$$\dot{\underline{\nu}} = [H]\,\underline{\nu} \tag{7.24}$$

where

$$[H] = [A_{SS}]^{-1} \quad [B_{SS}] \tag{7.25}$$

Now it is possible to analyse the static and dynamic stability of a AAMV configuration (chapter 8) and the influence of the configuration characteristics on the AAMV dynamics (section 9.4).

The mathematical model illustrated in this chapter has been presented by the author at the *2nd International Conference on Marine Research and Transportation, 2007* [8].

Chapter 8

Stability

8.1 Introduction

The AAMV configuration is characterized, as shown in chapter 6 and chapter 7, by a model of dynamics different from that one of airborne and waterborne vehicles. In chapter 6 a model to estimate the AAMV equilibrium attitude is shown, and in chapter 7 the behaviour of an AAMV in the small disturbances framework is analyzed, developing a system of equations of motion. In this chapter this analysis proceeds developing a method to assess the stability of an AAMV configuration.

8.2 Static Stability

Analyzing the forces and moments under the small disturbances hypothesis, the static stability of an AAMV is derived using the Routh-Hurwitz criterion. A brief insight of the Routh-Hurwitz criterion is given in appendix C.

In particular, Staufenbiel [51] showed how the last coefficient A_0 of the characteristic polynomial of a WIGe vehicle can be used to estimate its static stability. In

general, given the characteristic polynomial of a system:

$$A_n\, s^n + A_{n-1}\, s^{n-1} + \ldots + A_1\, s^1 + A_0 = 0 \tag{8.1}$$

if the condition

$$\frac{A_0}{A_n} > 0 \tag{8.2}$$

is fulfilled, the system is statically stable.

8.2.1 AAMV characteristic polynomial and static stability condition

In chapter 7 the author develops a mathematical model to study the longitudinal dynamics of an AAMV. A system of ordinary differential equations of motion is derived for the longitudinal plane in the frame of small-disturbance stability theory. Starting from this model, the Routh-Hurwitz condition is used to derive a mathematical expression to estimate the AAMV static stability.

8.2.1.1 Complete order system

By defining a state space vector $\underline{\nu}$ as

$$\underline{\nu} \;=\; \begin{bmatrix} \dot{\eta}_1 & \dot{\eta}_3 & \dot{\eta}_5 & \eta_3 & \eta_5 & \eta_0 \end{bmatrix}^T \tag{8.3}$$

the system of equations of motion can be rearranged in the Cauchy standard form (or state-space form), showed in eq. 7.21. The characteristic polynomial of the complete order system can be derived:

$$A_6\, s^6 + A_5\, s^5 + A_4\, s^4 + A_3\, s^3 + A_2\, s^2 + A_1\, s^1 + A_0 = 0 \tag{8.4}$$

With $A_6 = 1$, the static stability is assured when:

$$A_0 = \frac{num_0}{\Delta} > 0 \tag{8.5}$$

where num_0 is equal to

$$num_0 = V_0 \left[D_{10} \left(B_{31} \, C_{53} - B_{51} \, C_{33} \right) - B_{11} \left(C_{35} \, D_{50} - C_{53} \, D_{30} \right) \right] \tag{8.6}$$

and Δ is equal to

$$\begin{aligned} \Delta = & \left(I_{55} + A_{55} \right) \left[m^2 + m \left(A_{11} + A_{33} \right) + A_{11} \, A_{33} - A_{31} \, A_{13} \right] + \\ & - \left(m + A_{11} \right) A_{53} A_{35} - \left(m + A_{33} \right) A_{51} \, A_{15} + A_{53} \, A_{31} \, A_{15} + A_{51} \, A_{13} \, A_{35} \end{aligned} \tag{8.7}$$

A_{ij}, B_{ij}, C_{ij}, and D_{ij} stability derivatives are illustrated, respectively, in eq. 7.15, 7.16, 7.17, and 7.18.

8.2.1.2 Reduced Order System

This mathematical method should be validated against experimental data. Unfortunately, no experimental data on static stability of a AAMV configuration is available in the public domain.

To plan experiments to obtain these data, it is necessary to have a physical insight of the condition stated in eq. 8.2. This condition, applied to the complete order system in eq. 8.5, is relatively complex. Assuming that the surge degree of freedom (η_1) can be decoupled from heave (η_3) and (η_5) pitch degrees of freedom, a simplified version of the condition in eq. 8.5 can be obtained, leading to a better physical insight.

In chapter 7 the author derives a mathematical model of the dynamics of the AAMV starting from the systems of equations of motion of WIGe vehicles and

planing craft. As regard the dynamics of a planing craft, Martin [28] demonstrated that the surge motion can be decoupled from the heave and pitch motion. For the dynamics of WIGe vehicles, Rozhdestvensky [41] proposed a reduced order system where the surge motion is decoupled from heave and pitch motion. This hypothesis has been confirmed by, among others, Delhaye [12].

By defining the reduced order state space vector $\underline{\nu}$ as

$$\underline{\nu} = \begin{bmatrix} \dot{\eta_3} & \dot{\eta_5} & \eta_3 & \eta_5 & \eta_0 \end{bmatrix}^T \tag{8.8}$$

the Cauchy standard form (or state-space form) of the reduced order system is obtained. The characteristic polynomial can be derived:

$$A_5\, s^5 + A_4\, s^4 + A_3\, s^3 + A_2\, s^2 + A_1\, s^1 + A_0 = 0 \tag{8.9}$$

With $A_5 = 1$, the static stability is assured when

$$A_0 = \frac{V_0\,(C_{33}\,D_{50} - C_{53}D_{30})}{(A_{55} + I_{55})\,(A_3 + m) - A_{53}A_{35}} > 0 \tag{8.10}$$

8.2.2 Reduced order static stability: physical insight

Each coefficient in eq. 8.10 is the derivative with respect to:

- accelerations (Aij),
- heave position(Cij),
- height above the surface (Dij)

of the sum of aerodynamic and hydrodynamic forces (and moments). Referring to section 7.3.2, remembering that the superscript 'a' stands for aerodynamic and

'h' for hydrodynamic, and that Z is the heave force (positive downward) and M the pitch moment (positive bow up), the coefficients are equal to:

$$\begin{aligned} A_{33} &= A^a_{33} + A^h_{33} &&= -Z^a_{\ddot{\eta}3} - Z^h_{\ddot{\eta}3} \\ A_{35} &= A^a_{35} + A^h_{35} &&= -Z^a_{\ddot{\eta}5} - Z^h_{\ddot{\eta}5} \\ A_{53} &= A^a_{53} + A^h_{53} &&= -M^a_{\ddot{\eta}3} - M^h_{\ddot{\eta}3} \\ A_{55} &= A^a_{55} + A^h_{55} &&= -M^a_{\ddot{\eta}5} - M^h_{\ddot{\eta}5} \end{aligned} \tag{8.11}$$

$$\begin{aligned} C_{33} &= C^h_{33} &&= -Z^h_{\eta 3} \quad , \quad C^a_{33} = 0 \\ C_{53} &= C^h_{53} &&= -M^h_{\eta 3} \quad , \quad C^a_{53} = 0 \\ D_{30} &= D^a_{30} &&= -Z^a_{\eta 0} \quad , \quad D^h_{30} = 0 \\ D_{50} &= D^a_{53} &&= -M^a_{\eta 0} \quad , \quad D^h_{50} = 0 \end{aligned} \tag{8.12}$$

The aerodynamic derivatives can be estimated with the approach presented in appendix A and the hydrodynamic derivatives with expressions presented in [28] or [15]. Using these expressions for the configuration presented in section 5.3 we have

$$(A_{55} + I_{55})\,(m + A_{33}) - A_{53}\,A_{35} > 0 \tag{8.13}$$

therefore, being the denominator of eq. 8.10 greater than zero, the static stability condition of the reduced order becomes

$$\frac{D_{50}}{D_{30}} - \frac{C_{53}}{C_{33}} > 0 \tag{8.14}$$

8.2.2.1 Similarity with WIGe vehicles

To better understand the condition expressed in eq. 8.14, a parallel with WIGe vehicles static stability criteria is illustrated. The static stability condition derived by Staufenbiel [51] and Irodov [20] is:

$$\frac{M_w}{Z_w} - \frac{M_h}{Z_h} < 0 \tag{8.15}$$

that, using the present nomenclature corresponds to the condition

$$\frac{B_{53}}{B_{33}} - \frac{D_{50}}{D_{30}} < 0 \tag{8.16}$$

M_w and M_h are the derivatives of pitch moment with respect to the heave velocity and the height above the surface, Z_w and Z_h are the heave force same derivatives. Staufenbiel and Irodov define M_w/Z_w also as the aerodynamic center of pitch and M_h/Z_h as the aerodynamic center in height. Remembering that positive abscissa means ahead of the CG, the condition in eq. 8.15 and 8.16 can be expressed as (Rozhdestvensky) [42]:

> "the (aerodynamic) center in height should be located upstream of the (aerodynamic) center in pitch."

Dividing the lift due to a variation of the pitch angle (ΔL_{alpha}) from the lift due to a variation of the height above the surface (ΔL_{height}), condition in eq. 8.15 states that the point of action of force ΔL_{height} should be located upstream the point of action of force ΔL_{alpha}.

8.2.2.2 AAMV Static stability criterion (reduced order)

As regard the AAMV, using expressions 8.12, the static stability condition in eq. 8.14 can be expressed as:

$$\frac{M^a_{\eta 0}}{Z^a_{\eta 0}} - \frac{M^h_{\eta 3}}{Z^h_{\eta 3}} > 0 \tag{8.17}$$

The first term $M^a_{\eta 0}/Z^a_{\eta 0}$ is the analogue of the aerodynamic center in height of WIGe vehicles. The author proposes for the second term the name 'hydrodynamic center in heave', so that eq. 8.17 can be also expressed as:

"the hydrodynamic center in heave should be located downstream of the aerodynamic center in height."

As before, dividing the hydrodynamic lift due to a heave variation (ΔL_{hyd}) from the lift due to a variation of the height above the surface (ΔL_{height}), the point of action of ΔL_{hyd} should be located upstream the point of action of ΔL_{hyd}.

8.2.3 Reduced order system static stability: graphical insight

To better understand conditions expressed in eq. 8.17, a graphical representation of the aerodynamic center in height, the aerodynamic center in pitch and the hydrodynamic center in heave is given in fig. 8.1.

For a conventional aircraft the longitudinal static stability, without considering the influence of the aerodynamic control surfaces (the so called 'fixed stick analysis'), is determined only by the position of the 'neutral point 1', called 'aerodynamic center in pitch'. This point can be imagined as the point where the aerodynamic forces, due to an external disturbance of the pitch angle, act. To have an airplane statically stable, the aerodynamic center in pitch should be located rearward with respect to the CG, and the distance between the neutral point 1 and the CG is called static stability margin (ssm_1), since it is a measure of how statically stable the airplane is. This condition can be explained observing that if, due to a disturbance, the pitch angle augments the aerodynamic lift (proportional to the angle of attack, this being a function of the pitch angle) but, since the 'disturbance lift' generated in this way can be imagined acting on the neutral point 1, a pitch down moment is created, counteracting the pitch up disturbance. The pitch down moment, being proportional to the distance between the aerodynamic center in pitch and the CG, is proportional to ssm_1. The same applies, opposite in direction, if the pitch angle diminishes. It has to be noted that the optimum value of ssm_1

is within a range of values. In fact, if ssm_1 is too small, the static stability would be insufficient to counteract external disturbances, and the airplane can easily become unstable. On the other hand, if ssm_1 is too large, it will be very difficult to change the pitch attitude of the airplane, compromising the maneuverability of the airplane.

For wing in ground effect vehicles there is an additional neutral point, called 'neutral point 2', due to the fact that aerodynamic forces depend also on the height above the surface of the vehicle. As stated by Staufenbiel, Irodov and others, to have a statically stable WIGe vehicle, it should fulfill the condition 'neutral point 1 rearward the CG' plus another condition: the neutral point 2 should be located upstream with respect to the neutral point 1. The distance between the two neutral points can be assumed as a second static stability margin, indicated as ssm_2.

For an aerodynamically alleviated marine vehicle a third neutral point exists, due to the fact that the forces depend on:

- the pitch angle as for airplane and WIGe vehicles,
- the height above the surface as in WIGe vehicles,
- and also on the heave position.

In fact hydrodynamic forces depend heavily on the heave position of the AAMV. Furthermore, the condition expressed in eq. 8.17 is represented here by the fact that 'neutral point 3', also called 'hydrodynamic center in heave', is located downstream with respect to the 'neutral point 2', also called aerodynamic center in height. As for previous cases, the distance between the neutral point 2 and the neutral point 3 can be assumed as a measure of the static stability margin in heave (ssm_3).

The condition for the AAMV static stability is derived using the reduced order system of equations of motion, following an approach already used for WIGe vehicles. It should be noted that it is a thumbnail rule, useful for the preliminary design phase of the vehicle and to have a quick physical insight of the static stability of a AAMV.

8.3 Dynamic Stability

A system is defined as dynamically stable if it is statically stable and all the characteristic roots of the system have a negative real part.

Also if it is possible to calculate the real part of the roots, using a numerical program to solve the system of equations of motion illustrated in eq. 7.3.2, it is relatively complicate to derive the expressions and to have a physical insight of them. It is still complicate using the reduced order system of section 8.2.1.2.

The author, having a limited amount of time to investigate this aspect of the stability, has chosen to investigate numerically the dynamic stability of an AAMV configuration, and the results of this analysis are presented in section 9.4.2.

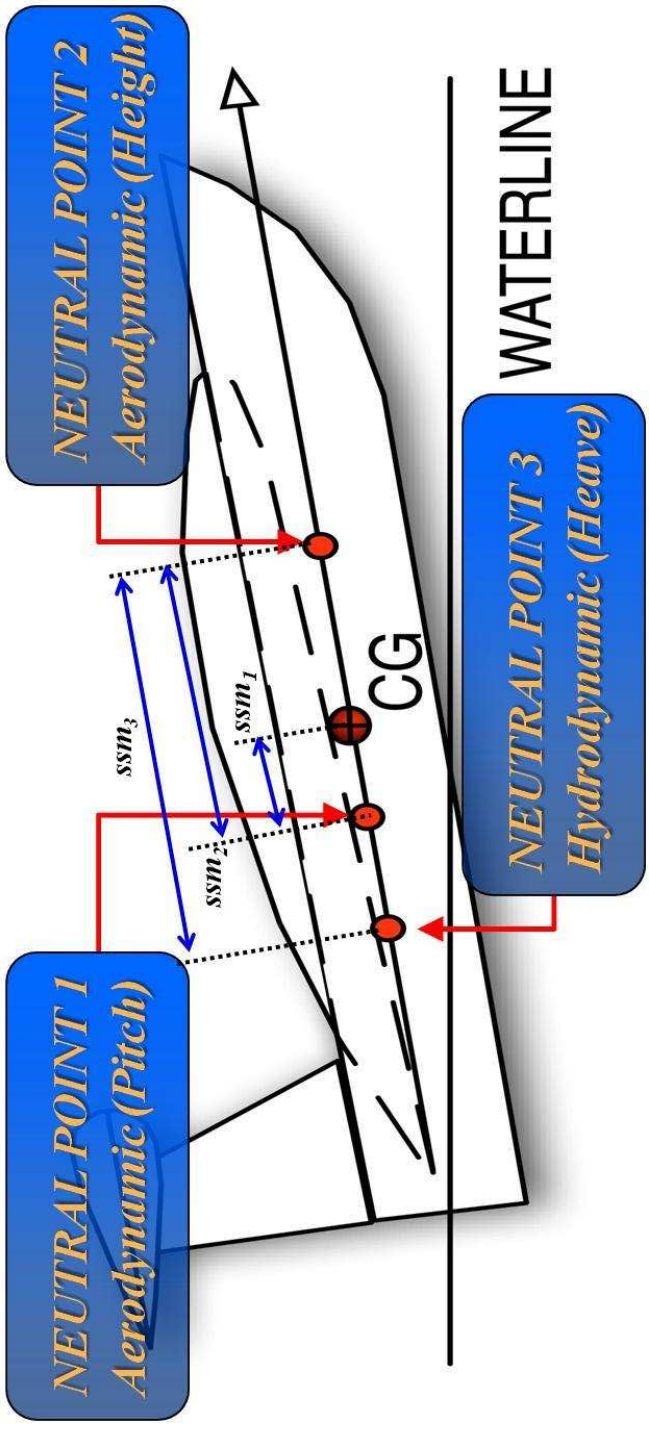

Figure 8.1: AAMV static stability: graphical analysis

Chapter 9

Design of a Hybrid Vehicle: Parametric Analysis

9.1 Introduction

In chapter 6 an equilibrium attitude estimation method is developed. In chapter 7 a method to study the static and dynamic stability of the vehicle is derived. In this chapter these two methods are used to conduct two parametric analyses. Taking the model C-01 as a baseline configuration, with characteristics illustrated in tab. 9.1, some key parameters of the configuration are changed across a range of values and the influences on the equilibrium attitude and static/dynamic stability characteristics are analyzed. Each key parameter influence is analyzed across a range speed from Fn = 1.0 to Fn = 3.5 (from 7.4 to 25.8 m/s or from 14 to 50 knots), except for speeds at which the system of equations of equilibrium do not have a solution. Typically, the system of equations of equilibrium do not have a solution if the sum of pitch moments around the CG cannot be balanced to zero.

Since the AAMV is still in a preliminary design phase, this parametric analysis has a dual purpose. Firstly, to plan experiments to acquire data. The mathemat-

ical models developed need validations against experimental data. Unfortunately no experimental data on the equilibrium attitude or on the static/dynamic stability of an AAMV configuration is available in the public domain. To plan such experiments, it is fundamental to have a rough estimation of the characteristics of the configuration that have the main influence on AAMV performance. Secondly, only doing a parametric analysis an optimized configuration can be proposed, calculating the best trade-off value of each parameter. This parametric analysis can be compared to the more familiar 'sensitivity analysis' of the airplane preliminary design [39] [40], where the optimum value of each configuration characteristic is presented along with its derivative with respect to a certain requirement. For example, analyzing the optimum total weight (at take-off) of the airplane, the derivatives of this weight with respect to number of passengers, payload, range, endurance, and so on are presented.

9.2 Comparison model: C-01

These parametric analysis take as comparison the model C-01, whose configuration is illustrated in tab. 9.1.

As illustrated in chapter 5, the configurations proposed in this work are composed by one or two aerodynamic surfaces, a prismatic planing hull and an aero- and/or a hydro-propulsion system. The model C-01 is composed by:

- a wing of aspect ratio equals to 1, which profile is a Glenn Martin 21, thickness-to-chord ratio equals to 11 %, with endplate,
- a prismatic planing hull whose characteristics are similar to the planing hull presented in [46] (tab.3) by Savitsky.

Characteristics		Dimensional	Dimensionless	
GEOMETRY				
Propulsion				
	ξ_{TP}	0 [m]	$\frac{\xi_{TP}}{B}$	0
	ζ_{TP}	0 [m]	$\frac{\zeta_{TP}}{B}$	0
	ϵ_{TP}	12 [deg]	/	/
Aerodynamic				
	First surface			
	mac	20 [m]	$\frac{mac}{B}$	3.606
	S_{a1}	400 [m^2]	$\frac{S_{a1}}{B^2}$	13
	η_{a1}	10 [deg]	/	/
	ξ_{ac1}	10 [m]	$\frac{\xi_{ac1}}{B}$	1.803
	ζ_{ac1}	-2 [m]	$\frac{\zeta_{ac1}}{B}$	-0.361
	profile	Glenn Martin 21, t/c 11, with endplate [2]		
Hydrodynamic				
	B (beam)	5.547 [m]	$\frac{B}{B}$	1
	β	14 [deg]	/	/
	A_h	20.067 [m^2]	$\frac{A_h}{B^2}$	0.652
INERTIAL CHAR.				
	lcg	8.656 [m]	$\frac{lcg}{B}$	1.560
	vcg	1.387 [m]	$\frac{vcg}{B}$	0.250
	m (mass)	52160 [kg]	$\frac{m}{\rho_{sw}*B^3}$	0.298
	$I_{55} = m * k_{55}^2$	2712318.1 [kg*m^2]	$\frac{k_{55}}{B}$	1.3

Table 9.1: Parametric analysis: characteristic of the basic model (model C-01)

As regard the profile Glenn Martin 21, in appendix A the aerodynamic coefficients of lift, drag and moment, along with its geometrical characteristics, are presented (fig. A.1, A.2). It is important to notice how the aerodynamic coefficients are function of both the angle of attach and of the height above the surface.

This configuration has only one aerodynamic surface. In general, the introduction of a secondary aerodynamic surface in an airplane or WIGe vehicle configuration is done to solve longitudinal stability issues. In particular, the horizontal stabilizer, along with the elevator, equilibrates the pitch-down moment of the main aerodynamic surface and makes the airplane statically stable. Since the AAMV is still in its conceptual/preliminary design phase, it is preferred here not to complicate the configuration, to have a better physical insight of the physics. Once the static and dynamics stability characteristics of the AAMV will be established, a secondary aerodynamic surface will be incorporated in the configuration and its influence on the equilibrium attitude performances and on the static and dynamic stability will be analyzed.

The hydrodynamic surface of the AAMV configuration analyzed, the prismatic planing hull, is similar to the planing craft analyzed in 2007 by Savitsky to exploit validated experimental data. As illustrated in chapter 6, the agreement between the equilibrium attitude model developed here and the Savitsky mathematical model is good, therefore also since no data are present in the public domain to validate the equilibrium attitude model and the static/dynamic stability model of an AAMV, this constitutes a validation basis for these analysis.

9.3 Equilibrium state performance optimization

In this section the influences of the chosen parameters on the equilibrium attitude variables are presented. Each variable is varied across a range of values, and these values are indicated as percentage of the comparison value. For example, 100 (%) indicates the value of the parameter as in the model C-01, therefore 50 indicates half and 200 double of the comparison value.

9.3.1 Parameters analyzed

The configuration parameters that can be varied are presented in tab. 9.1, but only a part of them are analyzed.

9.3.1.1 Propulsion

The point of action of the propulsion force (ξ_{TP}, ζ_{TP}) and the direction of the force, indicated as the angle between the keel of the planing hull and the T force (ϵ_{TP}), are not analyzed. This is because at this stage of the project a propulsion system has not been chosen, therefore it is preferred to exclude its influence from this analysis. The point of action of the thrust force is coincident with the CG, therefore no moment about the CG is generated. Furthermore, the direction ϵ is kept fixed at 12 deg, as in the Savitsky planing craft model used as planing hull for the AAMV C-01.

9.3.1.2 Aerodynamic surface geometry

The characteristics of the aerodynamic surface are the length of the mean aerodynamic chord (mac), the plan surface area (S_{a1}), the angle between the mean aerodynamic chord of the profile and the keel of the planing hull (η_{a1}), the position of the aerodynamic center (ξ_{ac1}, ζ_{ac1}), and the profile type.

The aspect ratio (width/mac) of the wing has been kept equal to 1, so as to have experimental data [29] to feed in the model. For the same reason the profile is always kept the same. With the aspect ratio fixed, a change of the mac leads to a change of the wing surface area, therefore only one of these two parameters is varied: the mac length. The longitudinal position of the aerodynamic center ξ_{ac1} and η_{a1} are analyzed as well, but the vertical position ζ_{ac1} is kept equal to -2 m. This is because a low vertical AC position limits the possible range of trim equilibrium angle, since the trailing edge of the wing can touch the water after a certain value of τ, and a too high position can severely reduce or nullify the positive effects of the WIGe.

9.3.1.3 Hydrodynamic surface geometry

The planing hull has a prismatic shape, therefore it can be defined by two parameters: the width of the hull (beam, B) and the deadrise angle β, the transverse slope of the bottom of the boat, measured in degrees. These are illustrated in fig. 4.1. A third parameter, A_h, estimates the average value of the frontal area of the hull above the waterline. It is useful to evaluate the aerodynamic drag experienced by the planing hull, following the method presented by Savitsky [46]. Only the deadrise angle is taken into account in the parametric analysis, the other parameters being kept equal to the Savitsky's planing hull values.

9.3.1.4 Inertial characteristics

The inertial parameters are the longitudinal and vertical positions of the center of gravity, respectively lcg and vcg, the total mass m, and the pitch moment of inertia, I_{55}. Only lcg and m have been analyzed, since vcg is limited by the lateral hydrostatic stability of the AAMV at rest and I_{55} does not have any influence on the equilibrium attitude.

9.3.1.5 Summary

It has to be specified that this is a sensitivity analysis to highlight the influence of each parameter independently. Due to the fact that the AAMV project is still in its conceptual phase, the configuration has not been set in detail. In fact, each parameter is varied without thinking about the effects of these changes on the other parameters. It is important to clarify that, on the opposite side, once an AAMV configuration is in its preliminary design phase, each design parameter is linked to the others. For example, a change of the mass of the vehicle will change the aerodynamic load on the aerodynamic surfaces, a very important design parameter. Therefore the mass of the vehicle and the area of the aerodynamic surfaces have to be investigated together.

In the present work, the configuration parameters analyzed are:

- mac, the mean aerodynamic chord of the aerodynamic surface,
- η_{a1}, the angle between the keel of the hull and the mac,
- ξ_{ac1}, the longitudinal position of the aerodynamic center of the wing,
- β, the deadrise angle of the planing hull,

Variable	C-01 value	Values analyzed	
mac	20 m	0, 50, 100, 150%	0, 10, 20, 30 m
η_{a1}	10 deg	0, 40, 80, 120%	0, 4, 8, 12 deg
ξ_{ac1}	10 m	-50, 0, 100, 150%	-5, 0, 10, 15m
β	14 deg	50, 100, 150	7, 14, 21 deg
lcg	8.656 m	85, 100, 115%	7.3576, 8.656, 9.9544 m
m	52160 kg	50, 100, 150%	26080, 52160, 78240 kg

Table 9.2: Equilibrium attitude parametric analysis: parameters analyzed

- lcg, the longitudinal position of the center of gravity of the vehicle,
- m, the total mass of the vehicle.

In tab. 9.2 are presented, for each parameter, the range of values analyzed. For each parameter, for each value, the range of speed values considered is between Fn = 1.0 and Fn = 3.5.

9.3.2 Influence of the chosen parameters on AAMV equilibrium attitude

The influence of each parameter is analyzed using the data obtained with the equilibrium attitude model MATLAB implementation (see appendix B).

9.3.2.1 Mean aerodynamic chord (mac)

First of all, it should be noticed that the curves of the configuration with a mac 150% of the original mac go up to about Fn = 2.8. Above this speed the system of equations of equilibrium does not have any solution. When further increasing

the mac, the total aerodynamic pitching up moment cannot be balanced by the total hydrodynamic pitching down moment. Therefore the vehicle does not have an equilibrium trim angle. The vehicle tends to flip over, which is a commonly known instability and one that can cause accident with such vehicles.

As shown in fig. 9.2, the aerodynamic lift, which increases as the wing area is increased, alleviates the weight of the vehicle. Therefore if the mac increases the CG height above the surface will increase and the draft at the transom of the planing hull will diminish. This is confirmed by fig. 9.3: the aerodynamic lift sustains a bigger part of the vehicle as the speed is augmented and as the wing area is increased.

As regard the resistance-to-weight ratio (fig. 9.4), it should be highlighted that for low speed marine vehicles it is not convenient to have a wing. In fact, below a certain speed, the hydrodynamic drag of the configuration with a wing is higher than the hydrodynamic drag of the configuration without any wing. It is due to a balance between the hydrodynamic lift, hydrodynamic drag, aerodynamic lift, and aerodynamic drag. If, at the same speed, the trim angle increases, the vertical components of hydrodynamic forces will diminish, and the horizontal component will increase. The vertical component is the hydrodynamic lift that, together with the aerodynamic lift, sustains the weight of the vehicle. Below the critical speed, the speed at which the R/W ratio curves cross each other (about Fn = 3.3-3.4 in fig. 9.4), the aerodynamic lift is not high enough to counterbalance the augment of the hydrodynamic drag due to a bigger trim equilibrium angle. In fact the sum of aerodynamic and hydrodynamic drags is higher for vehicles with wing with respect to the vehicle without any wing. Above the critical speed the trim angle is still higher for the configurations with wing, leading to a bigger horizontal component of hydrodynamic forces (drag), but the aerodynamic lift is sustaining a consistent part of the weight of the vehicle. This means that the

hydrodynamic lift needed is diminished enough to have the sum of aerodynamic and hydrodynamic drag lower for vehicles with wing with respect to the vehicle without wings.

9.3.2.2 Angle between mac and the keel (η)

η is the angle between the keel of the hull and the mac of the wing. As shown in fig. 9.5, if η angle is augmented the trim equilibrium angle is augmented, as the previous case. Anyway, as it can be observed in fig. 9.6 and fig. 9.7, the sensitivity of the aerodynamic lift with respect to η is less pronounced than the sensitivity with respect to mac. This is confirmed also by the smaller raise of the height above the surface of the CG and by the smaller draft reduction.

In fig. 9.8 the resistance-to-weight ratio curves confirm the previous observations. The qualitative trend is similar to fig. 9.4, but quantitatively the differences are less pronounced. The critical speed can be estimated around Fn = 3.3-3.4.

9.3.2.3 Longitudinal position of the aerodynamic center (ξ_{ac1})

ξ_{ac1} is the longitudinal position of the aerodynamic center of the wing. It has been varied between -5 m and + 15 m: from 5 m aft to 15 m fore the longitudinal position of the CG. As it can be seen, the behavior is different from previous parametric analysis.

Fig. 9.12 show the resistance to weight ratio. For high speed marine vehicles it is convenient to have the wing shifted forward as much as possible rather than having the wing behind the CG, while for low speed marine vehicle the opposite is valid. As previously defined, the resistance-to-weight ratio is the sum of aerodynamic and hydrodynamic drag divided by the weight of the vehicle. As shown in fig.

9.13, the aerodynamic drag (D_A) remains almost the same changing configuration, therefore the behavior of the resistance-to-weight ratio is due to the hydrodynamic drag (D_H). In fig. 9.11 it can be observed that the aerodynamic lift (L_A) and, consequently, the hydrodynamic lift (L_H) do not change varying the longitudinal position of the aerodynamic center.

The conclusion is that ξ_{ac1} does not influence aerodynamic lift and drag forces, as well as hydrodynamic lift forces. It effects only the hydrodynamic drag, in such a way that if the position of the aerodynamic center of the wing is shifted forward, the hydrodynamic efficiency (L_H/D_H) will be:

- decreased below the critical speed,
- increased above the critical speed.

as it can be observed in fig. 9.14.

9.3.2.4 Deadrise angle of the hull (β)

'Deadrise' is the transverse slope of the bottom of the boat, measured in degrees. A boat with a flat bottom has 0 degrees deadrise angle. This angle has an effect on calm water stability and on high speed performance. The majority of high-speed offshore planing hulls adopt a deadrise angle between 15 and 25 degrees, due to the superior seakeeping capability at high speed in rough water [3], also if a lower hydrodynamic efficiency corresponds to a higher deadrise angle. A parametric analysis on the influence of the deadrise angle of the planing hull on the AAMV equilibrium state performances is conducted. The results are similar to the results obtained for conventional planing hull without any aerodynamic lift. As it can be seen in fig. 9.17, the aerodynamic lift is not substantially influenced

by a change of the deadrise angle. Fig. 9.15 shows that if the deadrise angle is increased, the trim equilibrium attitude at the same speed will be higher. This is because if the deadrise angle increases the hydrodynamic lift generated will decrease, therefore to obtain the same hydrodynamic lift it is necessary to have a bigger trim equilibrium angle. In fig. 9.16 it can be seen as a higher τ leads to a higher draft, to a lower high above the surface of the CG and to a higher resistance to weight ratio (fig. 9.18). While the previous analysis showed a critical speed, here if the deadrise angle increases, the resistance to weight ratio will be higher across the whole speed range.

9.3.2.5 Longitudinal position of the center of gravity (lcg)

The longitudinal position of the CG is a fundamental parameter of planing craft design. It strongly influences the equilibrium attitude and the static and dynamic stability of the vehicle. Therefore it is essential to analyze its influence. It is not possible to widely vary the position of the center of gravity, because:

- shifting rearward the CG the equilibrium trim angle τ augments. If τ is too high the system of equations of equilibrium does not have any solution, basically because the AAMV tends to flip over,
- shifting forward the CG the equilibrium trim angle τ diminishes. If τ is lower than 2 degrees the model adopted, the Savitsky long form method [13], is no longer valid.

In fig. 9.21 it can be seen that shifting rearward or forward the CG, the percentage of the total weight sustained by the aerodynamic lift does not change substantially, as for the aerodynamic drag (fig. 9.23). Similarly to the longitudinal position of

the aerodynamic center ξ_{ac1} parametric analysis, lcg mainly influences the hydrodynamic efficiency of the AAMV, defined as the ratio between the hydrodynamic lift and the hydrodynamic drag (fig. 9.24). The conclusion is that, with respect to the resistance to weight ratio:

- at low speed it is better to have a forward shifted CG (higher lcg),
- at high speed it is better to have a rearward shifted CG (lower lcg).

9.3.2.6 Mass (m)

In a preliminary design, the mass is calculated starting from the requirements of the vehicle, in particular from the payload. In this work the vehicle configuration has not been fixed, it is still in its conceptual phase, therefore it is interesting to investigate the AAMV mass influence. For this reason the mass has been widely varied, from 50% to 150% of the baseline configuration mass, and the results are presented in fig. 9.25 through 9.30. The baseline configuration mass is equal to the mass of the planing craft presented by Savitsky in [46], tab. 3. It is important in this case to analyze the dimensionless parameters, since it is obvious that a heavier vehicle will experience a bigger hydrodynamic drag, also if some graphs have been kept dimensional, to give an idea of the order of magnitude of the forces. In fig. 9.28 is represented the resistance to weight ratio. It can be observed that, at high speed, the lowest R / W ratio is obtained with the heaviest configuration. As it can be seen in fig. 9.30, aerodynamic efficiencies of the three configurations are almost equals, instead hydrodynamic efficiencies are quite different. In general the hydrodynamic efficiency tends to diminish as the speed increases, but the red curve (m 26080 kg) has a derivative with respect to the speed more negative than the blue curve (m 78240 kg). The green curve (m 52160 kg) has an intermediate behavior. Therefore as the speed increases the best configuration, from a R / W

ratio point of view, changes from the lightest one to the heaviest one. This aspect is very similar to the planing hull R / W ratio, therefore the wing seems not to substantially influence the sensitivity with respect to the mass parameter.

9.4 Dynamic stability optimization

To analyse the influence of some configuration's parameter on the dynamic stability of the vehicle, an approach similar to the analysis of planing hull dynamic stability done by Payne [35] is adopted.

In this work a linear approximation of the stability derivatives is used, since the development of a nonlinear method is beyond the scope of this work. Troesch in 1993 [54] and later with Hicks [19] conducted a series of parametric analysis on the influence of some parameters of the planing hull configuration on its stability. He stated that a linear approach can be used to estimate the critical value of each parameter, that is the value at which the planing hull becomes unstable. Beyond this value nothing can be said using a linear approach, a nonlinear approach is needed to assess the characteristic of the unstable oscillation of the vehicle, such as frequency, amplitude, etc. Therefore the following analysis focus its attention on the boundary between the dynamic stability and instability. For each parameter a graph is presented, showing the values of this parameter that guarantee the dynamic stability of the vehicle, in function of the speed. Beyond this value the vehicle is unstable and nothing can be estimated with the linear approach used.

9.4.1 Parameters analyzed

In 1974 Payne [35] analyzed the coupled pitch and heave instability of high speed planing hull, instability also known as porpoising. In this analysis he presented several graphs showing the influence of some configuration parameters on the porpoising oscillation characteristics. In particular he stressed the importance of:

- the longitudinal position of the CG,
- the longitudinal radius of gyration (the pitch moment of inertia).

In this work, in addition to these parameters, since the AAMV also has aerodynamic surfaces, the following configuration characteristics are taken into account:

- the mean aerodynamic chord of the aerodynamic surface (mac),
- the angle between the keel and the mac (η),
- the position of the aerodynamic center of the wing (ξ_{AC1}),

The results of this analysis are presented with a graph. The x-axis represents the range of the parameter analyzed, the y-axis the speed range. Each point, having as coordinates (x = parameter value, y= speed), is represented by a symbol:

- 'o' if the vehicle is stable,
- 'x' if the vehicle is unstable,
- '*' if the vehicle cannot reach a trimmed equilibrium state.

For each parameter two figures are presented (see, for example, fig. 9.31 and 9.32). The first one shows the stable zone, the unstable zone and the zones where the

Variable	C-01 value	Range	Step	Range	Step
mac	20 m	0 to 150%	10%	0 to 30 m	2 m
η_{a1}	10 deg	0 to 120%	10%	0 to 12 deg	1 deg
ξ_{ac1}	10 m	-50 to 150%	25%	-5 to 15m	2.5 m
β	14 deg	50 to 150%	10%	7 to 21 deg	1.4 deg
lcg	8.656 m	85 to 115%	5%	7.36 to 9.95 m	0.4328 m
m	52160 kg	50 to 150%	10%	26080 to 78240 kg	7824 kg
k_{55}	1.3*beam	0 to 400%	50%	0 to 5.2*beam	0.65*beam

Table 9.3: Dynamic stability parametric analysis: parameters analyzed

vehicle cannot reach an equilibrium state, versus the speed range Fn = 1 to Fn = 3.5. The second one shows the same graph, but it focus the attention on the boundary zone between the stable and unstable zone.

9.4.2 Dynamic stability sensitivity

The parameters taken into account in this analysis are summarized in tab. 9.3.

To have a quick comparison between the influence magnitude of each parameter, the derivatives of the critical speed with respect to the value of the parameter are presented in tab. 9.4. For an increase of 100% of each parameter value, it is shown the change of the critical speed, the speed at which the AAMV becomes dynamically unstable. If this value is positive, it means that the critical speed is increased, therefore a positive effect is obtained. If negative, it means that the critical Froude number is decreased, leading to an undesiderable effect. The value is calculated through a speed range where the derivative is approximately constant.

Parameter	Calculation	Average ΔFn_{crit} / 100%
mac	$\frac{1.3-1.5}{150-70} * 100$	- 0.25
η	$\frac{1.42-1.53}{120-0} * 100$	- 0.09
ξ_{ac1}	$\frac{1.4-1.64}{150-(-50)} * 100$	- 0.12
β	$\frac{1.425-1.465}{150-50} * 100$	- 0.04
lcg	$\frac{1.62-1.24}{115-85} * 100$	+ 1.27
mass	$\frac{1.45-1.37}{150-50} * 100$	+ 0.08
k_{55}	$\frac{2.4-1.4}{400-100} * 100$	+ 0.33

Table 9.4: Dynamic stability sensitivity: critical Fn change for an increase of 100%

It should be highlighted that these derivative values are valuable from a qualitative point of view, since their actual values are linked with the stability derivatives estimation method and the geometric characteristics of the model C-01 configuration. Therefore quantitatively no extrapolation for others configurations should be made, but quantitatively these derivatives are a indicator of the parameters that influence the most the dynamic stability of an AAMV configuration.

9.4.2.1 Mean aerodynamic chord (mac)

The length of the mean aerodynamic chord of the wing is the third most important parameter to consider (tab.9.4) in order to analyse the dynamic behaviour of an AAMV, after the longitudinal position of the CG and the pich moment of inertia. As it can be seen in fig. 9.31 and fig. 9.32, if the mac augments, the critical Froude number decreases, therefore has a negative effect on the dynamics.

The value inticated in the table is the average derivative in the parameter range 70% to 150%. For a lower value of the mac the negative effect tens to diminishes, in fact between mac 0% (vehicle without a wing) and 60% the average derivative

is (fig. 9.32):

$$\frac{\Delta Fn_{crit}}{100\%} = -0.07$$

9.4.2.2 Angle between mac and the keel (η)

Fig. 9.33 and fig. 9.34 demonstrates that η has a slight influence on the AAMV dynamic behaviour, about one third if compared to the mac's influence. As the mac influence, increasing η the critical Fn diminishes, leading to a negative effect.

9.4.2.3 Longitudinal position of the aerodynamic center (ξ_{ac1})

ξ_{ac1} influence, represented in fig. 9.35 and fig. 9.36, is about one half of the mac's influence. In particular, if the position of the wing with respect to the hull is shifted forward (ξ_{ac1} increases), the vehicle will become less stable. In fact, the dynamic instability appears at a lower Fn.

9.4.2.4 Deadrise angle of the hull (β)

The effect of the deadrise angle, represented in fig. 9.37 and fig. 9.38, is the lowest among all parameters. It is about one fifth of the mac's influence and if the deadrise angle increases the critical Fn will slightly diminish, leading to a negative effect. Payne conducted a similar analysis of the influence of deadrise angle on the dynamic behaviour of prismatic planing hull (see fig. 13 of [35]), obtaining similar results: the deadrise angle has a slight influence on the dynamic stability of planing craft.

9.4.2.5 Longitudinal position of the center of gravity (lcg)

The longitudinal position of the center of gravity is the most important parameter to take into account in a dynamic stability analysis, as the average derivative value shows (tab. 9.4). It has an influence five times greater than the mac's influence, also if it should be noticed that the lcg cannot be largely varied. In fact if the CG is located in the hull too forward or too rearward, it is not possible to balance all the forces and moments in the longitudinal plane and the system of equations of equilibrium do not have a solution. In any case it remains the most important parameter, as it can be seen in fig. 9.39 and 9.40.

If the CG is shifted forward, the vehicle will experience a positive effect. According to Payne [35] this is a well known effect, as already stated by Savitsky [43], who affirms that a practical rule of thumb to eliminate or at least to diminish the porpoising instability is to move the CG forward.

9.4.2.6 Mass (m)

The mass is an important parameter to take into account in this analysis, but it has only a light positive effect on the dynamic stability, comparable to the effect of η (only as absolute value, the sign is opposite). As shown in fig. 9.41 and fig. 9.42, if the mass of the AAMV is diminished or augmented of 50% with respect to the C-01 mass, the critical Froude number will change, respectively, of - 0.07 and + 0.01. Also, as already said, these value cannot be taken to extrapolate a quantity for another AAMV configuration, qualitatively they indicates that the dependence of dynamic stability on the mass is lower than the dependence on other parameters.

This low dependence of the dynamic stability on the mass is a positive aspect.

In fact it extends the range of payload in which the dynamics characteristics do not substantially vary. From a customer point of view, a high dependence of the vehicle characteristics on the load is a negative aspect, since the desired behavior is constant performance.

9.4.2.7 Pitch radius of gyration (k_{55})

Referring to fig. 9.43, to fig. 9.44 and to tab. 9.4, the pitch radius of gyration is the second most important parameter, after lcg, from the dynamic stability point of view. If the value of the pitch moment of inertia increases, the critical Fn increases, leading to a positive effect.

As the longitudinal position of the CG, this is another well known effect (Payne [35], Savitsky [43]).

9.5 Conclusions

9.5.1 Resistance-to-weight ratio optimization

A general observation can be made for all the parametric analysis. The use of a wing can influence positively or negatively the behavior of an AAMV, therefore the characteristics of the wing have to be chosen carefully. In particular under a certain speed, dependent on which parameters are under analysis, it is disadvantageous to use an aerodynamic surface: the hydrodynamic efficiency is diminished, leading to an increased drag force having the same lift force, therefore having a worse R / W ratio. The main reason is the influence of the wing on the trim equilibrium attitude angle: it tends to increase it, leading to all these

negative consequences. Above this 'critical speed' the opposite situation happens: aerodynamic forces start to give their positive contribution, diminishing the R / W ratio. For these reasons, the key rule to choose the value of the parameter analyzed should be this one:

- to minimize, below critical speed, the influence of the wing,
- to maximize, above critical speed, the influence of the wing.

It should be noted that this is valid strictly from the R/W ratio point of view, but it can be counterproductive to think only about total resistance. Fig. 9.4 can illustrate this aspect. It can be seen that the configuration with the biggest wing has a critical Froude number lower than the other configurations (about Fn = 2.8), and this is a good aspect, since the lower is the speed at which the vehicle starts to experience a lower resistance (compared with the configuration without any wing) the better is. Anyway it can be seen also that, at a certain speed, the wing is so big that the aerodynamic pitch up moment cannot be balanced by the remaining moments about the CG. This means that the AAMV with the biggest wing *potentially* would have, at high speed, the lowest R/W ratio, but cannot reach the speed range where this happens.

At this point a configuration optimized with regard the resistance-to-weight ratio, called C-02, can be proposed. This configuration will be compared against the planing hull configuration of Savitsky [46], called C-00. To highlight the advantages given solely by the additional aerodynamic surface, the configuration C-02 is identical to C-00 as regard the propulsion, inertial and hydrodynamic characteristics, as it can be seen in tab. 9.5. The planing hull (C-00) configuration characteristics are illustrated in fig. 9.45, and the C-02 (Glenn Martin aerodynamic profile) characteristics are illustrated in fig. 9.46. As regard the C-02 aerodynamic characteristics, a trade-off value between the enhancement at high

speed of the wing positive influence and the danger of an excessive aerodynamic pitch up moment is chosen, as previously explained.

9.5.1.1 C-02 configuration performances

The comparison between the planing craft (C-00) and the AAMV (C-02) performances are illustrated in fig. 9.47 through fig. 9.53. As it can be seen, the configuration with a wing has, for the same speed:

- a higher trim equilibrium attitude,
- a lower draft at transom (for Fn $\geq$ 2),
- a higher CG position above the surface,
- a lower keel and chine wetted length.

As regard the Resistance-to-weight ratio, the speed range can be divided in two regions:

- 1 $\leq$ Fn $\leq$ Fn*, C-02 disadvantageous,
- Fn $\geq$ Fn*, C-02 advantageous.

Fn*, the critical speed, is about 3. Analyzing the numerical values presented in tab. 9.6, it can be seen that choosing carefully the aerodynamic surface characteristics (chord length, angle between the keel and the aerodynamic chord, position of the aerodynamic center, etc.), the R / W difference between the two configurations has been minimized in the "disadvantageous" speed range (Fn $\leq$ Fn*) and maximized in the "advantageous" speed range (Fn $\geq$ Fn*).

Characteristics		Dimensional		Dimensionless		
Configuration		C-00	C-02		C-00	C-02
GEOMETRY						
Propulsion						
	ξ_{TP}	0 [m]		$\frac{\xi_{TP}}{B}$	0	
	ζ_{TP}	0 [m]		$\frac{\zeta_{TP}}{B}$	0	
	ϵ_{TP}	12 [deg]		/	/	
Aerodynamic						
	First surface					
	mac	na	20 [m]	$\frac{mac}{B}$	na	3.606
	S_{a1}	na	400 [m^2]	$\frac{S_{a1}}{B^2}$	na	13
	η_{a1}	na	8 [deg]	/	na	/
	ξ_{ac1}	na	15 [m]	$\frac{\xi_{ac1}}{B}$	na	1.803
	ζ_{ac1}	na	-2 [m]	$\frac{\zeta_{ac1}}{B}$	na	-0.361
	profile	na	Glenn Martin 21, with endplate [2]			
Hydrodynamic						
	B (beam)	5.547 [m]		$\frac{B}{B}$	1	
	β	14 [deg]		/	/	
	A_h	20.067 [m^2]		$\frac{A_h}{B^2}$	0.652	
INERTIAL CHAR.						
	lcg	8.656 [m]		$\frac{lcg}{B}$	1.560	
	vcg	1.387 [m]		$\frac{vcg}{B}$	0.250	
	m (mass)	52160 [kg]		$\frac{m}{\rho_{sw}*B^3}$	0.298	
	$I_{55} = m * k_{55}^2$	2712318.1 [kg*m^2]		$\frac{k_{55}}{B}$	1.3	

Table 9.5: Planing hull configuration (C-00) vs AAMV configuration (C-02)

Fn	R/W		$\Delta_{R/W} = \frac{R/W_{C-02} - R/W_{C-00}}{R/W_{C-00}}$
	C-00	C-02	
1.0	0.068	0.072	+ 5.92 %
1.5	0.097	0.107	+ 10.61 %
2.0	0.120	0.132	+ 9.86 %
2.5	0.137	0.144	+ 5.02 %
3.0	0.156	0.155	- 0.64 %
3.5	0.182	0.169	- 7.52 %
4.0	0.216	0.181	-16.50 %
4.5	0.258	0.181	-29.77 %

Table 9.6: Resistance-to-weight ratio comparison, C-00 vs C-02

The configuration with the wing (C-02) experiences an increased drag with respect to the wingless configuration (C-00) for Fn $\leq$ Fn*, with a maximum at Fn = 1.7 ($\Delta_{R/W}$ = + 11.26 %), but in the advantageous speed range (Fn $\geq$ Fn*) the decrease of the resistance of the C-02 is, in module, much higher ($\Delta_{R/W}$ = - 29.77 % at Fn = 4.5).

This advantage is due to a higher total efficiency (defined as the ratio between the total lift and the total drag) of the C-02 configuration for a Fn $\geq$ Fn* (fig. 9.53). In fact, this lead to a lower total drag (fig. 9.51) experienced by the configuration with the wing.

9.5.1.2 Use of a DHMTU profile

As previously stated, the parametric analysis is conducted using a very poor efficiency aerofoil, a Glenn Martin 21, with endplates [2]. The reason is that it is very difficult to find, in the public domain, any experimental data on aerodynamic

profiles flying in ground effect, with or without endplates. As it can be seen in fig. 9.53, the aerodynamic efficiency of this profile, defined as the ratio between aerodynamic lift and drag, is about 5 through the entire speed range.

The Glenn Martin 21 was not designed to operate in ground effect, furthermore the aspect ratio of the tested wing is very low, around 1. For these reasons, its performances in this peculiar situation are very poor. In former Soviet Union, the Department of Hydro-mechanics of the Marine Technical University developed a series of profiles expressly designed for the Wing In Ground effect state. They are called DHMTU series, and several experimental campaigns have been carried out. Unfortunately very little detailed information on the performance of these sections have been published.

Only one paper has been found, presenting experimental data of one profile of the DHMTU family, obtained by N. Moore during his PhD at Southampton University, in 2002 [32]. Unfortunately the author found this article too late to fully integrate these useful data in the parametric analysis, and the C-02 configuration has been defined considering the results obtained using the Glenn Martin 21 profile. It has to be specified that the aspect ratios used in the present work, respectively 1 for the Glenn Martin profile and 3 for the DHMTU profile, have been chosen in accord with the geometrical characteristics of the models used in the relative experiments. The superior aerodynamic characteristics of the DHMTU profile are due also to this difference. Anyway, in order to compare the performance of the two different profiles, the author chose to keep equal the surface area of the two wings (396.75 m^2 for the DHMTU and 400 m^2 for the Glenn Martin), as shown in tab. 9.7.

In fig. 9.55 through fig. 9.60 are presented the graphs of the comparison between the planing craft configuration (C-00), the AAMV configuration C-02 with the Glenn Martin profile and the AAMV new configuration C-02 DHMTU, equipped

with the DHMTU profile analyzed by Moore in [32]. In tab. 9.7 are compared the two AAMV configurations, C-02 Glenn Martin and C-02 DHMTU, and in fig. 9.61 and fig. 9.62 are shown, respectively, the C-02 DHMTU configuration characteristics and a comparison between the C-02 configuration with the Glenn Martin profile (C-02 GM) and the C-02 configuration with the DHMTU profile (C-02 DHMTU).

The trim angle of C-02 DHMTU configuration is even higher than the C-02 GM configuration (fig. 9.55), also if for a fraction of a degree. Furthermore, C-02 DHMTU presents a lower draft at the transom (Fn $\geq$ 2) and a higher position of the CG above the surface than the other two configurations (fig. 9.54). The keel and chine wetted length, respectively L_K L_C in fig. 9.56, are both shorter using a DHMTU profile, yielding a reduced hydrodynamic friction drag. As shown in fig. 9.58, the use of a DHMTU profile instead of a Glenn Martin profile diminishes the aerodynamic drag and the hydrodynamic drag of the AAMV. Furthermore (fig. 9.60) this reduced drag is obtained also because of the much higher aerodynamic efficiency of the DHMTU profile (around 8) with respect to the Glenn Martin aerodynamic efficiency. It can be observed that while Glenn Martin aerodynamic efficiency is lower than the hydrodynamic efficiency, and being so it diminishes the total efficiency, the DHMTU aerodynamic efficiency , for Fn $\geq$ 1.7, raises the total efficiency.

The DHMTU profile is better than the Glenn Martin profile as regards all these aspects, and the superior performances are summarized in fig. 9.57, where the resistance-to-weight ratio curve of each configuration is shown. At high speed the C-02 DHMTU configuration experiences a lower total resistance than the C-02 Glenn Martin configuration. Furthermore, the critical speed, the speed at which the hybrid vehicle configuration becomes convenient compared with the simple planing hull, is much lower for the C-02 DHMTU configuration (Fn* = 2.4) than

Configuration characteristics	Dimensional		Dimensionless		
	C-02 DHMTU	C-02 Glenn Martin		C-02 DHMTU	C-02 GM
GEOMETRY					
Propulsion					
ξ_{TP}	0 [m]		$\frac{\xi_{TP}}{B}$	0	
ζ_{TP}	0 [m]		$\frac{\zeta_{TP}}{B}$	0	
ϵ_{TP}	12 [deg]		/	/	
Aerodynamic					
First surface					
mac	11.50 [m]	20 [m]	$\frac{mac}{B}$	2.073	3.606
S_{a1}	396.75 [m^2]	400 [m^2]	$\frac{S_{a1}}{B^2}$	12.89	13
η_{a1}	3 [deg]	8 [deg]	/	/	/
ξ_{ac1}	15 [m]	15 [m]	$\frac{\xi_{ac1}}{B}$	1.803	1.803
ζ_{ac1}	-2 [m]	-2 [m]	$\frac{\zeta_{ac1}}{B}$	-0.36	-0.36
profile	DHMTU 12-35.3-10.2-80.12	Glenn Martin 21, with endplate			
Hydrodynamic					
B (beam)	5.547 [m]		$\frac{B}{B}$	1	
β	14 [deg]		/	/	
A_h	20.067 [m^2]		$\frac{A_h}{B^2}$	0.652	
INERTIAL CHAR.					
lcg	8.656 [m]		$\frac{lcg}{B}$	1.560	
vcg	1.387 [m]		$\frac{vcg}{B}$	0.250	
m (mass)	52160 [kg]		$\frac{m}{\rho_{sw}*B^3}$	0.298	
$I_{55} = m * k_{55}^2$	2712318.1 [kg*m^2]		$\frac{k_{55}}{B}$	1.3	

Table 9.7: C-02 with DHMTU profile configuration vs C-02 with Glenn Martin profile configuration

for the C-02 GM configuration (Fn* = 3).

9.5.2 Dynamic stability optimization

Three are the analyzed parameters linked with the aerodynamic surface: the mean aerodynamic chord (mac), the angle between the keel of the hull and the mac (η), and the longitudinal position of the aerodynamic center (ξ_{ac1}). As it can be seen in tab. 9.4, η and ξ_{ac1} influences are about -0.10, meaning that for an increase of 100% of these parameters the critical Froude number, the speed at which the vehicle becomes unstable, decreases by 0.10. It is a slight negative effect. The influence of mac is stronger, around -0.25, and this is a very important parameter. In fact, to enhance the equilibrium attitude performances of the AAMV the mac length should be augmented, but it is the opposite from the point of view of dynamic stability. Therefore a convenient trade-off should be estimated during the design preliminary phase.

The other parameters investigated, linked with inertial (longitudinal position of the center of gravity (lcg), mass (m), pitch radius of gyration (k_{55})) or geometrical (deadrise angle, (β)) characteristics, show influences similar to the usual planing craft dynamics characteristics. Briefly, the most adopted approach to avoid porpoising instability is to shift the CG forward to augment the pitch moment of inertia, as already demonstrated by Savitsky [43] and Payne [35].

It should be noted that, as stated in section 9.4.2, quantitatively these results are strongly dependent on the aerodynamic, hydrodynamic and inertial characteristics of the vehicle, and also on the degree of approximation of the stability derivatives estimation method used. Therefore these numerical results should not be used for interpolation or extrapolation methods. Nonetheless, qualitatively a comparison analysis is conducted, and the results of this analysis can be used as a design tool

both to acquire experimental data and to design high speed marine vehicles with aerodynamic surfaces.

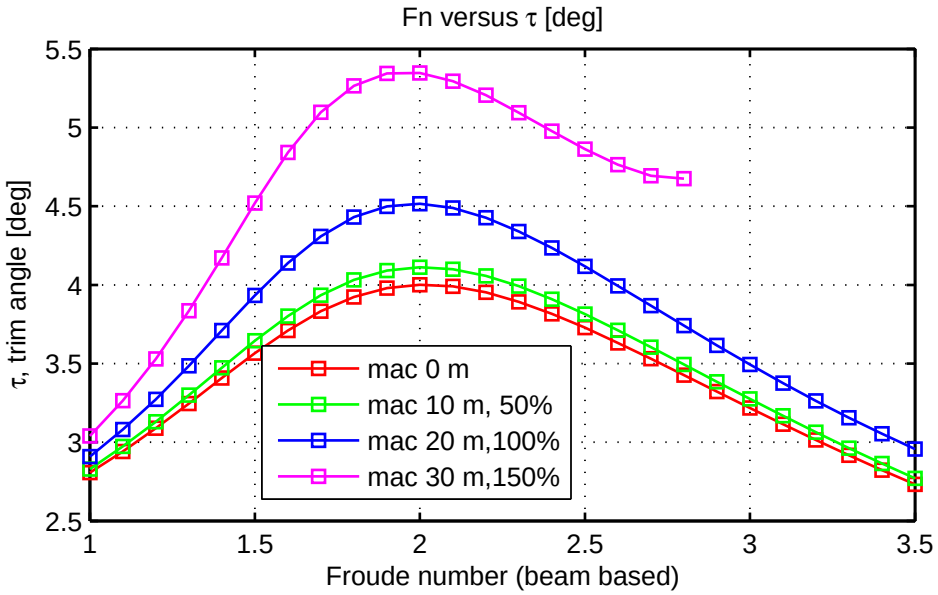

Figure 9.1: m.a.c. analysis: trim angle

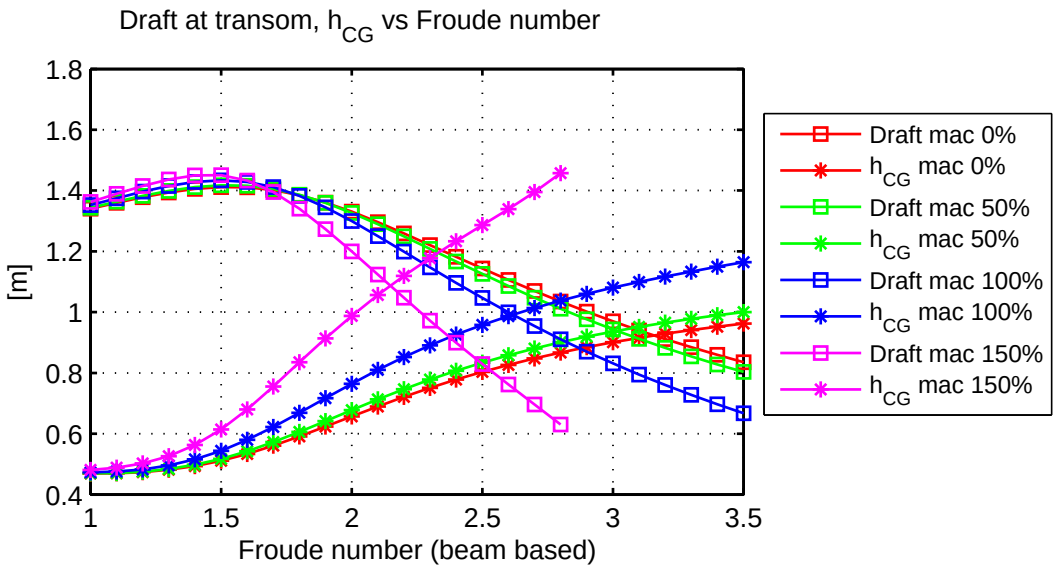

Figure 9.2: m.a.c. analysis: draft at transom & CG height above surface

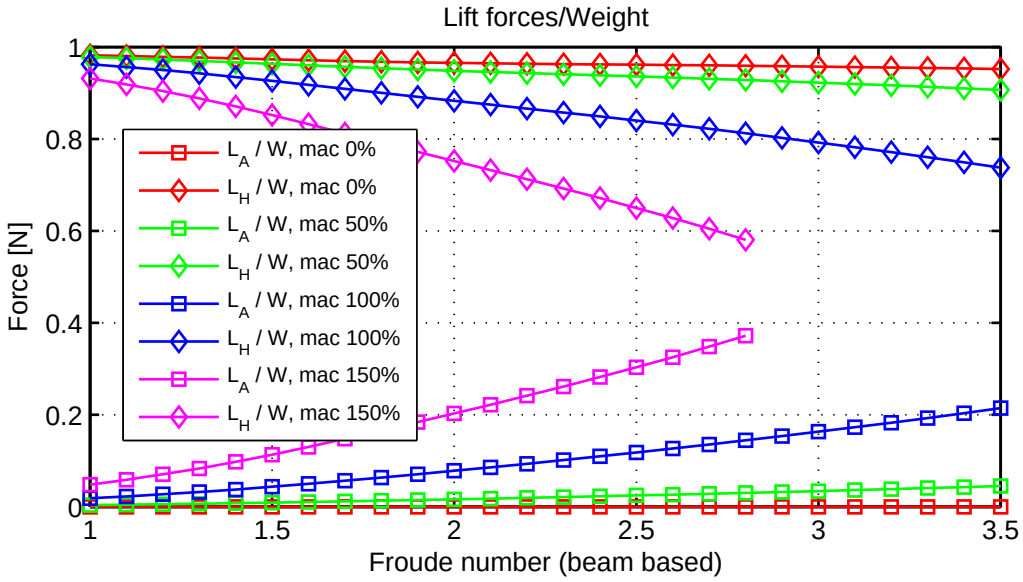

Figure 9.3: m.a.c. analysis: aerodynamic lift and hydrodynamic lift over weight

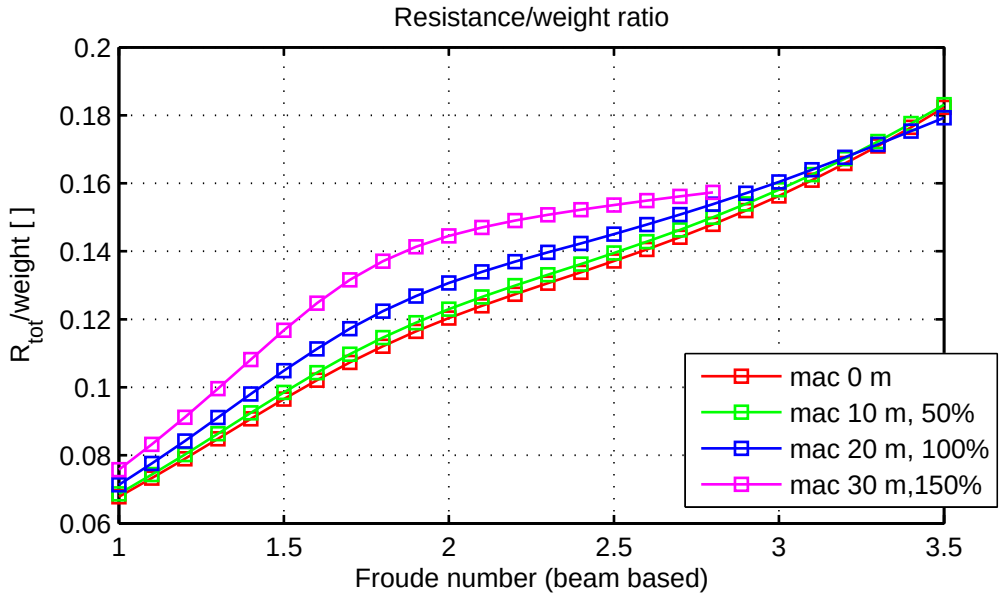

Figure 9.4: m.a.c. analysis: resistance-to-weight ratio

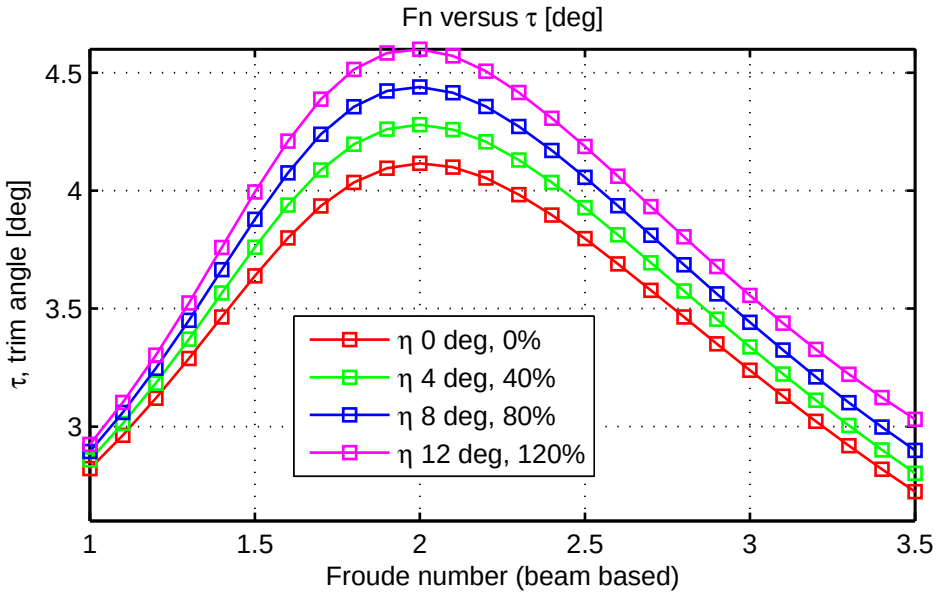

Figure 9.5: η analysis: trim angle

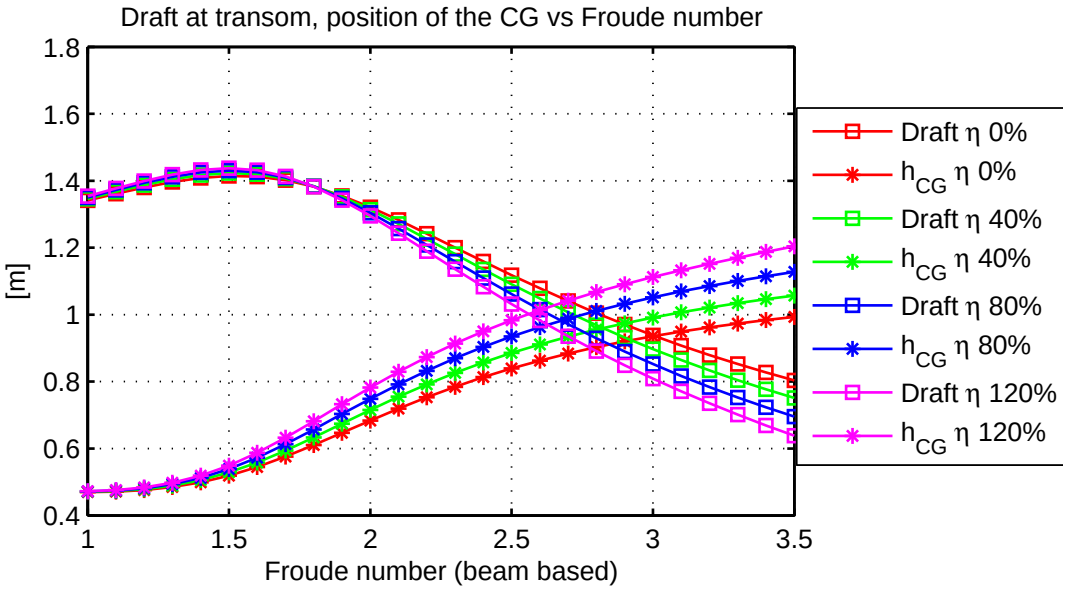

Figure 9.6: η analysis: draft at transom & CG height above surface

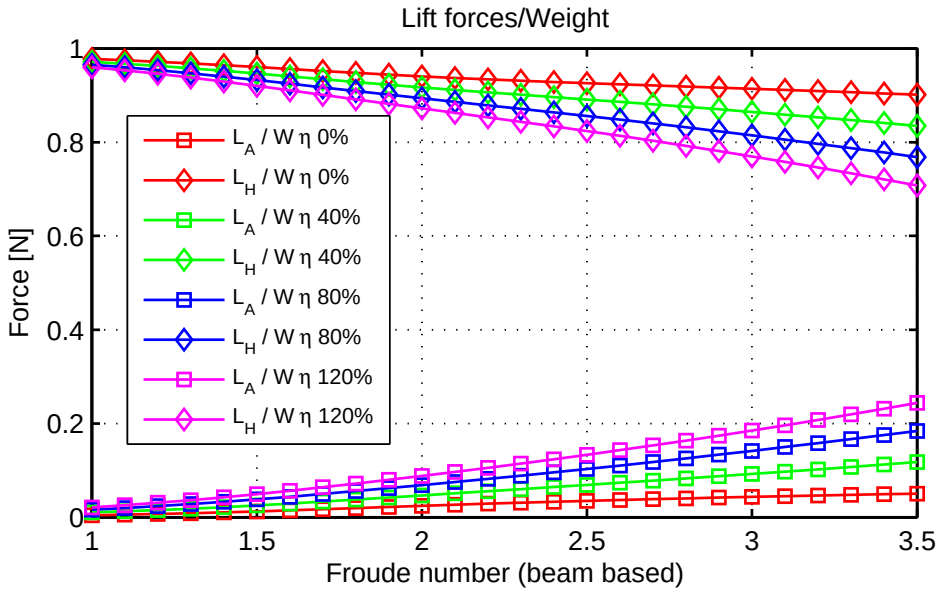

Figure 9.7: η analysis: aerodynamic lift and hydrodynamic lift over weight

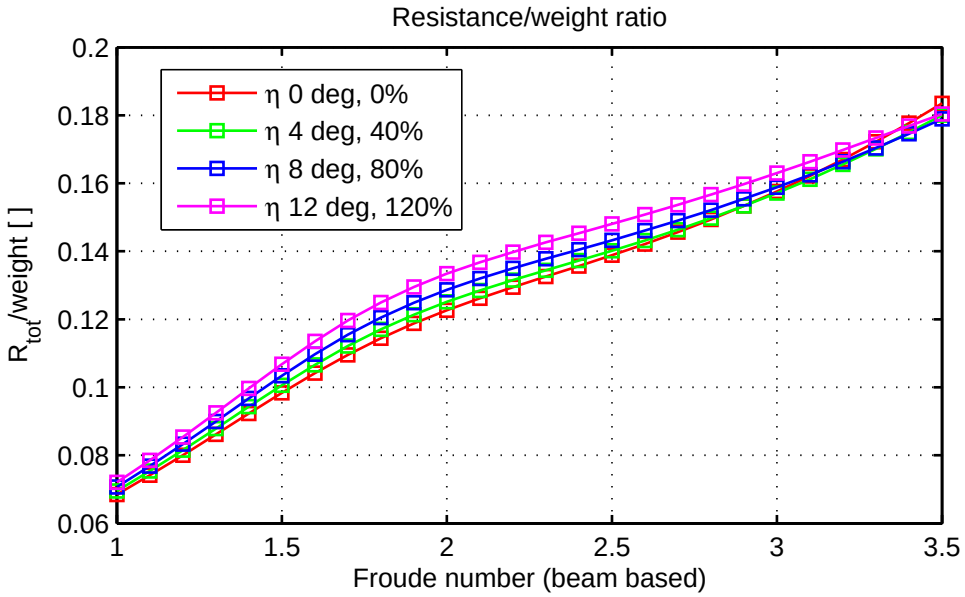

Figure 9.8: η analysis: resistance-to-weight ratio

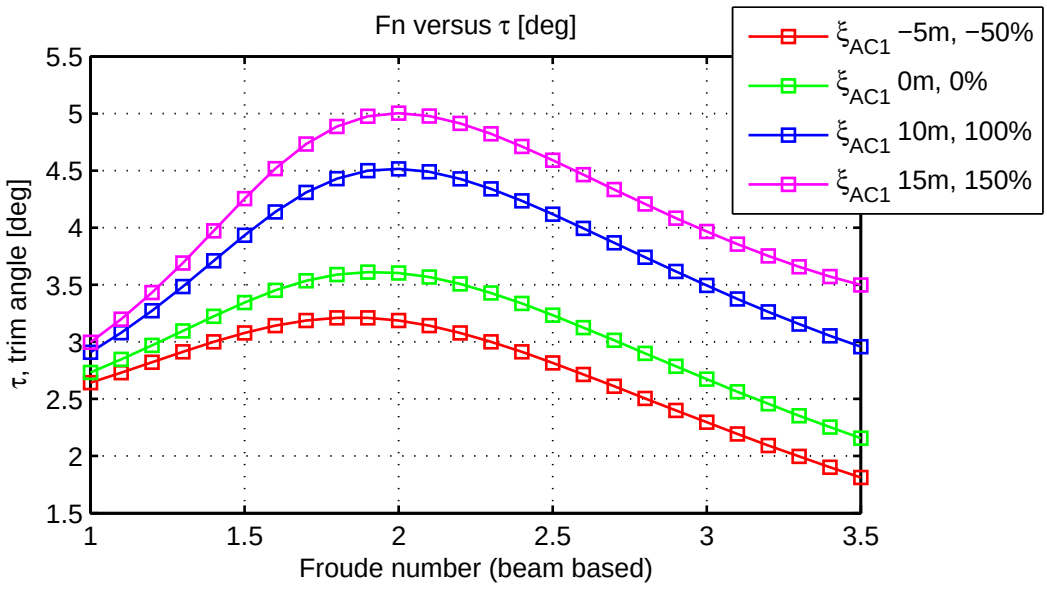

Figure 9.9: ξ_{AC1} analysis: trim angle

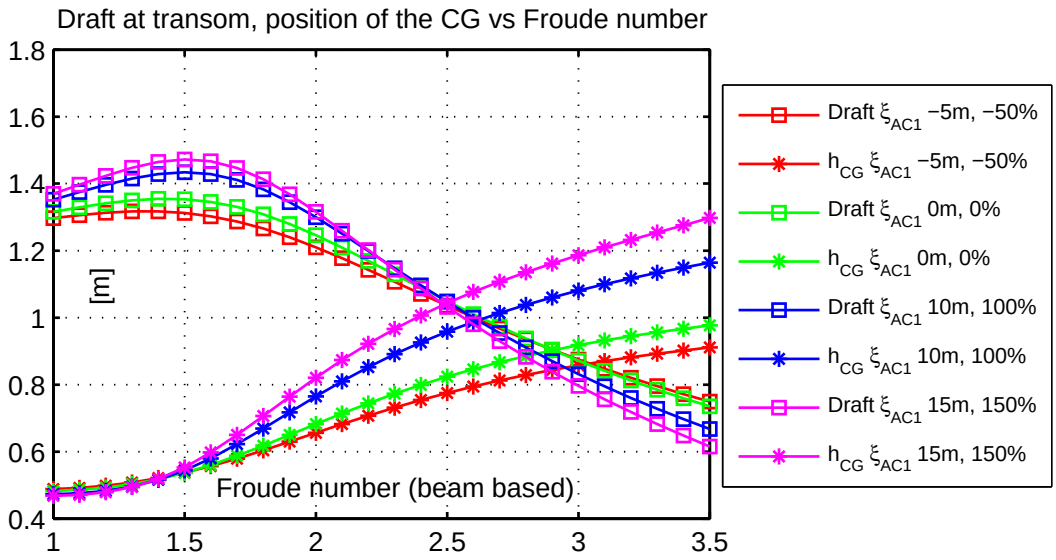

Figure 9.10: ξ_{AC1} analysis: draft at transom & CG height above surface

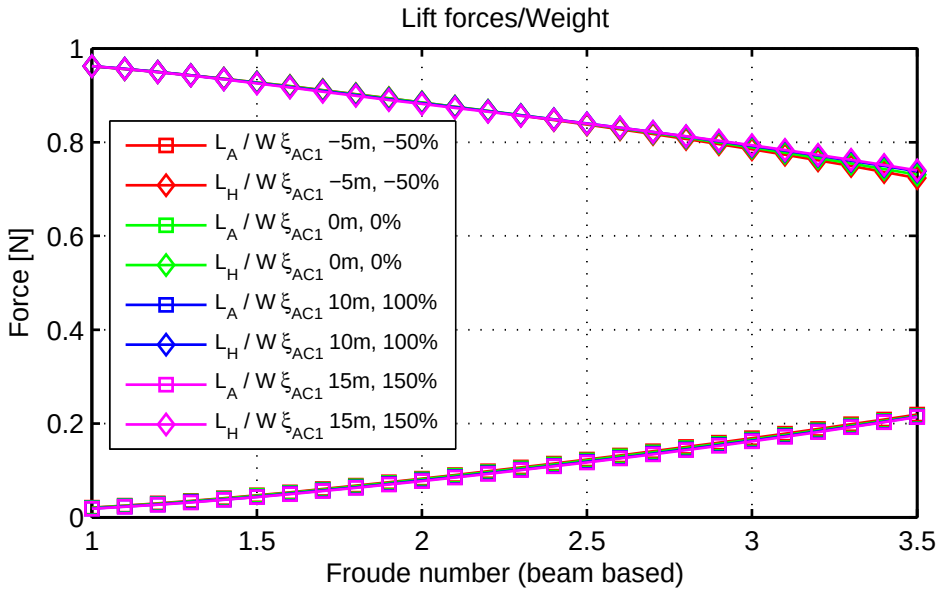

Figure 9.11: ξ_{AC1} analysis: aerodynamic lift and hydrodynamic lift over weight

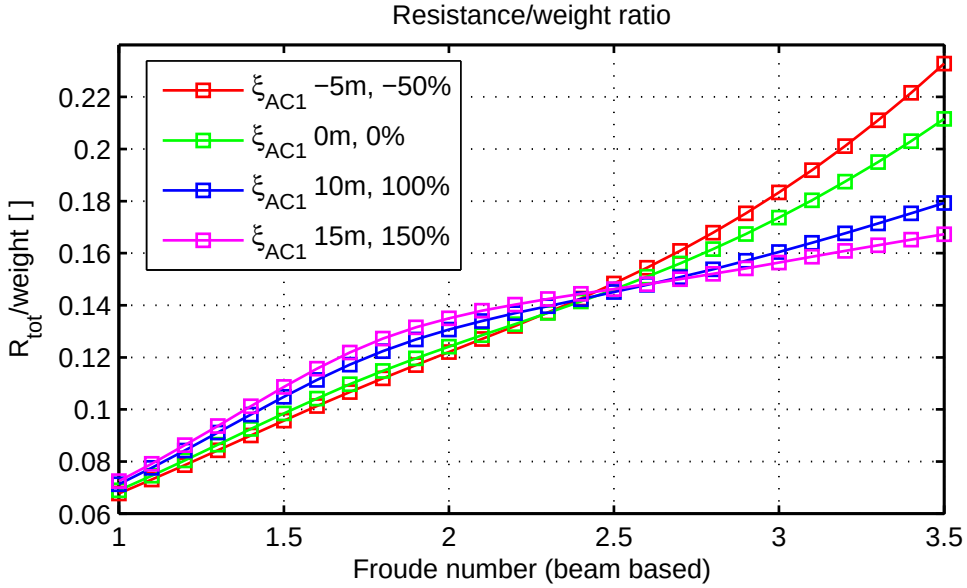

Figure 9.12: ξ_{AC1} analysis: resistance-to-weight ratio

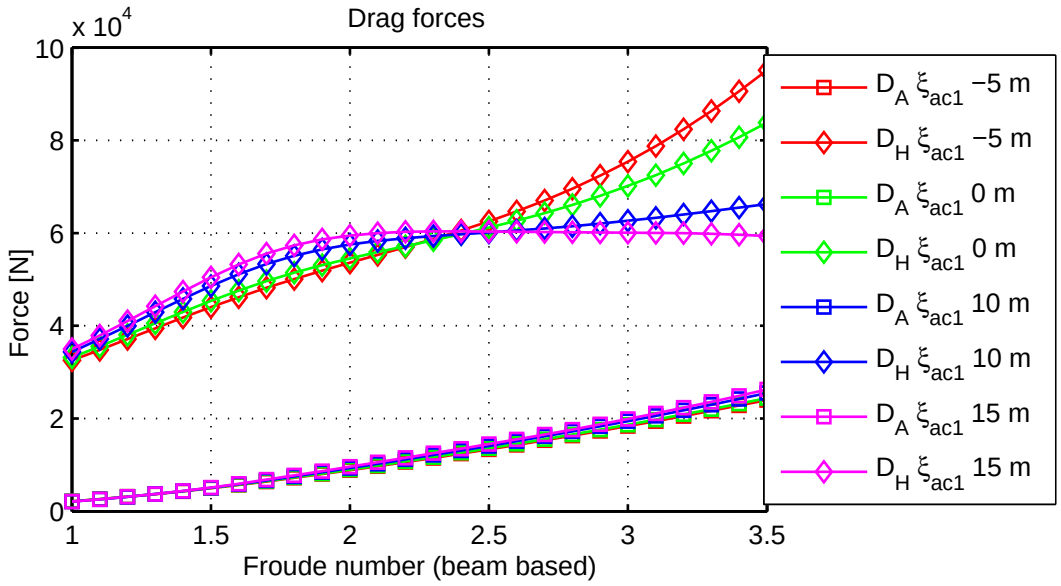

Figure 9.13: ξ_{AC1} analysis: drag forces

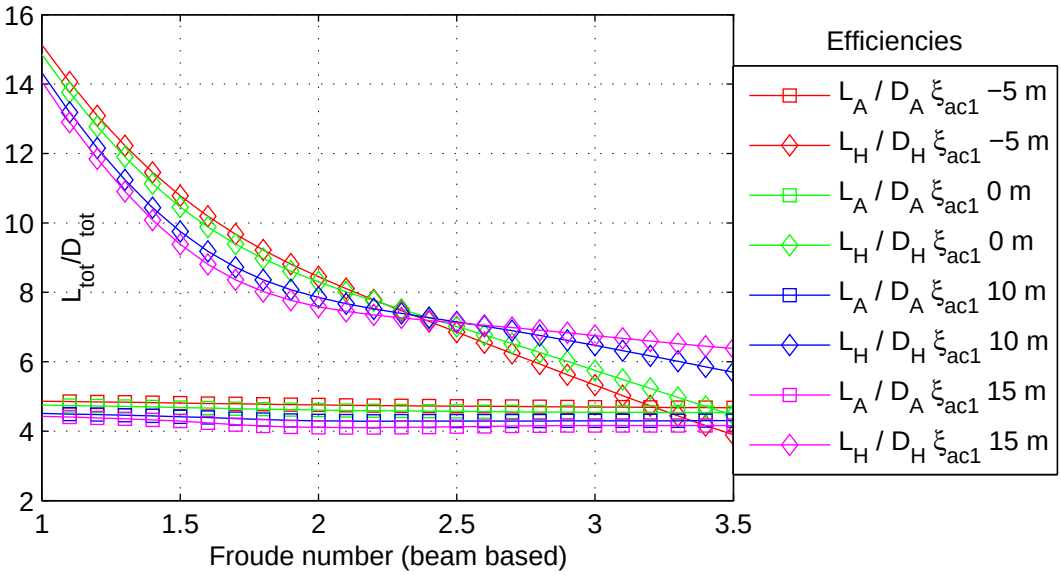

Figure 9.14: ξ_{AC1} analysis: aero- and hydrodynamic efficiencies

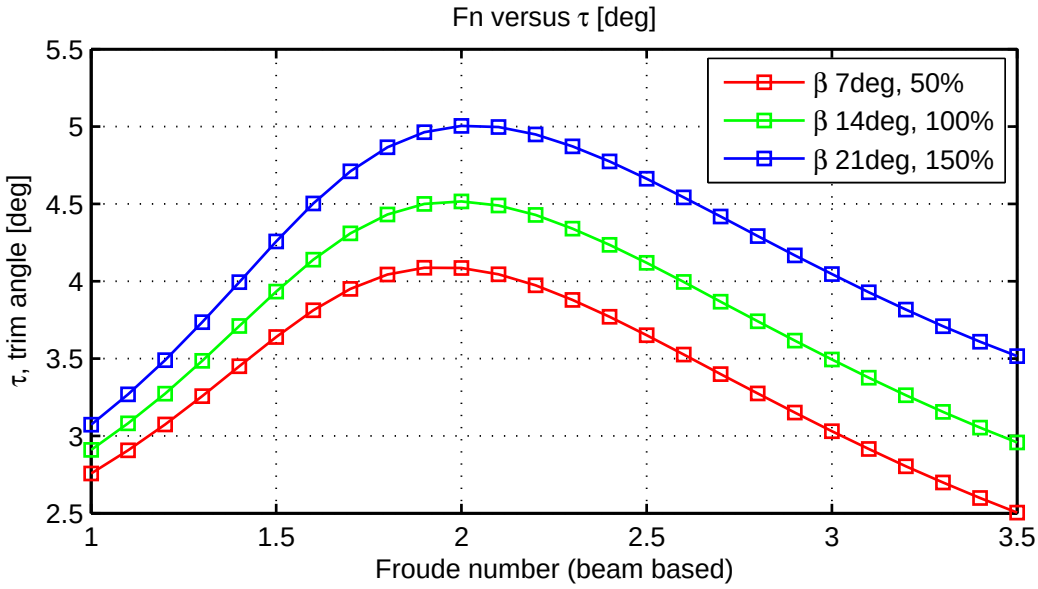

Figure 9.15: β analysis: trim angle

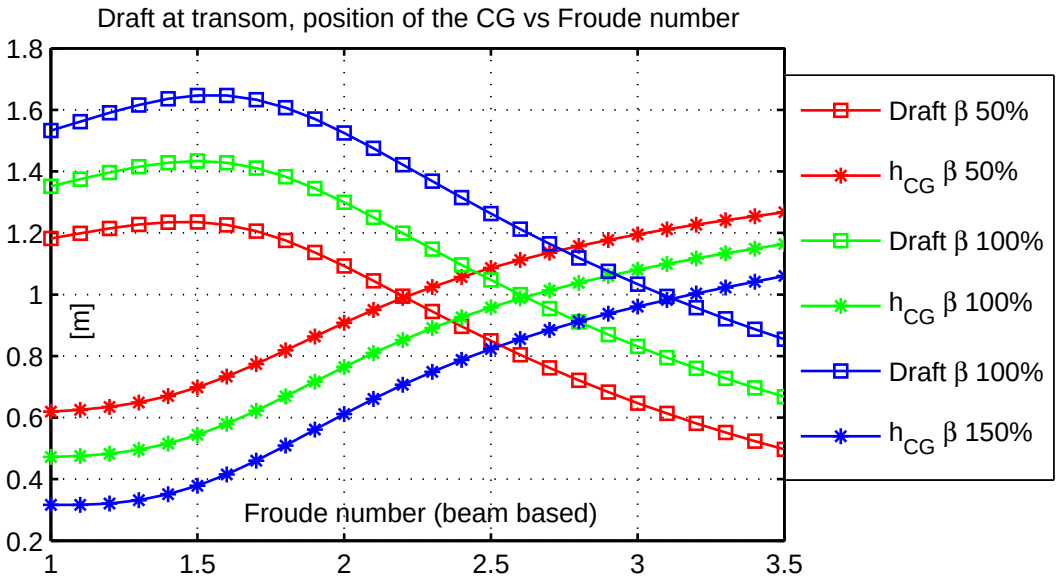

Figure 9.16: β analysis: draft at transom & CG height above surface

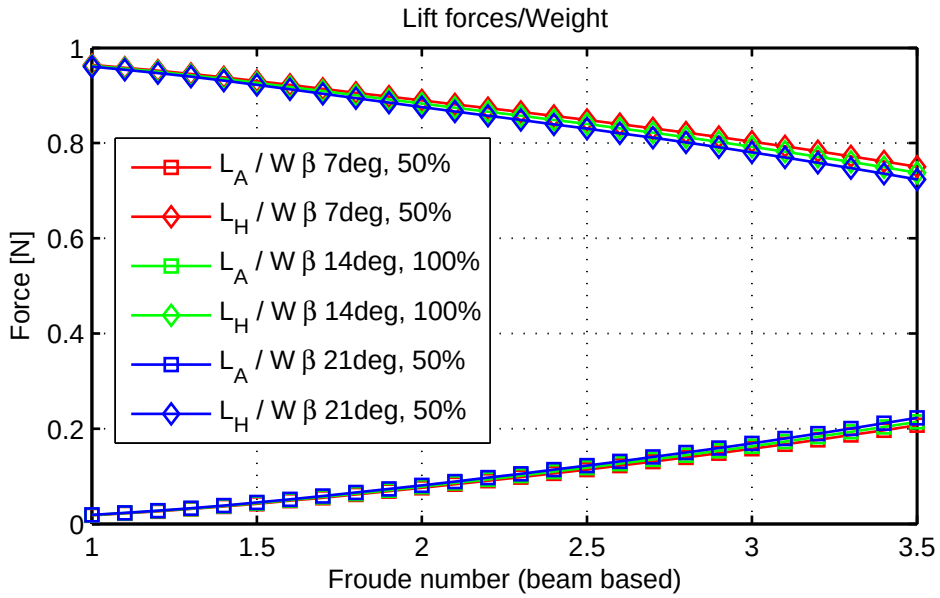

Figure 9.17: β analysis: aerodynamic lift and hydrodynamic lift over weight

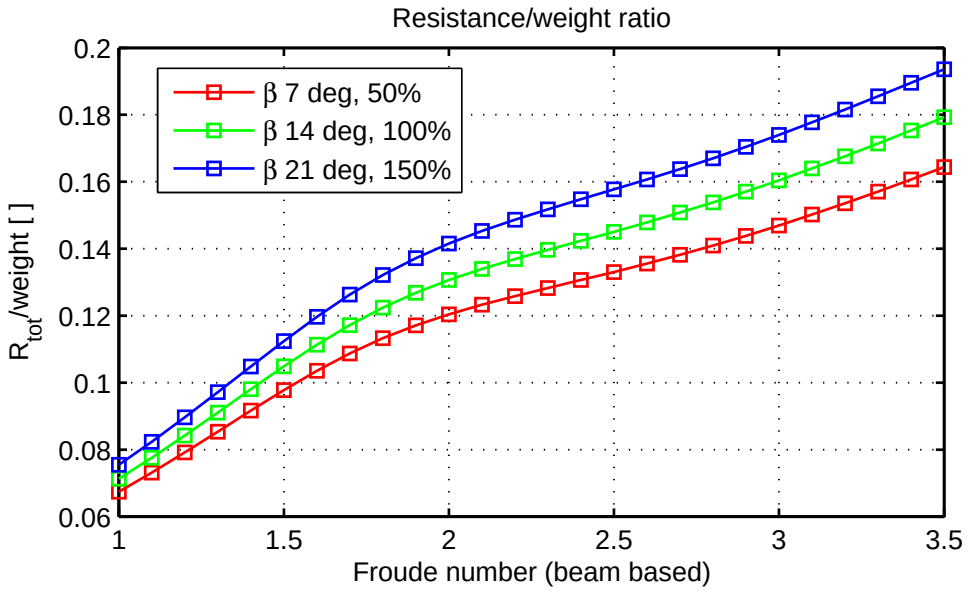

Figure 9.18: β analysis: resistance-to-weight ratio

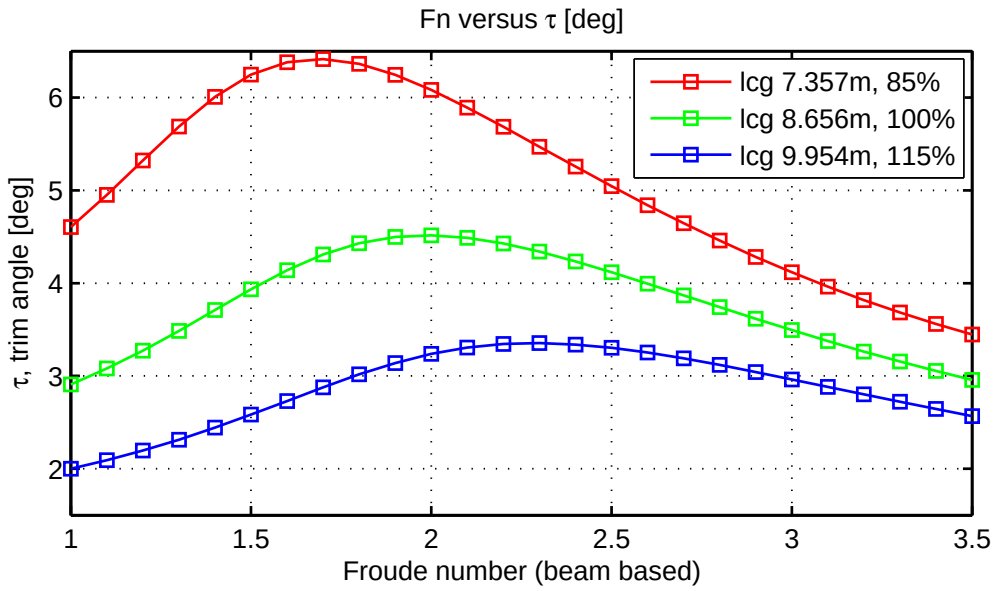

Figure 9.19: lcg analysis: trim angle

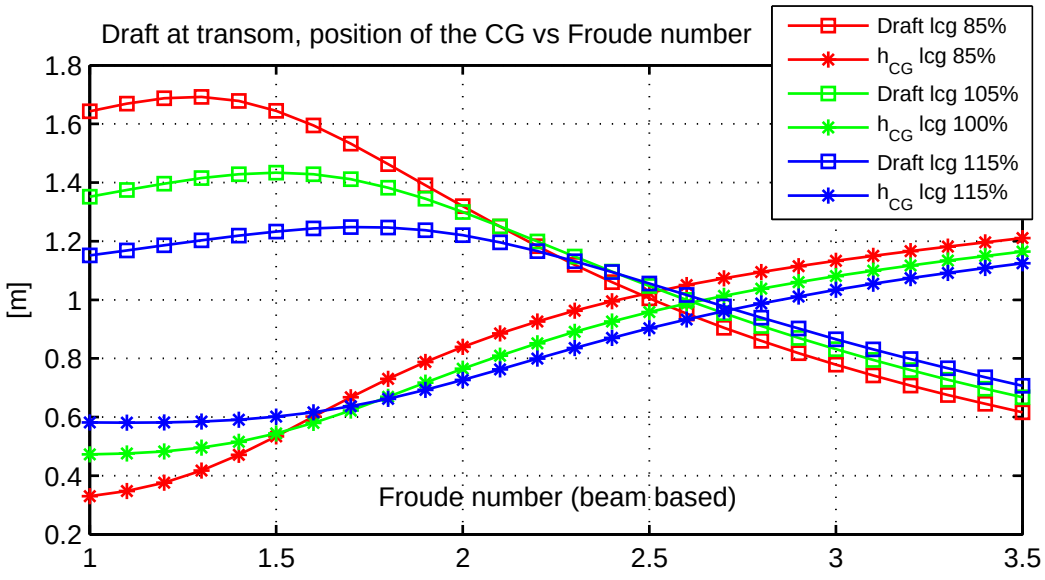

Figure 9.20: lcg analysis: draft at transom & CG height above surface

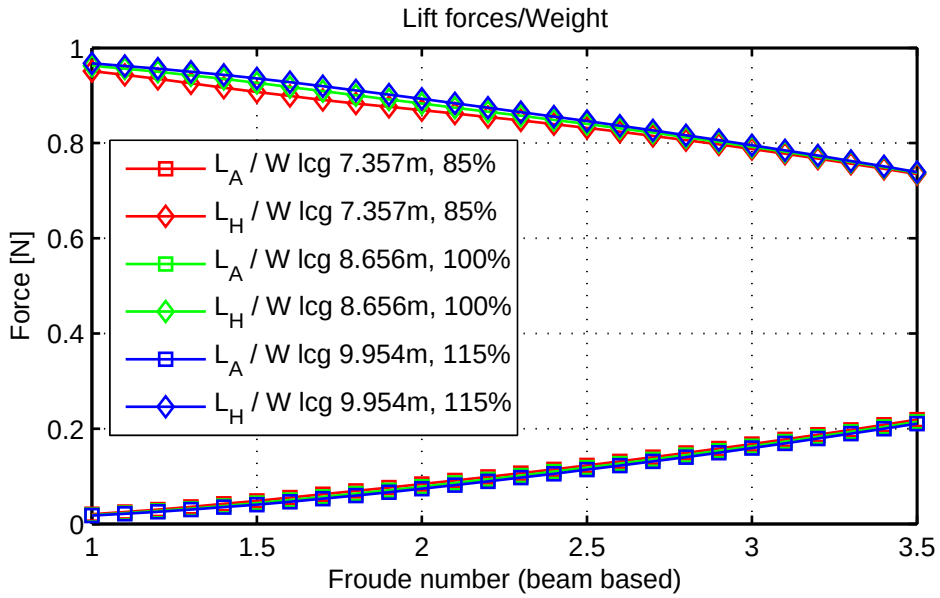

Figure 9.21: lcg analysis: aerodynamic lift and hydrodynamic lift over weight

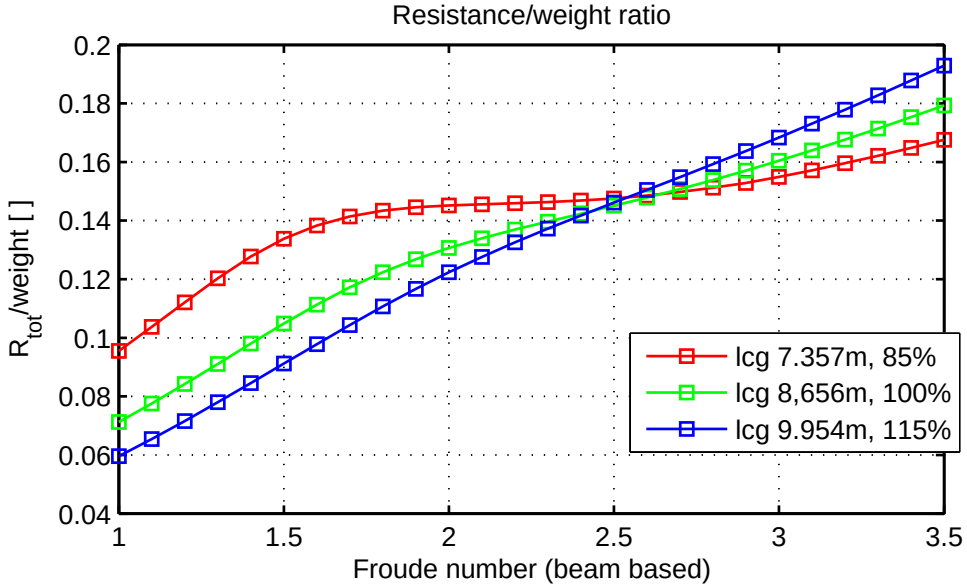

Figure 9.22: lcg analysis: resistance-to-weight ratio

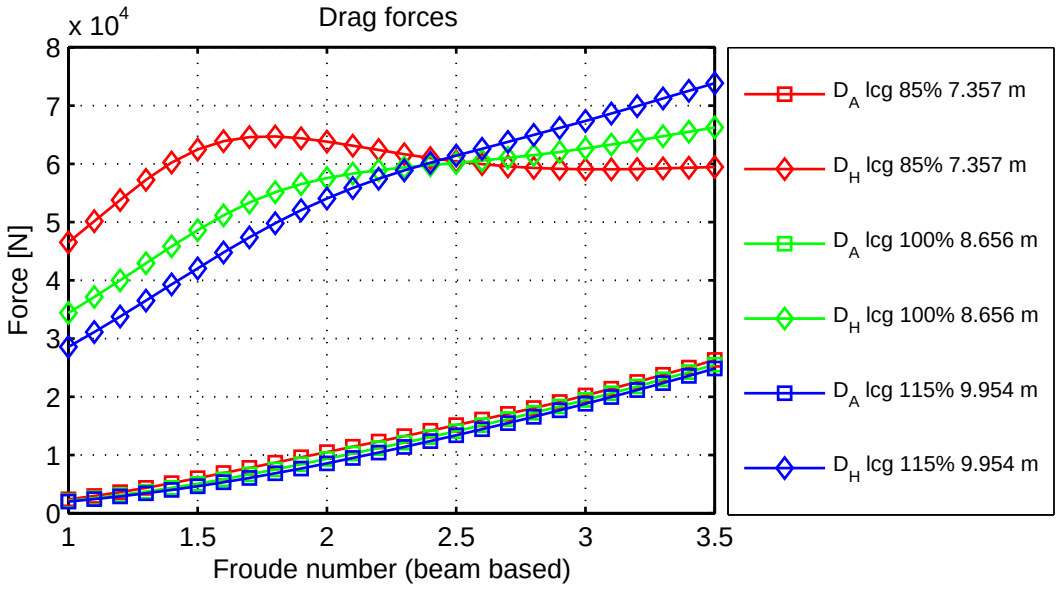

Figure 9.23: lcg analysis: drag forces

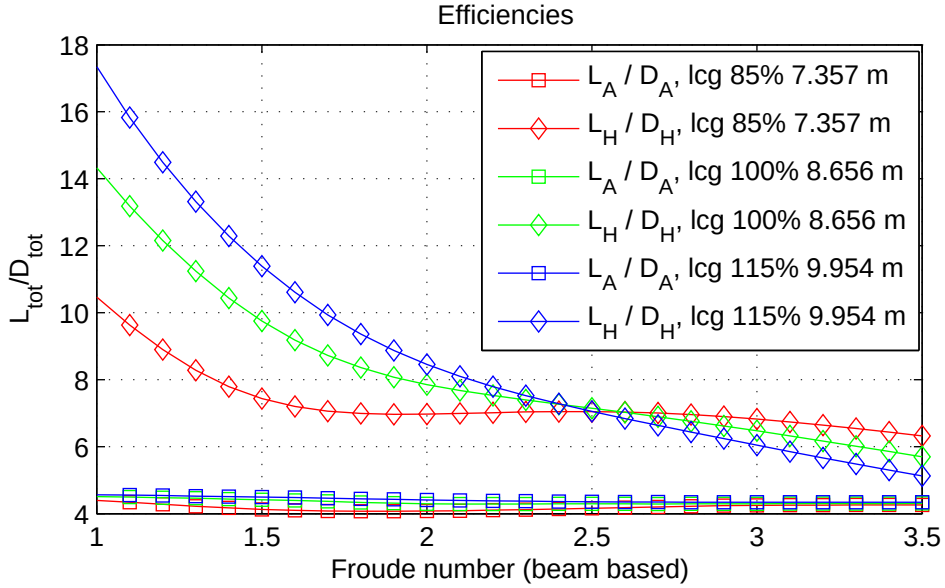

Figure 9.24: lcg analysis: aero- and hydrodynamic efficiencies

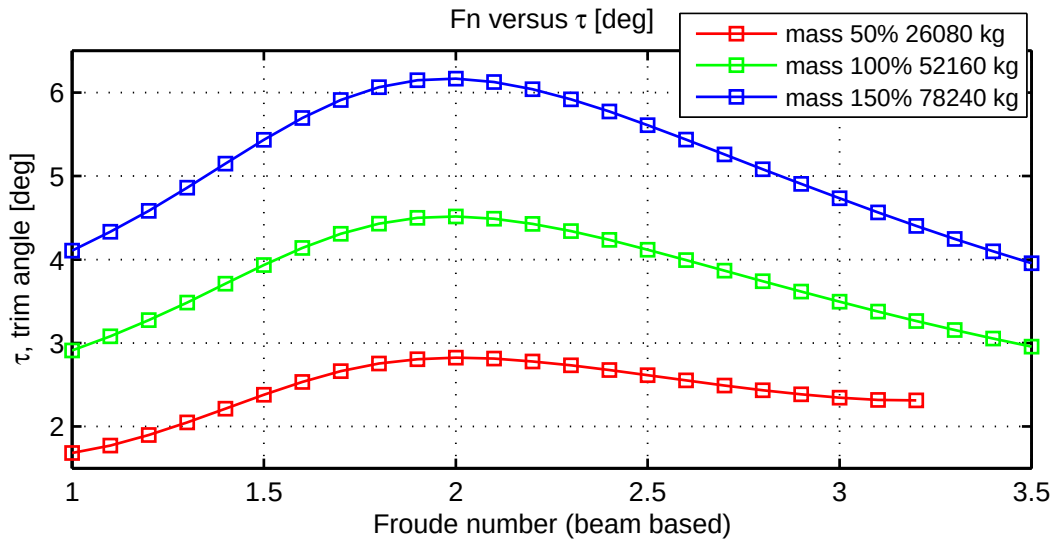

Figure 9.25: m analysis: trim angle

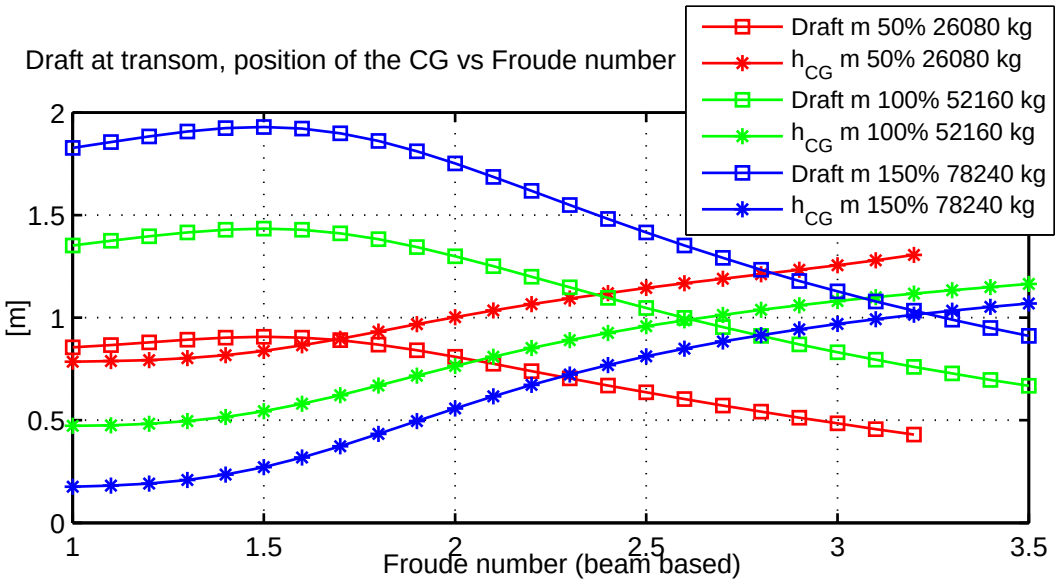

Figure 9.26: m analysis: draft at transom & CG height above surface

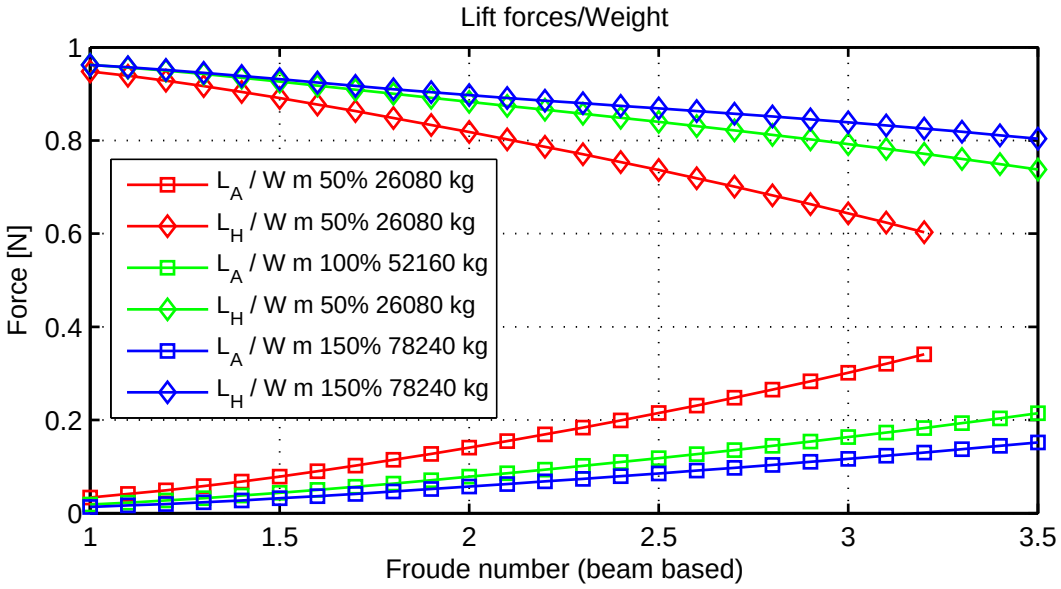

Figure 9.27: m analysis: aerodynamic lift and hydrodynamic lift over weight

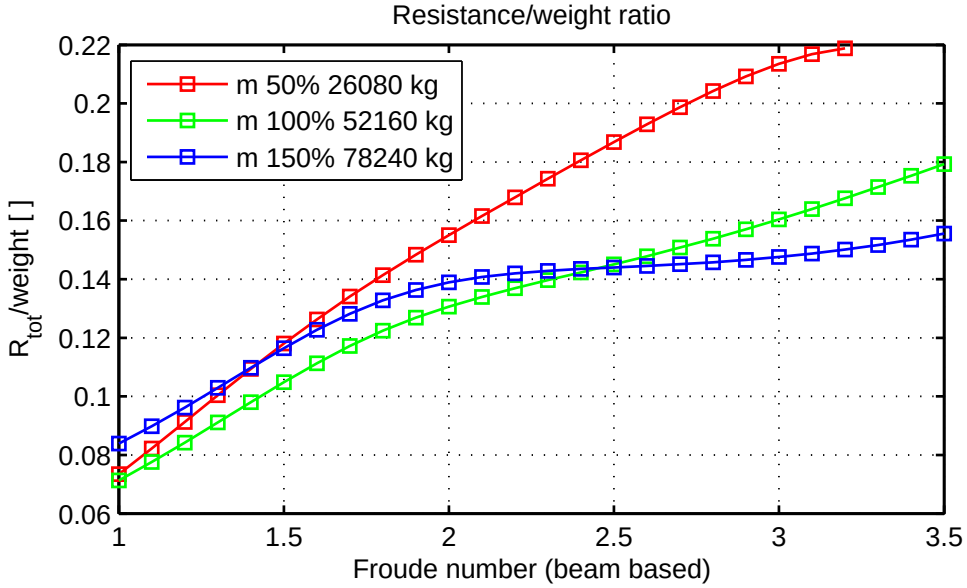

Figure 9.28: m analysis: resistance-to-weight ratio

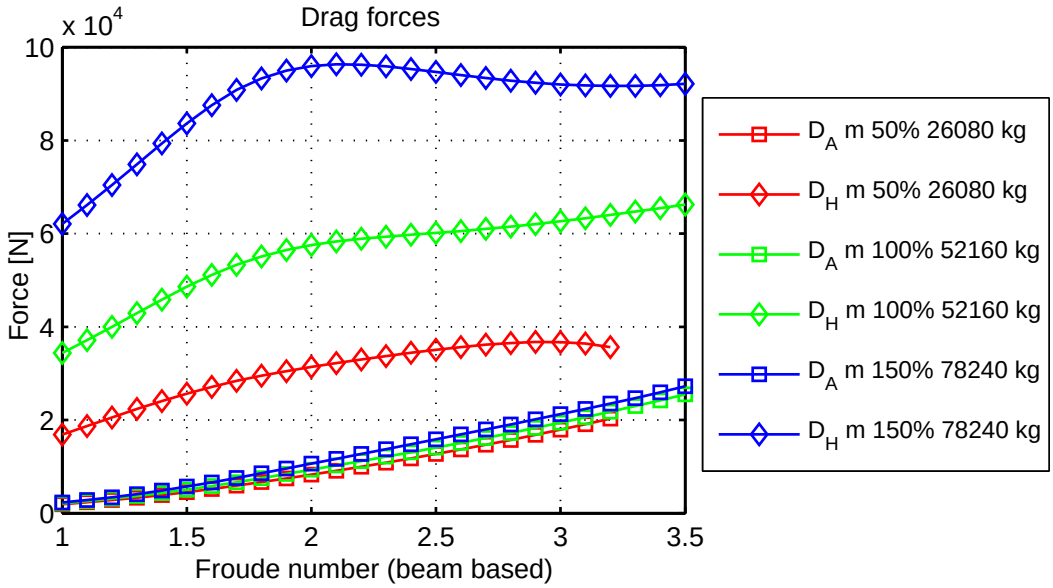

Figure 9.29: m analysis: drag forces

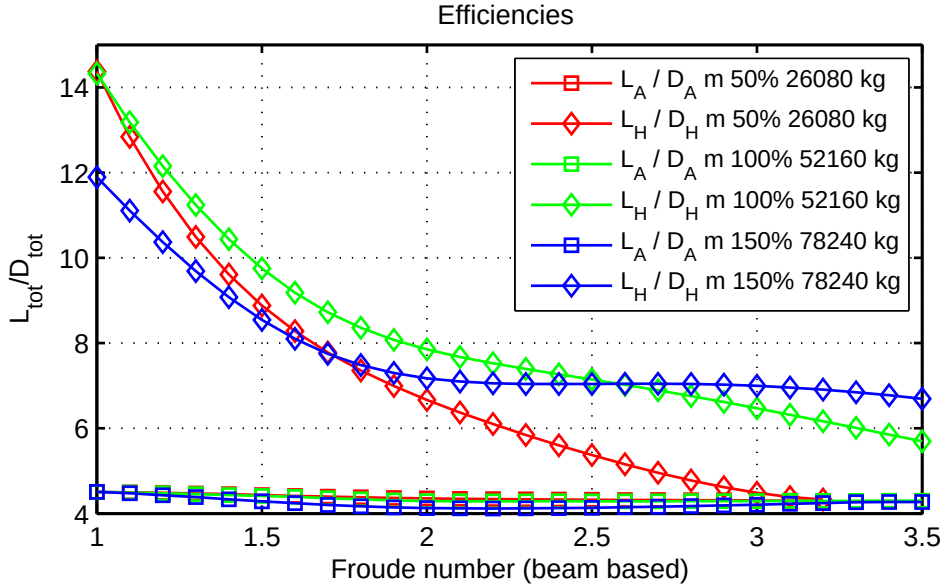

Figure 9.30: m analysis: aero- and hydrodynamic efficiencies

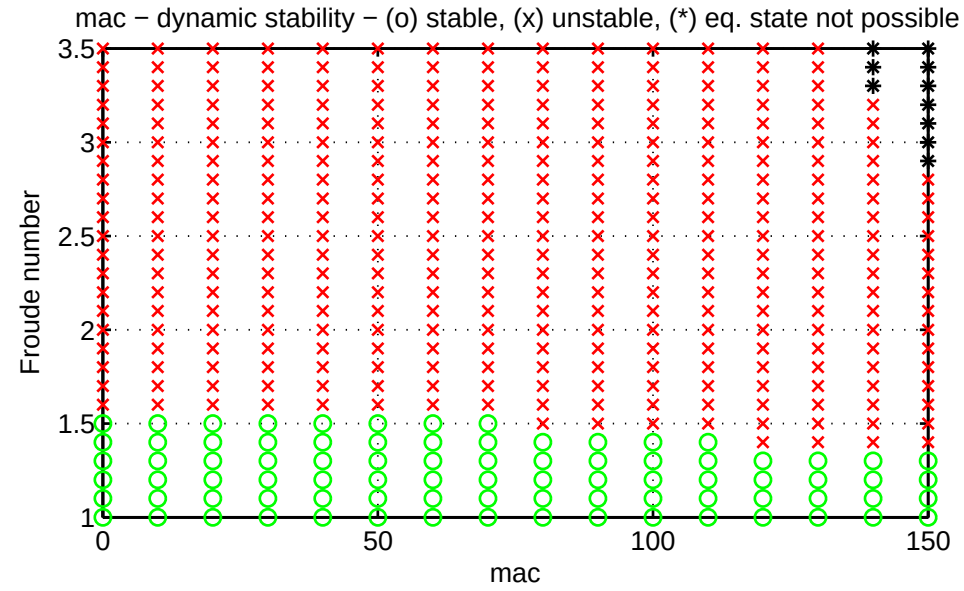

Figure 9.31: mac analysis: dynamic stability boundaries

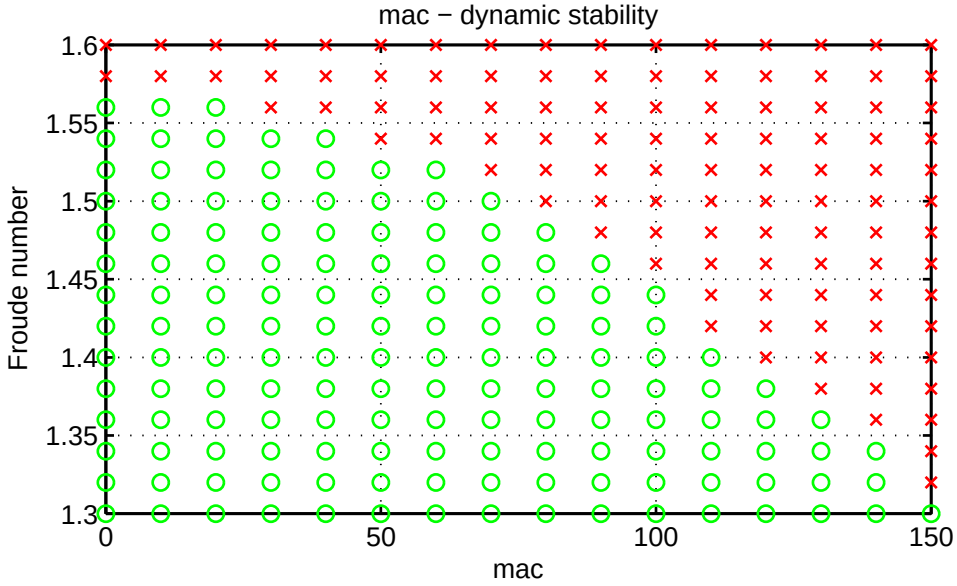

Figure 9.32: mac analysis: dynamic stability, focus on boundary

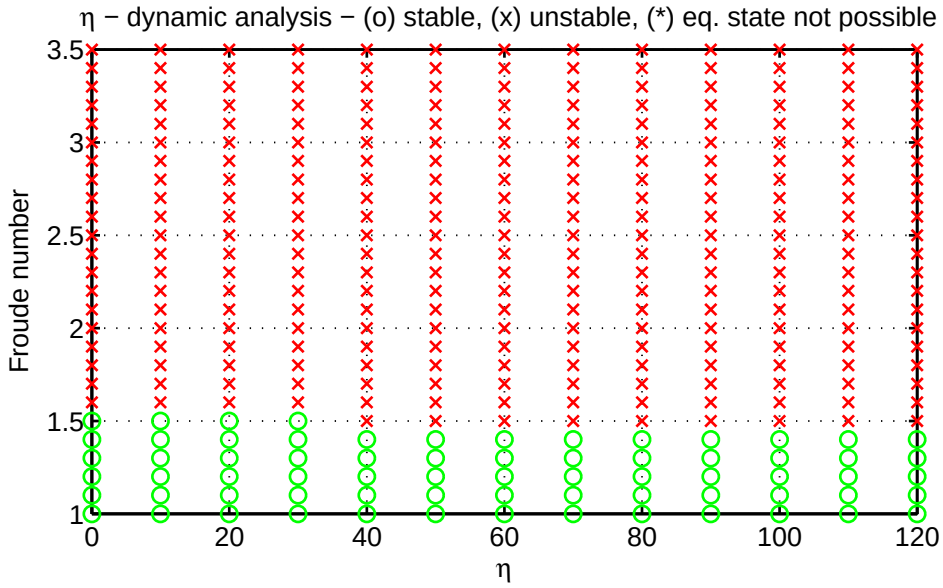

Figure 9.33: η analysis: dynamic stability boundaries

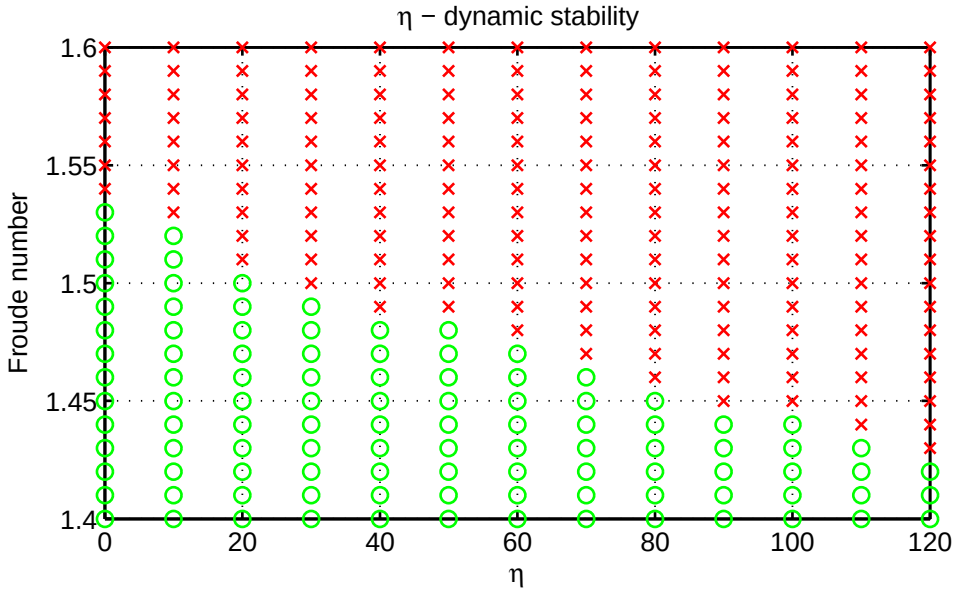

Figure 9.34: η analysis: dynamic stability, focus on boundary

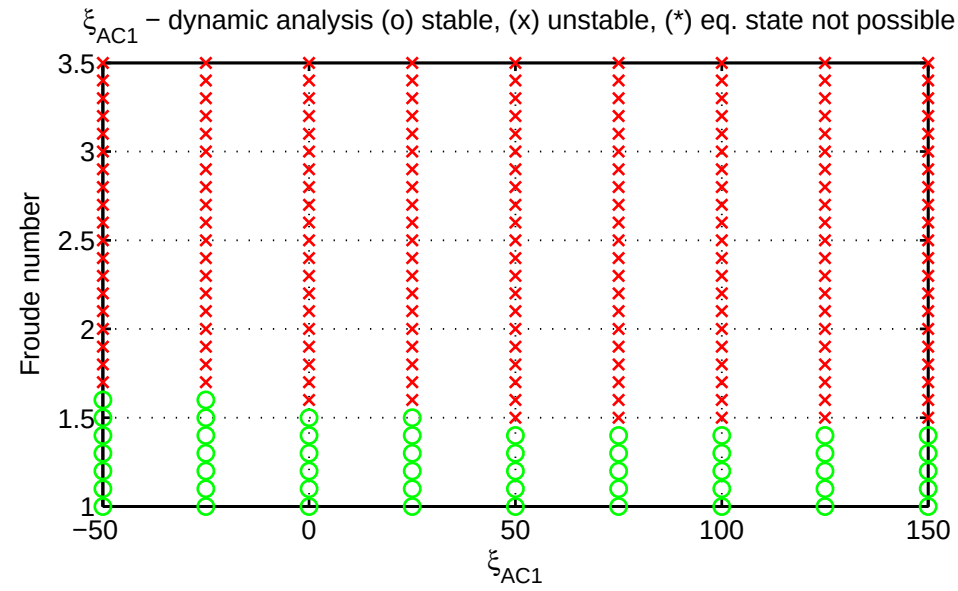

Figure 9.35: ξ_{AC1} analysis: dynamic stability boundaries

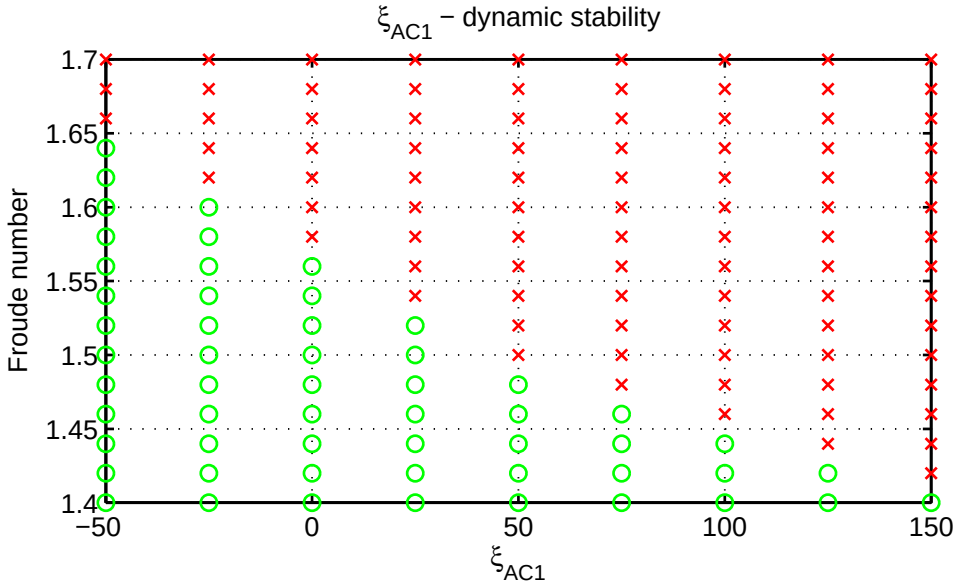

Figure 9.36: ξ_{AC1} analysis: dynamic stability, focus on boundary

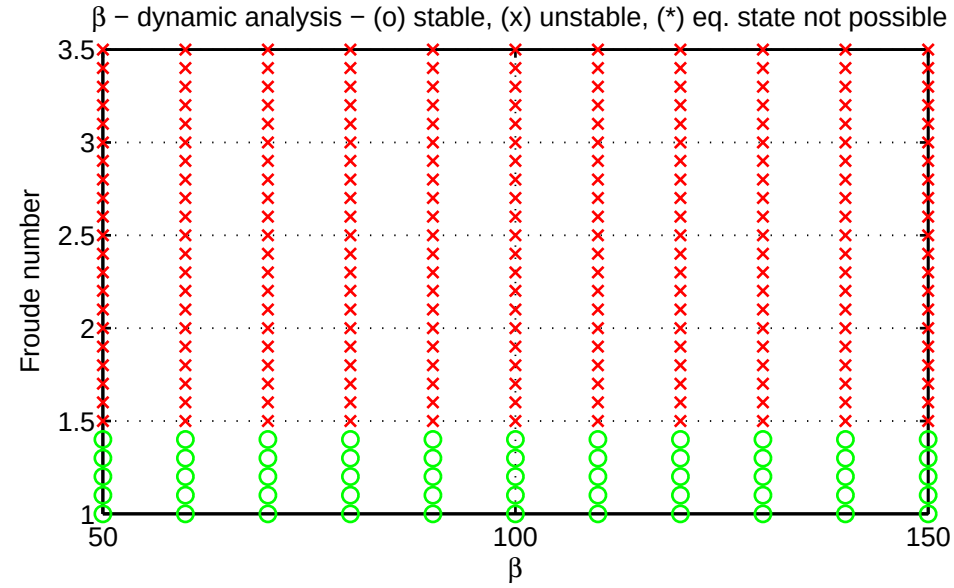

Figure 9.37: β analysis: dynamic stability boundaries

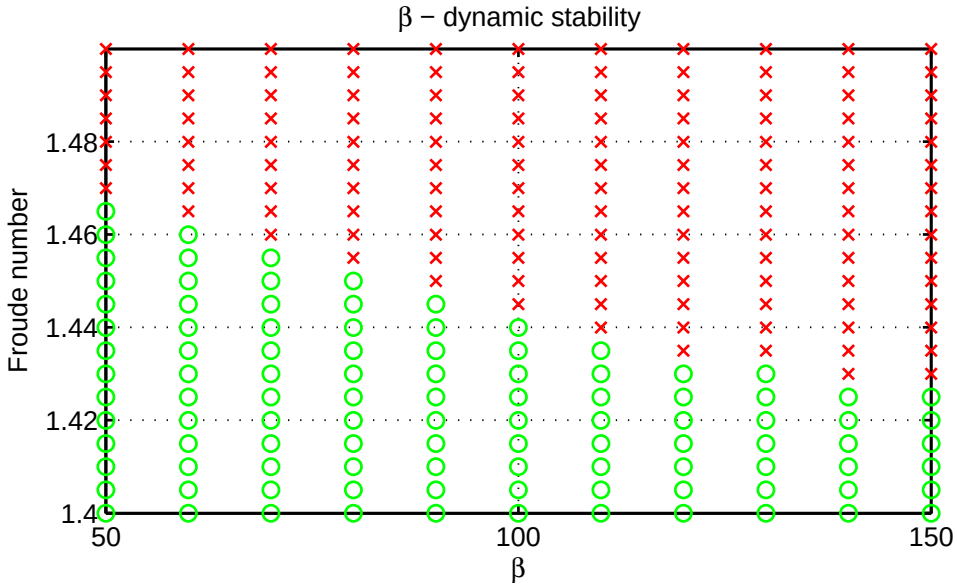

Figure 9.38: β analysis: dynamic stability, focus on boundary

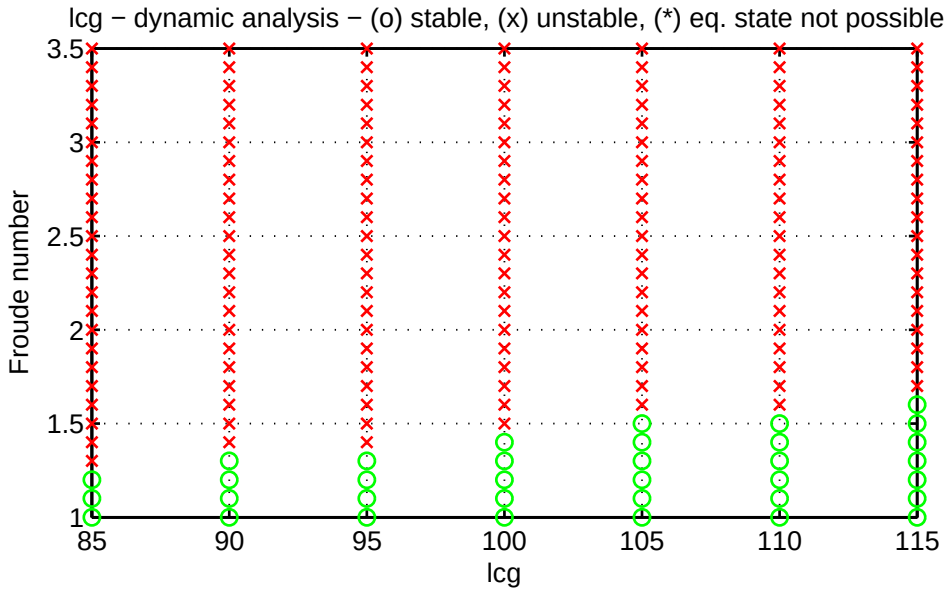

Figure 9.39: lcg analysis: dynamic stability boundaries

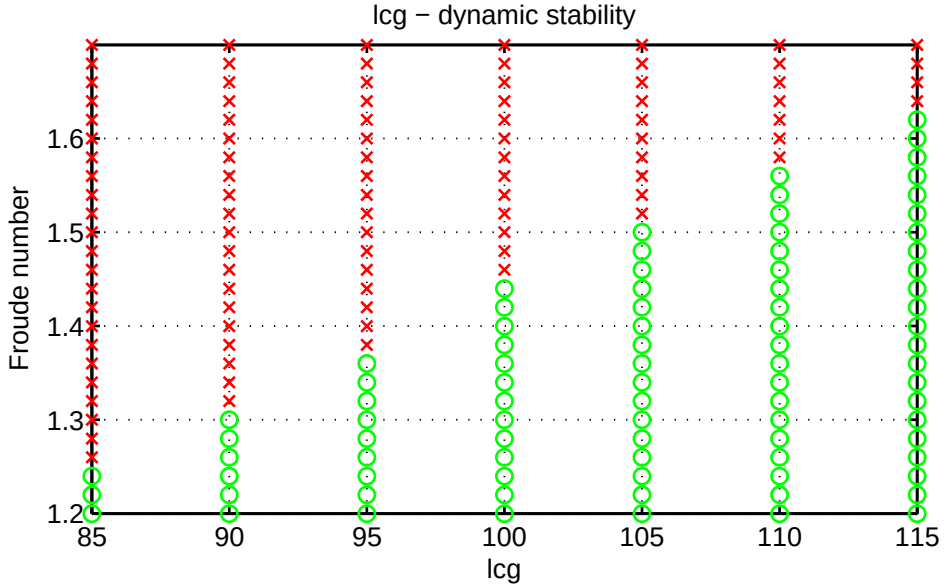

Figure 9.40: lcg analysis: dynamic stability, focus on boundary

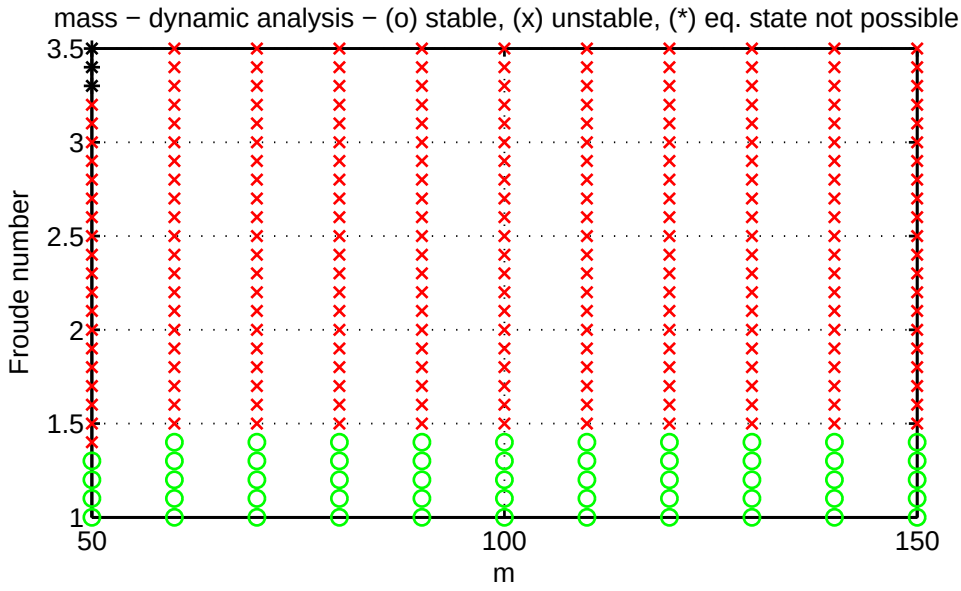

Figure 9.41: $mass$ analysis: dynamic stability boundaries

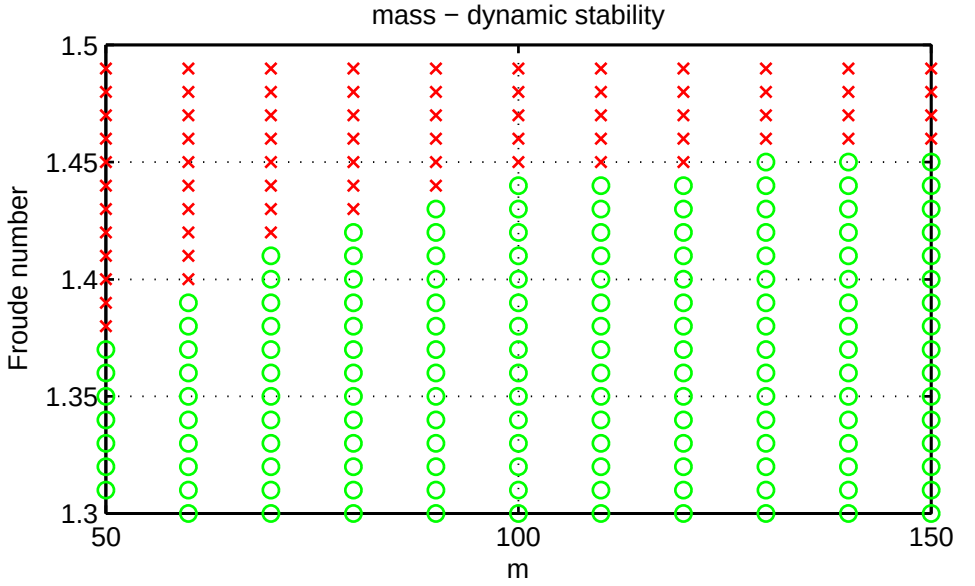

Figure 9.42: $mass$ analysis: dynamic stability, focus on boundary

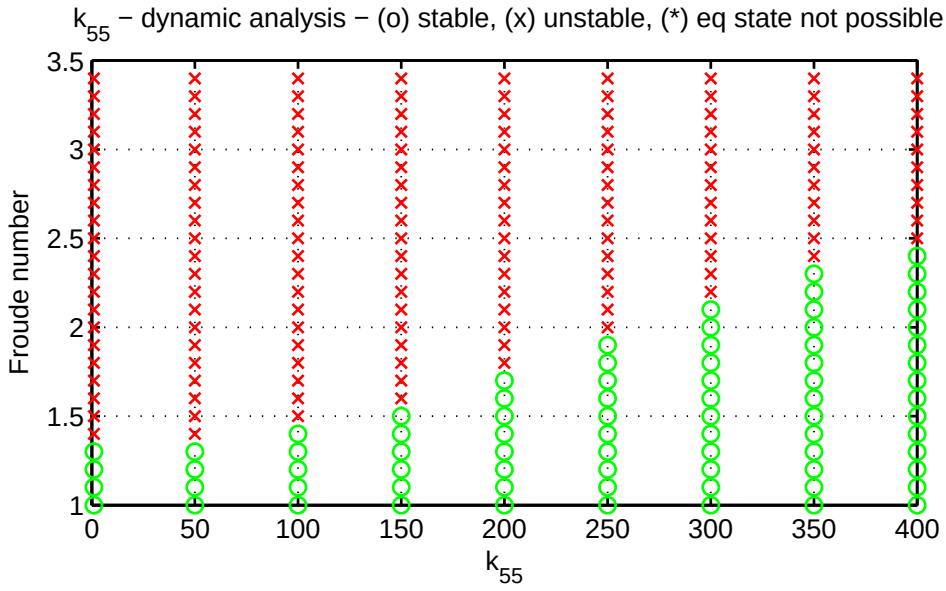

Figure 9.43: k_{55} analysis: dynamic stability boundaries

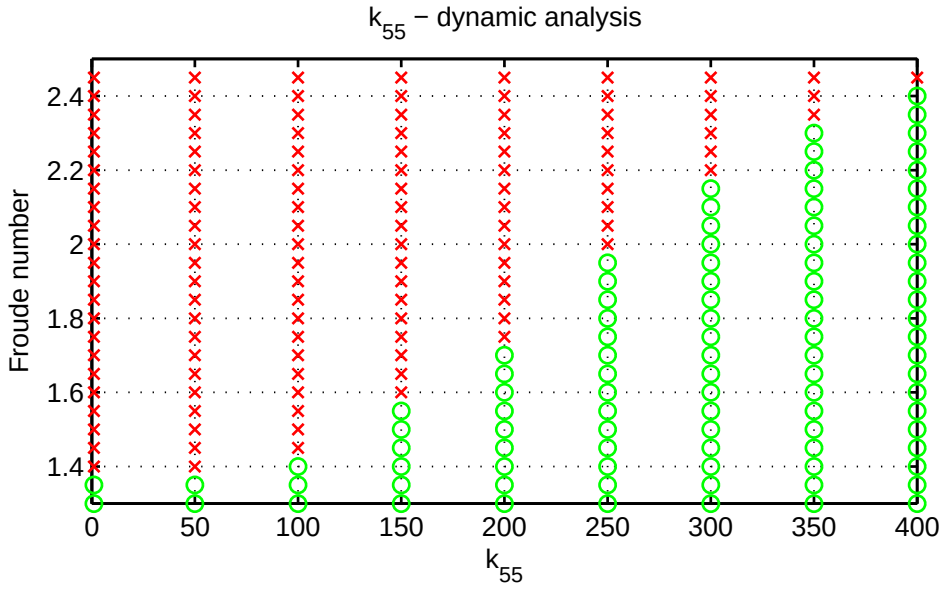

Figure 9.44: k_{55} analysis: dynamic stability, focus on boundary

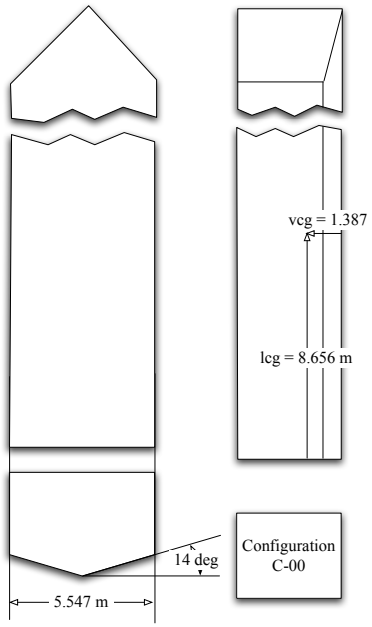

Figure 9.45: C-00 configuration characteristics

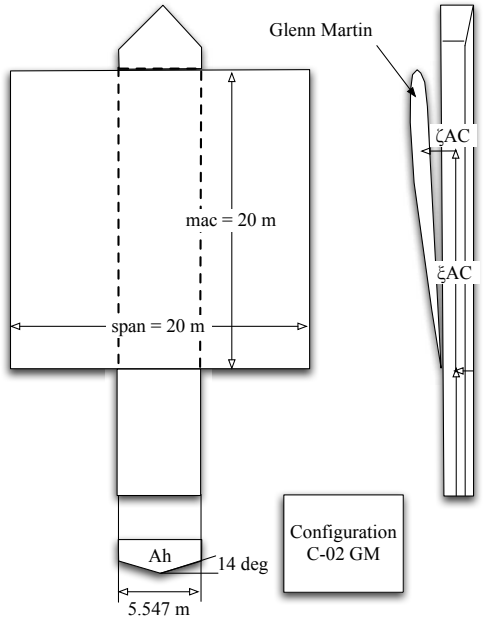

Figure 9.46: C-02 configuration characteristics

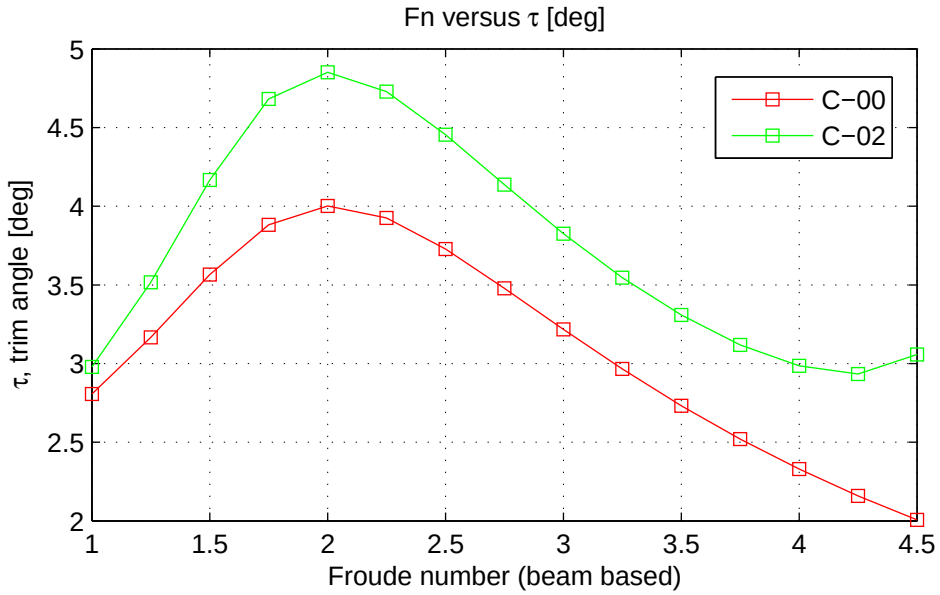

Figure 9.47: C-00 vs C-02: trim equilibrium angle

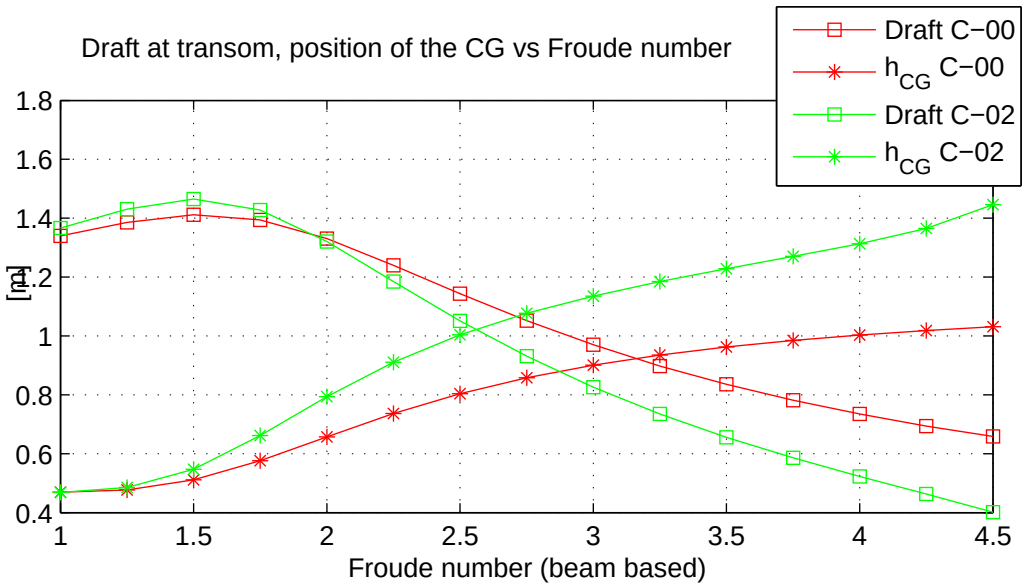

Figure 9.48: C-00 vs C-02: draft at transom & CG height above surface

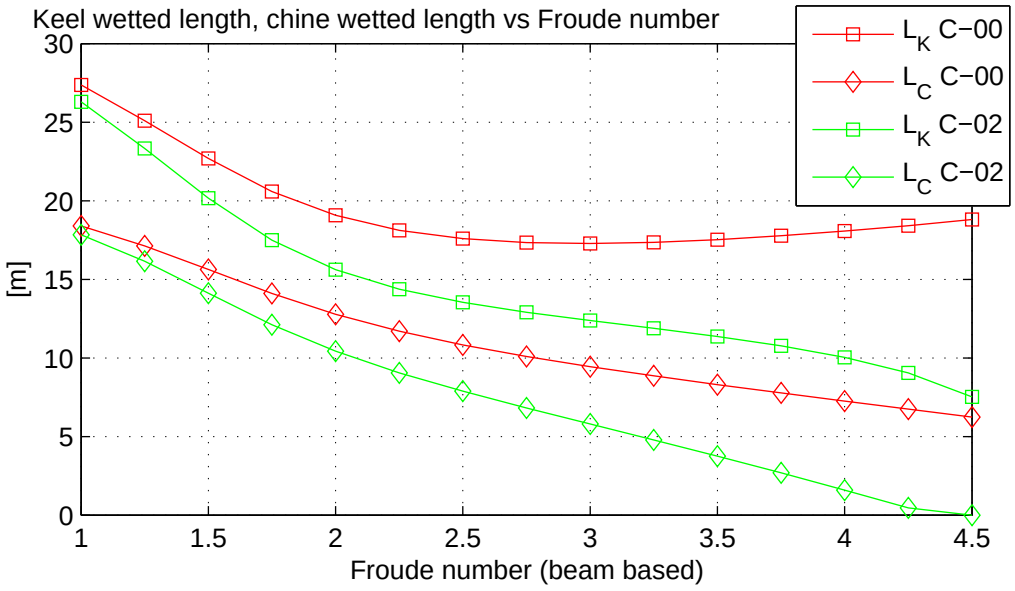

Figure 9.49: C-00 vs C-02: keel (L_K) and chine (L_C) wetted lengths

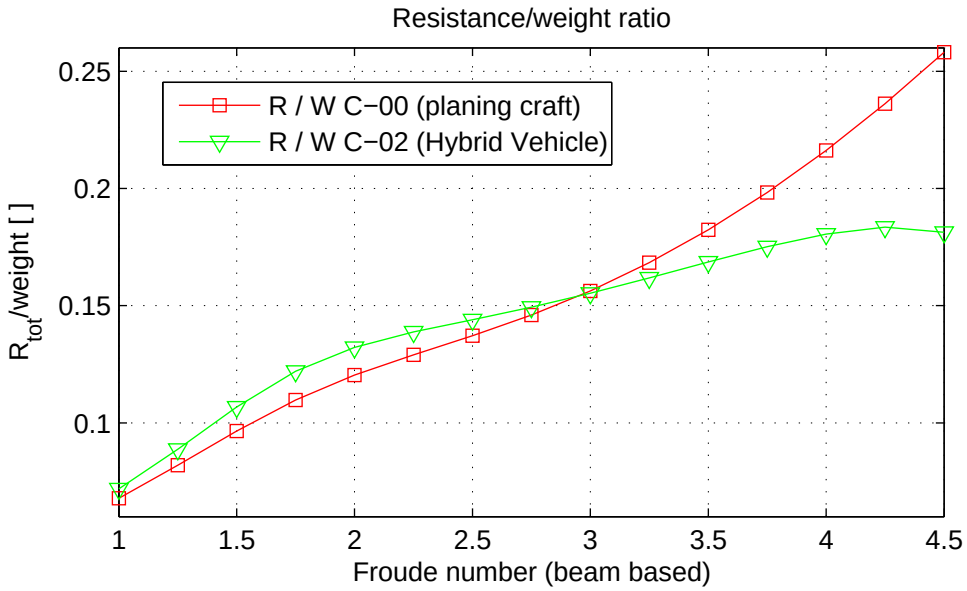

Figure 9.50: C-00 vs C-02: resistance-to-weight ratio

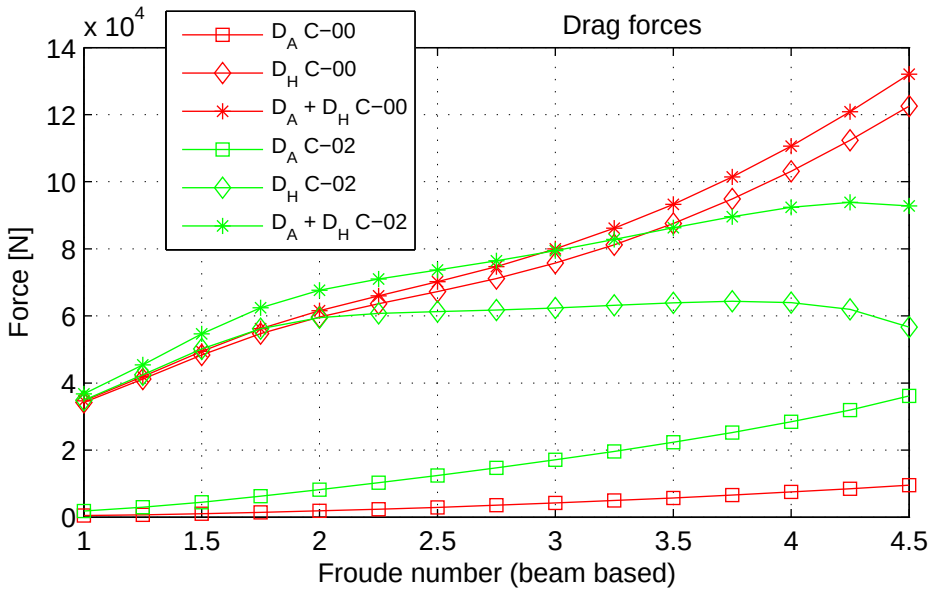

Figure 9.51: C-00 vs C-02: aerodynamic (D_A), hydrodynamic(D_H) and total drag

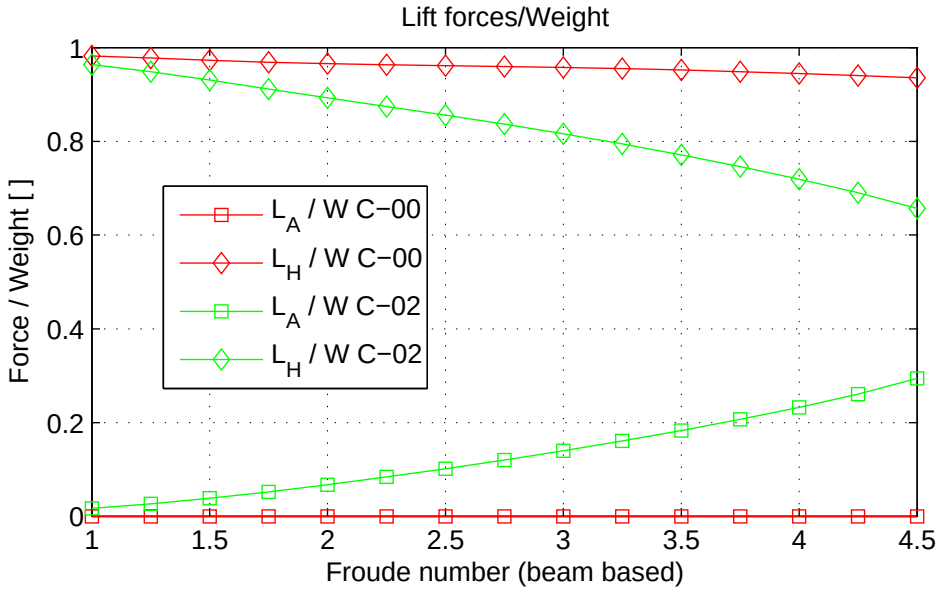

Figure 9.52: C-00 vs C-02: aerodynamic (L_A), hydrodynamic (L_H) lift-to-weight ratio

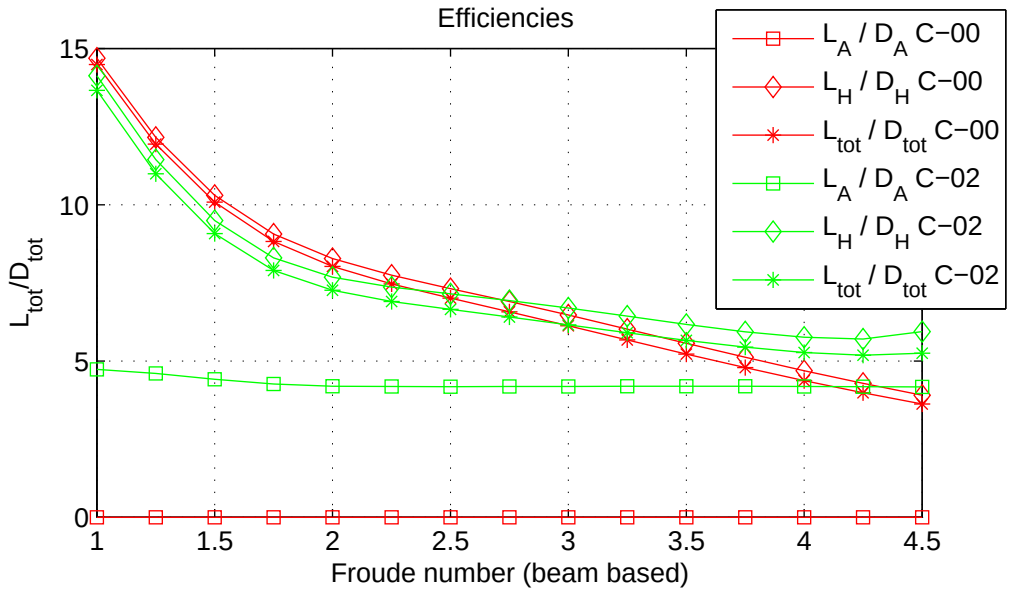

Figure 9.53: C-00 vs C-02: aerodynamic, hydrodynamic and total efficiencies

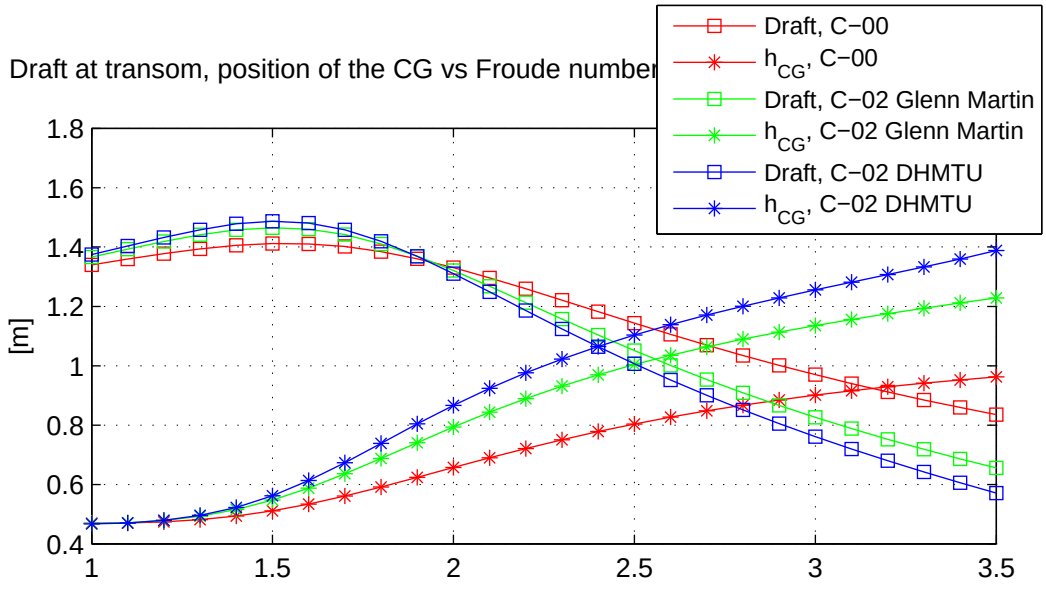

Figure 9.54: C-00 vs C-02 (Glenn) vs C-02 (DHMTU): draft at transom & CG height above surface

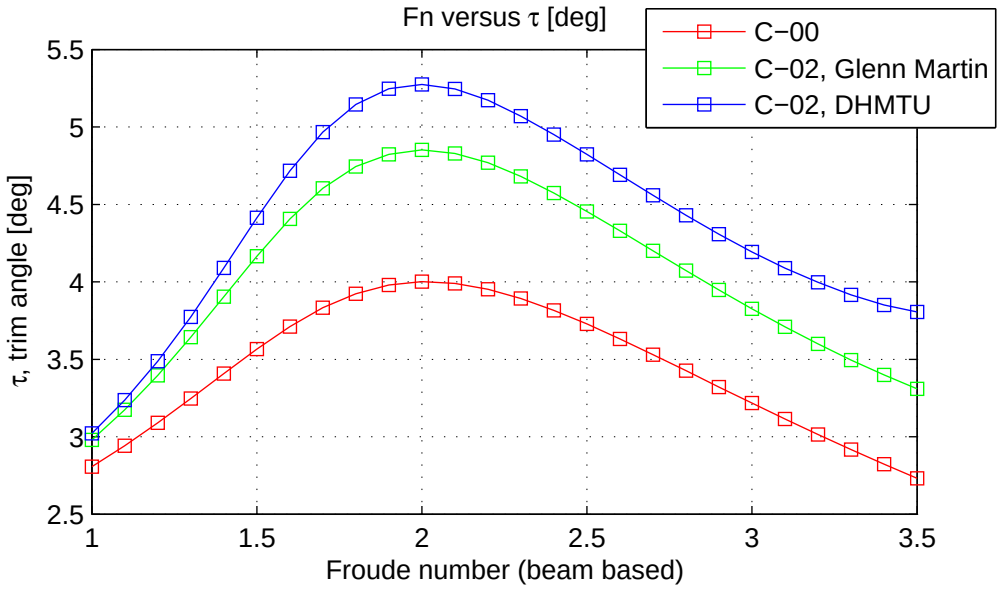

Figure 9.55: C-00 vs C-02 (Glenn) vs C-02 (DHMTU): trim equilibrium angle

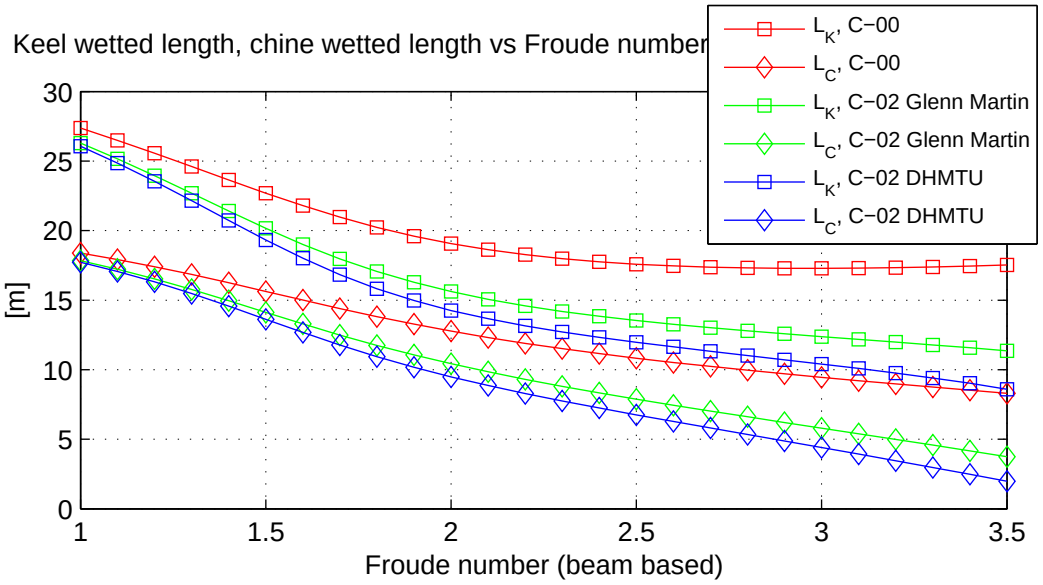

Figure 9.56: C-00 vs C-02 (Glenn) vs C-02 (DHMTU): wetted lengths

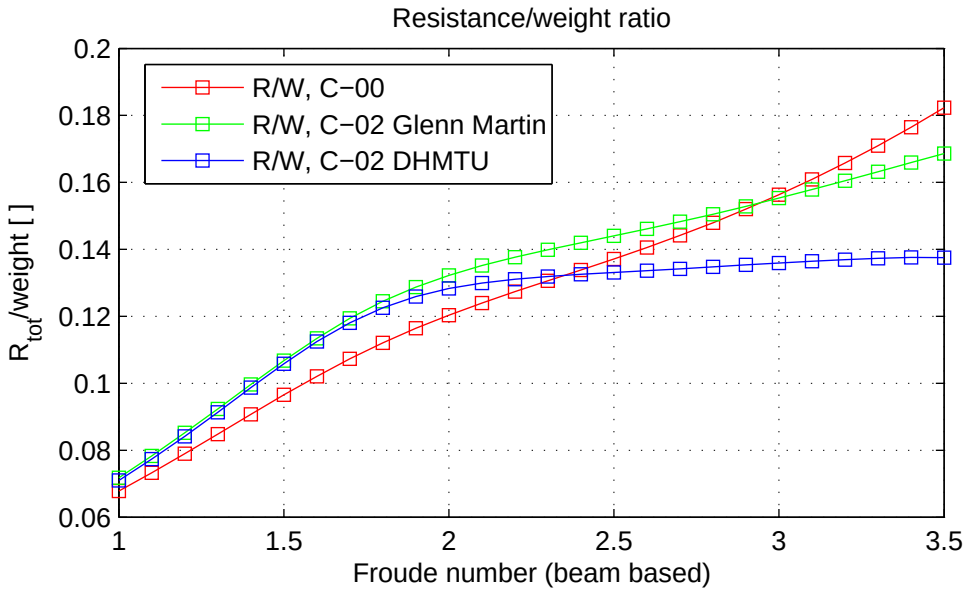

Figure 9.57: C-00 vs C-02 (Glenn) vs C-02 (DHMTU): resistance-to-weight ratio

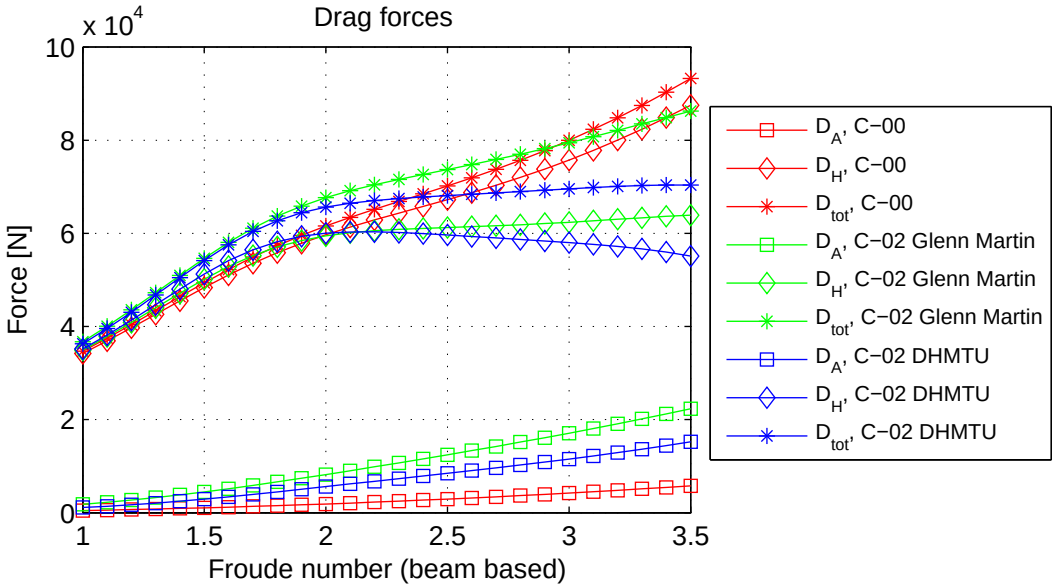

Figure 9.58: C-00 vs C-02 (Glenn) vs C-02 (DHMTU): drags

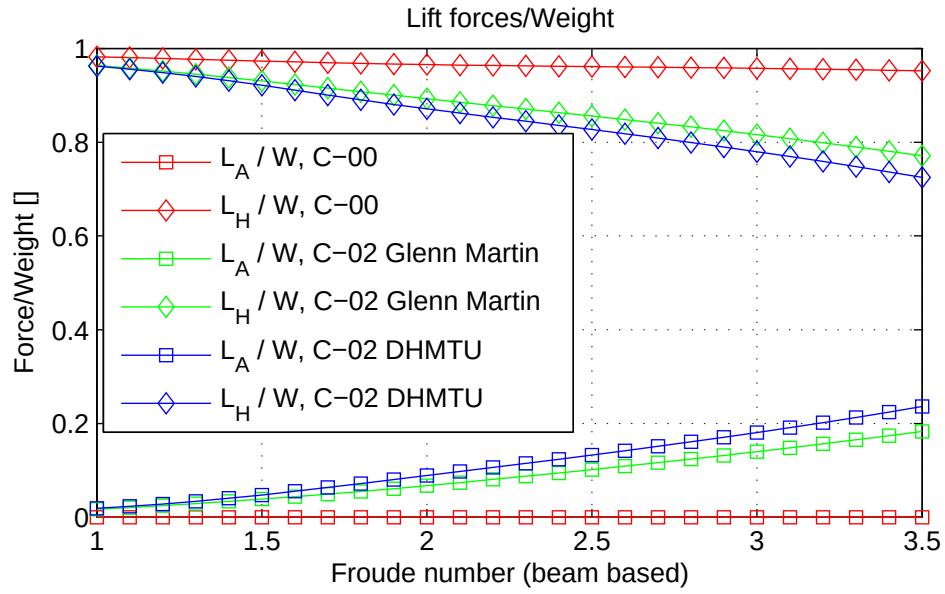

Figure 9.59: C-00 vs C-02 (Glenn) vs C-02 (DHMTU): lift to weight ratio

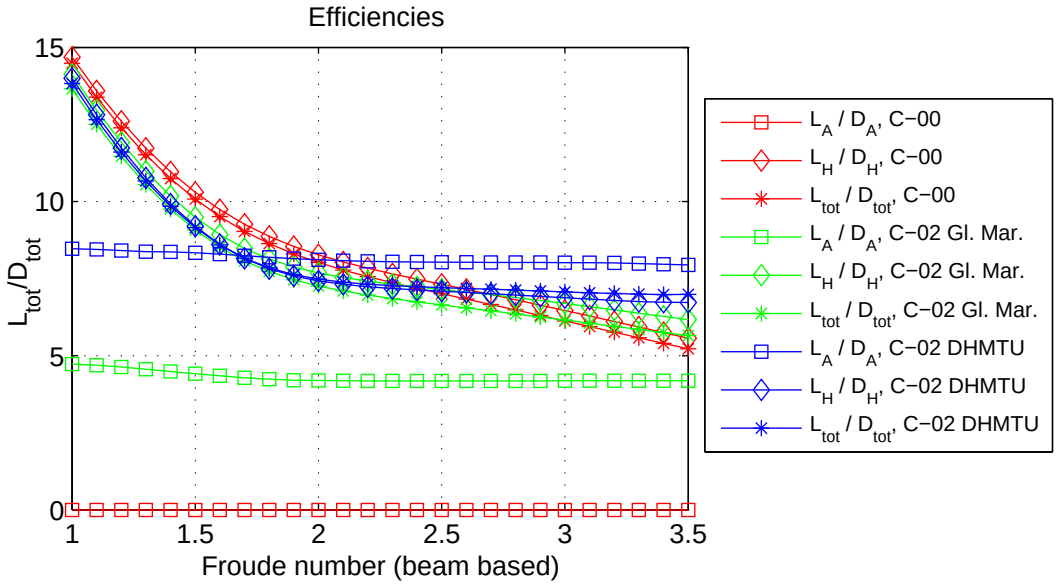

Figure 9.60: C-00 vs C-02 (Glenn) vs C-02 (DHMTU): efficiencies

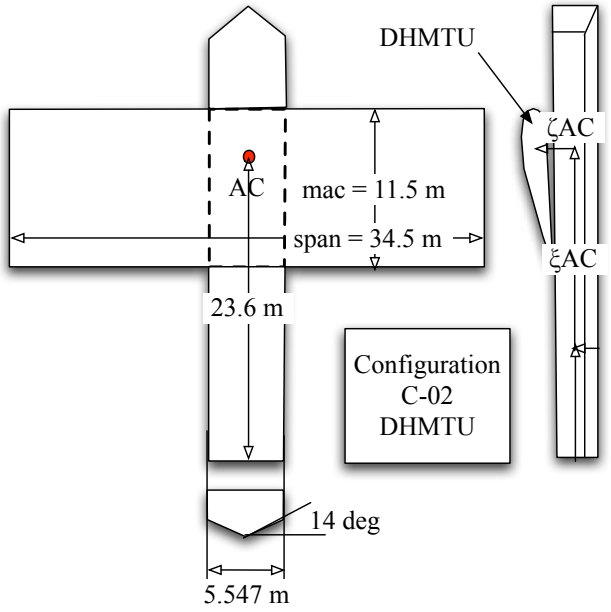

Figure 9.61: C-02 DHMTU configuration characteristics

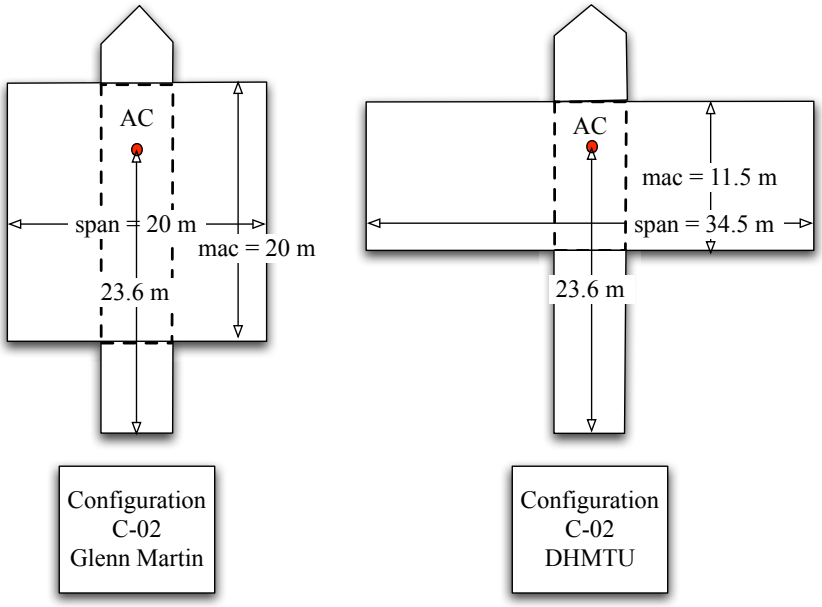

Figure 9.62: Comparison between C-02 GM and C-02 DHMTU configurations

Chapter 10

Practical Output: Novel Trim Control Device

10.1 Introduction

In chapter 4, the Savitsky mathematical model is presented. Its implementation in MATLAB is able to estimate, for a given speed range and a given configuration, the equilibrium attitude of a planing craft. The trim equilibrium angle, evaluated with the system of equations of equilibrium, is not necessarily the optimum angle from the resistance-to-weight ratio (R / W) point of view, and at high speed it can lead to instabilities, such as porpoising. In order to improve planing craft performance and to avoid dynamic instabilities, a number of 'trim control devices' have been developed: stern wedges [31] [22], stern flaps [22] [5] [10], shift of weight systems, wind spoilers. In 2005 Mosaad [33] analyzed and compared these control systems, drawing these conclusions:

- if a planing craft operates at the optimum trim angle it will experience a lower drag and it will avoid porpoising regime,

- the trim control device should be able to vary the trim across a range of angles, since the optimum trim angle varies depending on:
  - speed,
  - inertial characteristics, such as the mass and the CG position,
  - geometrical characteristics,
- the most efficient way to control the trim angle is shifting the weight, however its complicate mechanisms restrict the possible applications,
- the most common device are the transom flaps, due to its simply mechanisms and its immediate effect on the planing craft dynamics, however it is effective in a narrow speed range,
- the wind spoiler device is the least effective.

10.2 Device description

As described by Mosaad, the shifting-weight system is the most effective but it requires complicated mechanisms. Usually a certain amount of fuel is shifted fore or aft using two tanks, one aft tank and one forward tank. Its complexity makes this system attractive only for some ocean racers. The author proposes a shifting-weight system that does not require any tank, pump or whatever device used nowadays to shift part of the displacement aft and fore.

10.2.1 Physical principle

Similarly to chapter 4, the mathematical model adopted to explain the dynamics behaviour of the planing craft is the Savitsky model [43] [44] [45] [46].

In this model a fundamental parameter is the longitudinal position of the center of gravity of the planing craft with respect to the transom, called 'lcg'. To simulate the shifting-weight system it is necessary to vary the value of this parameter:

- an increased lcg corresponds to a forward weight shift,
- a diminished lcg corresponds to a rearward weight shift.

In fact, shifting some displacement from aft to fore (or vice versa) will affect the position of the CG. In particular it will shift the CG forward with respect to the transom of the planing craft, correspondent to an increase of lcg.

A change of lcg is equivalent to a weight shift. The novel system proposed by the author is based on the following consideration. As previously said, geometrically lcg is the longitudinal distance between the CG and the transom. This distance can be varied changing the CG position *or changing the position of the transom.* The position of the transom can be changed adopting a novel trim control device: it consists in a plate, with the same shape of the hull, able to slide aft and fore. In this way it can (sliding aft) extend lcg or (sliding fore) shorten lcg, and it has the same effect of actually shifting some displacement respectively forward or backward.

10.2.2 Hardware

A lateral view of the trim control device in three different positions is shown in fig. 10.1. It consists of a plate having the shape of the hull part between the keel and the chine, capable of sliding in and out. If the plate slides in, the effective length of lcg (lcg1 in the figure) is shorter than lcg of the unmodified hull. If the plate slides out, the effective length of lcg (lcg3) is longer than the lcg of the unmodified

hull. A rear view of the planing craft equipped with this plate is shown in fig. 10.2. The plate has a V shape.

10.3 Numerical results

The novel trim control device can optimize the trim angle from two points of view:

- to reduce the resistance to weight ratio,
- to avoid dynamic instabilities, such as porpoising.

As previously said in chapter 4, the planing craft Savitsky mathematical model is implemented in MATLAB, and it is used here to demonstrates the effects of the novel trim control device proposed by the author.

The baseline planing craft configuration is presented in tab. 10.1: it is called PC-00. It is the planing hull analyzed by Savitsky in [46] (tab. 3). To evaluate the effect of a change of the position of the CG, the configuration PC-00 is compared against other four configurations, PC-050, PC-075, PC-125 and PC-150. These configuration are identical to PC-00 except for the value of lcg, as illustrated in tab. 10.2.

10.3.1 Resistance-to-weight ratio reduction

In fig. 10.3 through 10.6 are compared the trim angle attitude, the resistance to weight ratio, the hydrodynamic drag force and the hydrodynamic efficiency of the five configurations illustrated in tab. 10.2. As it can be seen, to highlight the resistance-to-weight ratio reduction, the speed range has been divided in five

Characteristics		Dimensional	Dimensionless	
GEOMETRY				
Propulsion				
	ξ_{TP}	0 [m]	$\frac{\xi_{TP}}{B}$	0
	ζ_{TP}	0 [m]	$\frac{\zeta_{TP}}{B}$	0
	ϵ_{TP}	12 [deg]	/	/
Hydrodynamic				
	B (beam)	5.547 [m]	$\frac{B}{B}$	1
	β	14 [deg]	/	/
	A_h	20.067 [m^2]	$\frac{A_h}{B^2}$	0.652
INERTIAL CHAR.				
	lcg	8.656 [m]	$\frac{lcg}{B}$	1.560
	vcg	1.387 [m]	$\frac{vcg}{B}$	0.250
	m (mass)	52160 [kg]	$\frac{m}{\rho_{sw}*B^3}$	0.298
	$I_{55} = m * k_{55}^2$	2712318.1 [kg*m^2]	$\frac{k_{55}}{B}$	1.3

Table 10.1: Planing hull configuration (PC-00)

Configuration	lcg dimensional	$\frac{lcg_{PC-i}}{lcg_{PC-00}}$
PC-050	4.328 [m]	0.5
PC-075	6.492 [m]	0.75
PC-100	8.656 [m]	1
PC-125	10.82 [m]	1.25
PC-150	12.984 [m]	1.5

Table 10.2: Planing hull comparison configurations

ranges. In each range are shown only data for the configuration with the lowest total resistance, except for the data of the baseline configuration, evaluated through the entire speed range.

In fig. 10.4 are compared the resistance-to-weight ratios of each configuration. The baseline configuration has the optimal lcg length only in a narrow speed range, roughly between Fn 2.25 and Fn 2.65. At a lower speed it is better to have a longer lcg, while at higher speeds it is convenient to have a shorter lcg. In fig. 10.7 are shown the percentage resistance to weight ratio reductions obtained with the novel trim control device proposed by the author.

Basically, this reduction is due to the fact that each configuration needs the same amount of hydrodynamic lift generated by the hull (equal to the weight) but, as shown in fig. 10.6, the hydrodynamic efficiency can be increased by changing the lcg length. This means that less hydrodynamic drag is generated for the same amount of lift (fig. 10.5).

In fig. 10.3 are compared the trim equilibrium angles of the five configurations. At low velocities, a higher lcg leads to an increased keel and chine wetted lengths. Therefore the hydrodynamic center of pressure is shifted rearward, generating an additional pitch down moment, that leads to a lower trim equilibrium angle than that one of the baseline configuration. At high speeds, there is the opposite situation,leading to an increased trim equilibrium angle. As it can be seen, the trim angle curve is not continue. This is due to the fact that the change of the lcg length is not continue, but discrete, with steps of 25% of the PC-00 lcg length (2.164 m).

10.3.2 Keep the vehicle off dynamic instability regime

At high speed, a planing hull can experience dynamic instabilities, both in the longitudinal and lateral-directional plane: chine walking, corkscrewing, and porpoising [6].

Several investigations have been conducted to study the onset situations of these instabilities. Savitsky [43] proposes a critical trim angle, above which the planing hull experiences porpoising instability. This critical trim angle is a function of the hydrodynamic coefficient of lift and the deadrise angle (fig. 10.8). Celano [3] analyzed experimental data of Day and Haag [11] and derived a relatively simple relationship for the critical porpoising trim angle (in degrees), given the hydrodynamic coefficient of lift and the deadrise angle (eq. 10.1).

$$\tau_{critical} = 0.1197\,\beta^{0.7651}\,exp\left(15.7132\,\sqrt{\frac{C_L}{2}}\,\beta^{-0.2629}\right) \tag{10.1}$$

In fig. 10.3 are compared the trim angle of the five configurations of tab. 10.2. It can be seen how the trim equilibrium angle can be changed using the trim control device proposed by the author. In particular, if the trim equilibrium angle, for a given planing hull at a certain speed, is higher than the critical trim angle, it is possible to lower the trim angle with a higher lcg. As previously, if the novel trim control device slides out the lcg length increases. Therefore it is possible to control the trim angle to avoid porpoising instability.

10.4 Conclusion

For a conventional planing hull without any control device, the equilibrium trim angle (fixed the other parameters) depends only on speed. Anyway, if the trim an-

gle can be controlled, better performances will be achieved: with a lower resistance and the possibility of avoiding dynamic instabilities.

The most efficient way to control the trim angle is shifting the weight, however its complicated mechanisms restricts possible applications. The author proposes here a novel trim control device that does not require the complicated mechanisms needed by available shifting-weight systems. It consists in a plate able to slide in and out, illustrated in fig. 10.1 and fig. 10.2: this movement respectively diminishes or increases the value of the longitudinal position of the center of gravity (lcg).

Compared to the stern flap system, the advantages of the novel control trim device are:

- the trim angle can be increased and decreased, while stern flaps can only decrease the trim angle,
- thanks to the previous advantage, it can be used in a wider range of speed.

Compared to other shifting-weight systems, that use tanks to move a liquid (usually the fuel) fore and aft, advantages are:

- a shorter time to control the trim angle,
- no additional free surface effect problems (due to the additional tanks).

The potential of this novel control trim device, as shown also by numerical simulations (fig. 10.3 to fig. 10.7), is promising. It needs an experimental campaign to validate the theory and to evaluate the feasibility of the device from a hardware point of view.

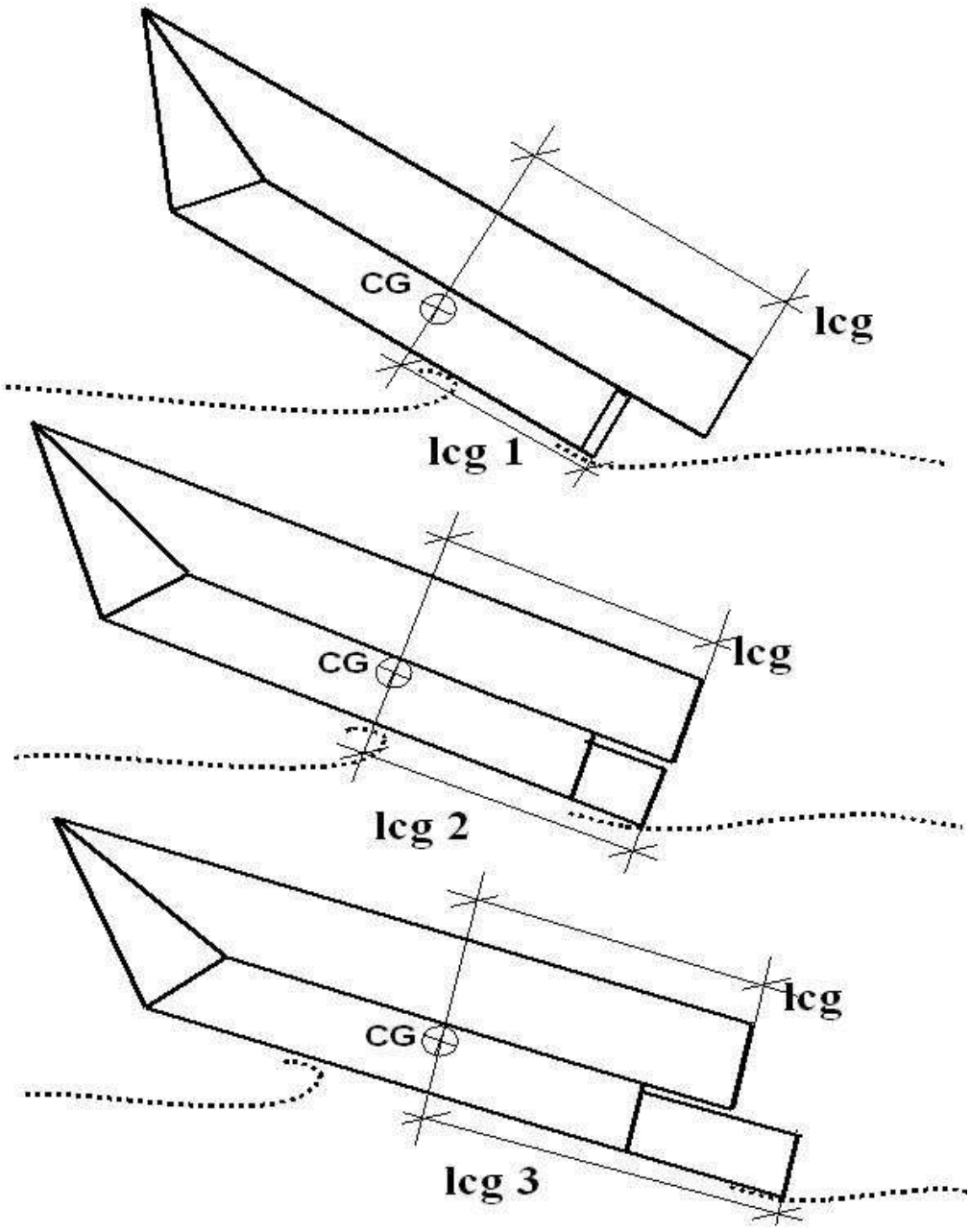

Figure 10.1: Novel trim control device: lateral view in three positions

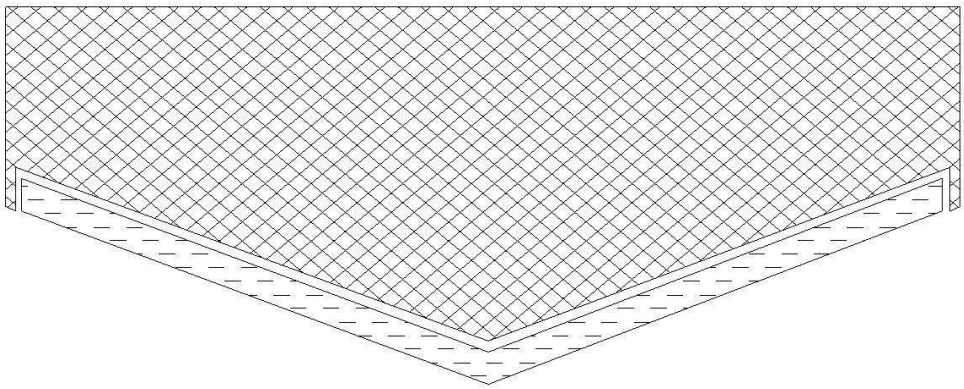

Figure 10.2: Novel trim control device: rear view

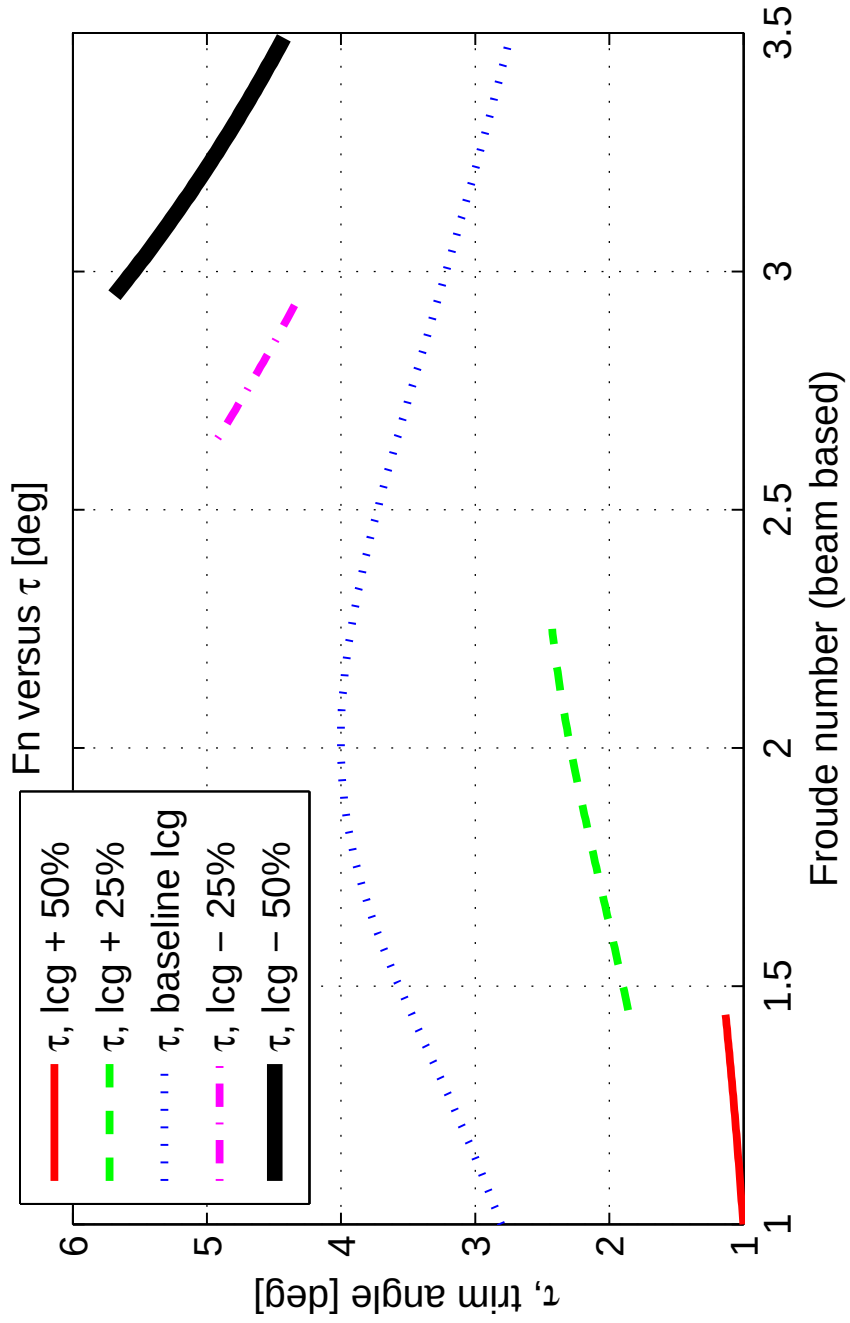

Figure 10.3: Influence of the CG longitudinal position on trim angle

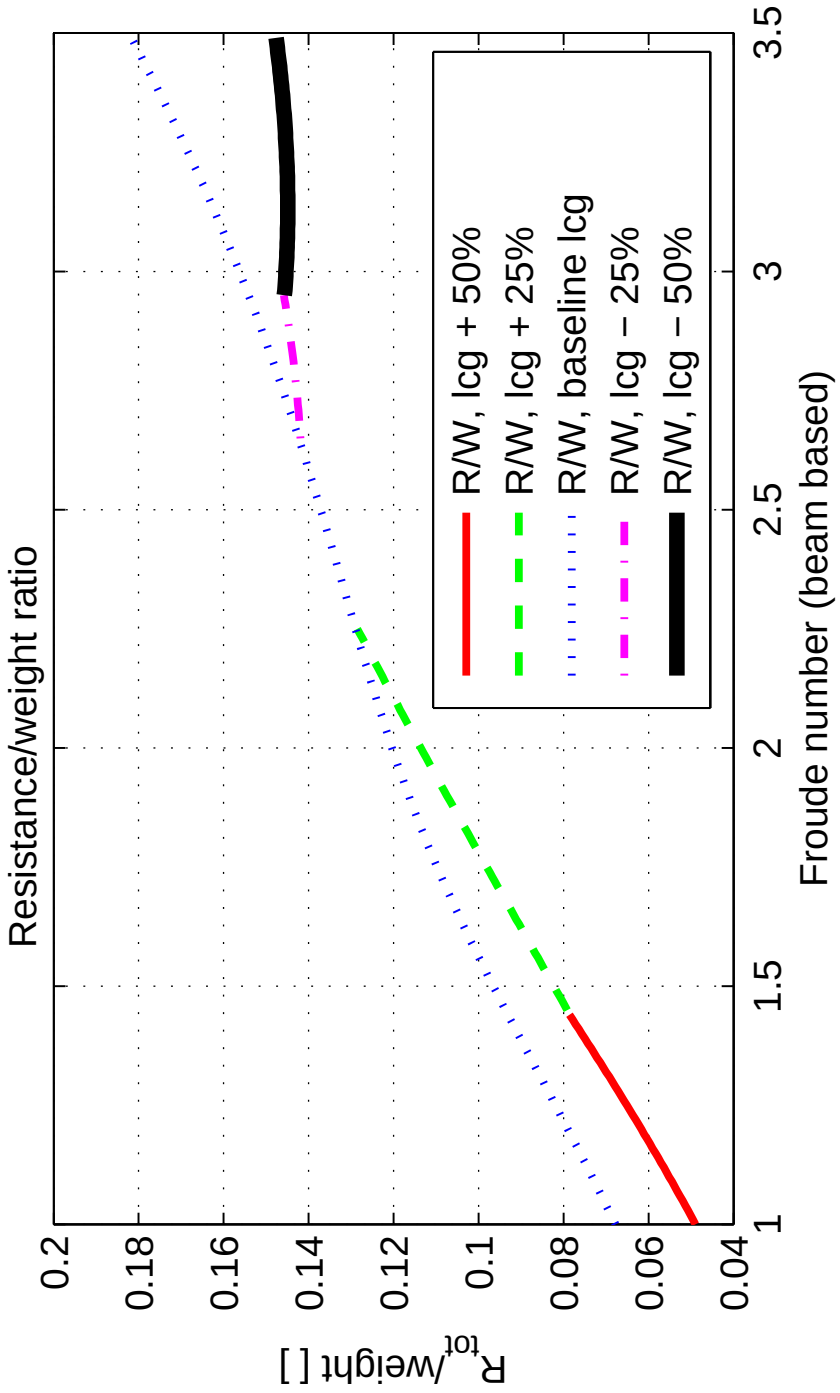

Figure 10.4: Influence of the CG longitudinal position on resistance to weight ratio

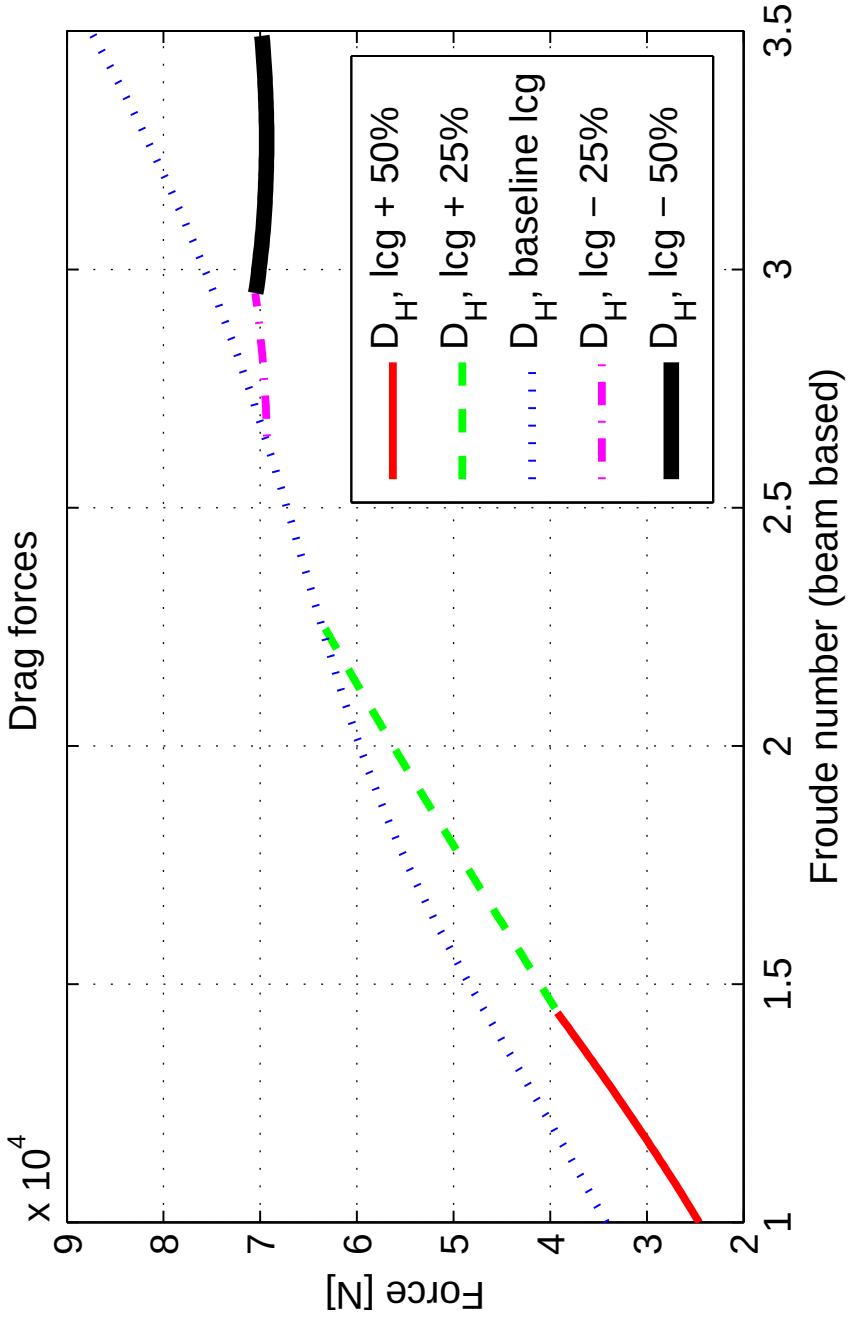

Figure 10.5: Influence of the CG longitudinal position on hydrodynamic drag

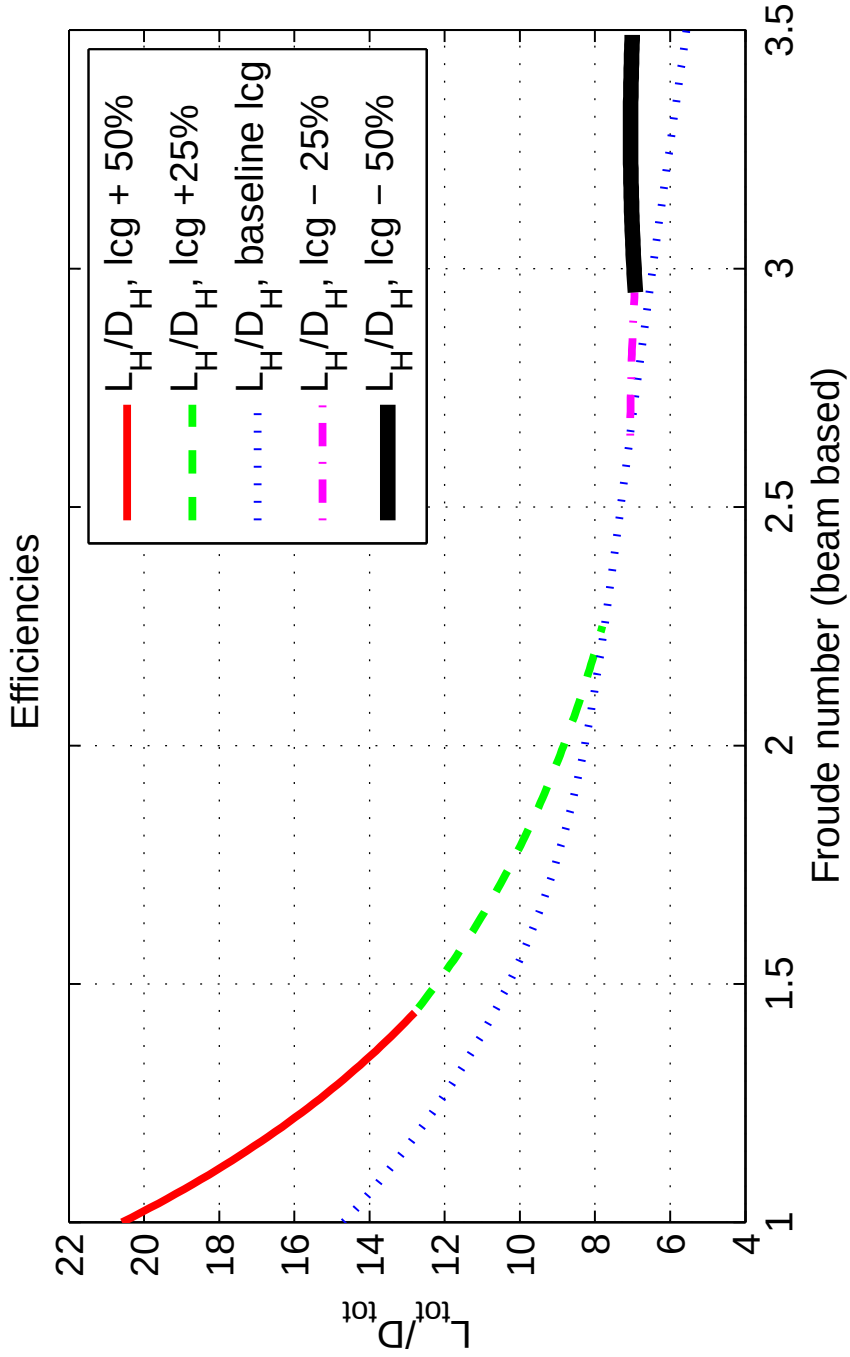

Figure 10.6: Influence of the CG longitudinal position on hydrodynamic efficiency

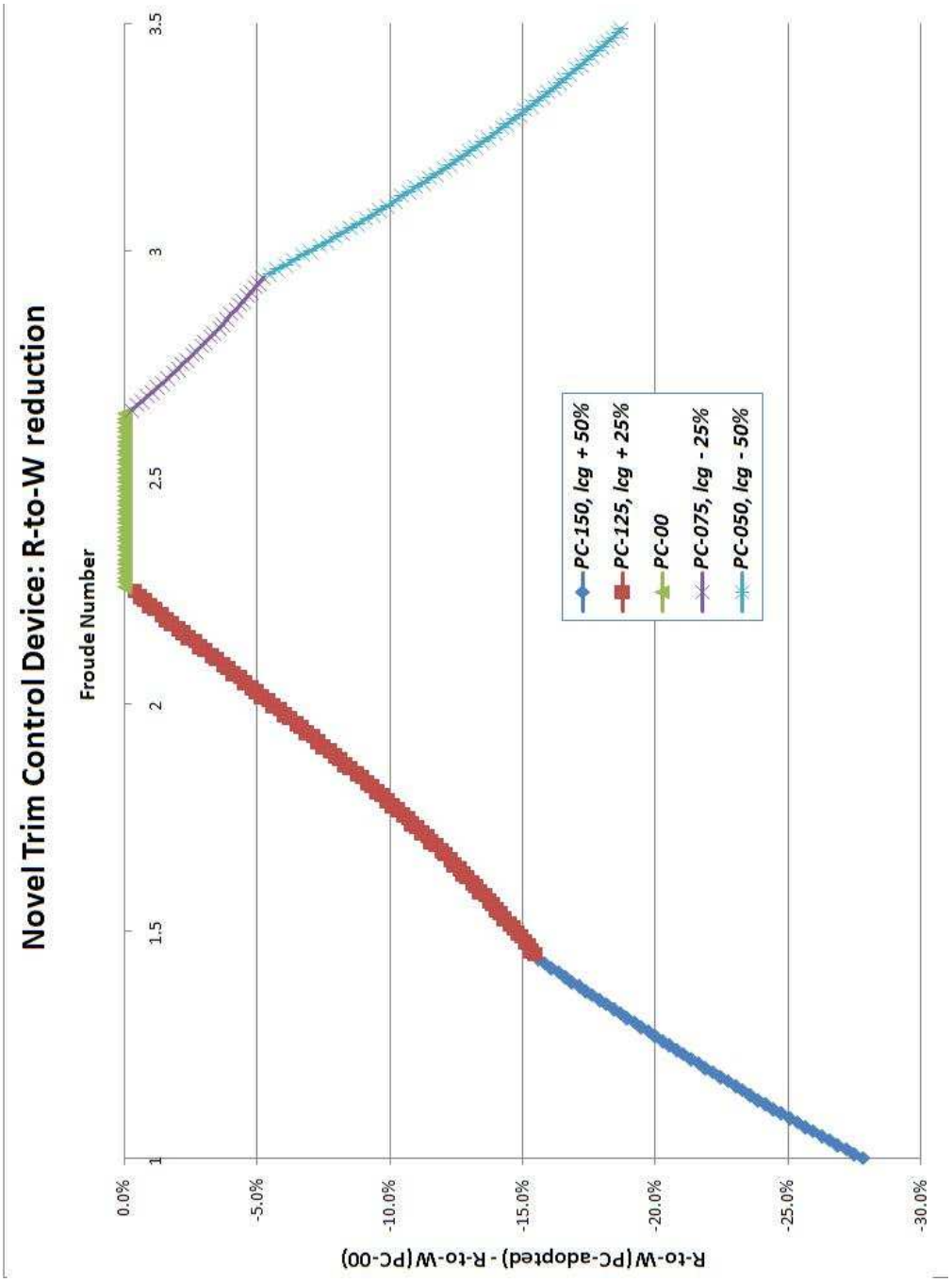

Figure 10.7: Resistance-to-weight percentage reduction

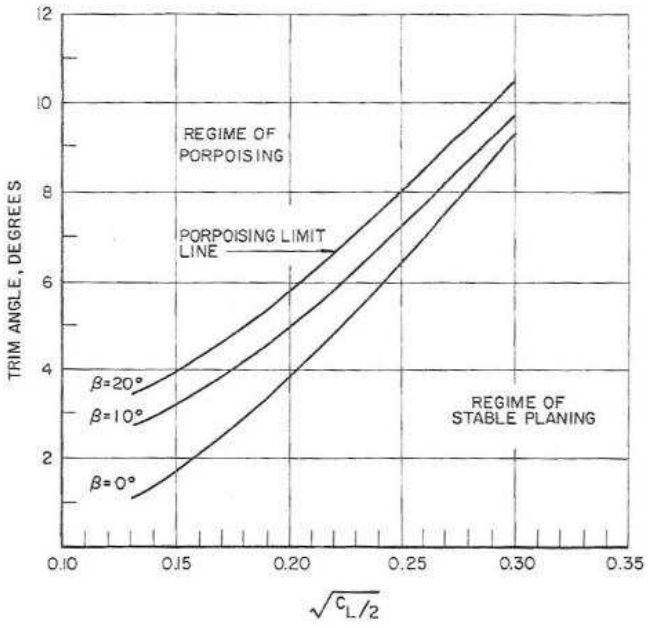

Figure 10.8: Porpoising limits, Savitsky [43]

Chapter 11

Discussion and General Observations

11.1 Introduction

In this chapter a discussion on main results of this work is presented. In fact, during the development of this work, many questions have been answered, but many more questions remain to be opened.

11.2 AAMV Lateral Stability

In chapter 9, an equilibrium attitude and a stability sensitivity analyses are presented, with the aim to help the preliminary design of an AAMV configuration. In chapter 8 the AAMV stability is discussed. Due to the huge amount of work and to the limited amount of time, only the longitudinal stability has been investigated, both static and dynamic. Nonetheless it is important to stress the importance of the lateral-directional stability.

The lateral-directional stability is related to the forces and moments acting in the lateral and in the directional plane. Referring to figure 11.1 (for a ship, but the

same system can be adopted for an AAMV configuration), basically they are:

- sway (also called side) force,
- roll moment,
- yaw moment.

Due to the complexity of the subject, only the static stability will be briefly discussed here, since the dynamic stability is beyond the scope of this chapter. In particular, the link between the CG vertical position and the roll static stability is discussed.

In chapter 9, to illustrate the advantages of an AAMV configuration, the C-00 planing hull configuration and two AAMV configurations, C-02 GM and C-02 DHMTU, are compared. As illustrated in tab. 9.7, all the three configuration has the same mass, around 50 metric tons. This is due to the aim to highlight all the advantages given by adding an aerodynamic surface to a planing hull configuration, without changing other parameters, but it can be explained also by thinking about how to use the additional volume of the aerodynamic surface.

For a conventional airplane configuration, wings are used as fuel tanks, due to many advantages. First of all, the wings are near the CG of the dry airplane, the weight of the fuel does not displace excessively the position of the center of gravity. Secondly, since the weight of the fuel acts where the aerodynamic lift is generated, the bending moment at the root of the wings, where the wings connect with the fuselage, is diminished, leading to a lighter structure. Similarly, in the AAMV the volume of the wing can be used as a fuel tank, leading to a diminished weight of the planing hull (which houses the fuel tank for the C-00 configuration), and it can justify a similar mass for the three different configurations.

From a roll static stability point of view, it is important to notice how this can greatly influence the 'transverse' stability of the AAMV. For a conventional displacement ship configuration, a measure of the transverse stability is the 'transverse metacentric height', being the distance between the CG and the transverse metacentre (M) of the ship. To have a transverse statically stable ship, M should lie above CG. Therefore, if the wing is used as a fuel tank, the vertical position of the CG is increased, and the distance between M and CG is diminished, leading to a diminished metacentric height, thus to a diminished transverse static stability.

11.2.1 Conclusion

As said in section (12.3.4), it is recommended in future work to further develop the AAMV's dynamics analysis into the lateral-directional plane, since it is of primary importance for the preliminary design of an AAMV configuration.

11.3 Configuration

In this work the configuration presented in fig. 5.3 is adopted, comprising one or more aerodynamic surfaces flying in ground effect and a prismatic planing hull.

Following the discussion in the previous section about lateral stability, from a 'transverse stability' point of view it would be better to have two planing hulls, with the wing between them. This 'catamaran' configuration, already adopted in the past for vehicles classifiable as AAMV (KUDU II in sec. 2.4, fig. 2.9), other than a superior lateral static stability, possess also other advantages. It is known that it is possible to further enhance the WIGe positive impact on aerodynamic efficiency adopting the so called 'end plates' [29]. These are two plates attached

at the tip of a wing, extending below the chord plane. In the catamaran configuration, if the wing is fitted between the two planing hulls (like in the KUDU II), the planing hulls will act as end plates. Williams [56] is conducting a parallel investigation on aerodynamic forces acting on a AAMV catamaran configuration, and the first performance estimate of this configuration seems to confirm the aforementioned considerations. The AAMV configuration studied by Williams is presented in fig. 11.2.

Nonetheless, in the present work a prismatic planing hull is preferred, to guarantee a wider applicability of the results and of the parametric analyses obtained. In fact, due to the complex hydrodynamic interactions between the two planing hulls of a catamaran configuration, the equilibrium attitude and stability estimate that would be obtained with the mathematical framework developed in this work would have been of a very limited applicability. In particular, the performance of a catamaran configuration depends strongly and non linearly on the length of the planing hulls and on the distance between them.

11.3.1 Conclusion

To guarantee a general applicability of the parametric analysis and of the other results obtained in this work, a prismatic planing hull has been adopted as the hydrodynamic surface. Nonetheless, as specified also in section 12.3.1, it is strongly advised that further development of the mathematical framework is carried out, in order to take into account different hydrodynamic surfaces, such as catamaran configurations.

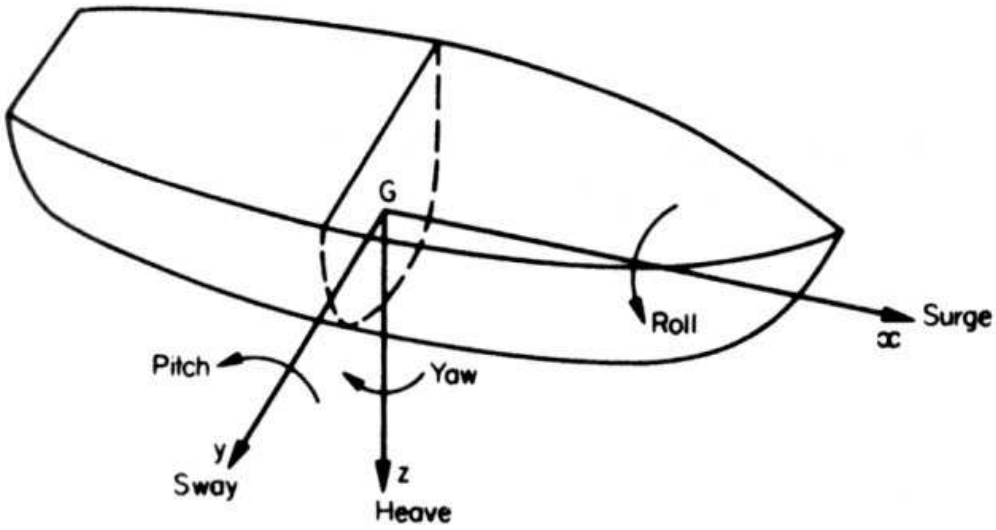

Figure 11.1: Longitudinal, lateral and directional forces and moments [38]

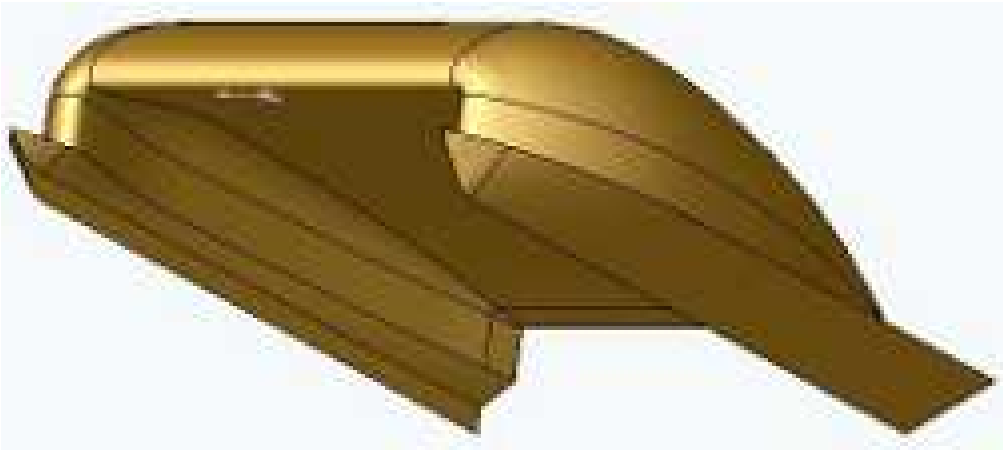

Figure 11.2: AAMV catamaran configuration [56]

Chapter 12

Conclusions and Future Developments

12.1 Introduction

In the last few decades, interest in high speed marine vehicles (HSMV) has been increasing, leading to several new configuration concepts. Among these, the 'aerodynamic alleviation concept' [14] consists of using one or more aerodynamic surfaces to alleviate the weight of the marine vehicle. Basically, the advantages are:

- a total drag, at high speed, up to 20-30 % lower than the same marine vehicle without aerodynamic surfaces (tab. 9.6),
- vertical and angular pitch accelerations, at high speed, 30-60% lower than conventional HSMV (see KUDU II in 2.4 and [21]),
- a vehicle bridging the speed gap and payload gap between conventional high speed marine vehicles and airplanes.

To classify this configuration concept, the author coined the new abbreviation AAMV, 'Aerodynamically Alleviated Marine Vehicle' (section 1.1.1).

Being a relatively recent configuration concept, it lacks a specifically developed mathematical framework to study its dynamics. The AAMV experiences aerodynamic and hydrodynamic forces of the same order of magnitude, therefore the mathematical frameworks developed separated so far for high speed marine vehicles and airplanes are not suitable.

With the present work the author has developed an integrated mathematical framework specifically for an AAMV configuration.

12.2 Conclusions

The main results of the present work can be summarized in the following points:

- development of a new system of equations of equilibrium, specifically developed to estimate the equilibrium attitude of a high speed marine vehicle using aerodynamic surfaces,
- development of a new system of equations of motion, specifically developed to estimate the dynamic behaviour of an AAMV,
- derivation of a new static stability criterion for the AAMV,
- development of two MATLAB programs, that implement the two new mathematical models,
- parametric analysis on the influence of the configuration characteristics on the AAMV performance,
- design of a novel trim control device, capable of reducing the resistance and to avoid the dynamic instability regime.

12.2.1 New system of equations of equilibrium

In chapter 6 a new system of equations of equilibrium specifically developed for the AAMV configuration is developed. To take into account all the forces and moments, shown in fig. 6.1, the author modified the system of equations of equilibrium developed by Savitsky [43]. Basically the aerodynamic lift, drag and moment of the aerodynamic surfaces are added to the basic system of equations of equilibrium of the Savitsky model.

Since the AAMV aerodynamic surfaces operate very close to the sea surface, they experiences the wing in ground effect. Therefore the aerodynamic forces are estimated taking into account their dependence not only on the angle of attack, but also on their height above the surface. This dependence, as shown for example by Moore [32], is strongly nonlinear and dependent on the airfoil and wing characteristic.

A method to solve the system of equations of equilibrium is developed. Unfortunately, no experimental data on vehicles classifiable as AAMV have been found in the public domain, so a direct validation of the model has not been possible. Nonetheless the author exploited the possibility of analyzing, with this mathematical model, other configurations, such as planing craft. The agreement between experimental data and computed data for such craft is good, as demonstrated in chapter 4.

The mathematical model developed has been presented at the *8th Symposium on High Speed Marine Vehicles, 2008* [9].

12.2.2 New system of equations of motion

In chapter 7 a mathematical model of the longitudinal dynamics of a AAMV configuration, developed in the small disturbances framework, is presented.

Coupling the systems of equations of motion, available in literature, used for Wing In Ground effect (WIGE) vehicles and for high speed planing craft, the author derived a new system of equations of motion. This mathematical model takes into account both aerodynamic and hydrodynamic (and hydrostatic) stability derivatives, leading to a new dynamics.

In fact, also if this AAMV mathematical model is obtained by combining the WIGe vehicles and the planing craft dynamics, the resultant dynamics is not simply the sum of these dynamics. As shown in tab. 12.1, the system of equations of motion developed by the author proposes a new dynamic feature, with a potential new mode of oscillation and a more complex dynamics with respect to WIGe vehicles, planing craft and conventional airplanes.

This novel system of equations of motion has been presented at the *2nd International Conference on Marine Research and Transportation, 2007* [8].

12.2.3 AAMV static stability criterion

As previously said, the AAMV dynamics differ substantially from planing craft dynamics and airplanes and WIGe vehicles dynamics. In section 8.2, the static stability of a AAMV configuration is analyzed, and a new static stability criterion is proposed.

Briefly, in the longitudinal plane, airplanes possess one neutral point, called aerodynamic neutral point in pitch (or also neutral point): if this point is rearward

Vehicle configuration	System of Equations of Motion	Roots
Airplane	4 equations $\frac{\partial x}{\partial t}, \frac{\partial z}{\partial t}, \frac{\partial \theta}{\partial t}, \theta$	2 oscillatory sol.s: phugoid, SPPO
Planing craft	4 equations $\frac{\partial z}{\partial t}, z, \frac{\partial \theta}{\partial t}, \theta$	2 oscillatory sol.s: porposing (least stable root)
WIGe vehicles	5 equations $\frac{\partial x}{\partial t}, \frac{\partial z}{\partial t}, \frac{\partial \theta}{\partial t}, \theta, h$	2 oscillatory sol.s, 1 real root: phugoid, SPPO, subsidence mode
AAMV	6 equations $\frac{\partial x}{\partial t}, \frac{\partial z}{\partial t}, z,$ $\frac{\partial \theta}{\partial t}, \theta, h$	(for the reduced order system, without $\frac{\partial x}{\partial t}$, 2 oscillatory sol.s, 1 real root)

Table 12.1: Comparison between the dynamics characteristics of conventional configurations and the AAMV dynamics

with respect to the CG of the vehicle, the airplane is statically stable. By contrast, WIGe vehicles have an additional neutral point, called aerodynamic neutral point in height, due to the fact that aerodynamic forces depend also on the height above the surface. To have a WIGe vehicle statically stable in height, this second neutral point should be upstream with respect to the first neutral point, as investigated by Staufenbiel [50], Irodov [20], and Rozhdestvensky [41]. For a aerodynamically alleviated marine vehicles (AAMV), a third neutral point exists, due to the fact that the forces depend on:

- the pitch angle as for an airplane and WIGe vehicles,
- the height above the surface as in WIGe vehicles,
- the heave position.

In fact the hydrodynamic forces depend heavily on the heave position of the AAMV. The condition expressed in eq. 8.17 can be expressed saying that the third neutral point, also called the hydrodynamic center in heave, should be located downstream with respect to the neutral point 2, to have an AAMV that is statically stable in heave. The relative position of each point is shown in fig. 8.1. In airplane dynamics, the distance between the CG and the (aerodynamic) neutral point (in pitch) is called 'static stability margin' (ssm_1). Following the same approach, the distance between the second neutral point and the first neutral point can be called 'static stability margin in height' (ssm_2). As already said, for a AAMV configuration a third neutral point exists, and the distance between the second and the third neutral point can be called 'hydrodynamic static stability margin in heave' (ssm_3).

12.2.4 Numerical implementation programs: AAMV design tools

The mathematical models developed, to estimate the equilibrium attitude of the AAMV and to study the dynamics of the AAMV in the small disturbances framework, are implemented in two MATLAB programs.

An extended markup language (xml) file structure is chosen as an input data file, due to its simplicity and versatility. A first program estimates the equilibrium attitude of the given AAMV configuration, in the chosen speed range. Then an excel file with the calculated variables is written (tab. B.3 and B.4) and a number of graphs are shown (fig. B.1 through B.7). A second program, starting from the equilibrium attitude parameters calculated with the first program, estimates the aerodynamic and hydrodynamic stability derivatives of the AAMV. Then it evaluates the roots of the characteristic polynomial of the AAMV system. An example of the roots calculated is shown in fig. B.8.

An example of an AAMV configuration analysis conducted using the two MATLAB programs is illustrated in appendix B.

12.2.5 Results of the AAMV parametric analysis

In chapter 9 a parametric analysis of the influence of some key parameters of an AAMV configuration is conducted. Both the influence on the equilibrium attitude characteristics and on the dynamic stability is shown.

The numerical estimations shown are valuable from a qualitative point of view, since their actual values are strongly influenced by the geometric characteristics of configuration C-01. Therefore quantitatively no extrapolation for others config-

urations should be made, but quantitatively these values are a indicator of which are the parameters that influence the most the equilibrium attitude and the dynamic stability of a AAMV configuration. These analysis are useful design tools for the preliminary phase of a AAMV design project.

12.2.5.1 Influence of the AAMV configuration on the equilibrium attitude

The key parameters chosen are:

- the length of the chord of the aerodynamic surface (mac),
- the angle between mac and the keel of the hull (η_{a1}),
- the longitudinal position of the aerodynamic center of the wing (ξ_{ac1}),
- the deadrise angle of the hull (β),
- the longitudinal position of the CG (lcg),
- the mass of the AAMV (m).

In general, a wing on a high speed marine vehicle can influence positively or negatively its behaviour: the characteristics of the aerodynamic surface/s have to be chosen carefully. In particular, under a certain speed, called 'critical speed', it is disadvantageous to use an aerodynamic surface: the hydrodynamic efficiency is diminished, leading to an increased drag force for the same lift force, therefore having a worse R / W ratio. The main reason is the influence of the wing on the trim equilibrium attitude angle: it tends to increase it, leading to all these negative consequences. Above this 'critical speed' the opposite situation happens: aerodynamic forces start to give their positive contribution, diminishing the R/W

ratio. For these reasons, the key rule to choose the value of the parameter analyzed should be this one:

- to minimize, below critical speed, the influence of the wing,
- to maximize, above critical speed, the influence of the wing.

Taking into account the results of these parametric analysis, an 'optimum' AAMV configuration is proposed, called C-02, and it is compared against a simple planing craft configuration, identical to C-02 but without the aerodynamic surface, called C-00. The two configurations are illustrated in tab. 9.5. Referring to tab. 9.6, the optimized AAMV configuration, C-02, experiences a slightly higher resistance below the critical speed (10% higher), while above the critical speed the resistance-to-weight ratio is up to 30% lower than the planing hull configuration, C-00.

12.2.5.2 Influence of the AAMV configuration on the dynamic stability

The key parameters chosen are:

- the length of the chord of the aerodynamic surface (mac),
- the angle between mac and the keel of the hull (η_{a1}),
- the longitudinal position of the aerodynamic center of the wing (ξ_{ac1}),
- the deadrise angle of the hull (β),
- the longitudinal position of the CG (lcg),
- the mass of the AAMV (m).
- the pitch moment of inertia of the AAMV (k_{55}, pitch radius of inertia).

In tab. 9.4 are summarized the results of the influence of the key parameters on the dynamic stability of the vehicle. Briefly, there is a speed, for each parameter, at which the AAMV configuration becomes unstable: it is because one or more roots of the characteristic polynomial have a real part. Each key parameter has been increased of 100%, and it has been analyzed how this 'instability onset speed' changes. Basically, the most important parameter is the longitudinal position of the center of gravity, *lcg*. Referring to tab. 9.4, if the *lcg* length is increased of 100%, the 'instability onset speed' can be shifted positively (that means shifted to a higher value) of 1.27 Fn. The second most important parameter is the value of the pitch moment of inertia, with a positive effect. The influences of these two parameters have been already known for the planing craft dynamics. The new result is the relatively strong influence of the length of the aerodynamic surface, represented by the mean aerodynamic chord (*mac*). The order of magnitude of its influence is comparable with the influence of the pitch moment of inertia, but its effect is negative. It means that if *mac* is increased of 100%, the 'instability onset speed' will be lowered of Fn 0.25.

12.2.6 Novel trim control device

For a conventional planing hull, the equilibrium trim angle (with the inertial and geometrical characteristics of the hull fixed) depends only on speed. Anyway, if the trim angle is controlled, a lower resistance and the possibility of avoiding dynamic instability can be obtained.

Nowadays, the most efficient way to control this angle is to adopt a shifting weight system. A novel trim control device is proposed here that does not require the complicated mechanisms needed by available shifting weight systems. This novel device is illustrated in fig. 10.1 and fig. 10.2. There is a plate able to slide

in and out: this movement respectively diminishes or increases the value of the longitudinal position of the center of gravity (lcg). It achieves the same objective of shifting part of the displacement fore and aft.

In fig. 10.4 and 10.7 are illustrated some numerical results, the reduction of the resistance-to-weight ratio that can be obtained compared to the performance of a conventional planing hull and of a planing hull equipped with the novel device. The reduction can be up to 25%.

In fig. 10.8 is illustrated the porpoising instability theory of Savitsky. Briefly, for each velocity there is a critical trim equilibrium angle beyond which the planing hull becomes unstable. With the novel device is possible to control the trim angle so as to avoid trim angles at which porpoising can occur.

12.3 Future Developments

The AAMV configuration is a relatively recent concept, therefore it needs further theoretical and experimental investigations. In the following sections the author proposes the main directions that should be investigated.

The research needed to design an AAMV will give a possibility to the hydrodynamics and aerodynamics research community of creating a unique vehicle.

12.3.1 Hydrodynamic surfaces: hull characteristics analysis

In this work the long-form Savitsky model is adopted to estimate the hydrostatic and hydrodynamic forces acting on the hull. This model is developed for high speed prismatic hulls, with one keel, one chine and a constant deadrise angle.

A major improvement of the model would be the possibility of analyzing a multiple hull configuration. A catamaran configuration would have the following advantages:

- lower accelerations in the longitudinal plane with respect to a planing hull of the same size,
- the space between the two planing hulls would be perfect to accommodate a wing,
- the two planing hulls would act as endplates of the wing, enhancing the WIGe advantages.

Furthermore, many solutions are adopted in modern planing hull configurations to enhance the performance, such as multiple chines, warped hulls (deadrise angle not constant), spray rails, stepped hulls, and so on. These solutions can be integrated in the equilibrium mathematical model to evaluate if they can be advantageous also for an AAMV configuration.

12.3.2 Aerodynamic surfaces: aerofoil analysis

In general, every aerofoil family can be adopted as an aerodynamic surface for an AAMV configuration. Anyway, the performance of an AAMV can be greatly enhanced with a careful choice of the profile.

In the former Soviet Union, an aerofoil family specifically developed to exploit the 'Wing In Ground effect' has been developed. This family is called DHMTU, after the Department of Hydromechanics of the Marine Technical University (DHMTU) of St. Petersburg, where this family was developed. Section 9.5.1.2 shows how the use of a particular DHMTU profile can greatly increase the performance of an

AAMV configuration. The problem is the lack of information about this aerofoil family in the public domain. In fact some authors, like Moore [32], are forced to build an actual model of a DHMTU profile to collect experimental data.

A theoretical and experimental comparative study between aerofoil families would be necessary to build an aerofoil database. This database, together with the parametric analysis presented in chapter 9, would be a useful tool to optimize the AAMV configuration in the preliminary design phase.

12.3.3 Stability Derivatives Estimation Method Development

The AAMV system of equations of motion (eq. 7.14), developed in the small disturbances framework, is composed by aerodynamic and hydrodynamic stability derivatives. The numerical values of the aerodynamic stability derivatives are estimated using the methods developed for WIGe vehicles (appendix A), while the hydrodynamic stability derivatives are evaluated using the method presented by Martin [28] and Faltinsen [15].

These methods are developed for configurations different from the AAMV. They can be adopted as a first approximation, but the relatively new configuration studied in this work would need a specifically developed method to estimate its stability derivatives. In particular, hydrodynamic stability derivatives are better approximated using a non-linear mathematical method, as shown by Troesch and Falzarano [54], by Hicks et al. [19] and, more recently, by Katayama and Ikeda [23].

12.3.4 From Longitudinal to Lateral-Directional Dynamics

In this work the AAMV dynamics in the longitudinal plane is analyzed, developing a system of equations of motion. The horizontal (x) and vertical (z) displacements and the pitch rotational displacement (θ) degrees of freedom have been decoupled by the the lateral displacement (y) and the yaw and roll rotational displacements (respectively ψ and ϕ). It is important to expand the AAMV dynamics analysis to the lateral-directional plane, to analyse the static and dynamic stability in this plane as well as the manoeuvre capabilities of this new configuration.

12.3.5 Hybrid Vehicle Preliminary Design Method

In [39] and [40], Roskam presents a preliminary design method for airplanes. Starting from a set of requirements as the payload, the range, the endurance, and so on, it presents a method to estimate the size of the vehicle, to limit the number of possible configurations and how to choose and integrate a possible propulsion system.

Taking this method as model, it is possible to develop a similar aproach to design a AAMV. The approach proposed is similar to that one used in this work to develop the mathematical system of equations of equilibrium and the system of equations of motion: it starts from available mathematical methods already developed for airborne and waterborne vehicles, then it modifies and couples the two approach to obtain a mathematical framework specific for the AAMV configuration. This work would benefit also from the parametric analysis presented in chapter 9.

References

[1] Associates, A. A. Rich passage research - passenger only fast ferry project. Tech. Rep. Appendix E-a, Art Anderson Associates, September 2004.

[2] Carter, A. W. Effect of ground proximity on the aerodynamic characteristics of aspect ratio 1 airfoils with and without plates. Technical Note TN D-970, NASA, Washington, October 1961. Langley Research Center, Langley Air Force Base, Va.

[3] Celano, T. The prediction of porpoising inception for modern planing craft. *SNAME Transactions 106* (1998), 269–292.

[4] Chun, H. H., and Chang, C. H. Longitudinal stability and dynamic motion of a small passenger wig craft. *Ocean Engineering 29* (2002), 1145–1162.

[5] Cocklin, M. R., Parsons, M. G., and Troesch, A. W. Stern flap powering performance prediction for the coast guard 110-foot wpb island class patrol boat. *Marine Technology 37*, 2 (2000), 100–110.

[6] Cohen, S. H., and Blount, D. L. Research plan for the investigation of dynamic instability of small high-speed craft. *Sname Transactions 94* (1986), 197–214.

[7] Collu, M. High speed marine vehicles exploiting aerodynamic lift: Dynamic model. Mid point review report, October 2007.

[8] Collu, M., Patel, M. H., and Trarieux, F. A unified mathematical model for high speed hybrid (air and waterborne) vehicles. In *2nd International Conference on Marine Research and Transportation* (2007).

[9] Collu, M., Patel, M. H., and Trarieux, F. A mathematical model to analyze the static stability of hybrid (aero-hydrodynamically supported) vehicles. In *8th Symposium on High Speed Marine Vehicles, HSMV 2008* (2008), Royal Institution of Naval Architects, pp. 148–161.

[10] Cusanelli, D. S. Stern flaps–a chronicle of success at sea (1989-2002). In *SNAME Innovations in Marine Transportation, Pacific Grove, California* (2002).

[11] Day, J. P., and Haag, R. J. Planing boat porpoising: A study of the critical boundries for a series of prismatic hulls. Master's thesis, Webb Institute of Naval Architecture, 1952.

[12] Delhaye, H. An investigation into the longitudinal stability of wing in ground effect vehicles. Master's thesis, Cranfield University - College of Aeronautics, 1997. Supervisor: P. G. Thomasson.

[13] Doctors, L. *Hydrodynamics of High-Speed Small Craft.* University of Michigan, 1985, ch. 4, pp. 137–205,269,270.

[14] Doctors, L. J. Analysis of the efficiency of an ekranocat: A very high speed catamaran with aerodynamic alleviation. In *International Conference on Wing in Ground Effect Craft (WIGs 97)* (December 1997), RINA, Ed.

[15] Faltinsen, O. M. *Hydrodynamics of High-Speed Vehicles*, 1st ed. Cambridge University Press, 2005.

[16] Gera, J. Stability and control of wing-in-ground effect vehicles or wingships. In *33rd Aerospace Sciences Meeting and Exhibit* (1995), AIAA.

[17] Hall, I. A. An investigation into the flight dynamics of wing in ground effect aircraft operating in aerodynamic flight. Master's thesis, Cranfield University - College of Aeronautics, 1994. Supervisor: P. G. Thomasson.

[18] Hicks, J. D. Analysis method for planing hull vertical motions. Master's thesis, University of Michigan, Department of Naval Architecture and Marine Engineering, 1993. Ann Arbor, Michigan, USA.

[19] Hicks, J. D., Troesch, A. W., and Jiang, C. Simulation and nonlinear dynamics analysis of planing hulls. *Transactions of the ASME 117* (February 1995), 38–45.

[20] Irodov, R. D. Wig longitudinal stability criteria (kriterii prodol'noy ustoychivosti ekranoplana). Translated document from Russian Vol 1 No 4 Pages 63-72, TsAGI (Central Institute of Aerohydrodynamics im. N. Ye. Zhukovskij), 1970.

[21] Kallio, J. A. Results of full scale trials on two high speed planing craft (kudu ii and kaama). Tech. Rep. DTNSRDC/SPD-0847-01, David W. Taylor Naval Ship Research and Development Center, July 1978.

[22] Karafiath, G., Cusanelli, D., and Lin, C. W. Stern wedges and stern flaps for improved powering - u. s. navy experience. *SNAME Transactions 107* (1999), 67–99.

[23] Katayama, T., and Ikeda, Y. Hydrodynamic forces acting on porpoising craft at high-speed. *Journal of Shipe and Ocean Technology 3*, 2 (1999), 17–26.

[24] Kumar, P. E. Stability of ground effect wings. Cranfield CoA Report Aero No. 198, Cranfield College of Aeronautics, May 1967.

[25] Kumar, P. E. On the longitudinal dynamic stability of a ground effect vehicle. Tech. rep., Cranfield College of Aeronautics, 1968.

[26] Lee, T.-S. Interference factor for catamaran planing hulls. *AIAA Journal 20*, 10 (October 1982), 1461–1462.

[27] Liu, C. Y., and Wang, C. T. Interference effect of catamaran planing hulls. *Journal of Hydronautics 13* (January 1979), 31–32.

[28] Martin, M. Theoretical determination of porpoising instability of high-speed planing boats. *Journal of Ship Research 22*, 1 (1978), 32–53.

[29] Marvin, P. F., and Lastinger, J. L. Aerodynamic characteristics of low-aspect-ratio wings in close proximity to the ground. Technical Note TN D-926, NASA, Washington, July 1961.

[30] Meyer, J. R., Clark, D. J., and Ellsworth, W. M. The quest for speed at sea. Technical digest, Carderock Division, NSWC, 2004.

[31] Millward, A. Effect of wedges on the performance characteristics of two planing hulls. *Journal of Ship Research 20*, 4 (December 1976), 224–232.

[32] Moore, N., Wilson, P. A., and Peters, A. J. An investigation into wing in ground effect airfoil geometry. In *Symposium on Challenges in Dynamics, System Identification, Control and Handling Qualities for Land, Air, Sea and Space Vehicles* (2002), no. RTO-MP-095, NATO, pp. 11–1 11–20.

[33] Mosaad, M. A., Gaafary, M. M., and Amin, I. A. Energy saving and dynamic stability of planning hull due to hydrodynamic control of trim angles. In *Maritime Transportation and Exploitation of Ocean and Coastal Resources - Guedes Soares, Garbatov & Fonseca (eds)* (2005), Soares, Grabatov, and Fonseca, Eds., vol. 1, pp. 229–242.

[34] Ollila, R. G. Historical review of wig vehicles. *Journal of Hydronautics 14*, 3 (July 1980), 65–76.

[35] Payne, P. R. Coupled pitch and heave porpoising instability in hydrodynamic planing. *Journal of Hydronautics 8*, 2 (April 1974), 58–71. AIAA-62979-655.

[36] Pensa, C. Appunti per le lezioni del corso di architettura navale ii - i catamarani. Universita' degli Studi di Napoli Federico II, January 2003.

[37] Privalov, E. I., and Kirillovikh, V. N. Transport amphibious platforms: a new type of high-speed craft. In *Workshop Proceedings of Ekranoplans & Very Fast Craft* (1996). The University of New South Wales, Sydney, Australia on 5-6 December 1996.

[38] Rawson, K. J., and Tupper, C. *Basic Ship Theory*, 5th ed., vol. 1, 2. Rawson K. J., Tupper C., 2001.

[39] Roskam, J. *Airplane Design Part I: Preliminary Sizing of Airplanes.* Design Analysis & Research, 1989.

[40] Roskam, J. *Airplane Design, Part II: Preliminary Configuration Design and Integration of the Propulsion System.* Design Analysis & Research, 1999.

[41] Rozhdestvensky, K. V. Ekranoplans - the gem's of fast water transport. *Transactions of The Institute of Marine Engineer 109*, Part 1 (November 1996), 47–74.

[42] Rozhdestvensky, K. V. Wing-in-ground effect vehicles. *Progress in Aerospace Sciences 1*, 42 (2006), 211–283.

[43] Savitsky, D. Hydrodynamic design of planing hulls. *Journal of Marine Technology 1*, 1 (1964), 71–95.

[44] Savitsky, D. Planing craft. *Naval Engineers Journal 97*, 2 (February 1985), 113–141.

[45] Savitsky, D. On the subject of high-speed monohulls. Presented to the Greek Section Of the Society Of Naval Architects and Marine Engineers Athens, Greece. October 2, 2003, October 2003.

[46] Savitsky, D., DeLorme, M. F., and Datla, R. Inclusion of whisker spray drag in performance prediction method for high-speed planing hulls. *Marine Technology 44*, 1 (January 2007), 35–56.

[47] Savitsky, D., and Dingee, A. Some interference effects between two flat surfaces planing parallel to each other at high speed. *Journal of Aeronautical Sciences 21* (June 1954), 419–420.

[48] Seydel, R. *From Equilibrium to Chaos: Practical Bifurcation and Stability Analysis*. Seydel, R., 1988.

[49] Shipps, P. R. Hybrid ram-wing/planning craft - today's raceboats, tomorrow's outlook. In *AIAA/SNAME Advanced Marine Vehicles Conference* (1976), no. AIAA 76-877. Arlington, Virginia, September 20-22.

[50] Staufenbiel, R. W., and Bao-Tzang, Y. Flugeigenschaften in der langsbewegung von bodeneffekt-fluggeraten, teil i und ii. *ZFW 24* (1976), Jan/Febr pp3–9, Marz/April pp.65–70.

[51] Staufenbiel, R. W., and Bao-Tzang, Y. Stability and control of ground effect aircraft in longitudinal motion (translation). Tech. Rep. DTNS RDC 77-0048, David W. Taylor Naval Ship Research and Development Center, June 1977.

[52] Staufenbiel, R. W., and Kleineidam, G. Longitudinal motion of low-flying vehicles in nonlinear flowfields. In *International Council of the*

Aeronautical Sciences, Congress, 12th (October 1980), American Institute of Aeronautics and Astronautics, AIAA, pp. 293–308.

[53] Troesch, A. W. On the hydrodynamics of vertically oscillating planing hulls. *Journal of Ship Research 36*, 4 (1992), 317–331.

[54] Troesch, A. W., and Falzarano, J. W. Modern nonlinear dynamical analysis of vertical plane motion of planing hulls. *Journal of Ship Research 37*, 3 (September 1993), 189–199.

[55] Ward, T. M., Goelzer, H. F., and Cook, P. M. Design and performance of the ram wing planing craft - kudu ii. In *AIAA/SNAME Advanced Marine Vehicles Conference* (1978). San Diego, CA; Apr. 17-19.

[56] Williams, A. G. W. *Aerodynamic Forces on High-Speed Multihulled Marine Vehicles*. PhD thesis, Cranfield University, 2008.

[57] Xi, H., and Sun, J. Nonlinear feedback stabilization of high-speed planing vessels by a controllable transom flap. In *American Control Conference* (June 2005), AACC. 2005 American Control Conference June 8-10, 2005, Portland, OR, USA.

[58] Xi, H., and Sun, J. Vertical plane motion of high speed planing vessels with controllable transom flaps: Modeling and control. In *Proceedings of IFAC Congress* (July 2005).

[59] Zarnick, E. E. A nonlinear mathematical model of motions of a planing boat in regular waves. Tech. Rep. DTNSRDC-78/032, David W. Taylor Naval Ship Research and Development Center, 1978.

[60] Zhukov, V., Maskalik, A., and Kolyzaev, B. *Ekranoplans, Peculiarity of the theory and design.* Saint Petersburg "Sudostroyeniye", 2000.

Appendix A

WIGe Vehicle Aerodynamic Stability Derivatives

A.1 Introduction

To evaluate the dynamic stability of a vehicle it is necessary to know its dynamic stability derivatives. Once these are evaluated, it is possible to estimate the roots of the system of equations of motion: if all the roots have a negative real part, the system will be dynamically stable.

In this section are presented some expressions to evaluate the aerodynamic stability derivatives, using the aerodynamic coefficients, and the equations to evaluate the coefficients of the polynomial characteristic of a WIGe vehicle, useful to evaluate its dynamic stability using the Routh-Hurwitz criterion.

In fig. A.1 and A.2 are shown, respectively, the Glenn Martin geometrical characteristics and its coefficients of lift, drag and moment, obtained thriugh several experiments by Carter [2]. This aerofoil and these data have been used for the parametric analyses presented in chapter 9.

A.2 Aerodynamic stability derivatives

As already shown in chapter 3, the aerodynamic derivatives of a WIGe system of equations of equilibrium, in the longitudinal plane, are the derivatives of the surge force (X), the heave force (Z), and the pitch moment (M) with respect to the height above the surface (h, η_0), the surge velocity (u, $\dot{\eta}_1$), the heave velocity (w, $\dot{\eta}_3$), the pitch angular velocity (q, $\dot{\eta}_5$), and the heave acceleration ($\dot{w}$, $\ddot{\eta}_3$). To estimate these derivatives, Staufenbiel [50] in Germany, Irodov [20] and Rozhdestvensky [41] in Russia, and others in UK as Kumar [24] and Hall [17] have given different sets of expressions. In his master thesis Delhaye [12] presents a comparison between these different methods, he showed that the three approaches (German, Russian and UK style) are very similar. In this appendix the UK-style expressions are presented.

A.2.1 Input aerodynamic coefficients

To estimate the aerodynamic stability derivatives, the coefficients presented in tab. A.1 are needed. Furthermore, if a secondary wing is present, the coefficients presented in tab. A.1 are also needed.

A.2.2 Aerodynamic stability derivatives expression

Once known the value of the parameters presented in tab. A.1 and tab. A.2, it is possible to evaluate the aerodynamic stability derivatives using the expressions given in tab. A.3

Table A.1: Aerodynamic coefficients needed to evaluate the aerodynamic stability derivatives (1)

C_L	coefficient of lift
$\partial C_L/\partial V$	C_L derivative wrt the velocity
$\partial C_L/\partial \alpha$	C_L derivative wrt the angle of attack
$\partial C_L/\partial (h/c)$	derivative of C_L wrt dimensionless h
C_D	coefficient of drag
$\partial C_D/\partial V$	C_D derivative wrt the velocity
$\partial C_D/\partial \alpha$	C_D derivative wrt the angle of attack
$\partial C_D/\partial (h/c)$	derivative of C_D wrt dimensionless h
$\partial C_m/\partial V$	C_m derivative wrt the velocity
$\partial C_m/\partial \alpha$	C_m derivative wrt the angle of attack
$\partial C_m/\partial (h/c)$	derivative of C_m wrt dimensionless h

Table A.2: Aerodynamic coefficients needed to evaluate the aerodynamic stability derivatives (2)

$\partial C_{LT}/\partial \alpha$	C_L derivative wrt the angle of attack
S_{LT}	area of the secondary airfoil
l_T	distance of aerodynamic center of the secondary wing aft of the CG
ϵ_α	downwash derivative at secondary wing
C_{LT}	coefficient of lift of the secondary airfoil)

Table A.3: Aerodynamic stability derivatives expressions, UK-style

Aerodynamic derivatives		
Derivative	Dimensional conversion	Dimensionless expression
X_h^a	$1/2\ \rho^a\ S^a\ V_0^2/c$	$\left(-\frac{\partial C_D}{\partial(h/c)}\right)$
$X_{\dot{\eta}_1}^a$	$1/2\ \rho^a\ S^a\ V_0$	$\left(-2C_D - V_0\frac{\partial C_D}{\partial V}\right)$
$X_{\dot{\eta}_3}^a$	$1/2\ \rho^a\ S^a\ V_0$	$\left(C_L - \frac{\partial C_D}{\partial \alpha}\right)$
$X_{\dot{\eta}_5}^a$	$1/2\ \rho^a\ S^a\ V_0\ c$	negligible (0)
$X_{\ddot{\eta}_3}^a$	$1/2\ \rho^a\ S^a\ c$	negligible (0)
Z_h^a	$1/2\ \rho^a\ S^a\ V_0^2/c$	$\left(-\frac{\partial C_L}{\partial(h/c)}\right)$
$Z_{\dot{\eta}_1}^a$	$1/2\ \rho^a\ S^a\ V_0$	$\left(-2C_L + V_0\frac{\partial C_L}{\partial V}\right)$
$Z_{\dot{\eta}_3}^a$	$1/2\ \rho^a\ S^a\ V_0$	$\left(-C_D - \frac{\partial C_L}{\partial \alpha}\right)$
$Z_{\dot{\eta}_5}^a$	$1/2\ \rho^a\ S^a\ V_0\ c$	$\left(-\frac{\partial C_{LT}}{\partial \alpha}\frac{S_T l_T}{S\ c}\right)$
$Z_{\ddot{\eta}_3}^a$	$1/2\ \rho^a\ S^a\ c$	$\left(-\frac{\partial C_{LT}}{\partial \alpha}\frac{S_T l_T}{S\ c}\ \epsilon_\alpha\right)$
M_h^a	$1/2\ \rho^a\ S^a\ V_0^2$	$\left(\frac{\partial C_m}{\partial(h/c)}\right)$
$M_{\dot{\eta}_1}^a$	$1/2\ \rho^a\ S^a\ V_0\ c$	negligible (0)
$M_{\dot{\eta}_3}^a$	$1/2\ \rho^a\ S^a\ V_0\ c$	$\left(\frac{\partial C_m}{\partial \alpha}\right)$
$M_{\dot{\eta}_5}^a$	$1/2\ \rho^a\ S^a\ V_0\ c^2$	$\left(-\frac{\partial C_{LT}}{\partial \alpha}\frac{S_T l_T^2}{S\ c^2}\right)$
$M_{\ddot{\eta}_3}^a$	$1/2\ \rho^a\ S^a\ c^2$	$\left(-\frac{\partial C_{LT}}{\partial \alpha}\frac{S_T l_T^2}{S\ c^2}\ \epsilon_\alpha\right)$

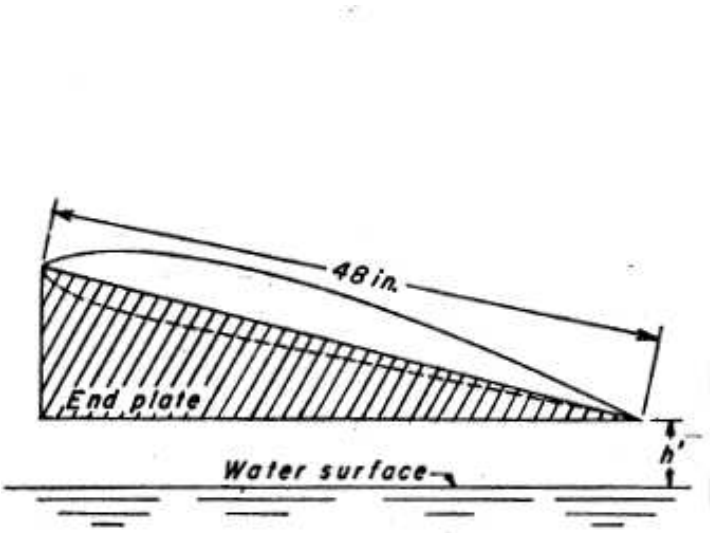

Station, percent chord	Airfoil ordinates, percent chord	
	Upper	Lower
0	4.43	4.43
1.25	6.10	3.02
2.5	6.90	2.40
5	7.99	1.66
7.5	8.82	1.18
10	9.46	.86
15	10.36	.38
20	10.84	.14
30	11.06	0
40	10.56	0
50	9.60	0
60	8.32	0
70	6.68	0
80	4.72	0
90	2.50	0
95	1.28	0
100	0	0

Figure A.1: Glenn Martin profile geometrical characteristics [2]

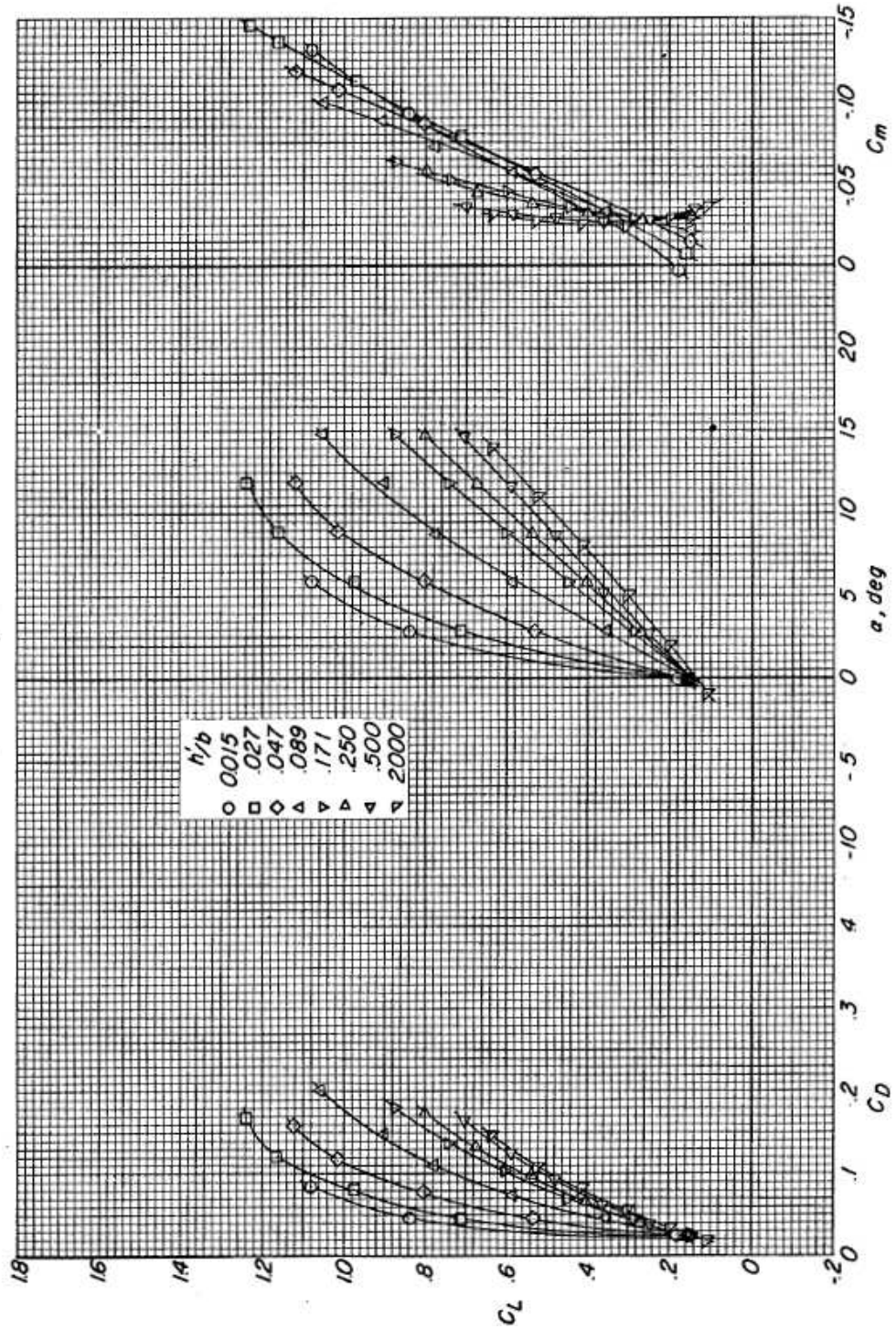

Figure A.2: Glenn Martin profile coefficients of lift, drag and moment, function of angle of attack and height above the surface [2]

Appendix B

AAMV configuration analysis: example

To better clarify how the AAMV equilibrium attitude program works, the procedure to analyse a AAMV configuration is illustrated step by step, from the input xml data to the output files and graphs.

B.1 Configuration and xml input data file

B.1.1 Configuration characteristics

The configuration analyzed in this example is illustrated in tab. B.1 and tab. B.2.

B.1.2 Aerodynamic coefficients excel input file

The excel file 'DHMTU.xls' is composed by $n + 1$ worksheets, where n is the number of heights above the surface. The first worksheet is illustrated in fig. 6.4. In this worksheet, called 'data', are contained the following data:

Table B.1: Xml input data example (1)

Branch of the tree	Name	Value
medium	rho_a $[kg\,m^{-3}]$	1.23
”	rho_h $[kg\,m^{-3}]$	1025.9
”	g $[m\,s^{-2}]$	9.81
”	nu_h $[m^2\,s]$	0.00000119
motion	Fn_min [ ]	1.0
”	Fn_max [ ]	3.5
”	Fn_delta [ ]	0.1
vehicle		
geometry		
prop	xi_tp $[m]$	0
”	zeta_tp $[m]$	0
”	eps_deg $[deg]$	12
aero		
first surface	mac_a1 $[m]$	11.50
”	S_a1 $[m^2]$	396.75
”	eta_a1 $[deg]$	3.0
”	xi_ac1 $[m]$	15.0
”	zeta_a1 $[m]$	-2.0
”	profile	DHMTU.xls
hydro	beam $[m]$	5.547
”	beta $[deg]$	14
”	A_h $[m^2]$	20.067
dynamics		
prop	T_V $[N\,m^{-1}\,s]$	0

Table B.2: Xml input data example (2)

vehicle		
dynamics		
aero		
stabDer	type	calculated
”	axes	wind-stability
”	Z_qWB	0
”	M_qWB	0
”	M_dwWB	0
”	eps_alpha	0
”	c_LTalpha	0
inertial	lcg $[m]$	8.656
”	vcg $[m]$	1.387
”	m $[kg]$	52160
”	I_55 $[kg\,m^2]$	2712318.1
computational_parameters		
tau_deg_start $[deg]$	2	
tau_deg_stop $[deg]$	10	
tau_deg_step $[deg]$	0.1	
h_CG_0 $[m]$	1.05	
h_CGEps $[m]$	0.1	
derivativesMethod	Faltinsen	

- heights analyzed,
- AR, aspect ratio of the wing,
- Mach number,
- Reynold number,
- the exact name of the profile.

In the others n worksheets are contained the lift, drag and aerodynamic coefficients, function of the angle of attack, as shown in fig. 6.5.

B.1.3 Xml input file

The xml input data file will be structured in the following way

```
<data>
   <medium>
           <rho_a um="[kg/m^3]">1.23</rho_a>
           <rho_h um="[kg/m^3]">1025.9</rho_h>
           <g um="[m/s^2]">9.81</g>
           <nu_h um="m^2/s">0.00000119</nu_h>
   </medium>
   <motion>
           <Fn_min>1.0</Fn_min>
           <Fn_max>3.5</Fn_max>
           <Fn_delta>0.1</Fn_delta>
   </motion>
   <vehicle>
            <geometry>
                     <prop>
                           <xi_tp um="[m]">0</xi_tp>
                           <zeta_tp um="[m]">0</zeta_tp>
                           <eps_deg um="[deg]">12</eps_deg>
                     </prop>
                     <aero>
```

```
                    <first>
                        <mac_a1 um="[m]">11.50</mac_a1>
                        <S_a1 um="[m^2]">396.75</S_a1>
                        <eta_a1 um="[deg]">3.0</eta_a1>
                        <xi_ac1 um="[m]">15.0</xi_ac1>
                        <zeta_ac1 um="[m]">-2.0</zeta_ac1>
                        <profile>
                            <xlsFileName_a1>DHMTU.xls</xlsFileName_a1>
                        </profile>
                    </first>
                </aero>
                <hydro>
                    <beam um="[m]">5.547</beam>
                    <beta um="[deg]">14</beta>
                    <A_h  um="[m^2]">20.067</A_h>
                </hydro>
        </geometry>
        <dynamics>
                <prop>
                    <T_V info="Thrust derivative wrt speed">0</T_V>
                </prop>
                <aero>
                    <stabDer>
                        <type>calculated</type>
                        <axes>wind-stability</axes>
                        <Z_qWB>0</Z_qWB>
                        <M_qWB>0</M_qWB>
                        <M_dwWB>0</M_dwWB>
                        <eps_alpha>0</eps_alpha>
                        <C_LTalpha>0</C_LTalpha>
                    </stabDer>
                </aero>
        </dynamics>
        <inertial>
                <lcg um="[m]">8.656</lcg>
                <vcg um="[m]">1.387</vcg>
                <m um="[kg]">52160</m>
                <I_55 um="[kg*m^2]">2712318.1</I_55>
        </inertial>
</vehicle>
<computational_parameters>
                    <tau_deg_start um="[deg]">2.000</tau_deg_start>
                    <tau_deg_stop um="[deg]">10.000</tau_deg_stop>
```

```
                        <tau_deg_step um="[deg]">0.1</tau_deg_step>
                        <h_CG_0 um="[m]">1.05</h_CG_0>
                        <h_CGEps um="[m]">0.01</h_CGEps>
                        <derivativesMethod>Faltinsen</derivativesMethod>
   </computational_parameters>
</data>
```

B.2 MATLAB elaboration

B.2.1 Launching the program

In MATLAB, the following commands are needed:

```
data(1).nameXmlFile = 'HV7_DHMTU.xml';

option  = 1;
graph   = 1;

HV_Dynamics_Analysis(data,option,graph)
```

The command $data(1).nameXmlFile = `HV7\_DHMTU.xml'$; set as first case the configuration specified in the xml file $HV7\_DHMTU.xml$. It is possible to compare several configurations performance. To insert the $i-th$ configuration to compare the command is:

```
data(i).nameXmlFile = '<name of the i-th configuration xml file>';
```

The command:

```
option = 1;
```

it is used to set if only the equilibrium attitude estimation is desired ($option = 1$) or if also the modes of oscillation will be calculated ($option = 2$).

The other option is to set if the graphs are desired ($graph = 1$) or not desired ($graph = 0$). To launch the program the command is:

```
HV_Dynamics_Analysis(data,option,graph)
```

B.2.2 Screen feedback

If everything is ok, MATLAB will show the following code:

```
data_in =

                nameXmlFile: 'HV7_DHMTU.xml'
                     medium: [1x1 struct]
                     motion: [1x1 struct]
                    vehicle: [1x1 struct]
    computational_parameters: [1x1 struct]
                    results: [1x1 struct]

Equilibrium Attitude Analysis Started
The vehicle has a AAMV configuration, monohull
%%%%% Analysis of the airfoil DHMTU.xls - START %%%%%
%%%%%
%%%%% Attention - do not open the DHMTU.xls file while the program is running
      Progress:
     Aerodyn. coeff. of height 1 of 7 analyzed
     Aerodyn. coeff. of height 2 of 7 analyzed
     Aerodyn. coeff. of height 3 of 7 analyzed
     Aerodyn. coeff. of height 4 of 7 analyzed
     Aerodyn. coeff. of height 5 of 7 analyzed
     Aerodyn. coeff. of height 6 of 7 analyzed
     Aerodyn. coeff. of height 7 of 7 analyzed
%%%%% Analysis of the airfoil DHMTU.xls - END
1 Fn      3.02deg      1.164e-010 N (vert)       5.513e-012 N (horiz)       -6.142 N*m
1.1 Fn      3.23deg      0 N (vert)       4.433e-012 N (horiz)       1.140 N*m
1.2 Fn      3.48deg      -1.164e-010 N (vert)       -4.661e-012 N (horiz)       -1.187 N*m
1.3 Fn      ...
1.4 Fn      ...
...
```

```
...
3.4 Fn      3.85deg      -5.820e-011 N (vert)       -5.456e-012 N (horiz)       0.574 N*m
3.5 Fn      3.80deg      0 N (vert)       -1.818e-012 N (horiz)       0.271 N*m
Case HV7_DHMTU.xml analyzed
Case 1 of 1 ( 100 %) of the total
```

First, the aerodynamic coefficients data in the excel file are acquired. Then MATLAB shows, for each speed analyzed, the equilibrium trim angle and the sum of vertical forces (vert), the sum horizontal forces (horiz) and the sum of pitch moments. In this way it is possible to check if the system of equations of equilibrium is satisfied.

B.3 Output

The AAMV program creates two kind of outputs:

- graphs,
- excel files.

The output variables are shown in several graphs and their numerical values are stored in two excel files.

B.3.1 Graphs

B.3.1.1 Equilibrium attitude

As regard the equilibrium attitude estimation, the program shows seven graphs.

Fig. B.1 shows the trim equilibrium attitude curve versus the dimensionless speed range.

Fig. B.2 shows the draft at transom and the AAMV center of gravity height above the surface, versus the dimensionless speed range.

Fig. B.3 shows the keel and the chine wetted lengths versus the dimensionless speed range. These data are useful to evaluate if these lengths, in particular the keel wetted length, do not are bigger than the actual length of the AAMV vehicle.

Fig. B.4 shows the AAMV resistance to weight ratio versus the dimensionless speed range. As defined previously, the R / W ratio is the sum of aerodynamic and hydrodynamic drag forces divided by the total weight of the vehicle.

Fig. B.5 shows the aerodynamic total drag, the hydrodynamic total drag and their sum versus the dimensionless speed range.

Fig. B.6 shows the aerodynamic total lift and hydrodynamic total lift, divided by the total weight of the vehicle, versus the dimensionless speed range. Here it is shown the percentage of weight sustained by aerodynamic and hydrodynamic forces.

Fig. B.7 shows the aerodynamic and hydrodynamic lift to drag ratio versus the dimensionless speed range. The lift to drag ratio is also called efficiency.

B.3.1.2 Modes of oscillation

As regard the modes of oscillation estimation, the program shows one graph, illustrated in fig. B.8. Here are represented the roots of the modes of oscillation for each speed evaluated in the equilibrium attitude program. Since the roots of

the modes of oscillation are of the form:

$$s = Re(s) \pm Im(s) \cdot i$$

the x axis represents the real value, the y axis the imaginary value.

The modes of oscillation represented in the graph are of the AAMV reduced order system of equations of motion. It is a system of the 5th order, therefore there are 5 roots:

- 2 complex roots,
- 1 real root.

The two branches in the graph correspond to the complex roots, and the roots near the origin represent the real roots.

B.3.2 Excel files

As previously said, two are the output excel files:

- *xml file name.xml.xls*, it contains the equilibrium attitude variables numerical values,
- *xml file name.xml-derivatives method name.xls*, it contains the numerical values of the variables describing the modes of oscillation.

B.3.2.1 Equilibrium attitude

The output equilibrium attitude excel file has the structure illustrated in tab. B.3 and tab. B.4.

Table B.3: AAMV program: equilibrium attitude output file (1)

Worksheet	Column Name	Description
Equilibrium state		
	Fn	Froude number
	Trim	Trim equilibrium angle τ
	Draft	Draft at transom
	Keel	Keel wetted length
	Chine	Chine wetted length
	CG height	CG height above the surface
Coefficients		
	Fn	Froude number
	Friction coeff.	Hydrodynamic friction coeff.
	Friction surface ref.	Reference area for the friction coeff.
	Aero. lift coeff., surf. 1	First surface, aerodynamic lift coeff.
	Aero. drag coeff., surf. 1	First surface, aerodynamic drag coeff.
	Hydro. lift coeff.	Hydrodynamic lift coefficient
Aerodynamic F and M		
	Fn	Froude number
	Lift 1	Aerodynamic lift force, 1st surface
	Drag 1	Aerodynamic drag force, 1st surface
	Lift 2	Aerodynamic lift force, 2nd surface
	Drag 2	Aerodynamic drag force, 2nd surface
	Drag hull above water	Aerodynamic drag of the part of the hull above the water

Table B.4: AAMV program: equilibrium attitude output file (2)

Worksheet	Column Name	Description
Hydrodynamic F and M		
	Fn	Froude number
	Potential Lift	Lift component of the potential force N
	Potential Drag	Drag component of the potential force N
	Friction drag	Friction drag force
	Whisker spray drag	Whisker spray drag force
	Total drag	Total hydrodynamic drag
RtoW		
	Fn	Froude number
	D_Aero/W	Aerodynamic drag divided by weight
	D_Hydro/W	Hydrodynamic drag divided by weight
	RtoW	Resistance-to-weight ratio
	% Aero drag	aerodynamic % of the total drag
	% Hydro drag	hydrodynamic % of the total drag

Table B.5: AAMV program: modes of oscillation output file

Worksheet	Column Name	Description
Root i-th		
	Fn	Froude number
	Real	Real part of the root
	Imaginary	Imaginary part of the root
	Period	Period length of the oscillation
	Time-to-half	Time to half the oscillation
	Omega	oscillation frequency $\sqrt{Re^2 + Im^2}$
	Zeta	oscillation damping ratio $\frac{-Re}{\omega}$

B.3.2.2 Modes of oscillation

The output modes of oscillation excel file has the structure illustrated in tab. B.5. For every root of the system of equations of motion there is a worksheet, and every worksheet has the same structure.

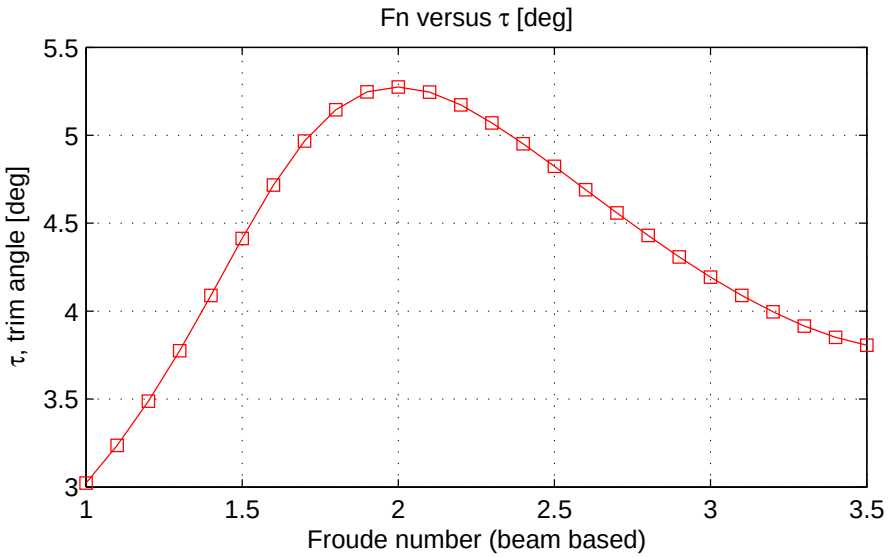

Figure B.1: AAMV program, output graph example: trim equilibrium angle vs speed

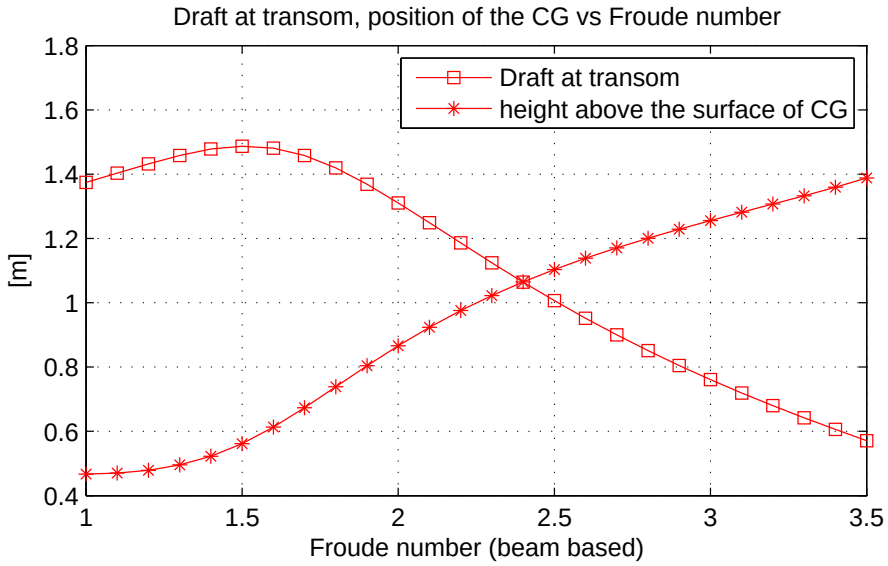

Figure B.2: AAMV program, output graph example: draft and CG height vs speed

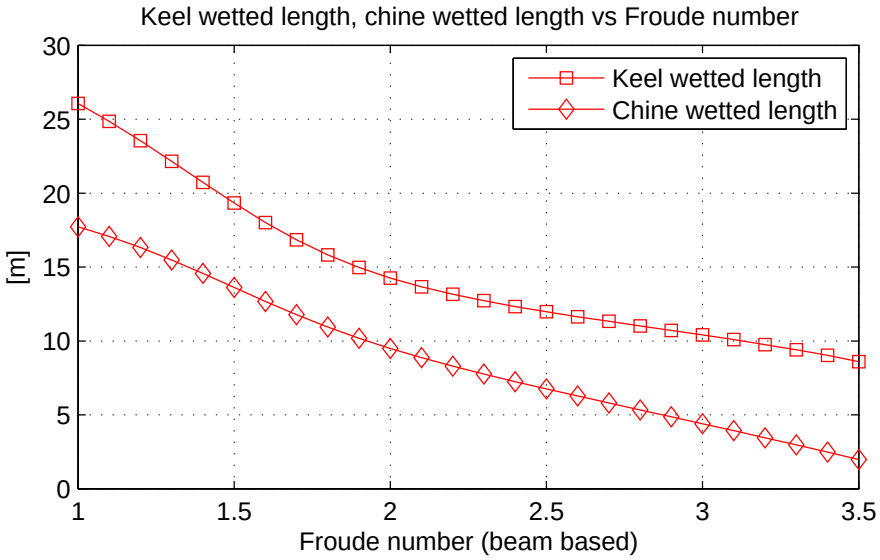

Figure B.3: AAMV program, output graph example: keel and chine wetted length vs speed

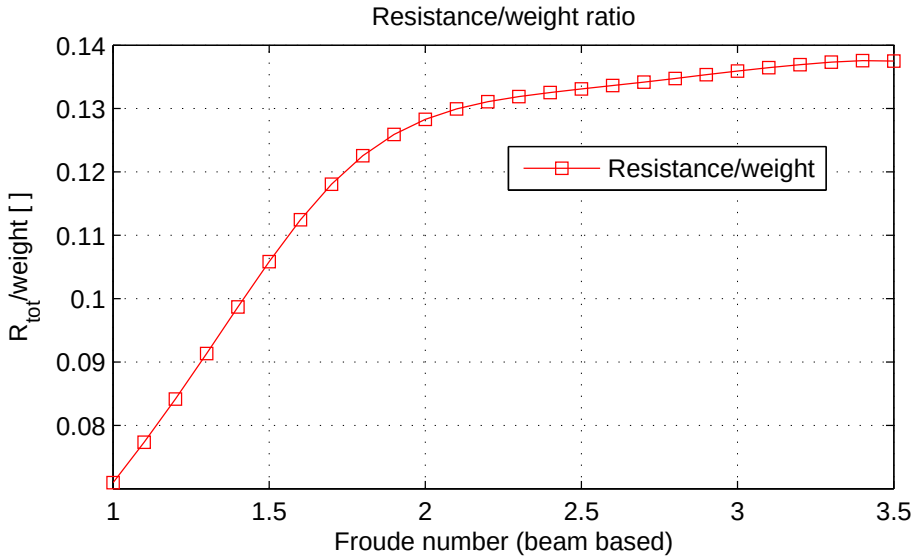

Figure B.4: AAMV program, output graph example: resistance to weight ratio vs speed

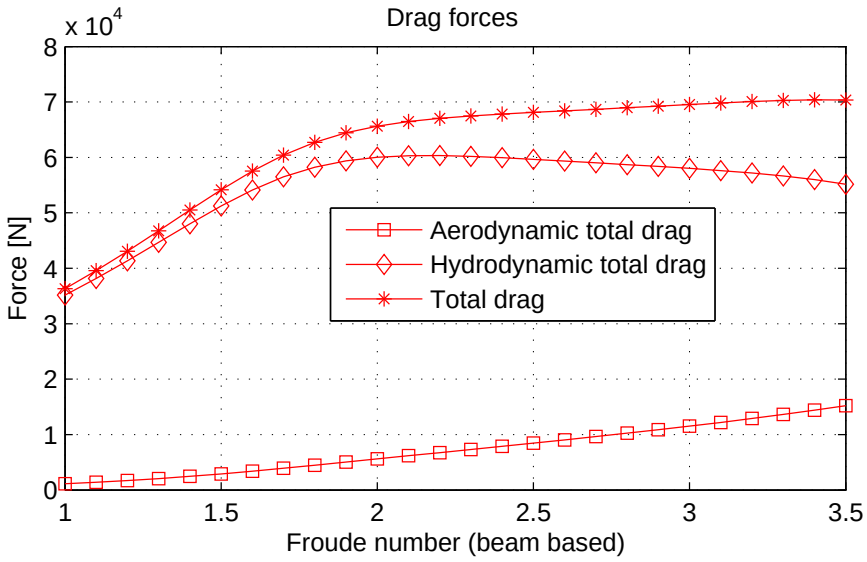

Figure B.5: AAMV program, output graph example: drags vs speed

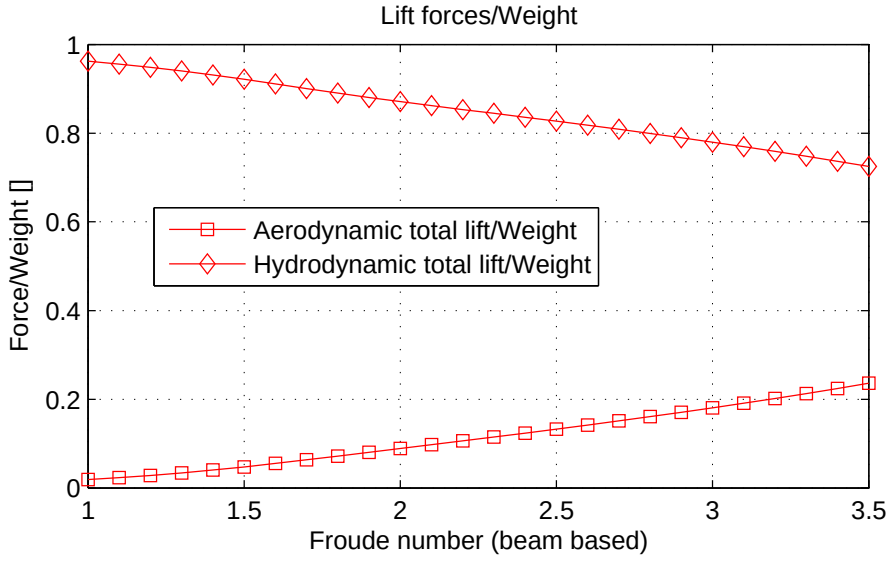

Figure B.6: AAMV program, output graph example: lifts to weight ratio vs speed

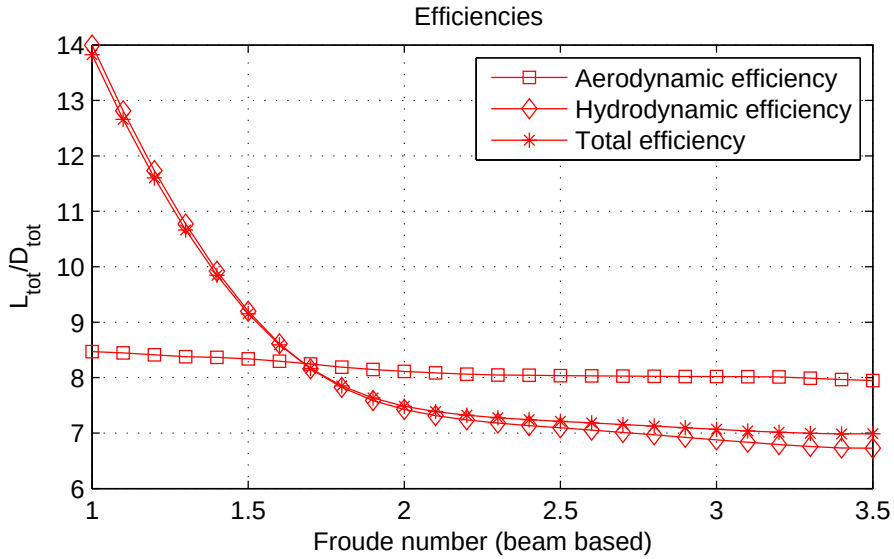

Figure B.7: AAMV program, output graph example: efficiencies vs speed

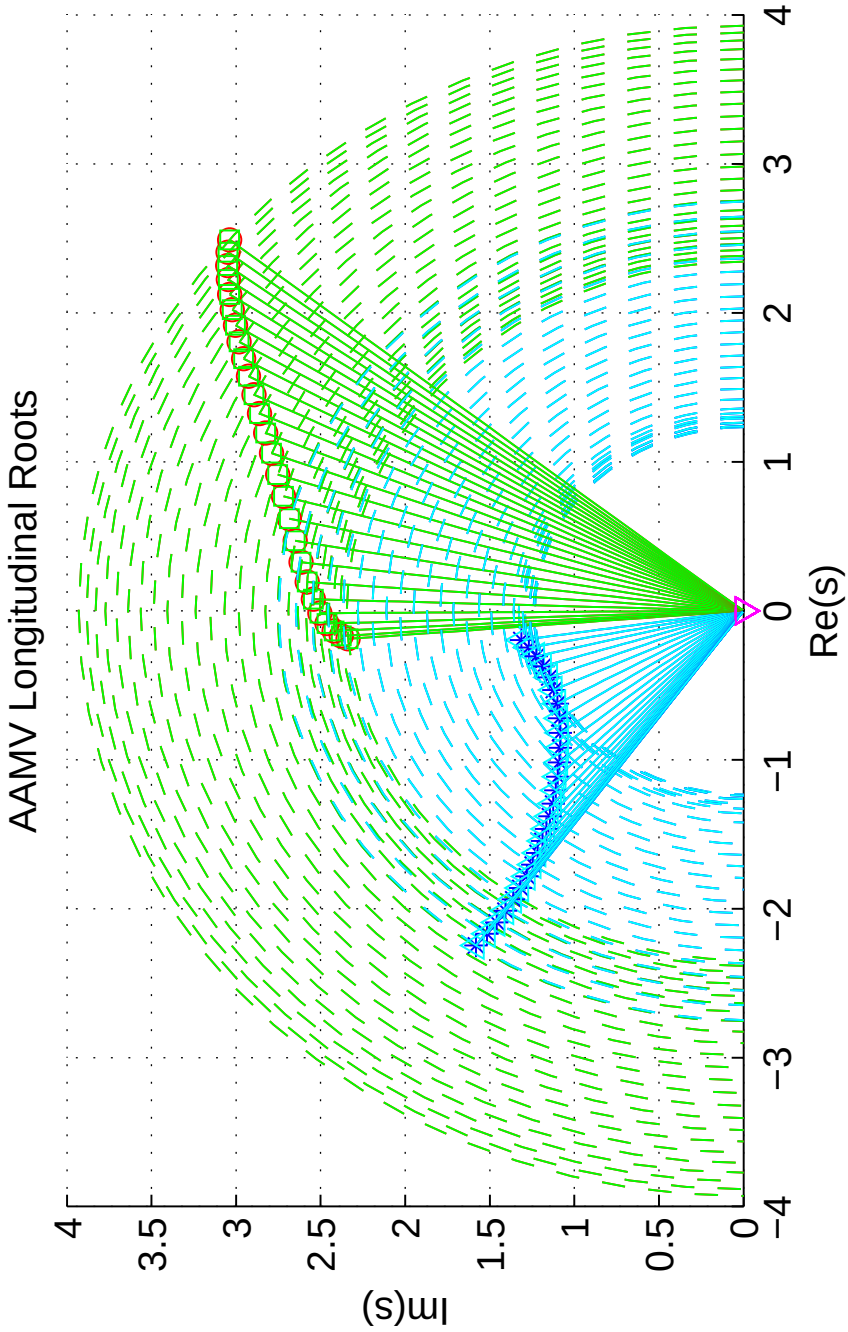

Figure B.8: AAMV program, output graph example: modes of oscillation roots

Appendix C

Routh Hurwitz Method

C.1 Introduction

Given a polynomial equation in s:

$$A_n \cdot s^n + A_{n-1} \cdot s^{n-1} + ... + A_1 \cdot s + A_0 = 0 \tag{C.1}$$

the Routh Hurwitz method is used to determine how many roots have positive real part. Therefore, if the polynomial equation is the characteristic polynomial equation of a dynamic system, this method can be used to estimate the stability of the system.

If eq. C.1 is the characteristic polynomial of the system of equations of motion of a vehicle, the Routh Hurwitz criterion can be used to derive the conditions to assure its static and dynamic stability.

C.2 Algorithm to derive the Routh Hurwitz matrix

The Routh Hurwitz matrix, also called Routh Hurwitz array, is a n+1 rows times h columns matrix.

$$\begin{cases} h = (n+2)/2 & \text{if n is even} \\ h = (n+1)/2 & \text{if n is odd} \end{cases}$$

C.2.1 First and second row

If n is even:

	Column 1	Column 2	...	Column h
Row 1	A_n	A_{n-2}	...	A_0
Row 2	A_{n-1}	A_{n-3}	...	0

If n is odd:

	Column 1	Column 2	...	Column h
Row 1	A_n	A_{n-2}	...	A_1
Row 2	A_{n-1}	A_{n-3}	...	A_0

C.2.2 From third row to n+1-th row

The generic element RH(i,j) of the Routh Hurwitz matrix can be obtained as follow.

$$RH(i,j) = \frac{RH(i-1,1) \cdot RH(i-2,j+1) - RH(i-2,1) \cdot RH(i-1,j+1)}{RH(i-1,1)} \tag{C.2}$$

	Column 1	...	Column j	Column j+1
Row i-2	$RH_{i-2,1}$	...	...	$RH_{i-2,j+1}$
Row i-1	$RH_{i-1,1}$	...	...	$RH_{i-1,j+1}$
Row i	...	...	$RH_{i,j}$	...

To calculate the h-th column elements, RH(...,j+1) = 0.

C.3 The Routh Hurwitz matrix and the vehicle stability

The Routh Hurwitz method states that if all the elements of the first column of the Routh Hurwitz matrix have the same sign, the real part of every root of the polynomial will be negative. For every sign change there is a root with a positive real part.

Therefore to assure the static and dynamic stability of a vehicle, the elements of the first row of its Routh Hurwitz matrix have to be of the same sign.